

Design, Synthesis, and Applications of Chiral Spiroketal (SPIROL)-Based Ligands

by

Siyuan Sun

A dissertation submitted in partial fulfillment
of the requirements for the degree of
Doctor of Philosophy
(Chemistry)
in the University of Michigan
2021

Doctoral Committee:

Associate Professor Pavel Nagorny, Chair
Professor Anna Schwendeman
Professor John P. Wolfe
Associate Professor Paul Zimmerman

Siyuan Sun

siyuans@umich.edu

ORCID iD: 0000-0002-1795-9336

© Siyuan Sun 2021

Dedication

To my dearest family.

Acknowledgements

I am pleased to express my gratitude to my supervisor, Dr. Pavel Nagorny, for his constant help, support, and encouragement, and without his guidance, this work would be impossible to complete. Dr. Pavel Nagorny is a knowledgeable scientist, who developed our innovative SPIROL project and orientated me towards the chiral catalysis. All trainings and unique experience in the Nagorny group continuously urge me to explore more chemistry in the future. Graduate school life is tougher than I thought, but I am glad that Dr. Pavel Nagorny is always a supportive mentor, who has valuable advice when I encountered all different problems and doubted myself. At the moment, I have learned a better way of viewing and solving different problems. In addition, this work would not have been possible without the support of the National Science Foundation (grant CHE-1350060 to P.N.).

I would also like to acknowledge and thank my dissertation committee Dr. John Wolfe, Dr. Paul Zimmerman and Dr. Anna Schwendeman for giving me this precious opportunity to share my research with them. I am especially grateful of their patience and understanding during the pandemic when all unexpected problems occurred.

I want to thank my undergraduate research advisor Dr. Mingji Dai at Purdue University for his guidance and support for me to pursue the graduate degree. It was my pleasure to meet Dr. Yu Bai, Dr. Yong Li, Wandi Zhang, Pui Leng Low and Xingyu Shen in the Dai group and be good friends to me since then.

I would like to thank all my colleagues at Nagorny group for their help over the past five years. I want to thank to our postdoctoral fellows, Dr. Iaroslav Khomutnyk for his valuable

advice on all mechanical and chemistry problems, and also grateful to have Dr. Alonso Argüelles as my mentor and coworker in this project, who did all valuable computational studies. I also cherish the opportunity to work with Kenta Yamamoto, Zachary Fejedelem, Nicolas Diaz and Solomon Song during all stages of the SPIROL project. I want to acknowledge my current and former lab mates Dr. Hem Khatri, Dr. Will Kaplan, Dr. Bijay Bhattarai, Dr. Tay Rosenthal, Dr. Jeonghyo Lee, Sibin Wang, Nolan Carney, Sungjin Kim, Ryan Rutkoski, Oleksii Zhelavskiy, Natasha Perry, Rami Hourani, Zhongzheng Li, Hao Guo, and Qingqin Huang. It is a blessing to meet many interesting souls from our department, including but limited to Dr. Shuo Guo, Dr. Yingfu Lin, Dr. Yanming Wang, Dr. Weixuan Nie, Yichao Yan, Mo Chen, Yishu Xu, and Liuhan Dai.

I am lucky to meet Xindie Huang at the University of Michigan and thank you for all the experience together and support along the way. I enjoyed the time to exchange non-chemistry related ideas and the communications of your grace to my soul.

Some special thanks go to my family in China, to whom this dissertation is dedicated, for their unconditioned love and support. They gave me the opportunity to explore the world when I first went to Nebraska, and it would be impossible for me to experience all different cultures in the last decade without their unlimited encouragement.

Table of Contents

Dedication	ii
Acknowledgements	iii
List of Tables	viii
List of Figures	ix
List of Schemes	xi
List of Abbreviations	xiv
Abstract	xviii
Chapter 1 Recent Developments of Chiral C₂-Symmetric Spirocyclic Ligands	1
1.1. Introduction	1
1.2. Recent developments with SPINOL and derivatives	3
1.3. Recent discovery and applications of SPIROL	16
1.4. Recent discovery and applications of O-SPINOL	22
1.5. Recent discovery and applications of aza-SPINOL	24
1.6. Recent discovery and applications of SPSiOL	26
1.7. Other asymmetric spirocyclic ligands	28
1.8. Concluding remarks	32

1.9. References	33
Chapter 2 Design, Synthesis, and Applications of Chiral Spiroketal-Containing (SPIROL)	
Ligands	42
2.1. Early developments of spiroketal-containing ligand SPIROL	42
2.2. Asymmetric alkylation with organozinc reagents	48
2.3. Introduction and synthesis of the aziridine-based catalysts for the highly enantioselective synthesis of chiral alcohols 2-4a	53
2.4. Second-generation asymmetric assembly of (<i>R,S,S</i>)-SPIROL core 2-2	55
2.5. Asymmetric catalysis with SPIROL-based ligands	60
2.6. Experimental information	65
2.7. References	99
Chapter 3 Exploration of Chiral Diastereomeric Spiroketal (SPIROL)-Based Phosphinite	
Ligands in Asymmetric Hydrogenation of Heterocycles	104
3.1. Introduction of iridium-catalyzed hydrogenation of aromatic heterocycles	104
3.2. Background of SPIROL-based phosphinite ligands	118
3.3. Design and synthesis of SPIRAPO ligands	120
3.4. Evaluation of all ligands in asymmetric hydrogenation of quinaldine	124
3.5. Results and discussion	127
3.6. Conclusions	130
3.7. Experimental information	131

3.8. References	187
Chapter 4 Exploration of Chiral Spiroketal (SPIROL)-Based Oxazoline Ligands (SPIROX) in Asymmetric Insertion of α-Diazocarbonyl Compounds	198
4.1. Introduction of carbene insertion	198
4.2. Introduction of BOX ligands	200
4.3. Synthesis of C ₂ -symmetric SPIROL-based bisoxazoline ligands (SPIROX)	209
4.4. Application of SPIROX ligands in asymmetric insertion of carbenoids into Si-H, N-H and O-H bonds	213
4.5. Conclusions	215
4.6. Experimental information	216
4.7. References	227
Chapter 5 Closing Remarks	232
Appendix A Experimental information for other important SPIROL-based ligands	235

List of Tables

Table 1.1 1) Asymmetric iridium-catalyzed hydroarylation and 2) asymmetric palladium-catalyzed allylic alkylation	18
Table 1.2 Palladium-catalyzed asymmetric Heck reaction.....	19
Table 1.3 Rhodium-catalyzed asymmetric hydrogenations.....	20
Table 2.1 Asymmetric hydrogenation of amino ester.....	61
Table 2.2 Studies of asymmetric hydroarylation	61
Table 2.3 Studies of asymmetric allylic alkylation.....	62
Table 2.4 Comparison of 3D structures of SPIRAP diastereomers and SDP.....	63
Table 3.1 Asymmetric hydrogenation of 2-methyl quinoline.....	112
Table 3.2 Asymmetric hydrogenation of 2-phenyl quinoline.....	114
Table 3.3 Asymmetric hydrogenation of 2-methyl quinoxaline.....	116
Table 3.4 Asymmetric hydrogenation of bezoxazinone	117
Table 3.5 Evaluation of ligands for the iridium(I)-catalyzed reduction of quinaldine	126
Table 4.1 Evaluation of SPIROX ligands for asymmetric insertion into a) Si-H and b) N-H....	213
Table 4.2 Evaluation of SPIROX ligands for Cu-catalyzed asymmetric O-H insertion.....	214

List of Figures

Figure 1.1 Selected examples for C ₂ -symmetric privileged ligands	2
Figure 1.2 Diastereomers of the Spirol 1-5.....	2
Figure 1.3 Early examples of chiral spirocyclic ligands.....	3
Figure 1.4 Example of chiral ligands with SPINOL-like backbone	5
Figure 1.5 Applications of SPINOL-like ligands	10
Figure 1.6 Chiral SPINOL-derived chiral organocatalysts.....	12
Figure 1.7 Selected applications with SPAs in name reactions	14
Figure 1.8 Applications of O-SPINOL-derived ligands	24
Figure 1.9 Applications with SPSiPhos ligands	28
Figure 1.10 Examples of SPAN-derived ligands.....	28
Figure 1.11 SKP 1-106 synthesis and the most recent application.....	30
Figure 1.12 Synthesis and applications of spirocyclic ligands 1-110 and 1-111	31
Figure 2.1 C ₂ symmetry in privileged ligands	42
Figure 2.2 Example of Nagorny group's diastereomeric SPIROLs	43
Figure 2.3 Early developments on enantioselective addition of dialkylzinc reagents	49
Figure 2.4 Selected examples of catalyst used in asymmetric alkylations	50
Figure 2.5 Syntheses of diphosphinite ligands	59
Figure 2.6 Privileged ligands used for comparison	60
Figure 2.7 Comparison of (R,S,S)-SPIRAP, (S,S,S)-SPIRAP, and SDP complexes of PdCl ₂	64

Figure 2.8 Recent developments of spirocyclic scaffold	64
Figure 3.1 Examples of bioactive tetrahydroquinoline-containing alkaloids	104
Figure 3.2 Asymmetric hydrogenation of furans	105
Figure 3.3 Asymmetric hydrogenation of pyrazine and derivatives.....	108
Figure 3.4 Effect of spiroketal and substituent configuration on diastereomeric SPIROL ligands	119
Figure 3.5 Asymmetric reduction of 2-substituted quinolines.....	127
Figure 3.6 Asymmetric reduction of quinoxalines and bezoxazinones	129
Figure 4.1 Example of different states of carbenes.....	199
Figure 4.2 Early studies with BOX ligands	201
Figure 4.3 Selected examples of the BOX and PyBOX ligand syntheses	202
Figure 4.4 Examples of asymmetric catalysis with BINOL-based oxazoline ligands.....	205
Figure 4.5 Asymmetric insertion of carbenoids into O-H with SpiroBOX ligand	208
Figure 4.6 Substrate scope of CuCl-catalyzed asymmetric O-H insertion	215
Figure 5.1 Selected examples of available ligands	233

List of Schemes

Scheme 1.1 Early developments of SPINOL.....	3
Scheme 1.2 Synthesis of cyclohexyl-fused SPINOL 1-29	6
Scheme 1.3 Synthesis of SPINOL-like scaffold 1-33.....	7
Scheme 1.4 Synthesis of 2,2'-dimethyl-SPINOL 1-36.....	7
Scheme 1.5 Synthesis of 3,3'-hexamethyl-SPINOL-like 1-38	8
Scheme 1.6 Phosphoric acid-catalyzed asymmetric synthesis of SPINOL 1-12.....	11
Scheme 1.7 Applications of immobilized SPA in desymmetrization of disubstituted oxetanes ..	16
Scheme 1.8 Design and synthesis of SPIROL 1-53.....	17
Scheme 1.9 Synthesis of SPIROL derivatives	21
Scheme 1.10 Asymmetric hydrogenation of α -dehydroamino acid esters	22
Scheme 1.11 Development and synthesis of O-SPINOL 1-80.....	23
Scheme 1.12 Synthetic routes of aza-SPINOLs	26
Scheme 1.13 Synthesis of SPSiOL 1-99.....	27
Scheme 2.1 Retrosynthetic plan for SPIROL scaffold	44
Scheme 2.2 Dr. Alonso Argüelles' racemic approach.....	45
Scheme 2.3 Dr. Alonso Argüelles' asymmetric synthesis.....	46
Scheme 2.4 Proposed mechanism for spiroketalization	47
Scheme 2.5 Spiroketalization with chiral alcohol 2-4a	48
Scheme 2.6 Yoshioka's work of asymmetric alkylation.....	50

Scheme 2.7 Seebach's work of asymmetric alkylation	51
Scheme 2.8 White's work of asymmetric alkylation.....	51
Scheme 2.9 Soai's work of asymmetric alkylation	52
Scheme 2.10 Early developments with catalysts 2-14 and 2-15.....	53
Scheme 2.11 Synthesis of aziridine catalysts 2-20 and 2-21	54
Scheme 2.12 Optimized synthesis for compound 2-2	55
Scheme 2.13 Synthesis of Bn- and MOM-protected spirocycles	55
Scheme 2.14 Selective deprotection and triflation	56
Scheme 2.15 Selective production of diphosphine ligands	57
Scheme 3.1 Asymmetric hydrogenation of benzofurans by Ding and Coworkers.....	106
Scheme 3.2 Asymmetric hydrogenation of protected indoles	107
Scheme 3.3 Asymmetric hydrogenation of unprotected indoles	107
Scheme 3.4 Asymmetric hydrogenation of pyridine	109
Scheme 3.5 Asymmetric hydrogenation of isoquinolines in total synthesis of (-)-Jorumycin by Stoltz and coworkers.....	110
Scheme 3.6 Development of SPIROL-based ligands	118
Scheme 3.7 Efficient synthesis towards SPIROL diastereomers.....	120
Scheme 3.8 Syntheses of diphosphinite ligands	121
Scheme 3.9 One-pot synthesis of diphosphinite from 3-32.....	122
Scheme 3.10 Initial synthetic attempt towards 3-35.....	122
Scheme 3.11 Synthesis of ligand L3-10	123
Scheme 3.12 Synthesis of (-)-(<i>R</i>)-angustureine 3-50.....	128
Scheme 4.1 Early study of asymmetric carbenoid insertion.....	200

Scheme 4.2 Early development of BINOL-based oxazoline ligands	203
Scheme 4.3 Optimized synthesis of BINOL-based oxazoline ligands	204
Scheme 4.4 Preparation of SpiroBOX ligand.....	206
Scheme 4.5 Asymmetric carbenoid insertion into N-H with SpiroBOX ligand.....	207
Scheme 4.6 Synthesis of compound 4-25	209
Scheme 4.7 Synthesis of SPIROX (R,R,R,R,R)-4-28	210
Scheme 4.8 Synthesis of SPIROX (R,R,R,S,S)-4-30	211
Scheme 4.9 Failed attempts towards (S,R,R)-4-31.....	212
Scheme 5.1 SPIROL synthesis	232

List of Abbreviations

μg	microgram
μmol	micromole
6-dEB	6-deoxy-erythronolide B
Å	angstrom
Ac	acetyl
Aq	aqueous
Ar	aryl
atm	atmosphere (unit)
BINOL	1,1'-bi-2-naphthol
Bn	benzyl
Boc	tert-butyloxycarbonyl
BOM	benzyloxymethyl
BRSM	based on recovered starting material
Bu	butyl
Bz	benzoyl
Calcd	calculated
Cat.	catalyst
CPA	chiral phosphoric acid
Cy	cyclohexyl
d	days
DBNE	<i>N,N</i> -dibutylnorephedrine
DBU	1,8-diazabicyclo[5.4.0]undec-7-ene

DCE	1,2-dichloroethane
DCM	dichloromethane
DDQ	2,3-dichloro-5,6-dicyano-1,4-benzoquinone
DFT	density functional theory
DMAP	4-dimethylaminopyridine
DMF	dimethylformamide
DPPA	diphenylphosphoric acid
d.r.	diastereomeric ratio
ee	enantiomeric excess
equiv.	equivalent
Et	ethyl
EtOAc	ethyl acetate
FDA	Food and Drug Administration
g	gram
h	hours
Hex	hexanes
HPLC	high-performance liquid chromatography
HRMS	high resolution mass spectrometry
HSQC	heteronuclear single quantum correlation
Hz	hertz
<i>i</i> -Pr	isopropyl
IR	infrared
<i>J</i>	coupling constant
kcal	kilocalorie
M	molar
Me	methyl

MeCN	acetonitrile
mg	milligram
min	minutes
mL	milliliters
mmol	millimoles
MS	molecular sieves
MW	molecular weight
NIH	National Institute of Health
NBS	<i>N</i> -bromosuccinimide
NMR	nuclear magnetic resonance
<i>n</i> -BuLi	<i>n</i> -butyl lithium
Nu	nucleophile
o/n	overnight
PG	protecting group
Ph	phenyl
PhMe	toluene
PMB	para-methoxybenzyl
PPA	polyphosphoric acid
ppm	parts per million
Pr	propyl
R	alkyl group (generic)
rac	racemic
R _f	retention factor
r.r.	regioisomeric ratio
rt	room temperature

SKP	(5 <i>aR</i> ,8 <i>aR</i>)-1,13-bis(diphenylphosphaneyl)-5 <i>a</i> ,6,7,8,8 <i>a</i> ,9-hexahydro-5 <i>H</i> -chromeno[3,2- <i>d</i>]xanthene
S _N 1	unimolecular nucleophilic substitution
S _N 2	bimolecular nucleophilic substitution
SPAN	spiro-2,2'-bichroman
SPINOL	1,1'-spirobiindane-7,7'-diol
t	time
TBAF	tetrabutylammonium fluoride
TBDPS	<i>t</i> -butyldiphenylsilyl
TBS	<i>t</i> -butyldimethylsilyl
<i>t</i> -Bu	<i>t</i> -butyl
TES	triethylsilyl
Tf	trifluoromethanesulfonyl
TFA	trifluoroacetic acid
TfOH	trifluoromethanesulfonic acid
THF	tetrahydrofuran
TLC	thin layer chromatography
Ts	<i>p</i> -toluenesulfonyl
UV	ultraviolet

Abstract

C_2 -symmetric axially chiral scaffolds are of significant importance in asymmetric catalysis. Over the past two decades, several chiral spirocyclic scaffolds have demonstrated great promise in both transition metal catalyzed reactions and various organocatalytic transformations. This dissertation describes the development and exploration of two novel diastereomeric C_2 -symmetric spirocyclic scaffolds termed “SPIROL”s. These studies include the development of convenient, and concise syntheses of both (*R,S,S*)- and (*S,S,S*)-diastereomeric series of SPIROLs on decagram scale in a highly enantioselective and diastereoselective fashion. Thus, obtained chiral spiroketal cores are subsequently elaborated into different types of C_2 -symmetric ligands that are explored in various Ir-, Rh-, Pd-, and Cu-catalyzed asymmetric transformations. In these studies, SPIROLs demonstrated excellent selectivity profiles in all of the explored transformations, and the observed selectivities and yields indicate that SPIROLS hold great promise as the ligands for the asymmetric transition metal catalysis.

Chapter 1 is an introduction and overview of recent developments with C_2 -symmetric spirocyclic ligands in the past five years. A summary of SPINOL-derived ligands and catalysts as well as SPIROL, O-SPINOL, aza-SPINOL and SPSiOL are included. Other interesting miscellaneous spirocyclic scaffolds are also presented in this chapter.

Chapter 2 describes the design and development of novel C_2 -symmetric spirocyclic scaffold SPIROL, which is a major breakthrough for ligands since the discovery of SPINOL. Three steps from commercially available starting material efficiently and selectively assemble

the spirocyclic core without need for the chiral resolution. Two structurally distinctive SPIROLs were produced from the same spirocyclic intermediate and independently exploited towards different ligands for future studies. SPIROL-derived ligands demonstrated good yields, excellent enantioselectivities and diastereoselectivities in many kinds of transformations.

Chapter 3 describes the development of new SPIROL-based diphosphinite ligands (SPIRAPO) for iridium-catalyzed asymmetric reduction of aromatic heterocycles. A new ligand core with isopropyl substituent on the backbone was also synthesized and studied. Our results suggested that SPIRAPO ligand performed better than other privileged scaffold-derived phosphinites under mild reaction conditions. The ligand is also well tolerated all changes in the heterocycle substitutions and frameworks. Two diastereomeric SPIROL-based phosphinites are compared in this study, and we discovered new properties with SPIROL scaffolds since our last report.

Chapter 4 describes the ongoing development of new SPIROL-based oxazoline ligands (SPIROX), and their applications in asymmetric insertion of copper carbenoids. The study showed excellent performance for the insertion into phenols, while unsatisfactory results were observed with silanes and anilines.

Chapter 1

Recent Developments of Chiral C₂-Symmetric Spirocyclic Ligands

1.1. Introduction

Chirality represents one of the most important topics to organic chemistry because the majority of biological molecules making up the living cells are either chiral compounds existing in an enantiopure form or comprised of the chiral enantioenriched building blocks.¹ As the result, chirality is of great importance for the molecular recognition, and, as the result, many therapeutic agents are enantioenriched chiral molecules. The nature has established enzymatic machinery to produce chiral building blocks, often with great levels of controls over the enantioselectivity. For a long time, chemists have tried to emulate these processes by developing different methods, including asymmetric catalysis,² to access the compounds of interest. Sustained research activities with chiral ligands could be traced back to Knowles' effort with CAMP and PMAP³ and Kagan's reports with DIOP.^{4,5} Since last century, there has been increasing research effort and specialization in chiral ligands and catalysts with an improvement in reactivity, catalyst loading, turnover rate, and especially enantioselectivity.⁶⁻⁸ The concept of "privileged ligands" was then introduced by Jacobson (Figure 1.1) and attributed to those ligands with a wide variety of transformations under high productivity and outstanding enantiocontrol.⁹

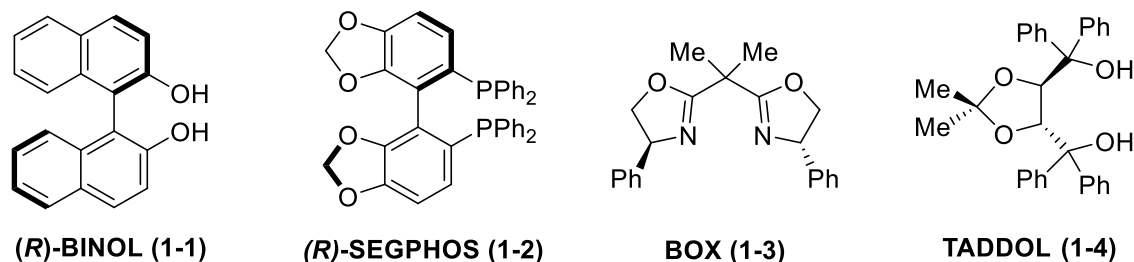


Figure 1.1 Selected examples for C₂-symmetric privileged ligands

Inspired from the most famous C₂-symmetric BINOL skeleton, the uniqueness of spirocyclic system having two rings linked by one common atom instead of a C-C bond led chemists to another class of axial chiral skeleton. In 1954, spiro[4,4]nonane-1,6-diol (**Spirol 1-5**) was first discovered by Cram and Steinberg¹⁰, and later Gerlach group¹¹ and Harada group¹² also independently reported their work to access this molecule. (Figure 1.2) The first application with chiral aluminum-**Spirol** complex was reported in 1992 in the asymmetric reduction of aromatic ketones,¹³ which marked the beginning of a new era of asymmetric catalysis with spirocyclic ligands.

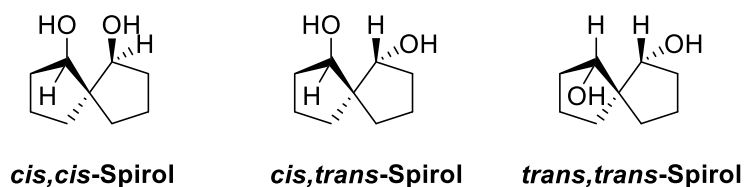


Figure 1.2 Diastereomers of the Spirol 1-5

For the past two decades, a large array of improvements was achieved with newly developed spirocyclic cores,^{14,15} such as SpirOP **1-6**,¹⁶ SDP **1-7**,¹⁷ SpinPHOX **1-8**¹⁸ and SPANphos **1-9**.¹⁹ (Figure 1.3) While significant number of new transformations have been developed with aforementioned ligands and catalysts, there are always motivations for scientists to develop more easily accessible spirocyclic cores and apply in unprecedented applications. Therefore, this chapter would mainly review rapid developments of new C₂-symmetric

spirocyclic ligands, as well as major breakthroughs with different applications in the past five years.

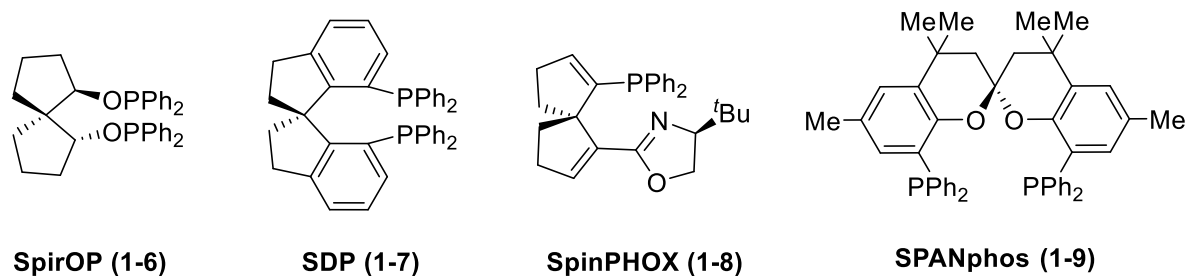
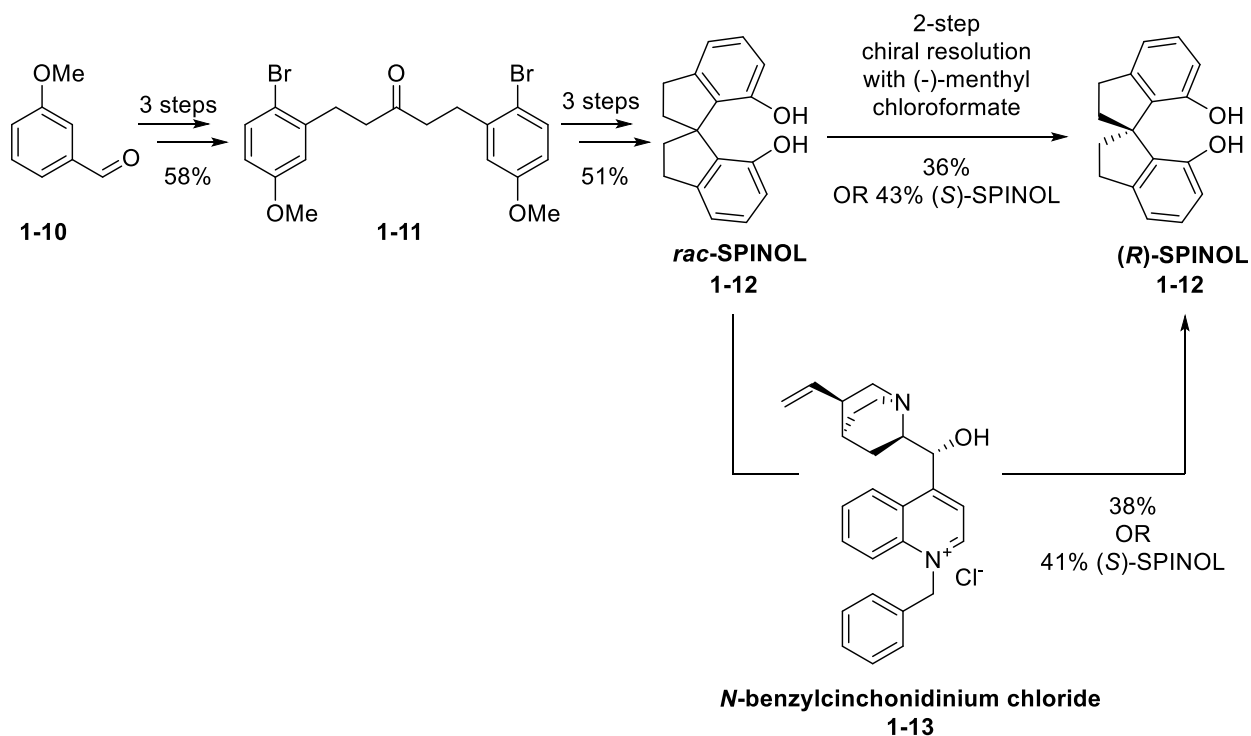


Figure 1.3 Early examples of chiral spirocyclic ligands

1.2. Recent developments with SPINOL and derivatives



Scheme 1.1 Early developments of SPINOL

The original synthesis of SPINOL **1-12** was reported by the Birman group, and they discovered that the ‘spiroanalog’ of BINOL presented a better configurational stability as well as

framework rigidity which are crucial in ligand design.²⁰ However, due to challenges associated with both polyphosphoric acid-catalyzed double cyclization and chiral resolution with *L*-menthyl chloroformate, operational barrier and overall yield following this method to either single enantiomer remained challenging. A following improved method from the Zhou group described the inclusion complexation with *N*-benzylcinchonium chloride **1-13**, which successfully separated racemic mixtures in only 1 step but low yields along with side reactions during the PPA-catalyzed cyclization could not be addressed.²¹ (Scheme 1.1) Up to today, when chemists want to explore more applications for various purposes, they more often would find themselves in a dilemma. They could either suffer during the process to first synthesize racemic SPINOL followed by one of the two above methods for chiral resolution or pay a premium for chiral SPINOLs. This predicament led to a partial solution that some SPINOL-like derivatives would be easier to access and expected to have similar reactivities comparing to the original SPINOL-derived ligands and catalysts.

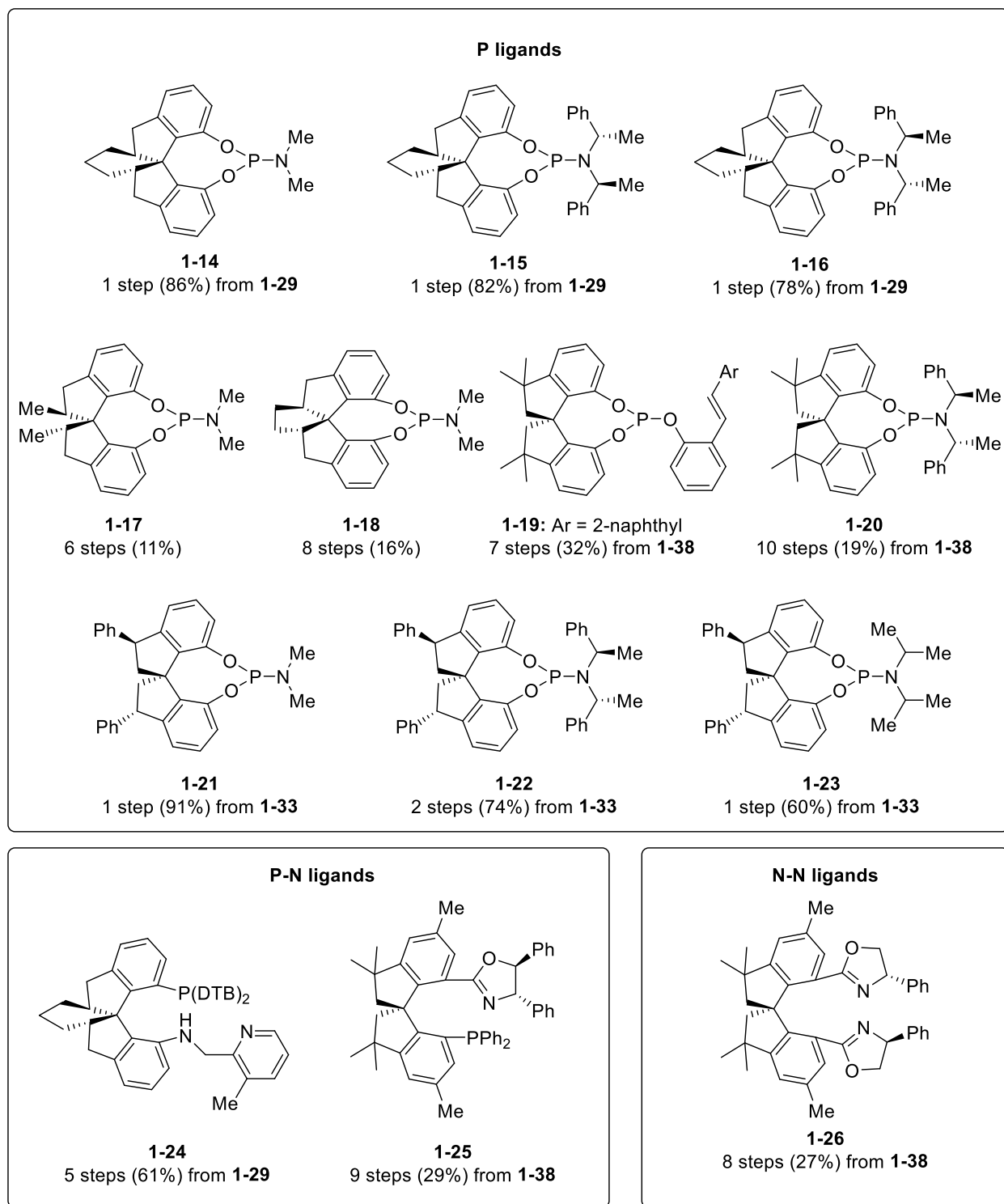
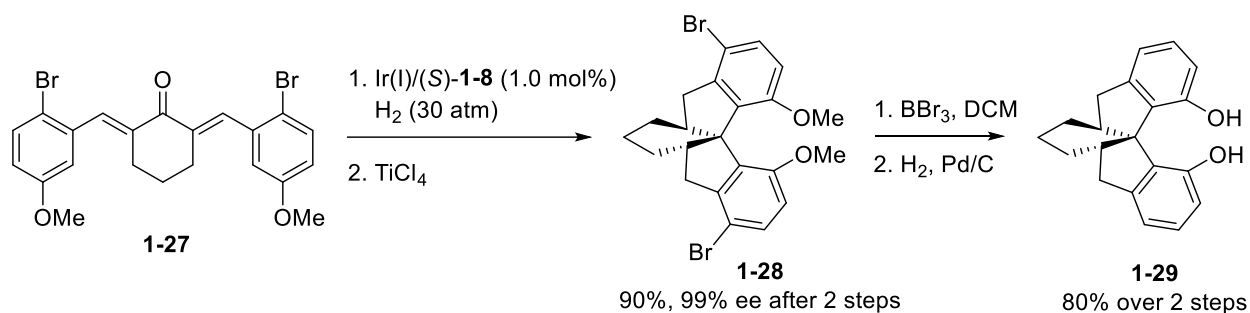
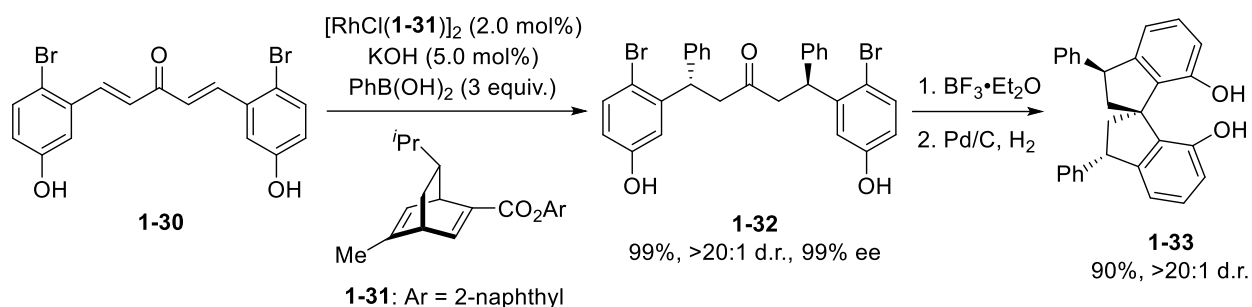


Figure 1.4 Example of chiral ligands with SPINOL-like backbone



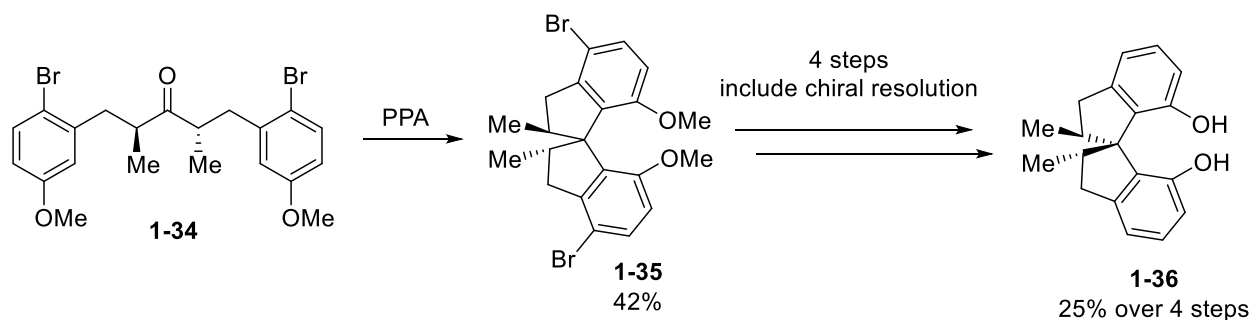
Scheme 1.2 Synthesis of cyclohexyl-fused SPINOL **1-29**

In 2018 a cyclohexyl-fused SPINOL skeleton was developed by Ding and coworkers, and the chiral resolution was successfully avoided in their report.²² (Scheme 1.2) The α,α' -bis(arylidene)-cyclohexanone **1-27** was subjected to the asymmetric reduction under 30 atm of H₂ with 1.0 mol% of commercially available Ir(COD)/(S)-**1-8** complex. The chiral α,α' -bis(benzyl)ketone product was obtained with excellent diastereoselectivities (trans/cis >20:1) and extremely high enantiopurities (>99% ee). A following selective spiroannulation towards cyclohexyl-fused **1-28** was achieved with TiCl₄ that internal steric constraints guided stereoselectivity in this step. The cyclohexyl-fused SPINOL **1-29** was synthesized after deprotection and hydrogenation with 80% yield for 2 steps. Various types of ligands (**1-14** to **1-16** and **1-24**) were successfully synthesized in 1 or 5 steps, and were examined in hydrogenations (Figure 1.5 reaction [1]), hydroacylations (Figure 1.5 reaction [2]), and [2+2] reactions (Figure 1.5 reaction [3]). They found that catalytic efficiencies were equal to privileged SPINOL-derived ligands and their synthesis did not involve a chiral resolution.



Scheme 1.3 Synthesis of SPINOL-like scaffold 1-33

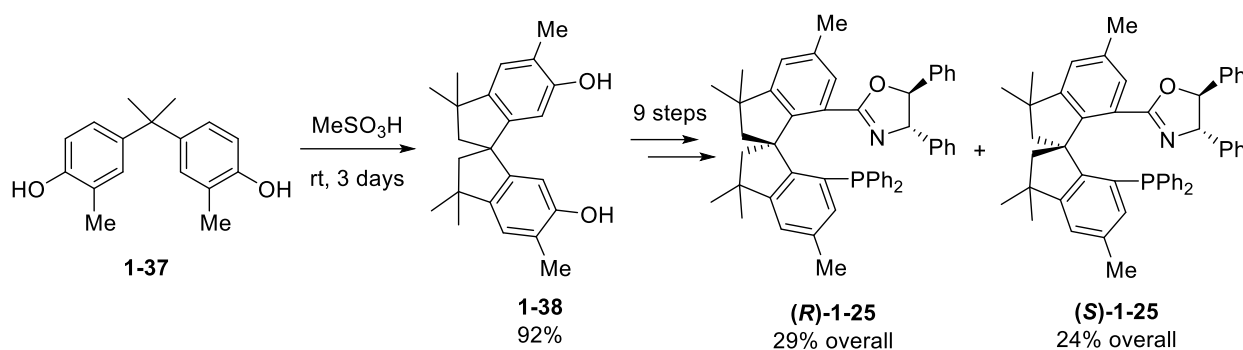
Another recent study with direct asymmetric access of SPINOL-like scaffold via spirocyclization was disclosed by Lu, Hayashi, and Lu *et al.*²³ (Scheme 1.3) Asymmetric additions of $\text{PhB}(\text{OH})_2$ to **1-30** assisted with chiral rhodium(I)-**1-31** complex was accomplished under the nonbasic condition. Two-fold conjugate phenylation product **1-32** was synthesized with excellent yield and selectivities (99%, >20:1 d.r., >99% ee). $\text{BF}_3 \cdot \text{Et}_2\text{O}$ promoted the spirocyclization with the excellent diastereoselectivity, followed by the hydrogenation to obtain **1-33** with 90% yield and >20:1 d.r. Further studies with derived phosphoramidite ligands (**1-21** to **1-23**) showed higher enantioselectivities in different metal-catalyzed hydrogenations (Figure 1.5 reaction [1]), hydroacylations (Figure 1.5 reaction [2]) and conjugate additions (Figure 1.5 reaction [5]) than the non-substituted SPINOL ligands.



Scheme 1.4 Synthesis of 2,2'-dimethyl-SPINOL 1-36

Meanwhile, a different attempt at synthesis was disclosed that SPINOL-like analogues with a 2,2'-dimethyl-, cyclopentyl-, or cyclohexyl-fused rings were accessed.²⁴ (Scheme 1.4) The

main difference between this work and previous work was that the challenging poly-phosphoric acid-promoted spirocyclization towards racemic **1-35** and the following optical resolution by semi-prep HPLC with a chiral column were required to access the diol **1-36**. Although **1-36**-based phosphoramidite ligands **1-17** and **1-18** showed excellent enantioselectivities (96-97% ee) in asymmetric hydrogenation of dehydro amino acid methyl esters (Figure 1.5 reaction [1]) and up to 92% ee in [4+2] cycloaddition of α,β -unsaturated imines with isocyanates (Figure 1.5 reaction [4]), additional substituents on 2,2'-position didn't seem to improve efficiencies in neither ligand synthesis nor catalytic abilities.



Scheme 1.5 Synthesis of 3,3'-hexamethyl-SPINOL-like **1-38**

An interesting approach to access enantiopure SPINOL-like ligands was done through a final-stage flash chromatography of diastereomeric products.²⁵ (Scheme 1.5) Bisphenol **1-37** was transformed to racemic hexamethyl-1,1'-spirobiindane-6,6'-diol **1-38** by methanesulfonic acid-catalyzed dimerization/rearrangement. It is to be noted that the diol **1-38** did not possess hydroxyl groups at 7,7'-positions, so additional steps would be taken to make the product SPINOL-like. Hence, the following 9-step synthesis along with the regular flash chromatography for the final step provided the enantiopure phosphine-oxazoline ligand **1-25**. In the asymmetric arylation of cyclic *N*-sulfonyl imines with arylboronic acids (Figure 1.5 reaction [6]), nickel(I)-**25** complex produced the desired imine up to 99% ee. In addition to the issue in structural

mismatch of **1-29** with SPINOL, later studies revealed that a challenging chiral resolution with *N*-tosyl-L-phenylalanine acid chloride,²⁶ *N*-benzylcinchonium chloride,²⁷ or (-)-menthyl chloroformate²⁸ was still required during the preparation of ligands **1-19**, **1-20**, and **1-26**. Fortunately, monophosphite-olefin **1-19** showed comparable selectivities in the Rh-catalyzed asymmetric arylation (Figure 1.5 **Error! Reference source not found.** reaction [6]), while phosphoramidite **1-20** demonstrated good enantioselectivities in palladium-catalyzed asymmetric hydroamination/arylation of alkenes (Figure 1.5 reaction [7]), and bisoxazoline **1-26** provided chiral α -silyl esters with 95% yield and 91% ee (Figure 1.5 reaction [8]). These reports indicated that efforts to synthesize SPINOL-like ligands were worth when they produced good results in various metal-catalyzed asymmetric transformations, but a tedious or difficult synthesis for core structures could be improved in near future.

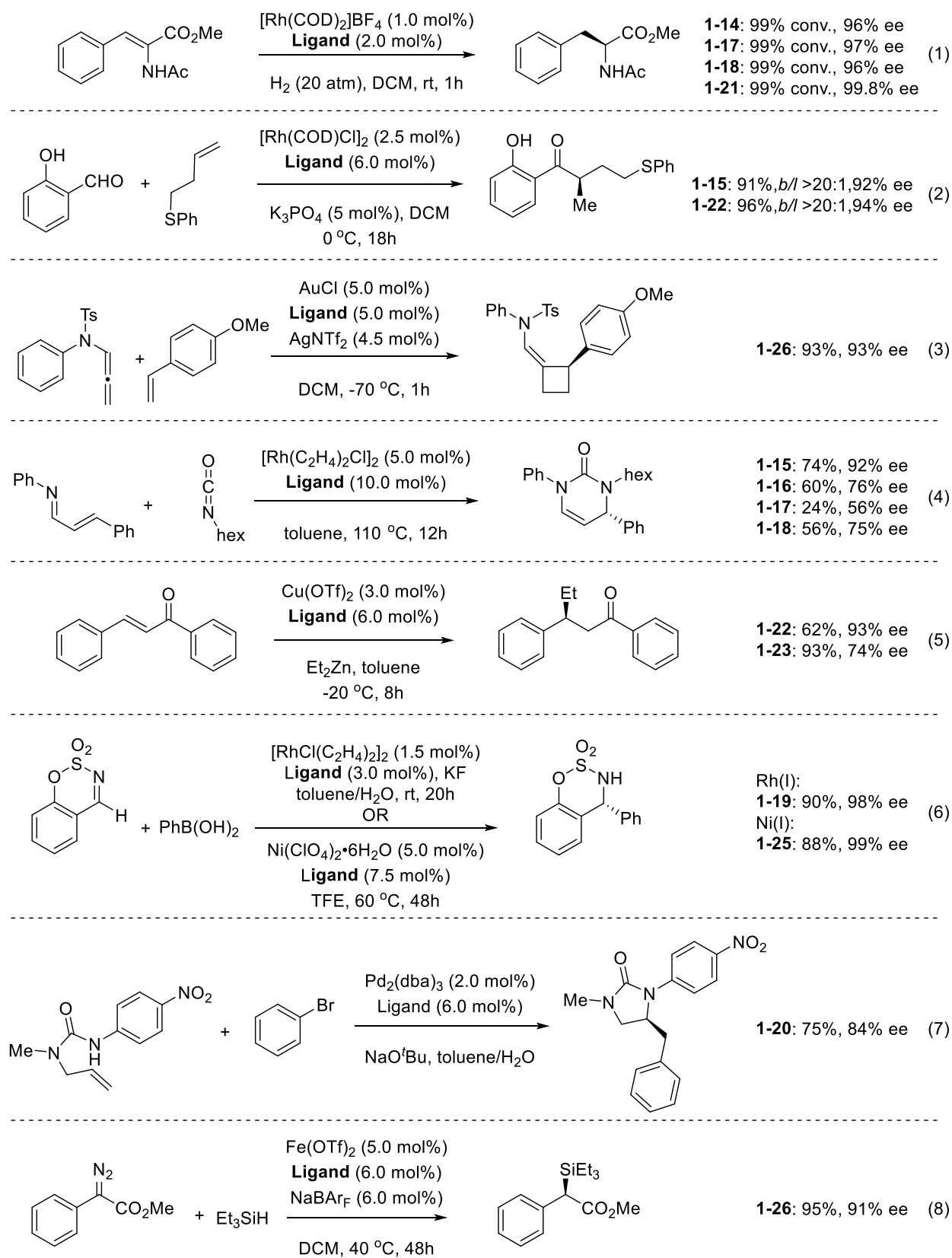
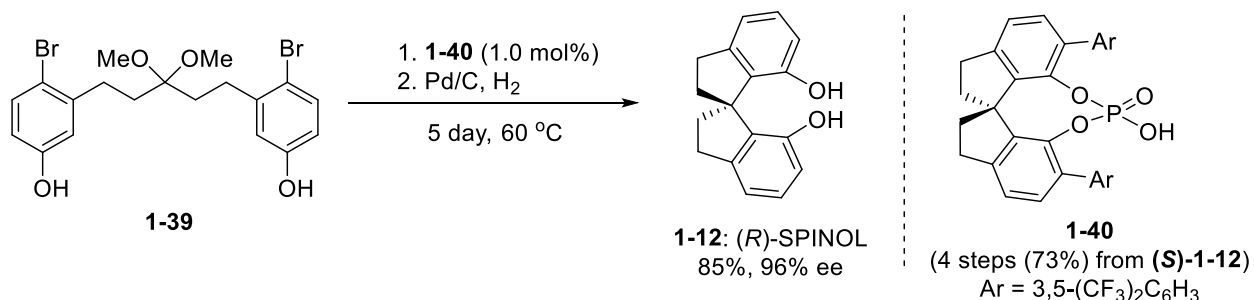


Figure 1.5 Applications of SPINOL-like ligands

Despite recent efforts were mainly on modifications in SPINOL core, scientists never gave up attempts to directly provide enantiopure SPINOL. The breakthrough work from Tan and coworkers finally eliminated the resolution step in the asymmetric synthesis of SPINOL **1-12**.²⁹ (Scheme 1.6) Compound **1-39** was subjected to the chiral phosphoric acid **1-40**-catalyzed enantioselective spirocyclization followed by the debromination, and the (*R*)-SPINOL **1-12** was obtained with 85% yield and 96% ee. Additional recrystallization with **1-12** could provide the desired single enantiomer, and more than 18 SPINOL derivatives were successfully synthesized. Although it is a milestone in asymmetric SPINOL synthesis, obtaining SPINOL-derived phosphoric acid for this reaction would not be economical and further studies with cheaper alternatives would be appreciated.



Scheme 1.6 Phosphoric acid-catalyzed asymmetric synthesis of SPINOL **1-12**

Since both of them are C₂-symmetrical but with different bite angles and dihedral angles, SPINOL-derived ligands have been often compared to BINOLs, and already successfully utilized in many Group 8, 9, 10 and 11 metal-catalyzed asymmetric transformations. In addition, SPINOL-derived chiral phosphoric acids (**SPA**) and phosphoramides (Figure 1.6) have been used to promote hundreds of asymmetric studies with excellent enantioselectivities in just ten years since the discovery.³⁰

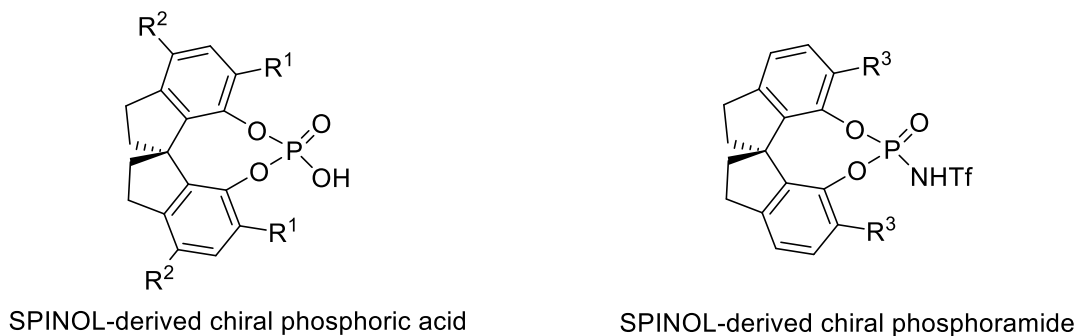


Figure 1.6 Chiral SPINOL-derived chiral organocatalysts

In 2010, the very first application with the new class of chiral phosphoric acids with SPINOL scaffold was achieved in Friedel-Crafts reaction of indoles.³¹ (Figure 1.7 reaction [1]) The new SPINOL-derived CPA **1-41** outperformed BINOL-based CPA with up to 80% yield and 96% ee at -60 °C. In recent years, SPINOL-derived CPAs have also been used to develop stereoselectivities in selected name reactions. Fischer indole synthesis is one of the most convenient methods to construct aromatic heterocycles,³² and in 2011 the first catalytic asymmetric Fischer indolization was achieved with catalyst **1-42**.³³ (Figure 1.7 reaction [2]) High enantioselectivity was achieved via the chiral hydrogen-bond-assisted ion pair, and various 3-substituted tetrahydrocarbazoles were stereoselectively synthesized under the mild condition. Piancatelli rearrangement is well-known for synthesizing highly functionalized cyclopentenone derivatives from 2-furylcarbinols,³⁴ and the Sun group reported the first example of enantioselective aza-Piancatelli rearrangement assisted with SPA.³⁵ (Figure 1.7 reaction [3]) Catalyst **1-43** provided excellent chemo-, enantio-, and diastereoselectivities in their study under mild reaction conditions, and chiral 4-amino-2-cyclopentenone products were readily available for transformations to valuable chiral building blocks. Pyrroles are commonly seen in natural products, and the acid-catalyzed Paal–Knorr reaction is a powerful tool to generate pyrroles, furans, or thiophenes.³⁶ A recent study featuring SPINOL-derived CPA **1-42** reported that high

enantiocontrol could be achieved in the Paal-Knorr reaction.³⁷ (Figure 1.7 reaction [4]) The unconventional, but possible enamine formation for the Paal-Knorr mechanism followed by the Lewis acid-CPA mediated dehydrative cyclization produced axially chiral arylpyrroles with high yields and ee. Latterly, the enantioselective Ugi reaction with an aldehyde or ketone, an amine, a carboxylic acid, and an isocyanide was achieved with SPA **1-44** by the Tan group.³⁸ (Figure 1.7 reaction [5]) It was exciting that peptide-like chiral α -acylaminoamides were quickly synthesized via the one-pot four-component Ugi reaction with wide substrate scope and high enantioselectivities. In 2019, chiral ketones bearing all-carbon quaternary stereocenters were synthesized via enantioselective House-Meinwald rearrangement.³⁹ (Figure 1.7 reaction [6]) With readily accessible racemic tetrasubstituted epoxides, both cyclic and acyclic ketones could be obtained with single regio-isomers. Up to 98% yield and 94% ee were observed in a wide range of substrates with SPA **1-43**, which led to important chiral all-carbon quaternary building blocks for future directions.

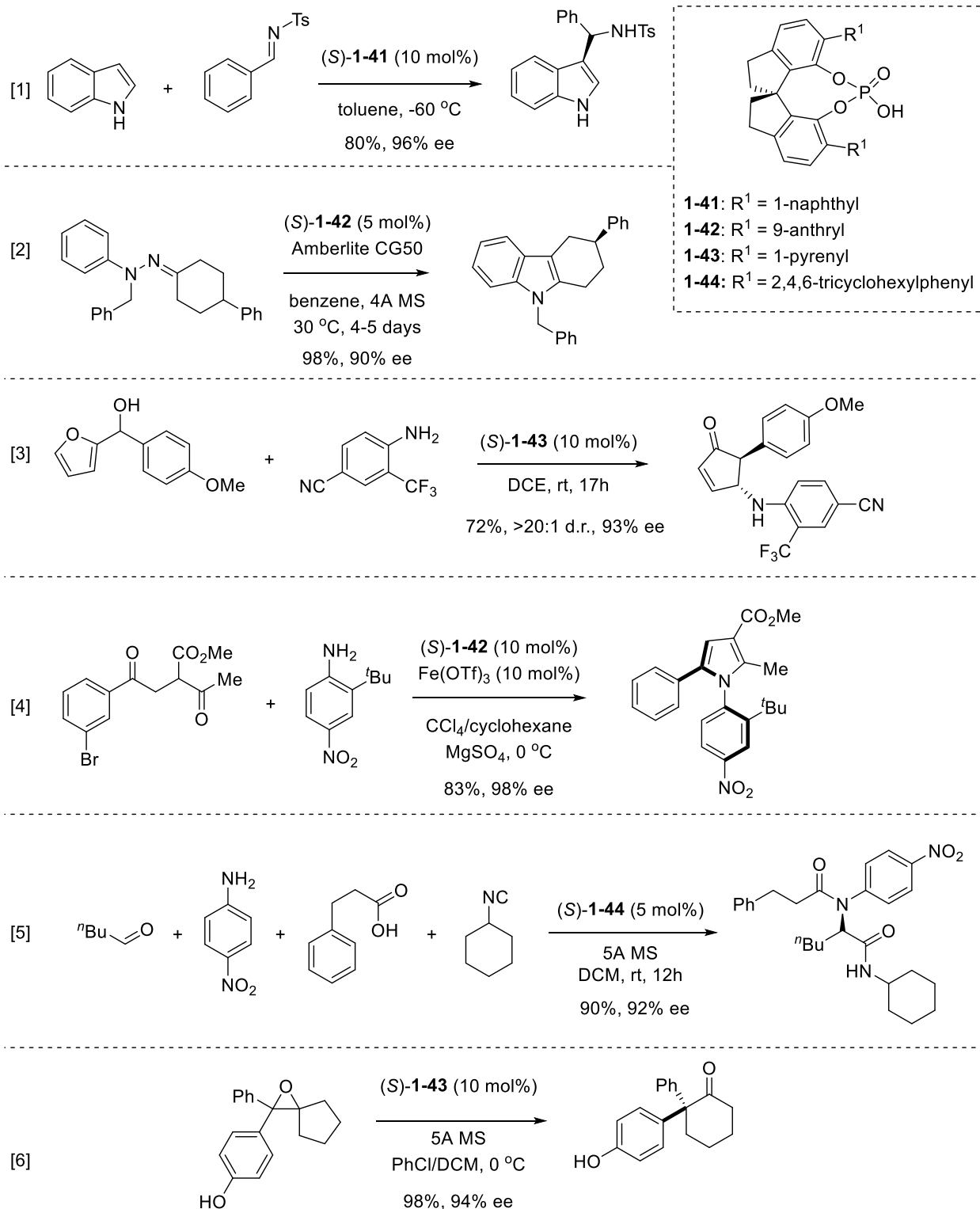
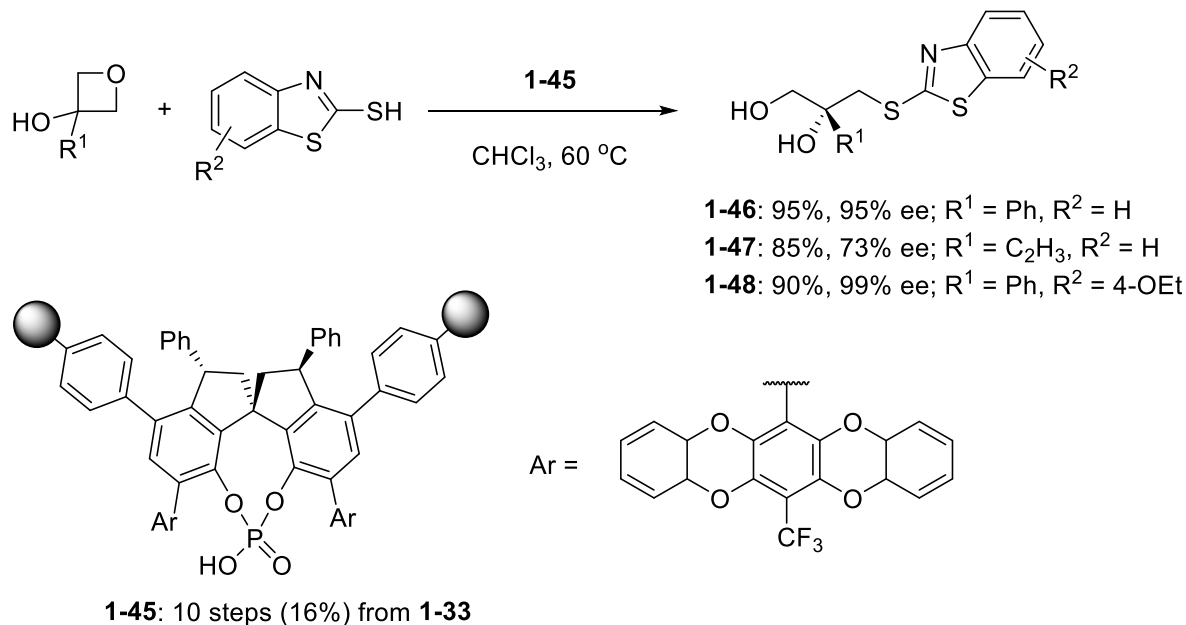


Figure 1.7 Selected applications with SPAs in name reactions

Besides excellent performances in name reactions, SPINOL-based organocatalysts are also versatile in many different kinds of transformations. In 2017, a CPA-catalyzed regiodivergent glycosylation of 6-dEB and Oleandomycin-derived macrolactone was achieved in the Nagorny lab.⁴⁰ It represented the first example of utilizing SPINOL-based CPAs to control regio selectivity in complex polyols. Impressively, CPAs have also been applied in photocatalytic transformations.⁴¹ In 2019, Fu and coworkers found that SPINOL-derived CPAs could smoothly replace expensive iridium and ruthenium-based photoredox catalysts in their study as a more economical and widely available catalyst. The reaction started with complexation between the redox-active ester and sodium iodide-triphenylphosphine complex, followed by the photo-induced fragmentation to generate the reactive alkyl radical. The *N*-heteroarene would then trap the radical to form a new chiral C-C bond with the presence of CPA. The new catalytic system enabled high enantioselectivities in this photo-redox decarboxylative alkylation with a variety of substrates. An interesting finding with SPINOL-derived *N*-triflylphosphoramidate was observed in another axially chiral ligand synthesis,⁴² where unique 1,1'-(ethene-1,1'-diyl)binaphthol (EBINOL) scaffold could be a great complement to existing privileged ligands. Asymmetric hydroarylation of alkynes assisted with SPINOL CPAs granted direct access to axially chiral EBINOL motifs. In fact, EBINOL-derived ligands proved their capabilities in difficult asymmetric applications and fully realized the value of precious SPINOL CPAs during the catalyst preparation.

Although significant attentions have been directed to solid-phase catalysts, such as BINOL-based immobilized CPAs,⁴³⁻⁴⁹ over the years, there is only one report regarding polymer-supported immobilized SPINOL-derived CPAs so far. In 2020, a family of immobilized SPINOL-derived CPAs were developed by Pericàs and coworkers for catalytic continuous flow

of desymmetrization with 3,3-disubstituted oxetanes.⁵⁰ (Scheme 1.7) It was surprising to see that a SPINOL-derived scaffold based on a previous report²³ was utilized in their study instead of using the original SPINOL. Nevertheless, the results showed that catalyst **1-45** not only had unlimited recyclability in both batch and flow, but also provided a diverse substrate scope with good yields and excellent enantioselectivities.

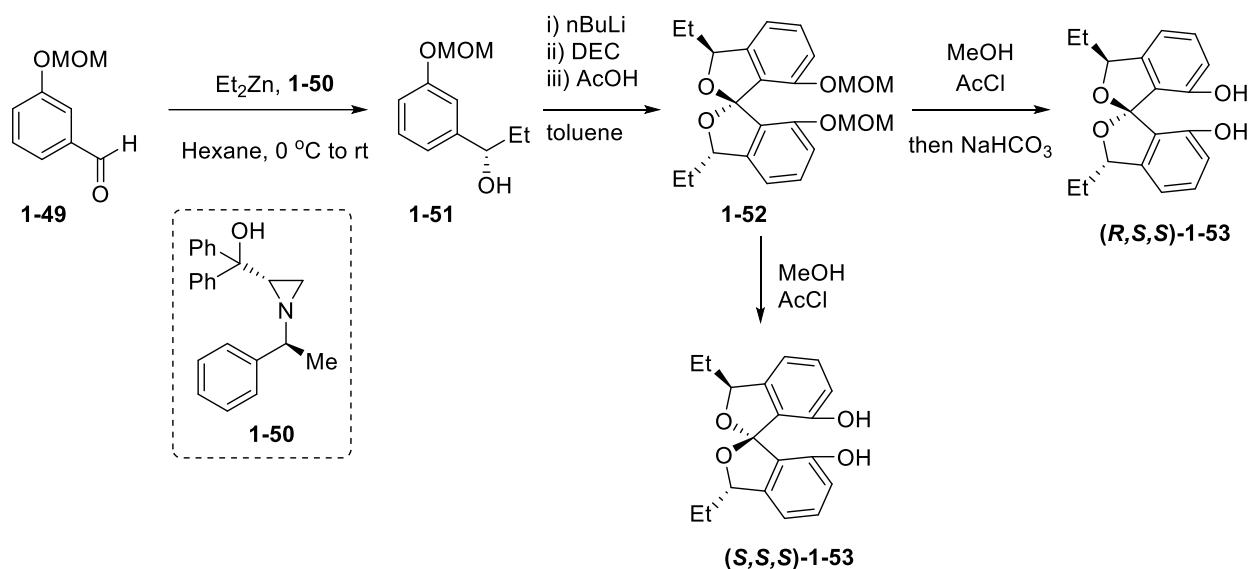


Scheme 1.7 Applications of immobilized SPA in desymmetrization of disubstituted oxetanes

1.3. Recent discovery and applications of SPIROL

Spirocyclic scaffolds have been proven unique and versatile in transition metal-catalyzed reactions, while most previous ligand synthesis shared a similar problem, stereocontrol during the spirocyclization. In 2018 an innovative synthesis towards a new class of spiroketal-based C₂-symmetric spirocyclic ligand, SPIROL, was developed by the Nagorny group.⁵¹ (Scheme 1.8) Starting with economical compound **1-49**, the asymmetric alkylation with diethylzinc and easily accessible aziridine catalyst **1-50** afforded product **1-51** with excellent yield (99%) and enantioselectivity (99%). The innovative asymmetric approach enabled the spirocyclization with

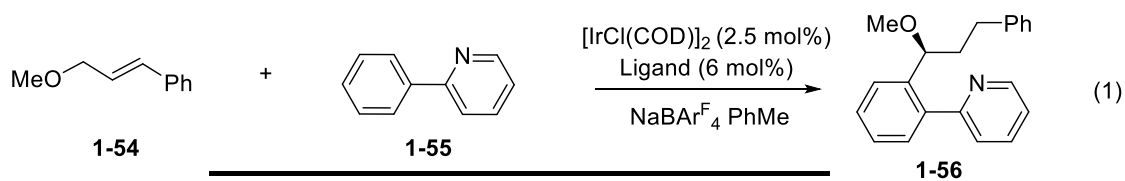
1-51 to produce MOM-protected spiroketal **1-52** with a perfect stereoselectivity (>128:1). Upon different deprotection conditions, two pseudoenantiomeric SPIROLs **1-53** were selectively synthesized, which could not be achieved in other spiroketal-containing skeletons synthesis. More details regarding design, synthesis and applications are disclosed in Chapter 2.



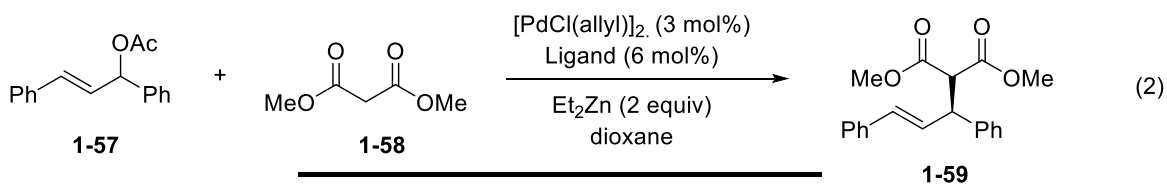
Scheme 1.8 Design and synthesis of SPIROL 1-53

Various SPIROL-based ligands were synthesized and compared in different transitional-metal-catalyzed reactions with BINOL-, SegPHOS- and SPINOL-derived ligands. In the iridium-catalyzed hydroarylation, (S,S,S) -SPIRAP provided better enantioselectivity in formation of **1-56** with 95% ee under milder conditions. Similarly, (S,S,S) -SPIRAP was also an exceptional ligand in the palladium-catalyzed allylic alkylation of chalcone derivative **1-57** that 94% yield and 97% ee were easily achieved. (Table 1.1)

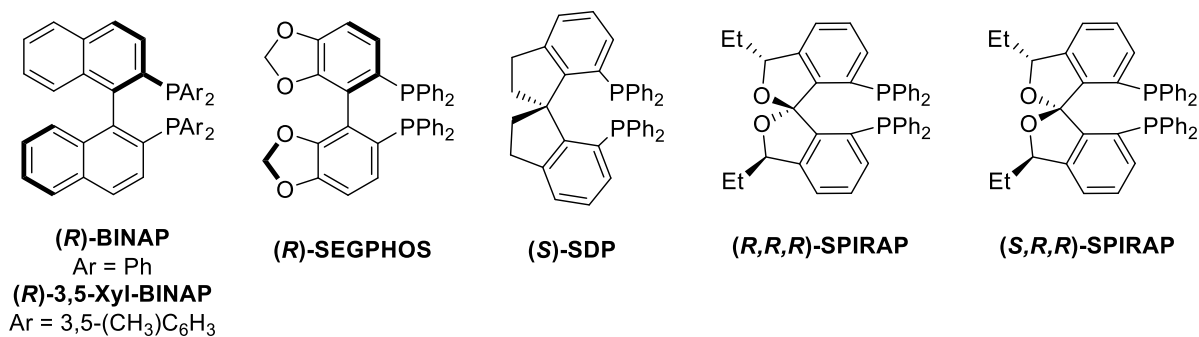
Table 1.1 1) Asymmetric iridium-catalyzed hydroarylation and 2) asymmetric palladium-catalyzed allylic alkylation



ligand	T [°C]	Yield [%]	ee [%]
(<i>R</i>)-BINAP	80	84	88
(<i>R</i>)-SEGPHOS	80	7	81
(<i>R</i>)-3,5-Xyl-BINAP	80	87	94
(<i>R</i>)-SDP	70	82	95
(<i>S,S,S</i>)-SPIRAP	70	96	95
(<i>R,S,S</i>)-SPIRAP	70	N.R.	–

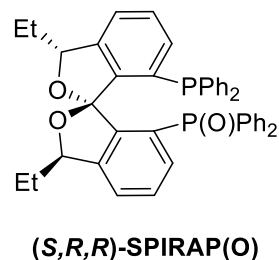
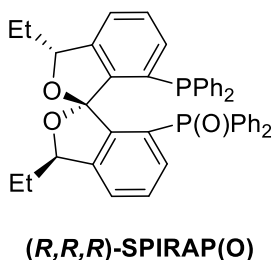
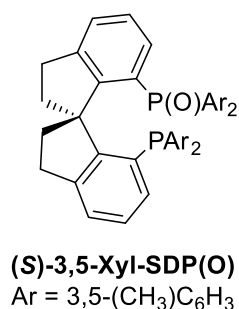
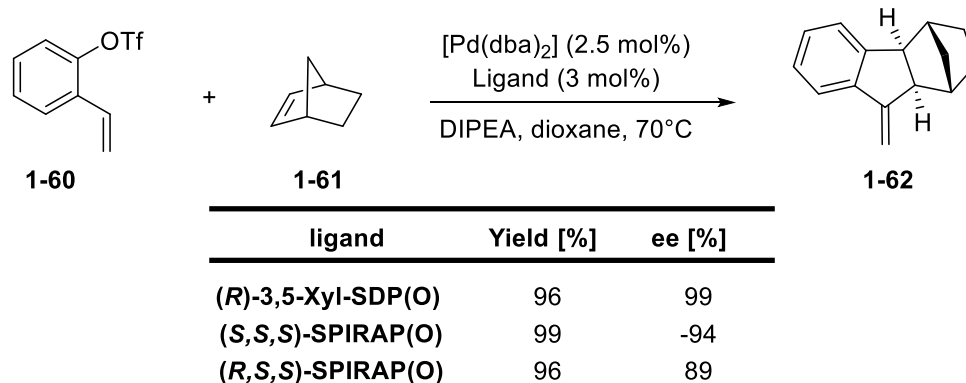


ligand	Yield [%]	ee [%]
(<i>S</i>)-SDP	97	97
(<i>S,S,S</i>)-SPIRAP	94	97
(<i>R,S,S</i>)-SPIRAP	98	-83

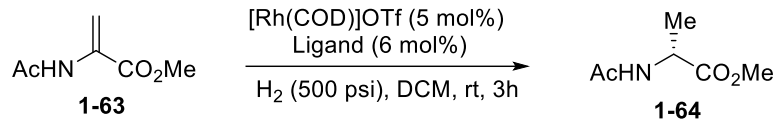


Excellent performance of (*S,S,S*)-SPIRAP(O) was observed in the palladium-catalyzed Heck reaction that 2-vinylphenyl triflate **1-60** reacted with norbornene **1-61** to produce **1-62** with 99% yield and 94% ee. (Table 1.2)

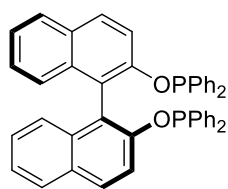
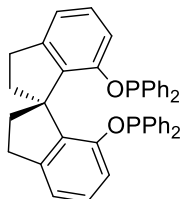
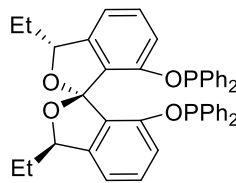
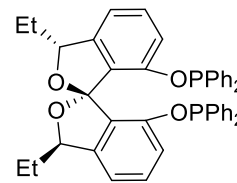
Table 1.2 Palladium-catalyzed asymmetric Heck reaction



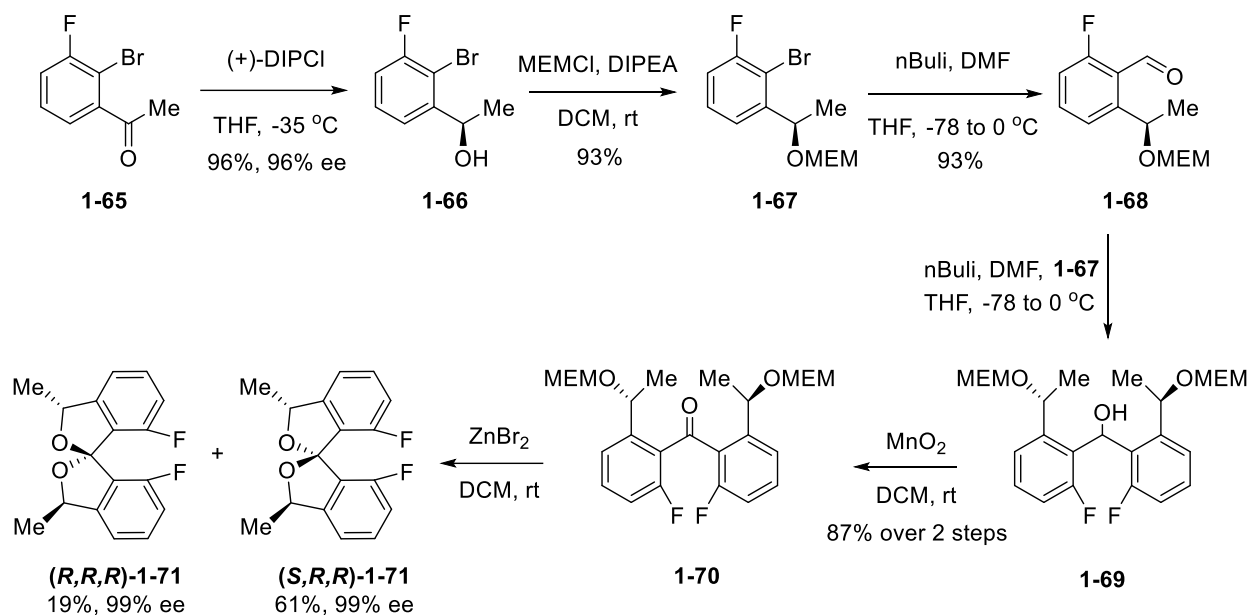
In the rhodium-catalyzed asymmetric hydrogenations of dehydroalanine **1-63**, *(S,R,R)*-SPIRAP(O) catalyzed the reaction with excellent results (85% yield and 93% ee). Pseudoenantiomer of *(S,R,R)*-SPIRAP(O) was evaluated in hydrogenation of aromatic heterocycles in a following report, which discussed interesting properties and findings about the structural differences between SPIROL and non-SPINOL-like ligands.⁵² (Table 1.3)

Table 1.3 Rhodium-catalyzed asymmetric hydrogenations

ligand	Yield [%]	ee [%]
(S)-BINAPO	84	89
(S)-SDPO	85	-93
(S,R,R)-SPIRAPO	87	-90
(R,R,R)-SPIRAPO	85	93

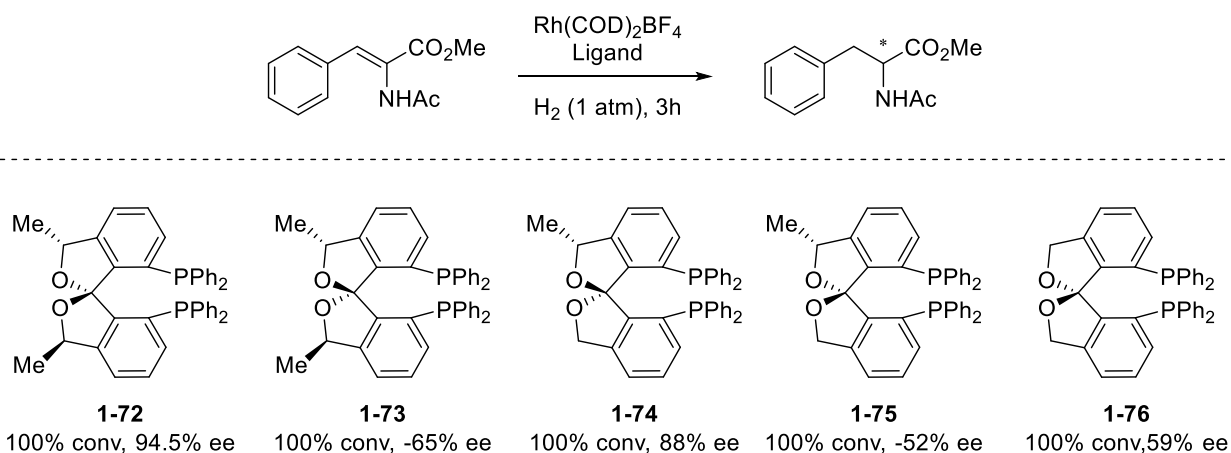
**(S)-BINAPO****(S)-SDPO****(S,R,R)-SPIRAPO****(R,R,R)-SPIRAPO**

Following our studies, several other SPIROL derivatives were disclosed by Sun and co-workers using the approach based on the intramolecular double cyclization method.⁵³ (Scheme 1.9) The synthesis commenced from an asymmetric reduction of 1-(2-bromo-3-fluorophenyl)ethanone **1-65** with (+)-DIPCl affording the chiral alcohol **1-66** with 96% yield and 96% ee. Sequential MEM protection, formylation, dimerization and oxidation provided the key intermediate **1-70** after 4 steps with 75% overall yield. Zinc bromide catalyzed the deprotection and spiroketal formation in one pot to produce both diastereomeric spiroketals **(R,R,R)-** and **(S,R,R)-1-71**. Also, due to additional chiral centers in the spiroketal skeleton, two diastereomers could be separated by column chromatography on normal silica gel with 61% and 19% yield, respectively. Additional modified structures bearing different substituents with 1,1'-spirobi(3*H*,3'*H*)isobenzofuran backbone were also synthesized, and reaction with KPPH₂ produced the final diphosphine ligands **1-72** to **1-76**.



Scheme 1.9 Synthesis of SPIROL derivatives

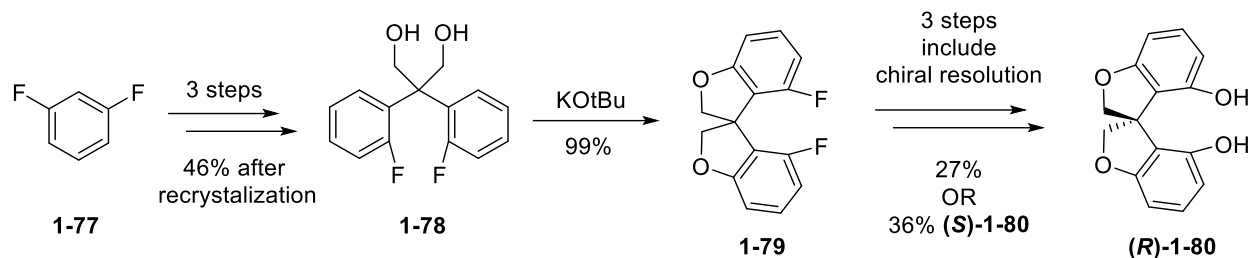
All ligands were evaluated in the asymmetric hydrogenation of α -dehydroamino acid esters with 1 atm of H_2 in DCM, and results showed excellent yields and enantioselectivities (up to 94.5% ee) with ligand **1-72** while SDP ligand gave only 10% ee under the same condition. Later optimization of the reaction condition to DCE improved the purity of product up to 98% ee. (Scheme 1.10)



Scheme 1.10 Asymmetric hydrogenation of α -dehydroamino acid esters

1.4. Recent discovery and applications of O-SPINOL

In addition to efforts devoted to SPIROL derivatives, a structurally unique oxaspirocyclic diphenol ligand (O-SPINOL) was recently developed by Zhang and coworkers, and used in the Ir-catalyzed asymmetric hydrogenation of lactones.⁵⁴ Due to the shorter nature of C–O bond, especially for the C(sp²)–O bond, replacing one carbon atom in SPINOL with an oxygen atom would lead to a ligand with different properties from SPINOL or SKP. The concise synthesis of the ligand started from **1-77** to establish the all-carbon quaternary center in **1-78** after 3 steps. A key double intramolecular S_NAr reaction to construct the spirocycle **1-79** with 45% overall yield, and the production scale could be done on >100 g. (Scheme 1.11) However, O-SPINOL was initially presented as the racemic mixture, and enantiomers of **1-80** had to be resolved with L-proline by control of the solvent accordingly.



Scheme 1.11 Development and synthesis of O-SPINOL 1-80

The derived tridentate ligand O-SpiroPAP **1-81** was synthesized and applied in the direct asymmetric reduction of Bringmann's lactones where excellent yields and enantioselectivities (up to 99% yield and >99% ee) were achieved.⁵⁵ With a slightly larger bite angle compared with that of SPINAP, O-SPINOL based diphosphine ligand (O-SDP) **1-83** was designed and synthesized.⁵⁶ It was applied in the enantioselective hydrogenation of tetra- and tri-substituted α,β -unsaturated carboxylic acids where high yields and enantioselectivities were achieved for a wide range of substrates (up to 99% yield and >99% ee) with high TON number. O-SPINOL-based phosphine–oxazoline ligands (O-SIPHOX) **1-82** was developed and they were used for the asymmetric synthesis of lorcaserins via iridium-catalyzed asymmetric hydrogenation.⁵⁷ (Figure 1.8)

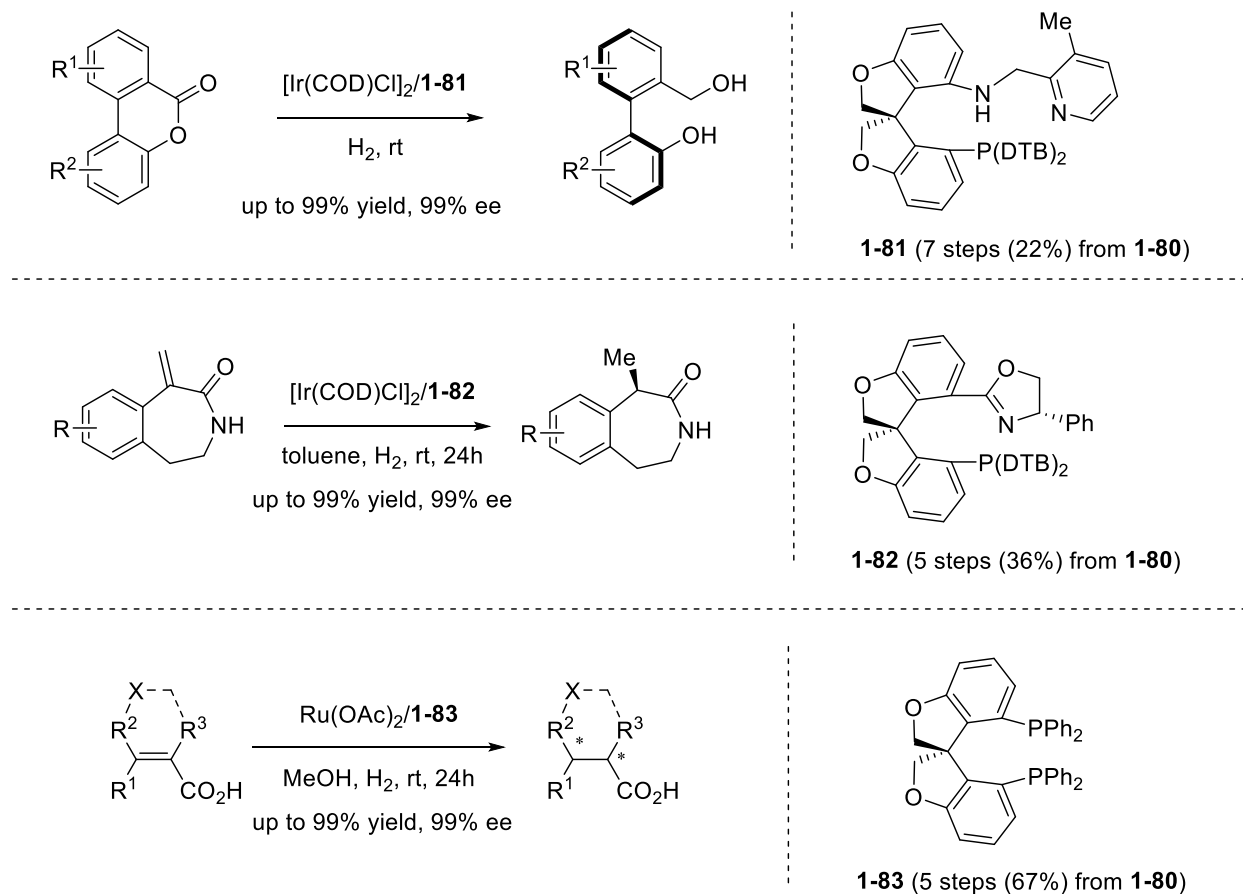
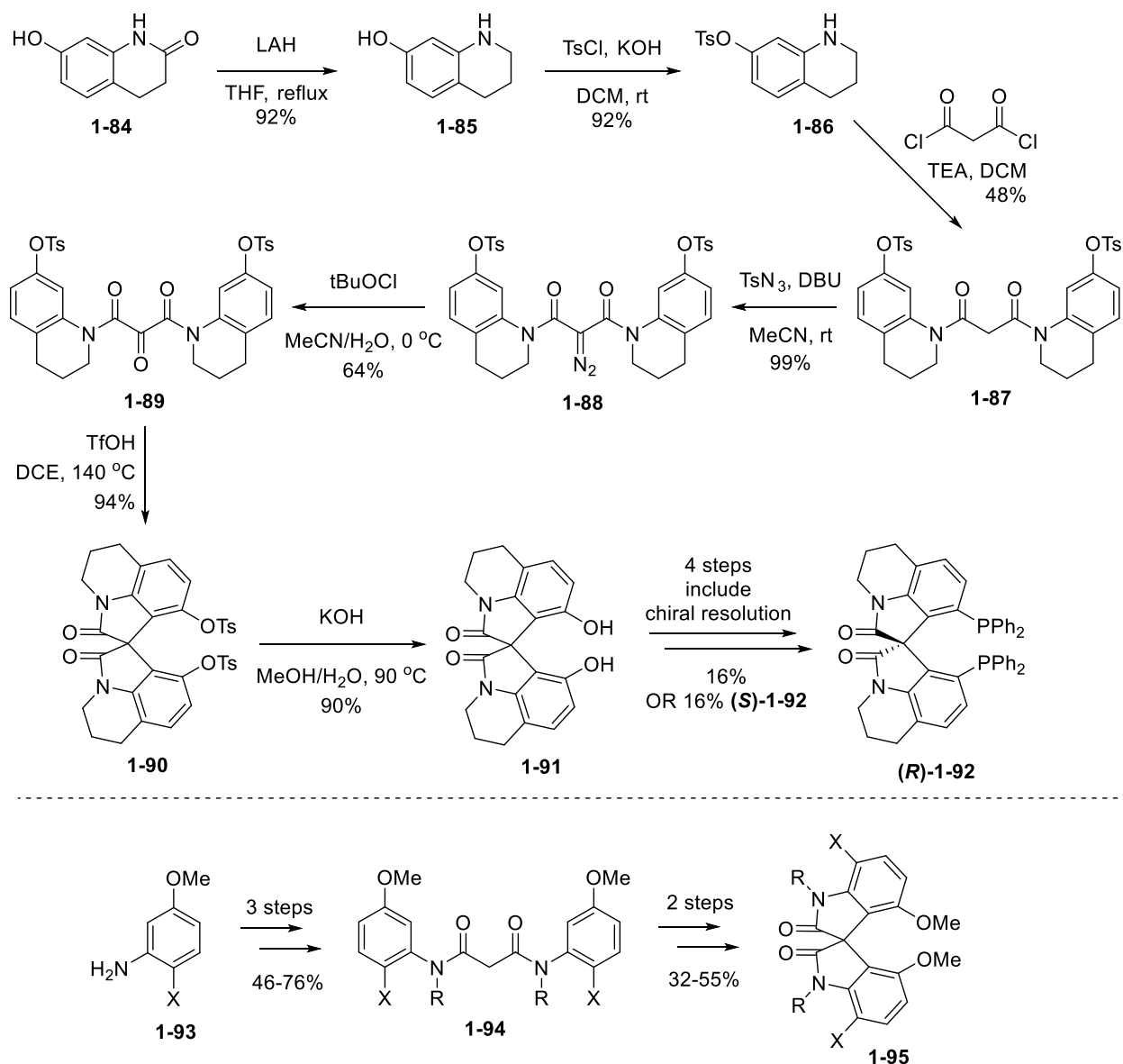


Figure 1.8 Applications of O-SPINOL-derived ligands

1.5. Recent discovery and applications of aza-SPINOL

Despite early efforts toward spirocyclic bisoxindoles,^{58–60} scientists might have overlooked the potential of constructing the ligand out of such backbone until recently. Following previously disclosed acid-promoted spirocyclization protocol, two elegant protocols of synthesizing C2-symmetric chiral aza-SPINOLs were recently reported.^{61,62} (Scheme 1.12) Wang and coworkers started their synthesis from commercially available 7-hydroxy-3,4-dihydroquinolin-2(1*H*)-one **1-84** and quickly access the diazo compound **1-88** in 4 steps bearing 41% yield. Oxidation of **1-88** with *t*-BuOCl afforded the key 2-oxomalonamide **1-89** with 64% yield. Treatment with TfOH afforded the spirocyclic **1-90**, followed by deprotection with KOH

to make final racemic diol **1-1**. Diphosphine ligand **1-92** was produced in just two steps from enantiopure diol. On the other hand, Zhang *et al* utilized different anilines **1-93** as the starting material and accessed the key intermediate **1-94** in 3 steps. Following oxidation with CrO₃ and Eaton's reagent-catalyzed double intramolecular Friedel–Crafts reaction, the aza-SPINOL core **1-95** was constructed with 60 to 82% yield. However, in both studies only the racemic diol had been produced and they were needed to be resolved with L-menthyl chloroformates before accessing enantiopure ligands. The derived diphosphine ligand **1-92** was tested in the desymmetrization of bisallylic amide, in which 55% yield and 72% ee were reported.



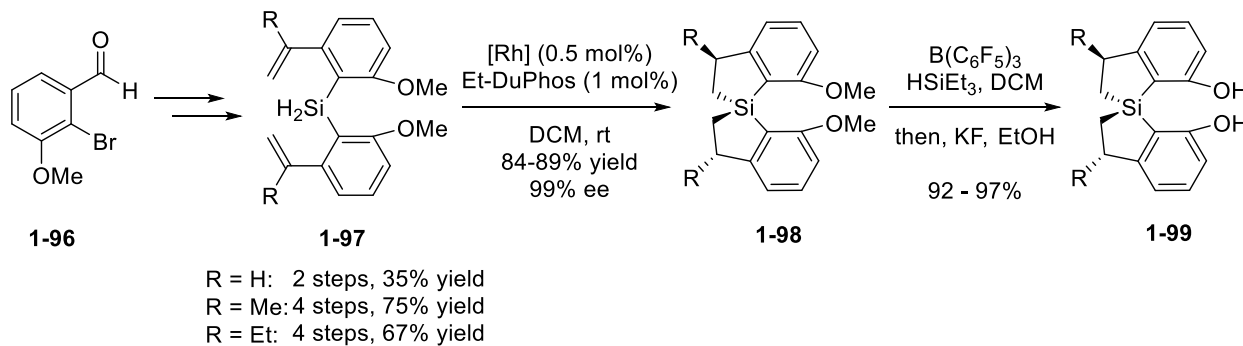
Scheme 1.12 Synthetic routes of aza-SPINOLs

1.6. Recent discovery and applications of SPSiOL

All aforementioned spirocyclic ligands have shown excellent enantioselectivities and great efficiencies in a broad spectrum of asymmetric transformations. However, since they are all designed based on carbon-centered spirocyclic scaffolds, many of these ligand syntheses still suffered from requirements of hard-to-obtain chiral intermediates for Friedel-Crafts reaction or

challenging chiral resolutions. In 2020 an innovative Si-centered chiral spiro-silabiindane ligand (SPSiOL) **1-99** was reported by Wang and coworkers.⁶³ Due to the longer C-Si bond⁶⁴ (ca 1.87 Å vs. ca. 1.53 Å of C-C) and bigger atomic radius of Si (111 pm vs. 67 pm of C), the silicon-centered spirocyclic scaffold had a constrained structure with a bigger bite angle comparing to SPINOL.

Key intermediate bis(alkenyl)dihydrosilanes **1-97** were readily prepared from 2-bromobenzaldehyde derivatives **1-96** in 4 or less steps bearing up to 75% overall yield. Chiral induction and diastereoselectivity were achieved in the following Rh-catalyzed double hydrosilylation of **1-97** with (*R,R*)-Et-DuPhos to obtain **1-98** with up to 89% yield and 99% ee. Lewis-acid catalyzed demethylation of **1-98** towards corresponding SPSiOLs **1-99** was mild enough to avoid any decomposition, and different ligands derived from SPSiOLs **1-99** could be produced easily on the gram scale. (Scheme 1.13)



Scheme 1.13 Synthesis of SPSiOL 1-99

Two SPSiOL-based monodentate phosphoramidites (SPSiPhos) were readily synthesized in 1 step from SPSiOLs and evaluated in the following studies. (Figure 1.9) In the Rh-catalyzed asymmetric hydrogenation of methyl 2-acetamidocinnamate, comparable excellent yields and enantioselectivities were observed (up to 99% yield and 99.8% ee) with ligand **1-100**. SPSiPhos **1-101** also demonstrated good enantioselectivities in the Pd-catalyzed intramolecular

carboamination. While high temperature was required for the SPINOL-based phosphoramidite complex, SPSiPhos **1-101** catalyzed the reaction under much milder reaction condition at only room temperature, and comparable yields and stereocontrol (80% and 85% ee) were observed. Further exploration of other SPSiOL-based ligands including the diastereomer of **1-99** are still undergoing.

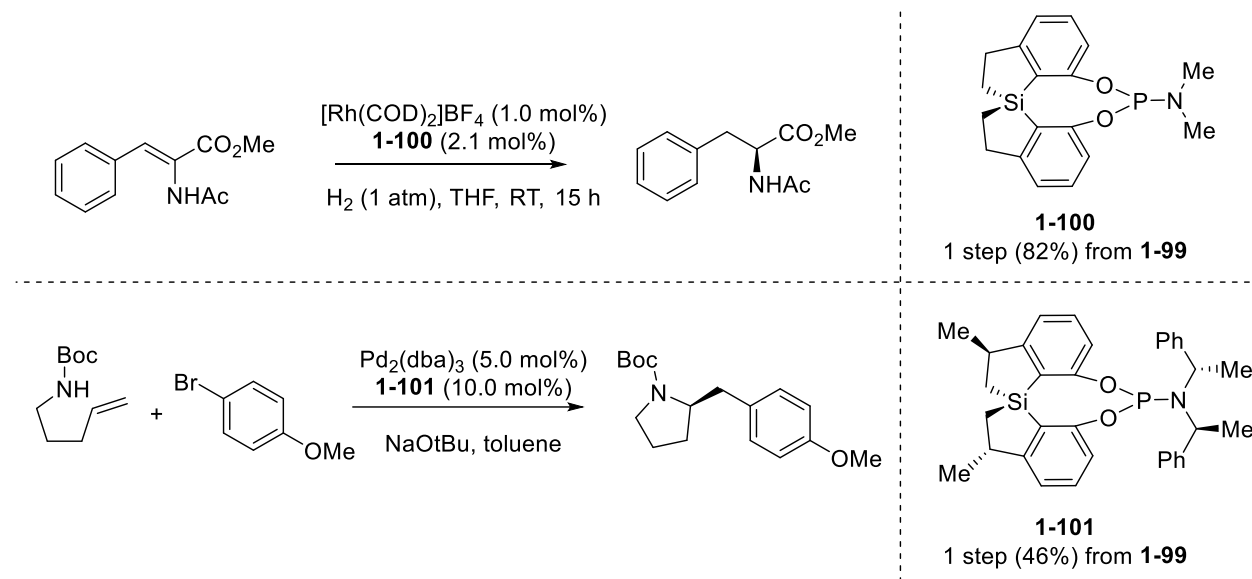


Figure 1.9 Applications with SPSiPhos ligands

1.7. Other asymmetric spirocyclic ligands

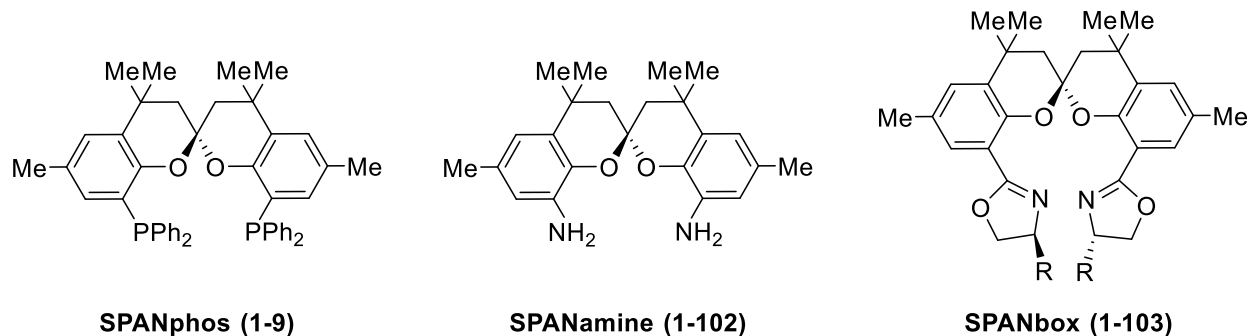


Figure 1.10 Examples of SPAN-derived ligands

SPINOL-based ligands have shown robust capabilities in asymmetric catalysis, but access to its original chiral spiro backbones remains a challenge for most research groups.

Considering installing spiroketal into the all-carbon spirocyclic backbone could provide a more convenient pathway, the new oxygen-containing spirocyclic skeleton was then designed and developed. Hence, ligands, such as SPANphos,¹⁹ SPANamine,⁶⁵ and, SPANbox⁶⁶, with the all-new spiroketal core (Figure 1.10) were synthesized and applied in different transformations, and more importantly structurally similar SKP⁶⁷ ligand quickly stood out in asymmetric catalysis due to its outstanding performances in various applications. Noteworthy, the high diastereo- and enantiocontrol to access key intermediate **1-105** were realized during the double asymmetric hydrogenation with (*S,S*)-Bn-SpinPHOX/Ir complex,⁶⁸ and subsequent functionalizations afforded SKP ligand **1-106**. A modified SKP ligand bearing 4-phenyl-substituted skeleton was reported by the Dou group based on their previous success in SPINOL modification.⁶⁹ There have been a good number of applications associated with SKP **1-106** in transition-metal catalyzed asymmetric transformations.^{70,71} With continual advances in SKP family, a new Pd-catalyzed regio- and enantioselective aminoarylation towards *N*-allyl 2-pyridones was recently achieved with good regioselectivities and excellent enantioselectivities (up to 86% yield, 96% ee, and b:l = 90:10).⁷² The three-component aminoarylation with allenols, aryl iodides and 2-pyridones spontaneously form a new carbon-carbon and a carbon-nitrogen bond in one pot. (Figure 1.11)

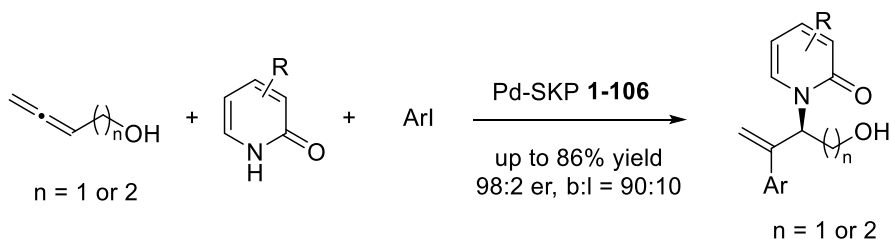
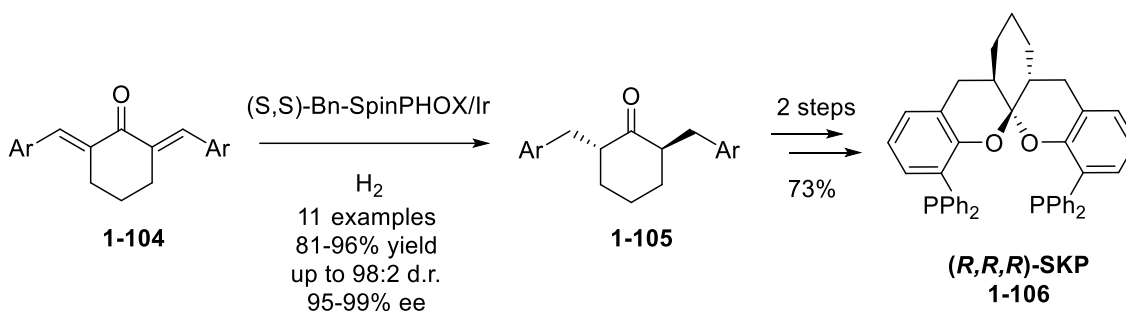


Figure 1.11 SKP 1-106 synthesis and the most recent application

In recent years, some chemists dedicated to exploring different approaches in the interest of constructing spirocyclic ligands. Early in 2004, a novel bidentate spiro phosphine–oxazoline ligand was developed and successfully applied in Pd-catalyzed asymmetric allylic alkylation.⁷³ Inspired from that work, a modified highly rigid spiro phosphine–oxazoline ligand was recently reported.⁷⁴ Starting with commercially available 7-bromo-1-indanone **1-107** and (*R*)-phenylglycinol, chiral trimethylsilylated aminonitrile **1-108** was obtained with quantitative yield. The key spiro oxazoline intermediates **1-109** could be accessed after 6 steps. Upon treatment with *n*-BuLi, compound **1-109** went through the lithium-halogen exchange following a nucleophilic attack with PPh₂Cl to afford ligands **1-110** and **1-111**. In the palladium-catalyzed asymmetric allylic alkylation with activated methylene carbonyl compounds or indoles, high yields (up to 99%) and enantioselectivities (up to 99.9% ee) were obtained with **1-110**. Following studies have also shown wide substrate scopes and excellent enantioselectivities in

palladium-catalyzed asymmetric arylation⁷⁵ and allylic etherification⁷⁶ with ligand **1-111**. (Figure 1.12)

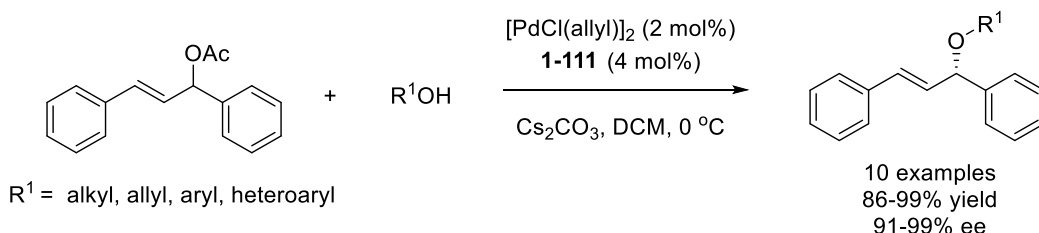
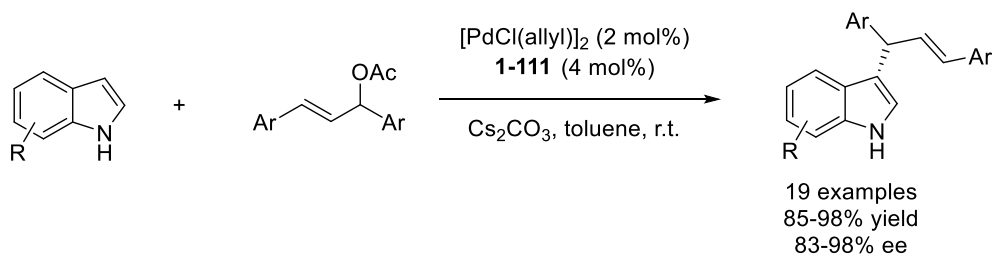
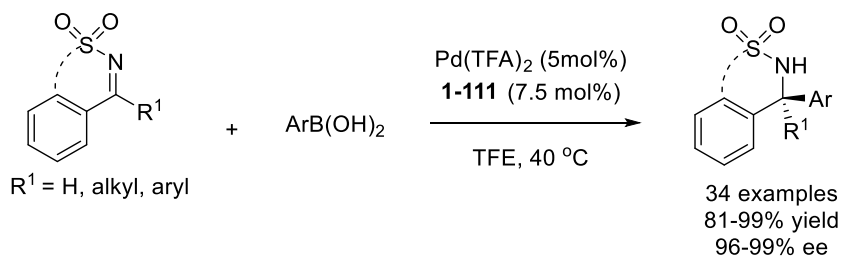
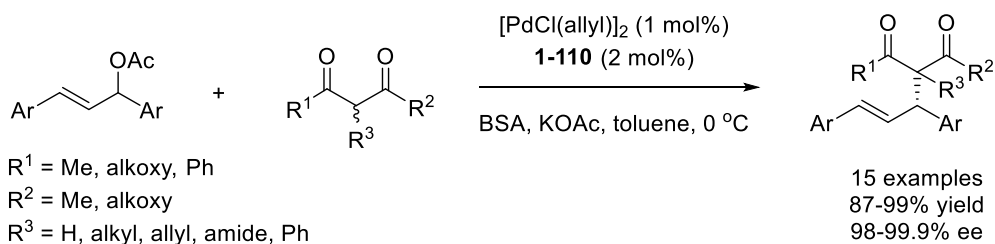
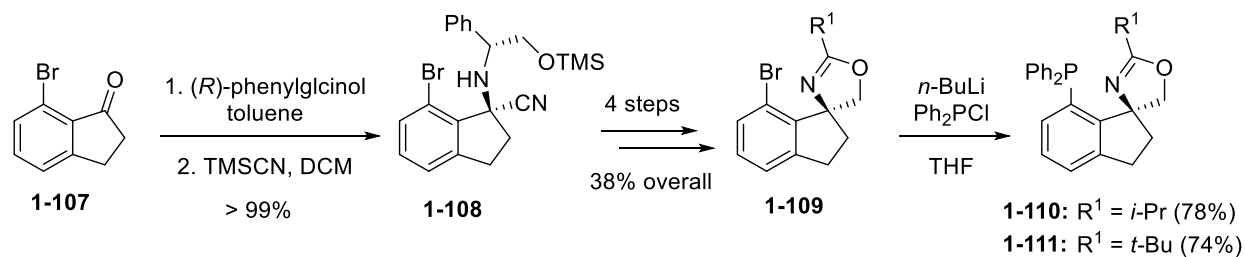


Figure 1.12 Synthesis and applications of spirocyclic ligands **1-110** and **1-111**

1.8. Concluding remarks

In the past two decades, the chemistry community has witnessed the rapid growth of spirocyclic ligands led by SPINOL. Structural advantages in SPINOL such as rigid backbone and optimal bite angle yielded promising and innovative results, which introduced SPINOL into hall of privileged ligands. Although current technologies still limit handy production of enantiopure SPINOLs, many research groups have alternatively developed their own spirocyclic ligands with extraordinary performances. It would not be surprised to see even more discussions with spirocyclic scaffolds under continual efforts.

1.9. References

- (1) Development of New Stereoisomeric Drugs <https://www.fda.gov/regulatory-information/search-fda-guidance-documents/development-new-stereoisomeric-drugs>.
- (2) Trost, B. M. Asymmetric Catalysis: An Enabling Science. *Proc. Natl. Acad. Sci.* **2004**, *101* (15), 5348–5355. <https://doi.org/10.1073/pnas.0306715101>.
- (3) Knowles, W. S.; Sabacky, M. J. Catalytic Asymmetric Hydrogenation Employing a Soluble, Optically Active, Rhodium Complex. *Chem. Commun. Lond.* **1968**, No. 22, 1445. <https://doi.org/10.1039/c19680001445>.
- (4) Dang, T. P.; Kagan, H. B. The Asymmetric Synthesis of Hydratropic Acid and Amino-Acids by Homogeneous Catalytic Hydrogenation. *J. Chem. Soc. Chem. Commun.* **1971**, No. 10, 481–481. <https://doi.org/10.1039/C29710000481>.
- (5) Kagan, H. B.; Dang, T.-P. Asymmetric Catalytic Reduction with Transition Metal Complexes. I. Catalytic System of Rhodium(I) with (-)-2,3-0-Isopropylidene-2,3-Dihydroxy-1,4-Bis(Diphenylphosphino)Butane, a New Chiral Diphosphine. *J. Am. Chem. Soc.* **1972**, *94* (18), 6429–6433. <https://doi.org/10.1021/ja00773a028>.
- (6) Pfaltz, A.; Drury, W. J. Design of Chiral Ligands for Asymmetric Catalysis: From C₂-Symmetric P,P- and N,N-Ligands to Sterically and Electronically Nonsymmetrical P,N-Ligands. *Proc. Natl. Acad. Sci.* **2004**, *101* (16), 5723–5726. <https://doi.org/10.1073/pnas.0307152101>.
- (7) Desimoni, G.; Faita, G.; Jørgensen, K. A. C₂-Symmetric Chiral Bis(Oxazoline) Ligands in Asymmetric Catalysis. *Chem. Rev.* **2006**, *106* (9), 3561–3651. <https://doi.org/10.1021/cr0505324>.
- (8) Liu, Y.; Li, W.; Zhang, J. Chiral Ligands Designed in China. *Natl. Sci. Rev.* **2017**, *4* (3), 326–358. <https://doi.org/10.1093/nsr/nwx064>.
- (9) Yoon, T. P.; Jacobsen, E. N. Privileged Chiral Catalysts. *Science* **2003**, *299* (5613), 1691–1693. <https://doi.org/10.1126/science.1083622>.
- (10) Cram, D. J.; Steinberg, H. Synthesis and Properties of Derivatives of Spiro[4.4]Nonane ¹. *J. Am. Chem. Soc.* **1954**, *76* (10), 2753–2757. <https://doi.org/10.1021/ja01639a046>.

- (11) Gerlach, H. Über Die Chiralität Der Enantiomeren Spiro[4.4]Nonan-1,6-Dione. *Helv. Chim. Acta* **1968**, *51* (7), 1587–1593. <https://doi.org/10.1002/hlca.19680510712>.
- (12) Harada, N.; Ochiai, N.; Takada, K.; Uda, H. (1S,5S,6R) Absolute Stereochemistry of (–)-Cis,Trans-Spiro[4.4]Nonane-1,6-Diyl Bis(p-Dimethylaminobenzoate) as Determined by the Exciton Chirality Method. *J. Chem. Soc. Chem. Commun.* **1977**, No. 14, 495–497. <https://doi.org/10.1039/C39770000495>.
- (13) Srivastava, N.; Mital, A.; Kumar, A. A Novel Chiral Auxiliary from Chiral Spiranes. Cis,Cis-(+)- and (–)-Spiro[4.4]Nonane-1,6-Diol as Chiral Modifier in Lithium Aluminium Hydride Reduction of Phenyl Alkyl Ketones. *J. Chem. Soc. Chem. Commun.* **1992**, No. 6, 493–494. <https://doi.org/10.1039/C39920000493>.
- (14) Bajracharya, G. B. Design and Synthesis of Chiral Spiro Ligands. *J. Nepal Chem. Soc.* **2011**, *28*, 1–23. <https://doi.org/10.3126/jncs.v28i0.8036>.
- (15) Zhu, S.-F.; Zhou, Q.-L. Spiro Ligands for Asymmetric Catalysis. In *Ligand Design in Metal Chemistry*; John Wiley & Sons, Ltd, 2016; pp 66–103. <https://doi.org/10.1002/9781118839621.ch4>.
- (16) Chan, A. S. C.; Hu, W.; Pai, C.-C.; Lau, C.-P.; Jiang, Y.; Mi, A.; Yan, M.; Sun, J.; Lou, R.; Deng, J. Novel Spiro Phosphinite Ligands and Their Application in Homogeneous Catalytic Hydrogenation Reactions. *J. Am. Chem. Soc.* **1997**, *119* (40), 9570–9571. <https://doi.org/10.1021/ja970955q>.
- (17) Xie, J.-H.; Wang, L.-X.; Fu, Y.; Zhu, S.-F.; Fan, B.-M.; Duan, H.-F.; Zhou, Q.-L. Synthesis of Spiro Diphosphines and Their Application in Asymmetric Hydrogenation of Ketones. *J. Am. Chem. Soc.* **2003**, *125* (15), 4404–4405. <https://doi.org/10.1021/ja029907i>.
- (18) Han, Z.; Wang, Z.; Zhang, X.; Ding, K. Spiro[4,4]-1,6-Nonadiene-Based Phosphine–Oxazoline Ligands for Iridium-Catalyzed Enantioselective Hydrogenation of Ketimines. *Angew. Chem. Int. Ed.* **2009**, *48* (29), 5345–5349. <https://doi.org/10.1002/anie.200901630>.
- (19) Freixa, Z.; Beentjes, M. S.; Batema, G. D.; Dieleman, C. B.; Strijdonck, G. P. F. van; Reek, J. N. H.; Kamer, P. C. J.; Fraanje, J.; Goubitz, K.; Leeuwen, P. W. N. M. van. SPANphos: A C₂-Symmetric Trans-Coordinating Diphosphane Ligand. *Angew. Chem. Int. Ed.* **2003**, *42* (11), 1284–1287. <https://doi.org/10.1002/anie.200390330>.

- (20) Birman, V. B.; L. Rheingold, A.; Lam, K.-C. 1,1'-Spirobiindane-7,7'-Diol: A Novel, C₂-Symmetric Chiral Ligand. *Tetrahedron Asymmetry* **1999**, *10* (1), 125–131. [https://doi.org/10.1016/S0957-4166\(98\)00481-9](https://doi.org/10.1016/S0957-4166(98)00481-9).
- (21) Zhang, J.-H.; Liao, J.; Cui, X.; Yu, K.-B.; Zhu, J.; Deng, J.-G.; Zhu, S.-F.; Wang, L.-X.; Zhou, Q.-L.; Chung, L. W.; Ye, T. Highly Efficient and Practical Resolution of 1,1'-Spirobiindane-7,7'-Diol by Inclusion Crystallization with N-Benzylcinchonidinium Chloride. *Tetrahedron Asymmetry* **2002**, *13* (13), 1363–1366. [https://doi.org/10.1016/S0957-4166\(02\)00360-9](https://doi.org/10.1016/S0957-4166(02)00360-9).
- (22) Zheng, Z.; Cao, Y.; Chong, Q.; Han, Z.; Ding, J.; Luo, C.; Wang, Z.; Zhu, D.; Zhou, Q.-L.; Ding, K. Chiral Cyclohexyl-Fused Spirobiindanes: Practical Synthesis, Ligand Development, and Asymmetric Catalysis. *J. Am. Chem. Soc.* **2018**, *140* (32), 10374–10381. <https://doi.org/10.1021/jacs.8b07125>.
- (23) Yin, L.; Xing, J.; Wang, Y.; Shen, Y.; Lu, T.; Hayashi, T.; Dou, X. Enantioselective Synthesis of 3,3'-Diaryl-SPINOLs: Rhodium-Catalyzed Asymmetric Arylation/BF₃-Promoted Spirocyclization Sequence. *Angew. Chem. Int. Ed.* **2019**, *58* (8), 2474–2478. <https://doi.org/10.1002/anie.201812266>.
- (24) Zheng, Z.; Cao, Y.; Zhu, D.; Wang, Z.; Ding, K. Development of Chiral Spiro Phosphoramidites for Rhodium-Catalyzed Enantioselective Reactions. *Chem. – Eur. J.* **2019**, *25* (40), 9491–9497. <https://doi.org/10.1002/chem.201900486>.
- (25) Sun, W.; Gu, H.; Lin, X. Synthesis and Application of Hexamethyl-1,1'-Spirobiindane-Based Phosphine-Oxazoline Ligands in Ni-Catalyzed Asymmetric Arylation of Cyclic Aldimines. *J. Org. Chem.* **2018**, *83* (7), 4034–4043. <https://doi.org/10.1021/acs.joc.8b00422>.
- (26) Shan, H.; Pan, R.; Lin, X. Synthesis and Application of a New Chiral Monodentate Spiro Phosphoramidite Ligand Based on Hexamethyl-1,1'-Spirobiindane Backbone in Asymmetric Hydroamination/Arylation of Alkenes. *Org. Biomol. Chem.* **2018**, *16* (34), 6183–6186. <https://doi.org/10.1039/C8OB01785A>.
- (27) Gu, H.; Han, Z.; Xie, H.; Lin, X. Iron-Catalyzed Enantioselective Si–H Bond Insertions. *Org. Lett.* **2018**, *20* (20), 6544–6549. <https://doi.org/10.1021/acs.orglett.8b02868>.
- (28) Shan, H.; Zhou, Q.; Yu, J.; Zhang, S.; Hong, X.; Lin, X. Rhodium-Catalyzed Asymmetric Addition of Organoboronic Acids to Aldimines Using Chiral Spiro Monophosphite-Olefin

- Ligands: Method Development and Mechanistic Studies. *J. Org. Chem.* **2018**, *83* (19), 11873–11885. <https://doi.org/10.1021/acs.joc.8b01764>.
- (29) Li, S.; Zhang, J.-W.; Li, X.-L.; Cheng, D.-J.; Tan, B. Phosphoric Acid-Catalyzed Asymmetric Synthesis of SPINOL Derivatives. *J. Am. Chem. Soc.* **2016**, *138* (50), 16561–16566. <https://doi.org/10.1021/jacs.6b11435>.
- (30) Lin, X.; Wang, L.; Han, Z.; Chen, Z. Chiral Spirocyclic Phosphoric Acids and Their Growing Applications. *Chin. J. Chem.* **2021**, *39* (4), 802–824. <https://doi.org/10.1002/cjoc.202000446>.
- (31) Xu, F.; Huang, D.; Han, C.; Shen, W.; Lin, X.; Wang, Y. SPINOL-Derived Phosphoric Acids: Synthesis and Application in Enantioselective Friedel–Crafts Reaction of Indoles with Imines. *J. Org. Chem.* **2010**, *75* (24), 8677–8680. <https://doi.org/10.1021/jo101640z>.
- (32) Fischer, E.; Jourdan, F. Ueber Die Hydrazine Der Brenztraubensäure. *Berichte Dtsch. Chem. Ges.* **1883**, *16* (2), 2241–2245. <https://doi.org/10.1002/cber.188301602141>.
- (33) Müller, S.; Webber, M. J.; List, B. The Catalytic Asymmetric Fischer Indolization. *J. Am. Chem. Soc.* **2011**, *133* (46), 18534–18537. <https://doi.org/10.1021/ja2092163>.
- (34) Piancatelli, G.; Scettri, A.; Barbadoro, S. A Useful Preparation of 4-Substituted 5-Hydroxy-3-Oxocyclopentene. *Tetrahedron Lett.* **1976**, *17* (39), 3555–3558. [https://doi.org/10.1016/S0040-4039\(00\)71357-8](https://doi.org/10.1016/S0040-4039(00)71357-8).
- (35) Li, H.; Tong, R.; Sun, J. Catalytic Enantioselective Aza-Piancatelli Rearrangement. *Angew. Chem. Int. Ed.* **2016**, *55* (48), 15125–15128. <https://doi.org/10.1002/anie.201607714>.
- (36) Paal, C. Ueber Die Derivate Des Acetophenonacetessigesters Und Des Acetonylacetessigesters. *Berichte Dtsch. Chem. Ges.* **1884**, *17* (2), 2756–2767. <https://doi.org/10.1002/cber.188401702228>.
- (37) Zhang, L.; Zhang, J.; Ma, J.; Cheng, D.-J.; Tan, B. Highly Atroposelective Synthesis of Arylpyrroles by Catalytic Asymmetric Paal–Knorr Reaction. *J. Am. Chem. Soc.* **2017**, *139* (5), 1714–1717. <https://doi.org/10.1021/jacs.6b09634>.
- (38) Zhang, J.; Yu, P.; Li, S.-Y.; Sun, H.; Xiang, S.-H.; Wang, J. (Joelle); Houk, K. N.; Tan, B. Asymmetric Phosphoric Acid-Catalyzed Four-Component Ugi Reaction. *Science* **2018**, *361* (6407), eaas8707. <https://doi.org/10.1126/science.aas8707>.

- (39) Ma, D.; Miao, C.-B.; Sun, J. Catalytic Enantioselective House–Meinwald Rearrangement: Efficient Construction of All-Carbon Quaternary Stereocenters. *J. Am. Chem. Soc.* **2019**, *141* (35), 13783–13787. <https://doi.org/10.1021/jacs.9b07514>.
- (40) Tay, J.-H.; Argüelles, A. J.; DeMars, M. D.; Zimmerman, P. M.; Sherman, D. H.; Nagorny, P. Regiodivergent Glycosylations of 6-Deoxy-Erythronolide B and Oleandomycin-Derived Macrolactones Enabled by Chiral Acid Catalysis. *J. Am. Chem. Soc.* **2017**, *139* (25), 8570–8578. <https://doi.org/10.1021/jacs.7b03198>.
- (41) Fu, M.-C.; Shang, R.; Zhao, B.; Wang, B.; Fu, Y. Photocatalytic Decarboxylative Alkylations Mediated by Triphenylphosphine and Sodium Iodide. *Science* **2019**, *363* (6434), 1429–1434. <https://doi.org/10.1126/science.aav3200>.
- (42) Wang, Y.-B.; Yu, P.; Zhou, Z.-P.; Zhang, J.; Wang, J. (Joelle); Luo, S.-H.; Gu, Q.-S.; Houk, K. N.; Tan, B. Rational Design, Enantioselective Synthesis and Catalytic Applications of Axially Chiral EBINOLs. *Nat. Catal.* **2019**, *2* (6), 504–513. <https://doi.org/10.1038/s41929-019-0278-7>.
- (43) Rueping, M.; Sugiono, E.; Steck, A.; Theissmann, T. Synthesis and Application of Polymer-Supported Chiral Brønsted Acid Organocatalysts. *Adv. Synth. Catal.* **2010**, *352* (2–3), 281–287. <https://doi.org/10.1002/adsc.200900746>.
- (44) Kundu, D. S.; Schmidt, J.; Bleschke, C.; Thomas, A.; Blechert, S. A Microporous Binol-Derived Phosphoric Acid. *Angew. Chem. Int. Ed.* **2012**, *51* (22), 5456–5459. <https://doi.org/10.1002/anie.201109072>.
- (45) Osorio-Planes, L.; Rodríguez-Esrich, C.; Pericàs, M. A. Enantioselective Continuous-Flow Production of 3-Indolylmethanamines Mediated by an Immobilized Phosphoric Acid Catalyst. *Chem. – Eur. J.* **2014**, *20* (8), 2367–2372. <https://doi.org/10.1002/chem.201303860>.
- (46) Clot-Almenara, L.; Rodríguez-Esrich, C.; Osorio-Planes, L.; Pericàs, M. A. Polystyrene-Supported TRIP: A Highly Recyclable Catalyst for Batch and Flow Enantioselective Allylation of Aldehydes. *ACS Catal.* **2016**, *6* (11), 7647–7651. <https://doi.org/10.1021/acscatal.6b02621>.
- (47) Clot-Almenara, L.; Rodríguez-Esrich, C.; Pericàs, M. A. Desymmetrisation of Meso-Diones Promoted by a Highly Recyclable Polymer-Supported Chiral Phosphoric Acid Catalyst. *RSC Adv.* **2018**, *8* (13), 6910–6914. <https://doi.org/10.1039/C7RA13471A>.

- (48) Zhang, X.; Kormos, A.; Zhang, J. Self-Supported BINOL-Derived Phosphoric Acid Based on a Chiral Carbazolic Porous Framework. *Org. Lett.* **2017**, *19* (22), 6072–6075. <https://doi.org/10.1021/acs.orglett.7b02887>.
- (49) Cheng, H.-G.; Miguélez, J.; Miyamura, H.; Yoo, W.-J.; Kobayashi, S. Integration of Aerobic Oxidation and Intramolecular Asymmetric Aza-Friedel–Crafts Reactions with a Chiral Bifunctional Heterogeneous Catalyst. *Chem. Sci.* **2017**, *8* (2), 1356–1359. <https://doi.org/10.1039/C6SC03849B>.
- (50) Lai, J.; Fianchini, M.; Pericàs, M. A. Development of Immobilized SPINOL-Derived Chiral Phosphoric Acids for Catalytic Continuous Flow Processes. Use in the Catalytic Desymmetrization of 3,3-Disubstituted Oxetanes. *ACS Catal.* **2020**, *10* (24), 14971–14983. <https://doi.org/10.1021/acscatal.0c04497>.
- (51) Argüelles, A. J.; Sun, S.; Budaitis, B. G.; Nagorny, P. Design, Synthesis, and Application of Chiral C_2 -Symmetric Spiroketal-Containing Ligands in Transition-Metal Catalysis. *Angew. Chem. Int. Ed.* **2018**, *57* (19), 5325–5329. <https://doi.org/10.1002/anie.201713304>.
- (52) Sun, S.; Nagorny, P. Exploration of Chiral Diastereomeric Spiroketal (SPIROL)-Based Phosphinite Ligands in Asymmetric Hydrogenation of Heterocycles. *Chem. Commun.* **2020**, *56* (60), 8432–8435. <https://doi.org/10.1039/D0CC03088K>.
- (53) Huang, J.; Hong, M.; Wang, C.-C.; Kramer, S.; Lin, G.-Q.; Sun, X.-W. Asymmetric Synthesis of Chiral Spiroketal Bisphosphine Ligands and Their Application in Enantioselective Olefin Hydrogenation. *J. Org. Chem.* **2018**, *83* (20), 12838–12846. <https://doi.org/10.1021/acs.joc.8b01693>.
- (54) Chen, G.-Q.; Lin, B.-J.; Huang, J.-M.; Zhao, L.-Y.; Chen, Q.-S.; Jia, S.-P.; Yin, Q.; Zhang, X. Design and Synthesis of Chiral Oxa-Spirocyclic Ligands for Ir-Catalyzed Direct Asymmetric Reduction of Bringmann's Lactones with Molecular H₂. *J. Am. Chem. Soc.* **2018**, *140* (26), 8064–8068. <https://doi.org/10.1021/jacs.8b03642>.
- (55) Chen, G.-Q.; Lin, B.-J.; Huang, J.-M.; Zhao, L.-Y.; Chen, Q.-S.; Jia, S.-P.; Yin, Q.; Zhang, X. Design and Synthesis of Chiral Oxa-Spirocyclic Ligands for Ir-Catalyzed Direct Asymmetric Reduction of Bringmann's Lactones with Molecular H₂. *J. Am. Chem. Soc.* **2018**, *140* (26), 8064–8068. <https://doi.org/10.1021/jacs.8b03642>.
- (56) Chen Gen-Qiang; Huang Jia-Ming; Lin Bi-Jin; Shi Chuan; Zhao Ling-Yu; Ma Bao-De; Ding Xiao-Bing; Yin Qin; Zhang Xumu. Highly Enantioselective Hydrogenation of Tetra-

- and Tri-Substituted α,β -Unsaturated Carboxylic Acids with Oxa-Spiro Diphosphine Ligands. *CCS Chem.* **2** (6), 468–477. <https://doi.org/10.31635/ccschem.020.202000176>.
- (57) Ye, X.-Y.; Liang, Z.-Q.; Jin, C.; Lang, Q.-W.; Chen, G.-Q.; Zhang, X. Design of Oxa-Spirocyclic PHOX Ligands for the Asymmetric Synthesis of Lorcaserin via Iridium-Catalyzed Asymmetric Hydrogenation. *Chem. Commun.* **2021**, *57* (2), 195–198. <https://doi.org/10.1039/D0CC06311H>.
- (58) Wang, J.; Yuan, Y.; Xiong, R.; Zhang-Negrerie, D.; Du, Y.; Zhao, K. Phenyliodine Bis(Trifluoroacetate)-Mediated Oxidative C–C Bond Formation: Synthesis of 3-Hydroxy-2-Oxindoles and Spirooxindoles from Anilides. *Org. Lett.* **2012**, *14* (9), 2210–2213. <https://doi.org/10.1021/ol300418h>.
- (59) Wu, H.; He, Y.-P.; Xu, L.; Zhang, D.-Y.; Gong, L.-Z. Asymmetric Organocatalytic Direct C(Sp²) H/C(Sp³) H Oxidative Cross-Coupling by Chiral Iodine Reagents. *Angew. Chem. Int. Ed.* **2014**, *53* (13), 3466–3469. <https://doi.org/10.1002/anie.201309967>.
- (60) Liu, T.; Feng, J.; Chen, C.; Deng, Z.; Kotagiri, R.; Zhou, G.; Zhang, X.; Cai, Q. Copper(I)-Catalyzed Intramolecular Asymmetric Double C-Arylation for the Formation of Chiral Spirocyclic Bis-Oxindoles. *Org. Lett.* **2019**, *21* (12), 4505–4509. <https://doi.org/10.1021/acs.orglett.9b01373>.
- (61) Guo, W.; Liu, Q.; Jiang, J.; Wang, J. Development of a C₂-Symmetric Chiral Aza Spirocyclic Diol. *Org. Lett.* **2020**, *22* (8), 3110–3113. <https://doi.org/10.1021/acs.orglett.0c00858>.
- (62) Sun, G.; Wang, Z.; Luo, Z.; Lin, Y.; Deng, Z.; Li, R.; Zhang, J. Design, Synthesis, and Resolution of Spirocyclic Bisoxindole-Based C₂-Symmetric Diols. *J. Org. Chem.* **2020**, *85* (16), 10584–10592. <https://doi.org/10.1021/acs.joc.0c01155>.
- (63) Chang, X.; Ma, P.-L.; Chen, H.-C.; Li, C.-Y.; Wang, P. Asymmetric Synthesis and Application of Chiral Spirosilabiindanes. *Angew. Chem. Int. Ed.* **2020**, *59* (23), 8937–8940. <https://doi.org/10.1002/anie.202002289>.
- (64) Oestreich, M. Chirality Transfer from Silicon to Carbon. *Chem. – Eur. J.* **2006**, *12* (1), 30–37. <https://doi.org/10.1002/chem.200500782>.
- (65) Sala, X.; Suárez, E. J. G.; Freixa, Z.; Benet-Buchholz, J.; Leeuwen, P. W. N. M. van. Modular Spiro Bidentate Nitrogen Ligands – Synthesis, Resolution and Application in

- Asymmetric Catalysis. *Eur. J. Org. Chem.* **2008**, 2008 (36), 6197–6205. <https://doi.org/10.1002/ejoc.200800913>.
- (66) Li, J.; Chen, G.; Wang, Z.; Zhang, R.; Zhang, X.; Ding, K. Spiro-2,2'-Bichroman-Based Bisoxazoline (SPANbox) Ligands for ZnII-Catalyzed Enantioselective Hydroxylation of β -Keto Esters and 1,3-Diester. *Chem. Sci.* **2011**, 2 (6), 1141–1144. <https://doi.org/10.1039/C0SC00607F>.
- (67) Wang, X.; Guo, P.; Wang, X.; Wang, Z.; Ding, K. Practical Asymmetric Catalytic Synthesis of Spiroketal and Chiral Diphosphine Ligands. *Adv. Synth. Catal.* **2013**, 355 (14–15), 2900–2907. <https://doi.org/10.1002/adsc.201300380>.
- (68) Wang, X.; Han, Z.; Wang, Z.; Ding, K. Catalytic Asymmetric Synthesis of Aromatic Spiroketal by SpinPhox/Iridium(I)-Catalyzed Hydrogenation and Spiroketalization of α, α' -Bis(2-Hydroxyarylidene) Ketones. *Angew. Chem. Int. Ed.* **2012**, 51 (4), 936–940. <https://doi.org/10.1002/anie.201106488>.
- (69) Liu, N.; Zhu, W.; Yao, J.; Yin, L.; Lu, T.; Dou, X. Catalyst-Controlled Chemodivergent Synthesis of Spirochromans from Diarylideneacetones and Organoboronic Acids. *ACS Catal.* **2020**, 10 (4), 2596–2602. <https://doi.org/10.1021/acscatal.9b05577>.
- (70) Wang, X.; Ding, K. Making Spiroketal-Based Diphosphine (SKP) Ligands via a Catalytic Asymmetric Approach. *Chin. J. Chem.* **2018**, 36 (10), 899–903. <https://doi.org/10.1002/cjoc.201800247>.
- (71) Wang, X.; Han, Z.; Wang, Z.; Ding, K. A Type of Structurally Adaptable Aromatic Spiroketal Based Chiral Diphosphine Ligands in Asymmetric Catalysis. *Acc. Chem. Res.* **2021**, 54 (3), 668–684. <https://doi.org/10.1021/acs.accounts.0c00697>.
- (72) Li, H.; Khan, I.; Li, M.; Wang, Z.; Wu, X.; Ding, K.; Zhang, Y. J. Pd-Catalyzed Regio- and Enantioselective Aminoarylation of Allenols with Aryl Iodides and 2-Pyridones. *Org. Lett.* **2021**. <https://doi.org/10.1021/acs.orglett.1c00959>.
- (73) Lait, S. M.; Parvez, M.; Keay, B. A. Synthesis of a Novel Spiro-Phosphino-Oxazine Ligand and Its Application to Pd-Catalyzed Asymmetric Allylic Alkylation. *Tetrahedron Asymmetry* **2004**, 15 (1), 155–158. <https://doi.org/10.1016/j.tetasy.2003.10.031>.
- (74) Qiu, Z.; Sun, R.; Teng, D. Synthesis of Highly Rigid Phosphine–Oxazoline Ligands for Palladium-Catalyzed Asymmetric Allylic Alkylation. *Org. Biomol. Chem.* **2018**, 16 (41), 7717–7724. <https://doi.org/10.1039/C8OB02265H>.

- (75) Qiu, Z.; Li, Y.; Zhang, Z.; Teng, D. Spiro Indane-Based Phosphine–Oxazoline Ligands for Palladium-Catalyzed Asymmetric Arylation of Cyclic N-Sulfonyl Imines. *Transit. Met. Chem.* **2019**, *44* (7), 649–654. <https://doi.org/10.1007/s11243-019-00329-z>.
- (76) Qiu, Z.; Sun, R.; Yang, K.; Teng, D. Spiro Indane-Based Phosphine-Oxazolines as Highly Efficient P,N Ligands for Enantioselective Pd-Catalyzed Allylic Alkylation of Indoles and Allylic Etherification. *Molecules* **2019**, *24* (8), 1575. <https://doi.org/10.3390/molecules24081575>.

Chapter 2

Design, Synthesis, and Applications of Chiral Spiroketal-Containing (SPIROL)

Ligands

(Excerpts of this chapter were adapted from following publications:

Nagorny, P.; Sun, S.; Arguelles, A. Spiroketal-Based C₂-Symmetric Scaffold for Asymmetric Catalysis. US10565015B2, February 18, 2020.

Argüelles, A. J.; Sun, S.; Budaitis, B. G.; Nagorny, P. *Angew. Chem. Int. Ed.* **2018**, *57*, 5325.)

2.1. Early developments of spiroketal-containing ligand SPIROL

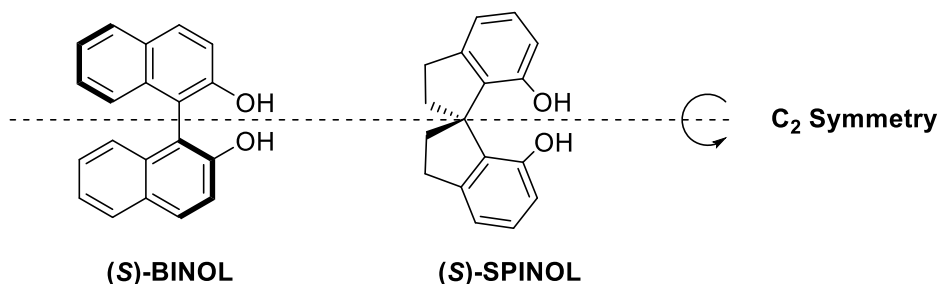


Figure 2.1 C₂ symmetry in privileged ligands

In the past decades, 1,1'-bis-spiroindane (SPINOL) based scaffold has been extensively used in asymmetric catalysis, and SPINOL-based chiral ligands demonstrate consistently excellent selectivity profiles across a wide range of transition metal catalyzed transformations.¹⁻³ Developed in the past century, BINOL-based ligands represent another important group of axially chiral ligands that are frequently employed in the modern asymmetric catalysis. (Figure 2.1) While both BINOL and SPINOL scaffolds share structural similarities, there are distinct structural features that distinguish these two classes of ligands. More rigid SPINOL scaffold

features different dihedral angles and a greater distance between the hydroxyl groups, which results in a more restricted binding pocket. Due to these unique features, SPINOL derivatives may outperform BINOL-derived ligands, and their evaluation is routinely involved in the cases when BINOL-ligands do not exhibit the desired reactivity and selectivity profiles. Over the past two decades, the chemists have developed and utilized a number of SPINOL-based ligands and catalysts (SPA,³ SDP,⁴ SIPHOS-PE,⁵ SITCP,⁶ *etc.*) in substantial numbers of metal-catalyzed asymmetric transformations and other organocatalyses. Unfortunately, since Birman group's original report of SPINOL,⁷ very few studies have effectively improved the accessibility of SPINOL and its derivatives in the past decade.^{8,9} Therefore, the cost to use and maintain the inventory of SPINOLs is still high for most groups. An important recent report from Tan and coworkers showcased SPINOL scaffold synthesis through enantioselective spirocyclization; however, its practical applications are significantly limited by the low availability of the SPINOL-based chiral phosphoric acid catalysts required to promote these transformations.⁹

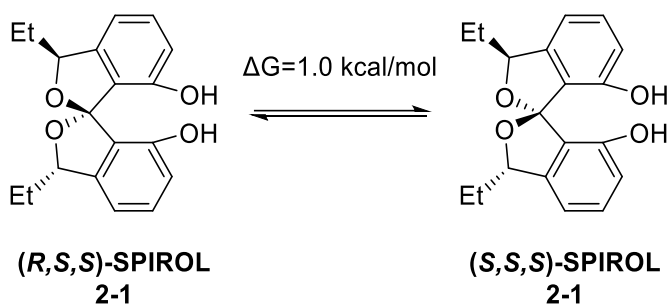
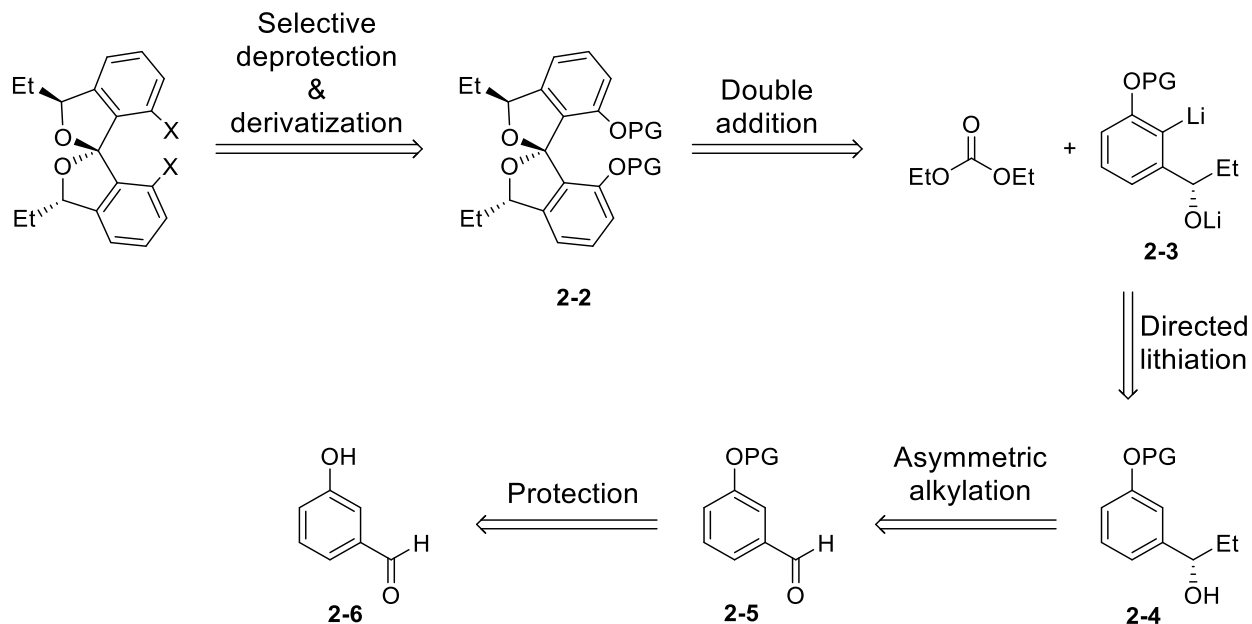


Figure 2.2 Example of Nagorny group's diastereomeric SPIROLs

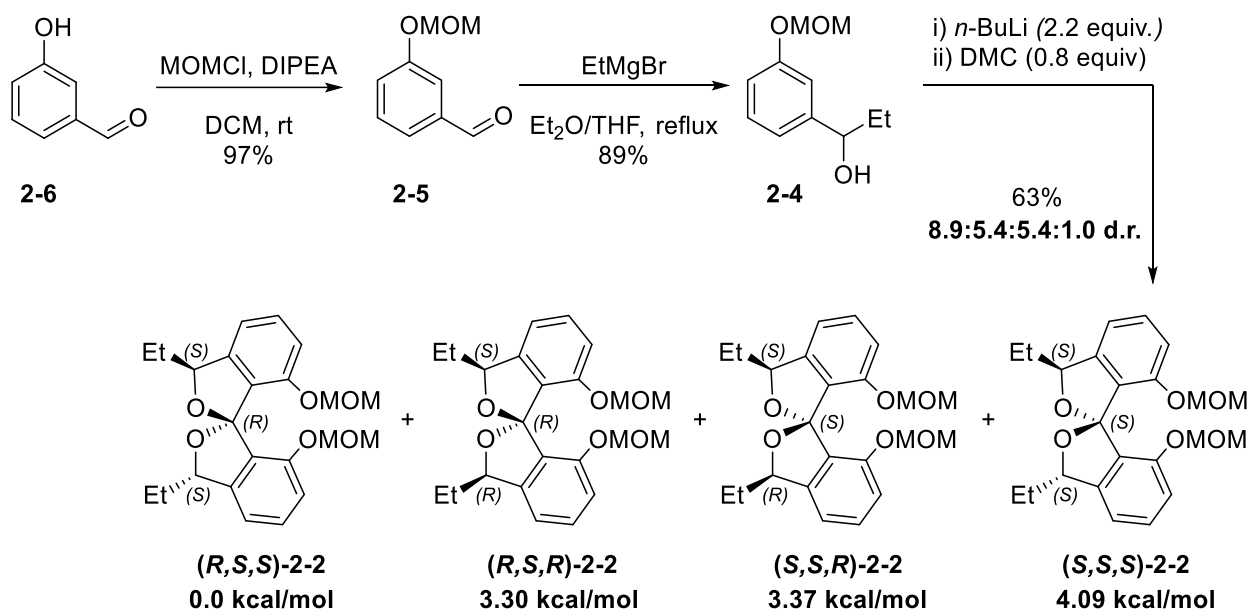
To address some of the challenges associated with the synthesis of SPINOL-based ligands, Nagorny group recently pursued the development of two structurally related spiroketal-based scaffolds (SPIROLs) that feature significantly easier preparation from the readily available building blocks.¹⁰ Two diastereomers would have different structural features, and (*S,S,S*)-

SPIROL **2-1** is 1.0 kcal/mol more stable over (*R,S,S*)-SPIROL **2-1** by gas-phase energy calculation. (Figure 2.2)



Scheme 2.1 Retrosynthetic plan for SPIROL scaffold

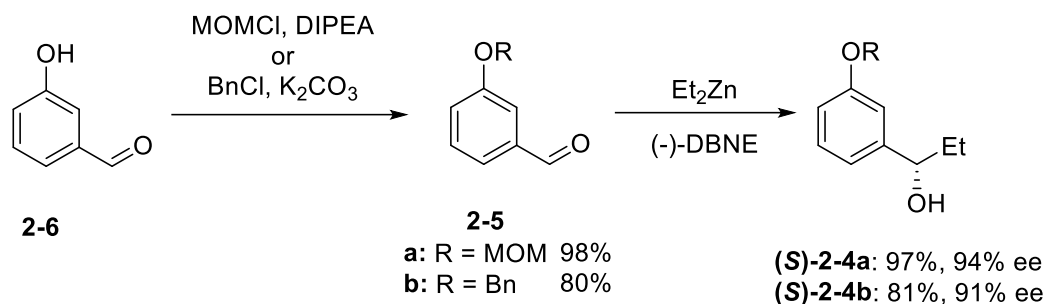
Our synthetic plan is depicted in Scheme 2.1. We envisioned that the SPIROL-based ligands would be accessed by functionalization of SPIROL core **2-2** that would be derived in one operation from the readily available chiral alcohol **2-4**. This operation is key to the synthesis and would involve the lithiation of **2-4** to form **2-3**, which would then react with diethyl carbonate (0.5 equiv) to form the spirocyclic product **2-2**. We also envisioned that the chiral precursor **2-4** would be readily derived by the enantioselective organometal addition to aldehydes **2-5** that are either commercially available or would be derived in one step from aldehyde **2-6**.



Scheme 2.2 Dr. Alonso Argüelles' racemic approach

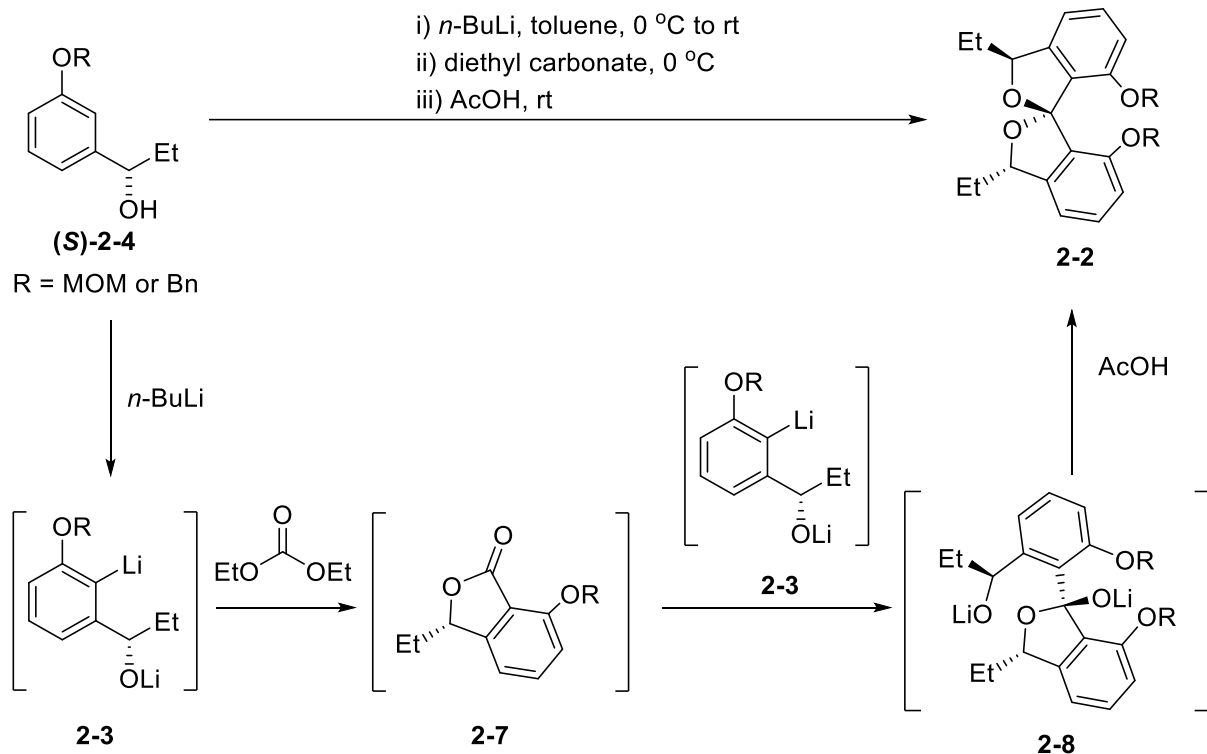
The initial execution of this plan was performed by Dr. Alonso Argüelles. (Scheme 2.2) He commenced the research from the cheap commercially available 3-hydroxybenzaldehyde **2-6** and protected the alcohols **2-5** with MOMCl and DIPEA with 97% yield. The MOM protecting group is required for the efficient ortho-lithiation in the following study. Reaction with ethylmagnesium(II) bromide produce racemic **2-4** with 89% yield. Spirocyclization was performed with racemic alcohol, and we were pleased to find spirocyclic products with 63% yield after isolation. Although the product seemed to be a single spot on the TLC, diastereomers were observed in the product's NMR. Methyl groups from MOM were integrated and used for calculation, and we determined that four diastereomers were formed in a ratio as 8.9:5.4:5.4:1.0. According to the gas phase energies (B97D/6-31G**) for all possible diastereomers, **(R,S,S)-2-2** was the dominant product. **(R,S,R)-2-2** and **(S,S,R)-2-2** had similar energy level, and the formation of them would use equal amount of both (*R*) and (*S*)-alcohol enantiomers in spiroketalization. **(R,S,R)-2-2** was the least favored product with the highest gas phase energy by

calculation. Hence, we proposed that with chiral alcohol **2-4**, discriminative formation of **2-2** would be observed.



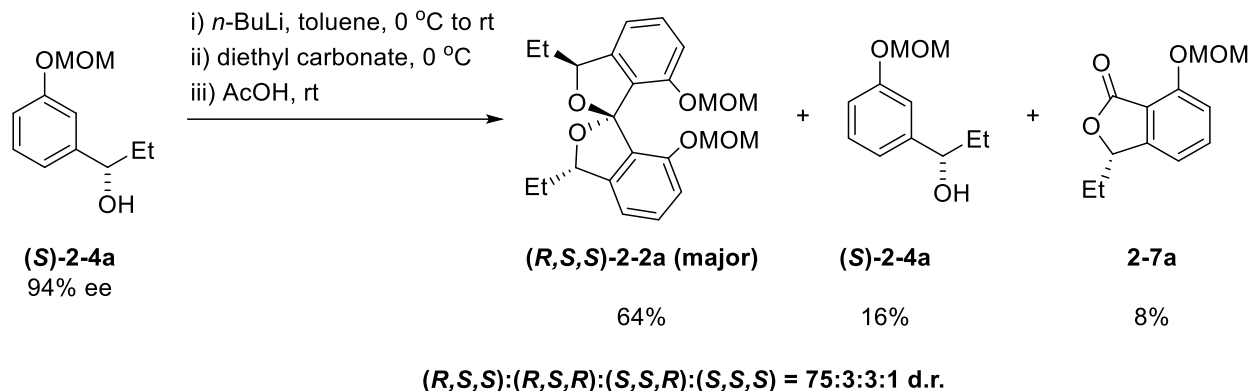
Scheme 2.3 Dr. Alonso Argüelles' asymmetric synthesis

Based on results and analysis from the racemic route, we began our asymmetric approach towards spirocyclic scaffold **2-2**. (Scheme 2.3) MOM and Bn protected alcohols **2-5** were synthesized from 3-hydroxybenzaldehyde **2-6** with 98% and 80% yield, respectively. These protecting groups are required for the efficient ortho-lithiation and could be removed under mild reaction conditions, such as *in situ* generated HCl or hydrogenation. Based on previous literature reports and catalyst availability, DBNE was the first choice for the preparation of the key chiral alcohol intermediates **2-4a** and **2-4b**. With the commercially available (-)-DBNE, the reaction with diethyl zinc and aldehyde **2-5a** yielded product **(S)-2-4a** with 97% yield and 94% ee. Bn group was also tolerated, and **(S)-2-4b** was produced with 81% yield and 91% ee.



Scheme 2.4 Proposed mechanism for spiroketalization

The key cyclization proceeds through the reaction mechanism proposed in Scheme 2.4. Alcohol **2-4** undergoes regioselective deprotonation with 2 equivalents of *n*-BuLi in toluene to produce lithiated intermediate **2-3**. This specie undergoes a subsequent reaction with diethyl carbonate to provide isobenzofuranone product **2-7**, which reacts with an additional equivalent of **2-3** to produce intermediate **2-8**. This product is protonated with acetic acid to provide hemiacetal precursor that further cyclizes to form the desired product **2-2** in excellent yields and selectivities. The dimerization of chiral alcohols **2-4a** and **2-4b** should lead to the enhancement in the enantiomeric excess of the resultant spiroketals **2-2a** and **2-2b** as the minor quantities of the minor enantiomers of **2-4** would produce diastereomeric products.



Scheme 2.5 Spiroketalization with chiral alcohol 2-4a

Indeed, subjecting alcohol **2-4a** containing the mixture of 97% of (*S*)-isomer and 3% of (*R*)-isomer (i.e., 94% ee) to the spiroketalization conditions resulted in the mixture of products depicted in Scheme 2.5. In addition to the desired product (**R,S,S**)-**2-2a** (64% yield), unreacted starting material (**S**)-**2-4a** (16% yield), isobenzofuran intermediate **2-7a** (8% yield) and stereoisomeric products (**R,S,R**)-**2-2a**, (**S,S,R**)-**2-2a** and (**S,S,S**)-**2-2a** were also observed. Although the d.r. between all diastereomers was improved to 75:3:3:1 in favor of (**R,S,S**)-**2-2a**, the presence of these multiple diastereomers arising from the different stereochemical configurations at the 1, 3 and 3' positions significantly complicated the analysis and purification of the main (1*R*, 3*S*, 3'*S*)-product (**R,S,S**)-**2-2a**. Hence, even we placed hopes on the following scale-up reactions to extract enough desired (**R,S,S**)-**2-2a**, the whole operation would be less economical or green than other SPINOL-like ligand preparations. Therefore, we decided to investigate different reaction conditions for a perfect chiral alkylation product **2-4a** and minimize the problem for following steps.

2.2. Asymmetric alkylation with organozinc reagents

Enantioselective alkylation is one of the most important transformations in the asymmetric catalysis towards biologically and pharmacologically valuable compounds.¹¹

Organozinc reagents are generally less reactive comparing to Grignard reagents or organolithium compounds as the source of alkyl carboanions. Therefore, alkyl- and arylzinc species are often used in asymmetric additions to carbonyl compounds with great stereo control due to their relative low reactivity.¹²⁻¹⁵ Early study from Oguni and Omi revealed that up to 49% ee could be achieved in asymmetric diethylzinc addition to benzaldehyde **2-9** with 2 mol% of (*S*)-leucinol.¹⁶ The first high enantioselective addition to aldehydes was observed with a nitrogen-based catalyst (-)-3-*exo*-(dimethylamino)isoborneol ((-)-DAIB).¹⁷ Noyori and coworkers reported up to 98% ee with diethyl zinc and 91% ee with dimethyl zinc to the benzaldehyde **2-9**. (Figure 2.3)

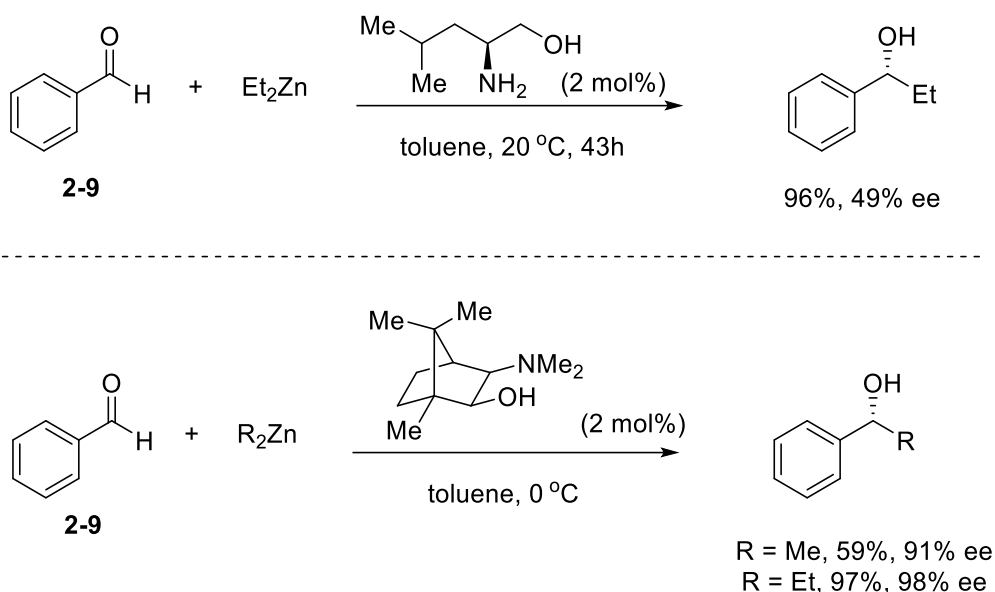


Figure 2.3 Early developments on enantioselective addition of dialkylzinc reagents

Over the years, numerous chiral ligands and catalysts for the asymmetric alkylation reactions have been reported in the scientific literature. (Figure 2.4) While many of these approaches have significant limitations, the modern state-of-the-art methods allows to achieve highly enantioselective formation of chiral benzylic alcohols such as (*S*)-**2-4a**. The overview of some of the methods for the enantioselective alkylation of aldehydes relevant to the work described in this chapter is provided below.

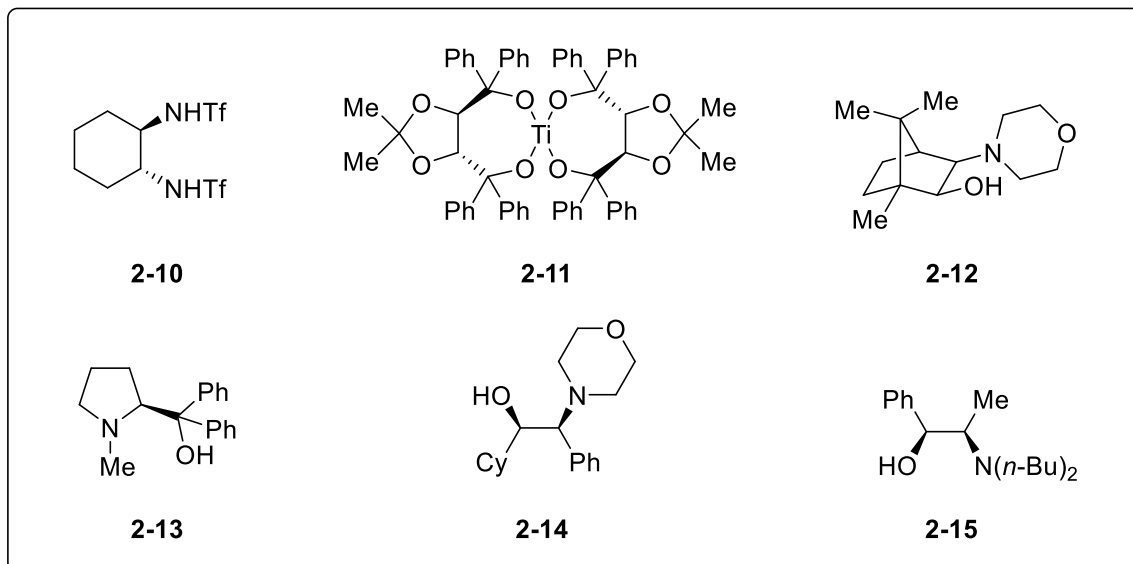
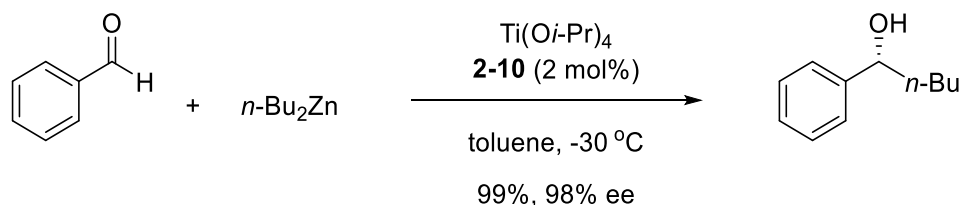


Figure 2.4 Selected examples of catalyst used in asymmetric alkylations

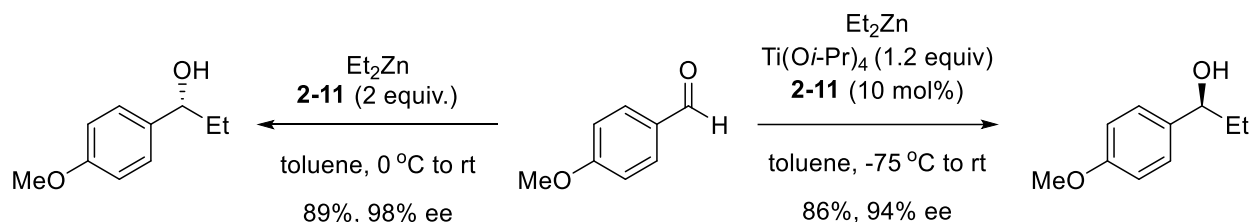
Yoshioka and coworkers synthesized ligands **2-10** made of conjugate bases of chiral proton acids.¹⁸ (Scheme 2.6) They suggested that the chiral sulfonamide **2-10**-titanate catalyst reacted with diethyl zinc to produce the dialkylzinc-orthotitanate complex for asymmetric addition to the benzaldehyde. The high selectivity was most likely introduced by the Lewis acidity and the strong effect from the chiral ligand near Zn. As low as 0.05 mol% of catalyst could produce the product with 97% yield and 98% ee in 2 hours.



Scheme 2.6 Yoshioka's work of asymmetric alkylation

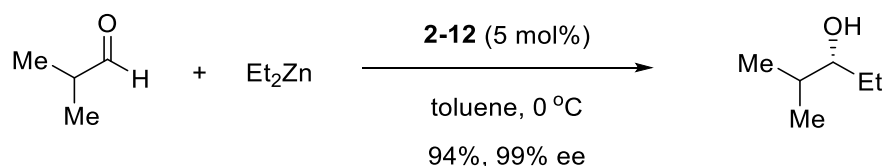
In 1991, Seebach and workers studied the asymmetric alkylation with a novel chiral spiro-titanate **2-11** without the need of amino alcohol or amide, and the catalyst was easy to prepare and more impressively air-stable.¹⁹ With 2 equivalent of catalyst **2-11**, the reaction proceeded at room temperature, and the product was obtained with 98% ee. However, they also

discovered that with 1.2 equivalent of $\text{Ti}(\text{O}i\text{-Pr})_4$, only catalytic amount of **2-11** was needed, and the configuration of the product was switch from *R* to *S*. They suggested that the enantioselectivity in this Lewisacid-catalyzed addition was due to the chiral Ti-based complex, but excess of achiral titanate would disturb the induction effects and produced the opposite enantiomer. (Scheme 2.7)



Scheme 2.7 Seebach's work of asymmetric alkylation

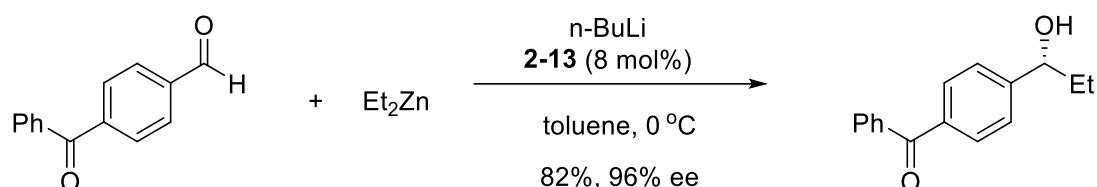
3-*exo*-morpholinoisoborneol (MIB) **2-12** was derived from (-)-DAIB, efficiently produced by the White group.²⁰ It was easier to prepare and more stable in storage according to the report from Nugent.²¹ Starting from *anti*-(1*S*)-(-)-camphorquinone 3-oxime, quick reduction with LAH followed by the reaction with commercially available bis(2-bromoethyl) ether afforded the MIB **2-12** with good yields and purity. It could be used to catalyzed asymmetric alkylation to aliphatic aldehydes in addition to aromatic aldehydes, and excellent enantiomeric excess (up to 99%) with α -branched secondary alcohol were observed in more than 10 substrates. (Scheme 2.8)



Scheme 2.8 White's work of asymmetric alkylation

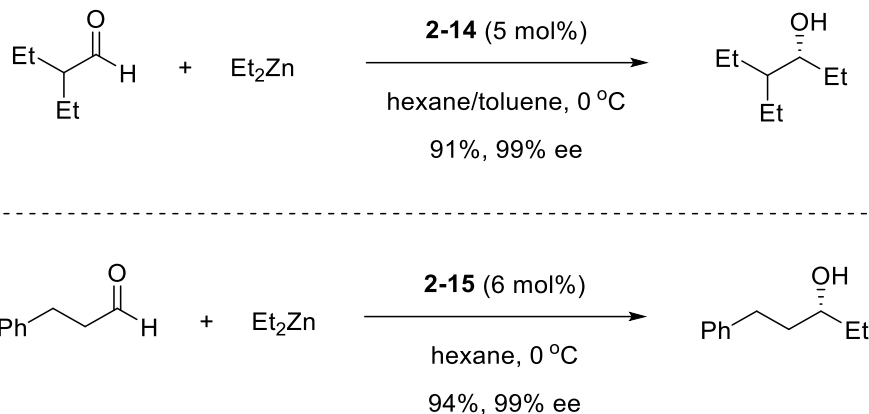
Catalyst **2-13** could be readily produced from inexpensive *L*-proline in just 4 steps with simple protections, deprotections and alkylations. In a report from Soai and Watanabe,

chemoselective alkylation, in addition to high enantioselectivity (96%), was observed in the presence of ketones. More than ten γ -hydroxy ketones and aromatic hydroxy ketones could be synthesized with up to 100% yield and 96% ee with catalyst **2-13**.²² (Scheme 2.9) Also, the chirality in the alcohol could be switch with the corresponding enantiomer of the chiral catalyst.



Scheme 2.9 Soai's work of asymmetric alkylation

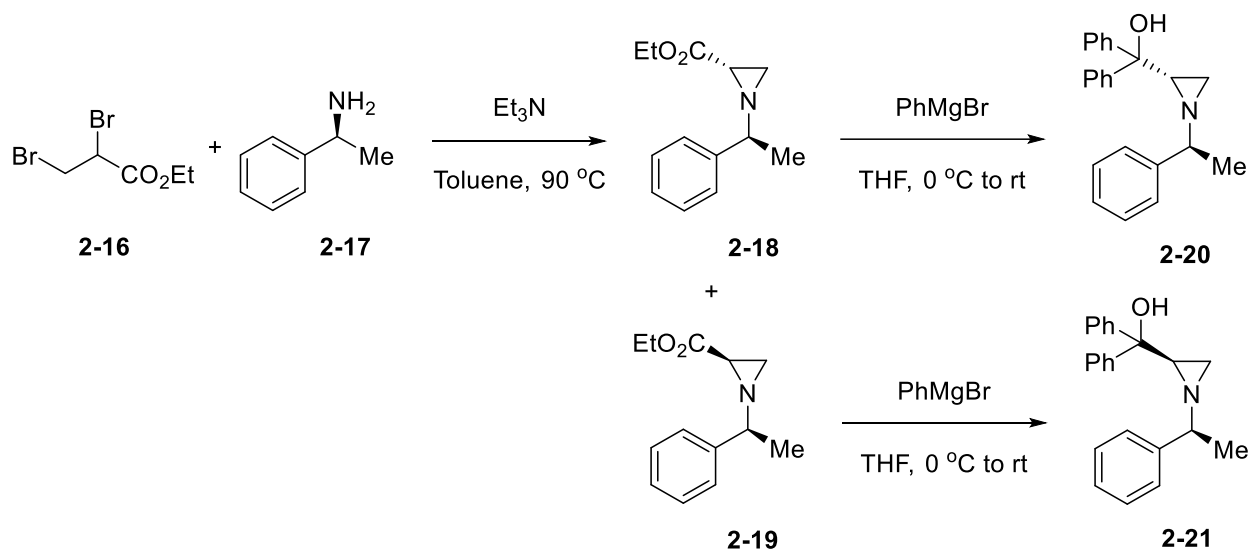
N,N-Dibutylnorephedrine (DBNE) **2-15** is often considered as one of the most versatile ligands in chiral addition to aliphatic and aromatic aldehydes,²³ and many derivatives, such as **2-14**, have been prepared for different applications.²⁴ Usage of (-)-DBNE **2-15** had already shown that the catalyst could promote not only aromatic aldehydes but more importantly aliphatic aldehydes too in early studies. DBNEs are widely commercially available nowadays, but they could not provide satisfied yields or enantioselectivity in all studies. Therefore, Nugent devoted his efforts towards DBNE-like amino alcohol catalysts development. In 2002 he synthesized catalyst **2-14** in just 2 steps from bis(2-bromoethyl) ether and commercially available (1*R*,2*S*)-2-amino-1,2-diphenylethanol, followed by Rh/alumina-catalyzed hydrogenation. The reaction with catalyst **2-14** at room temperature provided 14 chiral addition products with up to 99% ee. (Scheme 2.10)



Scheme 2.10 Early developments with catalysts **2-14** and **2-15**

2.3. Introduction and synthesis of the aziridine-based catalysts for the highly enantioselective synthesis of chiral alcohols **2-4a**

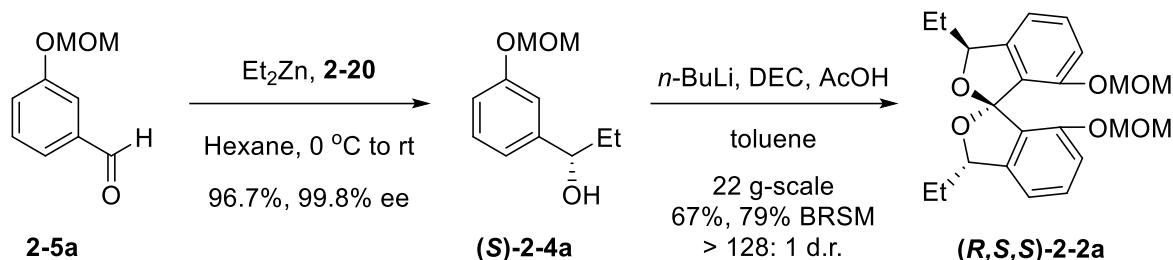
Aziridines have gained significant amounts of attention in synthesis and drug discovery as they are featured in various natural products.⁵ While less common in asymmetric catalysis, aziridines have been also used for chiral ligand design, and examples such as enantioselective arylation of aldehyde with arylboronic acid assisted with ligand **2-20**,²⁵ and a study of asymmetric alkylation of aromatic aldehydes with diethyl zinc²⁶ have been reported. In their study, multiple substituted aromatic aldehydes were tested, and extraordinary yields and enantioselectivities were observed. Moreover, the synthesis of the catalyst seemed easy and economical. Inspired by these promising published results, we decided to synthesize and employ aziridine catalysts in our own study.



Scheme 2.11 Synthesis of aziridine catalysts **2-20** and **2-21**

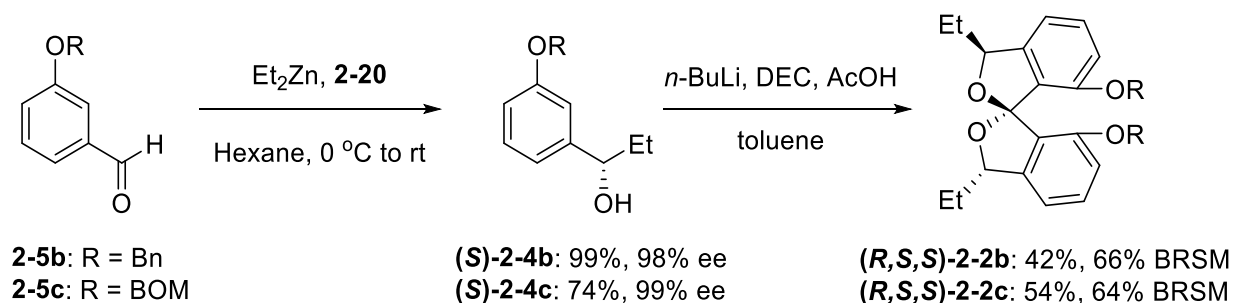
Our studies commenced with a known 2-step protocol that was modified for our synthesis.²⁶ Commercially available (*S*)-(-)-1-phenylethanamine **2-17** did the substitution reaction to widely available ethyl 2,3-dibromopropanoate **2-16** in toluene, and two diastereomeric aziridines **2-18** and **2-19** were already constructed. They could be separated by a simple column chromatography, and excellent yields of 43% and 38%, respectively, were obtained after the purification. Alkylation with phenylmagnesium(II) bromide was easily done on a multi-gram scale for either **2-18** or **2-19** with the yield at 91% or 95% respectively. Finally, aziridine catalysts **2-20** and **2-21** were quickly synthesized and readily available for our following studies. (Scheme 2.11)

2.4. Second-generation asymmetric assembly of (*R,S,S*)-SPIROL core 2-2



Scheme 2.12 Optimized synthesis for compound 2-2

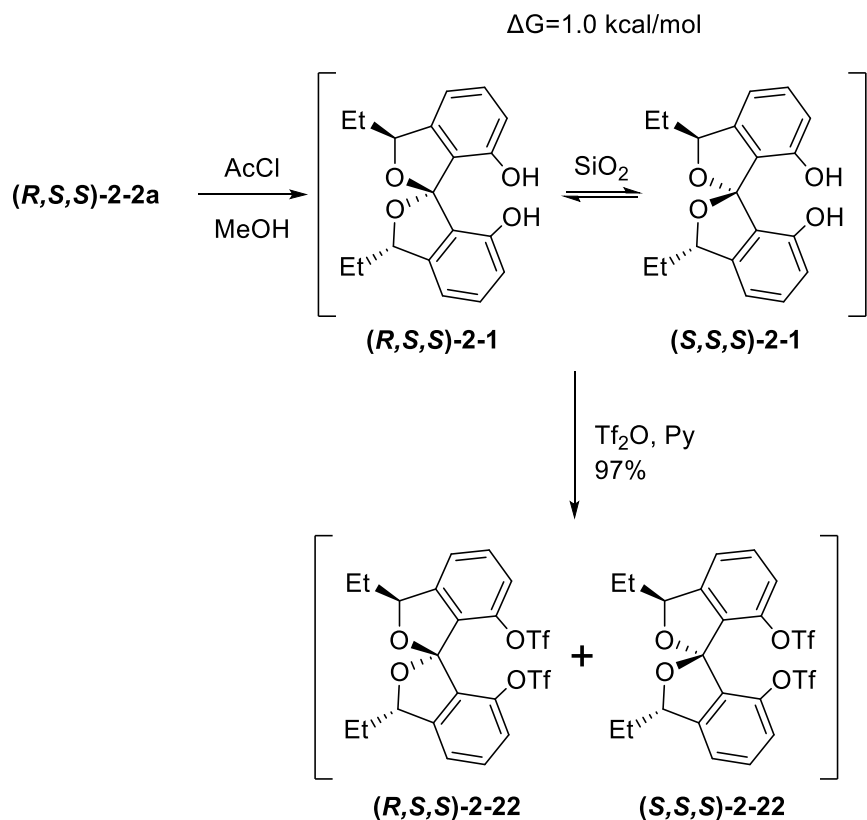
Our studies commenced with the enantioselective alkylation of MOM-protected benzaldehyde **2-5a** with diethyl zinc, and we were delighted to see that the alcohol **(S)-2-4a** was obtained practically enantiopure with 97% yield. Subjecting **(S)-2-4a** to two equivalents of *n*-BuLi in toluene followed by half equivalent of diethyl carbonate afforded the desired spiroketal **(R,S,S)-2-2a** in good yields (67%, 79% BRSM) and excellent diastereoselectivity (>128:1) thanks to the enantiopure starting material **(S)-2-4a**. More importantly, due to less than 0.1% of **(R)-2-4a** in the 99.8% ee chiral alcohol, other diastereomeric spiroketal products, such as **(R,S,R)-2-2a** and **(S,S,R)-2-2a**, were not detected. Impressively, the whole sequence was conveniently scaled to decagram scale. (*cf.* Scheme 2.12)



Scheme 2.13 Synthesis of Bn- and MOM-protected spirocycles

Additionally, enantioselective additions to Bn- and BOM-protected aldehydes with aziridine organocatalysts **2-14** also attained desired products. **(S)-2-4b** was obtained with 99% yield and 98% ee, and **(S)-2-4c** was almost enantiopure with 99% ee but slightly diminished

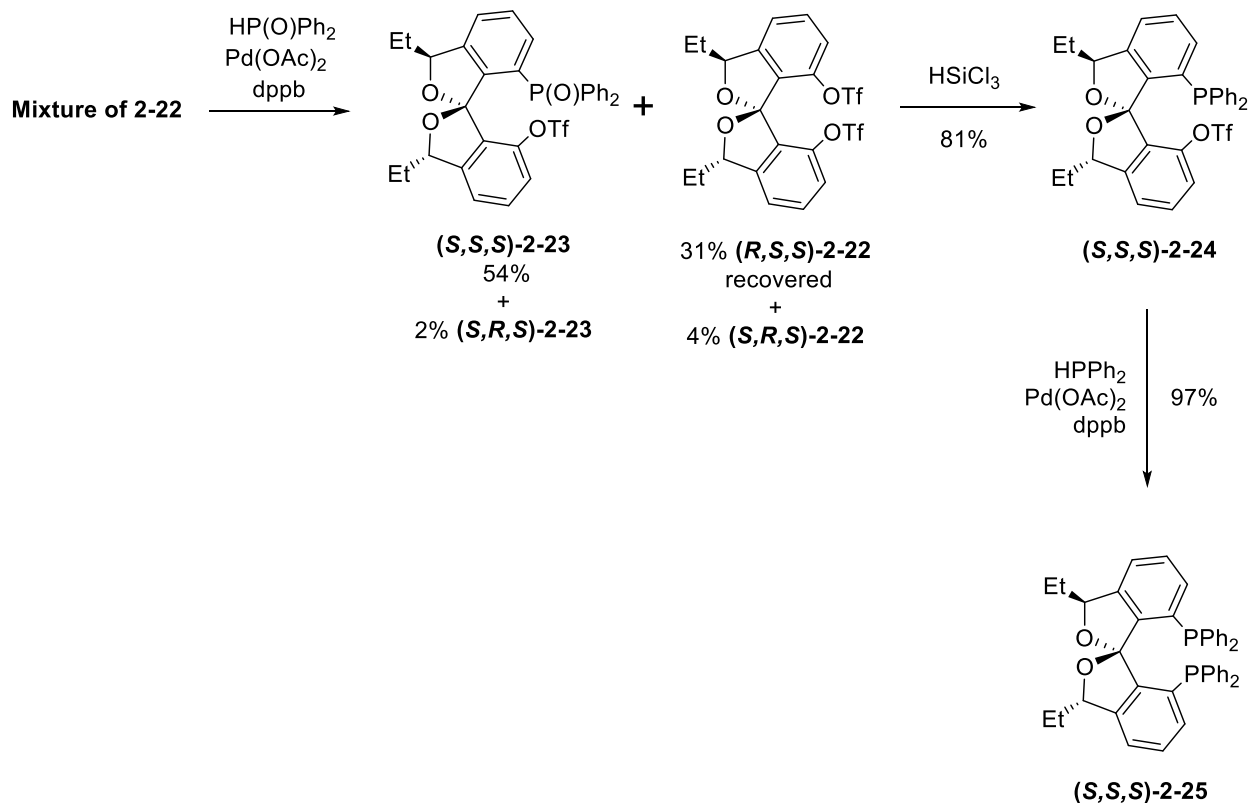
yield of 74%. Spirocyclization with resulting alcohols produced (*R,S,S*)-2-2b and (*R,S,S*)-2-2c with moderate yields (42% and 54%, respectively), but after starting materials were re-collected, both spirocycles were obtained with more than 60%. (Scheme 2.13)



Scheme 2.14 Selective deprotection and triflation

The deprotection of (*R,S,S*)-2-2a was carried out quantitatively (> 99% yield) under standard hydrogenolysis conditions. (cf. Scheme 2.14) The subsequent sodium bicarbonate work up was used to provide the mixture of (*S,R,S*)-2-1, (*S,S,S*)-2-1 and (*R,S,S*)-2-1 products in 1:3.1:11.7 d.r. However, 1:5.7:11 d.r. of (*S,R,S*)-2-1, (*R,S,S*)-2-1, and (*S,S,S*)-2-1 was observed if sodium bicarbonate work up was omitted. The major diastereomer (*R,S,S*)-2-1 could be separated and subsequently equilibrated to produce (*S,S,S*)-2-1 with moderate selectivities.

Computational studies showed that the *(S,S,S)*-**2-1** is favored by 1.0 kcal/mol by gas-phase energy over *(R,S,S)*-**2-1**. The diol mixture was almost quantitatively converted to the ditriflates **2-22** with unchanged d.r. under standard triflation conditions. Although the diastereomers of **2-22** did not interconvert and could be separated by flash column chromatography on silica, we found that a chemical resolution was far more convenient on a larger scale.



Scheme 2.15 Selective production of diphosphine ligands

A palladium-catalyzed coupling to diphenylphosphine oxide at 80 °C selectively reacted with *(S,S,S)*-**2-22** to afford phosphine oxide *(S,S,S)*-**2-23** in excellent yield, while ditriflate *(R,S,S)*-**2-22** was recovered quantitatively. The key in this route was recrystallization of *(S,S,S)*-**2-23** in cyclohexane to further increase its enantiopurity that allowed to generate highly pure ligands in the future. Phosphine oxide *(S,S,S)*-**2-23** was then elaborated to phosphine /triflate *(S,S,S)*-**2-24** by reduction with trichlorosilane. We also found conditions for the direct formation

of **(S,S,S)-2-25** from **(S,S,S)-2-24**, which we found essential to maintain an excellent yielding route. It should be noted that the sequence going from **(S,S,S)-2-23** to **(S,S,S)-2-25** is one step shorter than the reported/patented sequence for the actual SDP ligands as the introduction of the second phosphine functionality is done in a single step (vs. a known 2-step protocol). In addition, the recovered ditriflate **(R,S,S)-2-22** could be purified by recrystallization in cyclohexane, and then coupled to diphenyl phosphine oxide under similar conditions but at 100°C to afford **(R,S,S)-2-23** in good yield. This compound could then be elaborated in a similar fashion to diphosphine ligand **(R,S,S)-2-25** in good yields. It must be emphasized that the preparation of diphosphine ligands **(R,S,S)-SPIRAP 2-25** and **(S,S,S)-SPIRAP 2-25** is significantly shorter than for the construction of the corresponding SPINOL-based ligands. Altogether, the conciseness and robustness of this sequence allows achieving a faster, more efficient, and economical assembly of SPIROL-based ligands in comparison with the SPINOL-based ligands such as SDP. Therefore, we were pleased to accept the offer that Sigma-Aldrich commercialized both **(S,S,S)-SPIRAP** and **(R,R,R)-SPIRAP**.

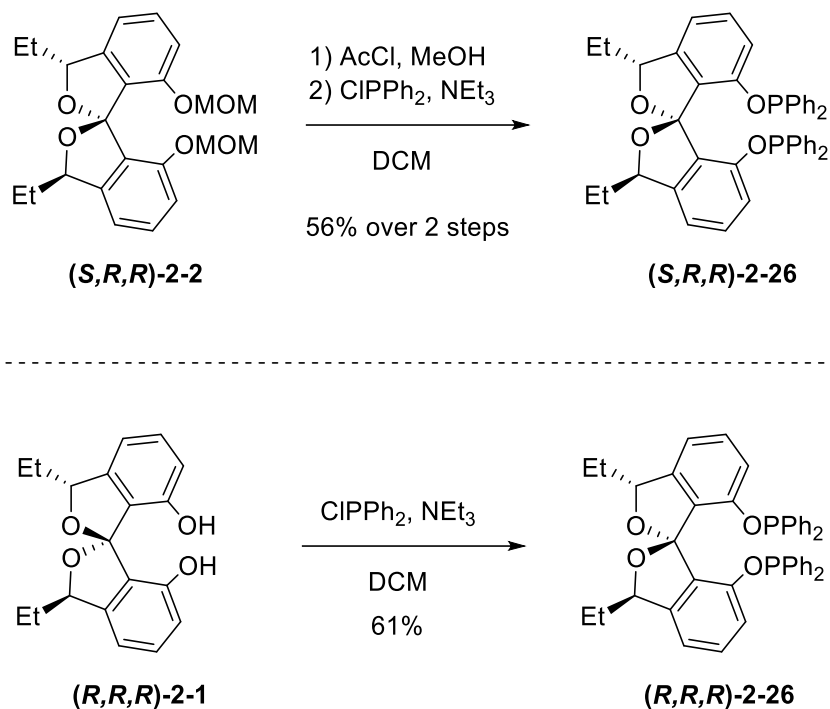


Figure 2.5 Syntheses of diphosphinite ligands

Another advantage of our preparation of SPIROL derivatives is that it is highly modular. We took advantage of the exceptionally direct route from the SPIROL core (*S,R,R*)-2-2 (or its (*R,S,S*)-counterpart) to obtain useful diphosphinites. The MOM deprotection of (*S,R,R*)-2-2 with a mild reaction environment of AcCl and MeOH, followed by the reaction with diphosphine chloride produced the ligand (*S,R,R*)-2-26 with 56% yield over 2 steps. However, (*R,R,R*)-2-26 (or its (*S,S,S*)-counterpart) was synthesized from (*R,R,R*)-2-1 with 61% yield. (Figure 2.5) This step would be optimized with better yields in our following studies described in Chapter 3.

2.5. Asymmetric catalysis with SPIROL-based ligands

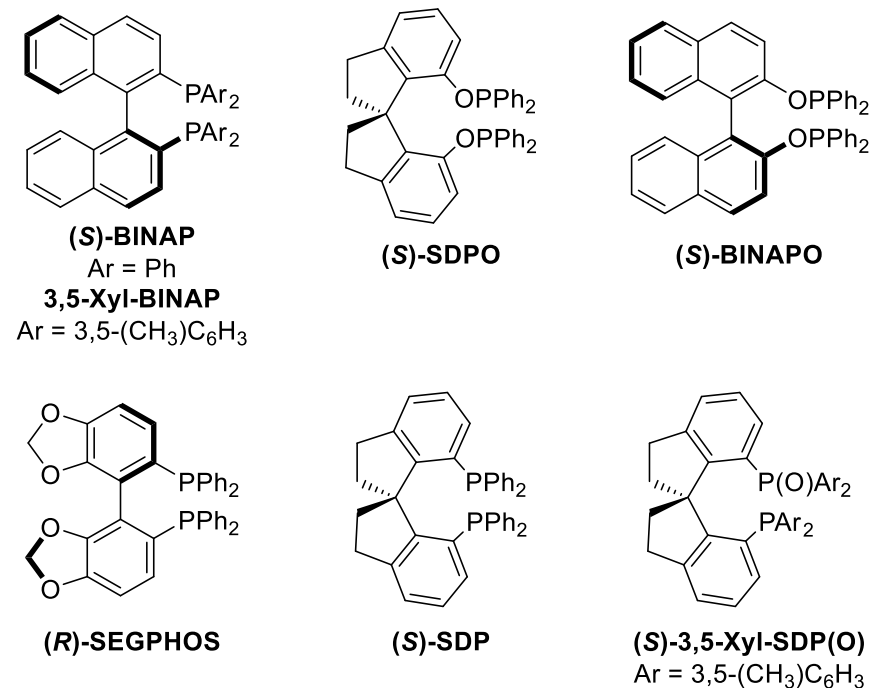
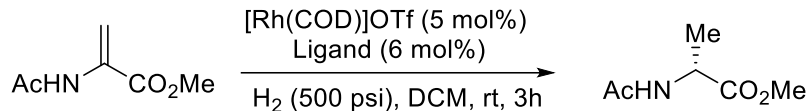


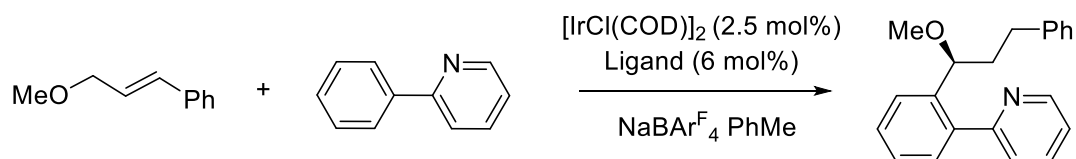
Figure 2.6 Privileged ligands used for comparison

Diphosphinite ligands (*S,R,R*)-**2-26** and (*R,R,R*)-**2-26** were applied in the Rh-catalyzed asymmetric hydrogenations of methyl 2-acetamidoacrylate. (Table 2.1) Due to stereo differences between two axial chiral structures, (*S*)-BINAPO and (*S*)-SDPO catalyzed the same reaction but with opposite enantiomers formed (entries 1 and 2). The result also indicated that the appearance of the chirality in the product was controlled by the chirality in the spirocyclic center of the ligand (entry 2, 3, and 4). (*R,R,R*)-**2-21** performed similarly to SPINOL-based ligand (*S*)-SDPO (entries 2 and 4).

Table 2.1 Asymmetric hydrogenation of amino ester

entry	ligand	yield [%]	ee [%]
1	(<i>S</i>)-BINAPO	84	89
2	(<i>S</i>)-SDPO	85	-93
3	(<i>S,R,R</i>)-2-26	87	-90
4	(<i>R,R,R</i>)-2-26	85	93

In the iridium-catalyzed hydroarylation, (*S,S,S*)-**2-25** provided better with 95% ee under milder conditions at only 70 °C. (Table 2.2) Although SPINOL-derived diphosphine ligand also catalyzed the reaction with 95% ee with the product, the yield (82%) was much lower comparing with SPIRAP (96%). Surprisingly, we didn't see any activity with the pseudoenantiomer (*R,S,S*)-**2-25**. Commercially available BINAPO and SegPhos were only reported with 7 to 84% yields and 81-88% ee, and the reaction condition was elevated to 70 °C as well.

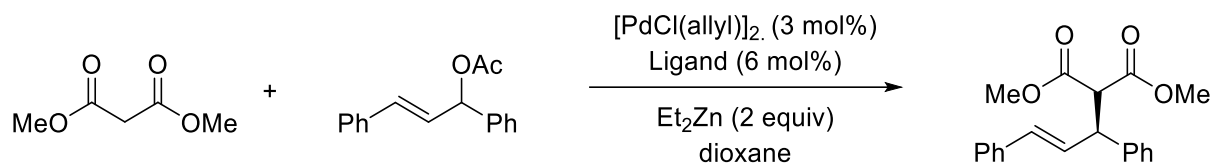
Table 2.2 Studies of asymmetric hydroarylation

entry	ligand	T [°C]	Yield [%]	ee [%]
1	(<i>R</i>)-BINAP	80	84	88
2	(<i>R</i>)-SEGPHOS	80	7	81
3	(<i>R</i>)-3,5-Xyl-BINAP	80	87	94
4	(<i>R</i>)-SDP	70	82	95
5	(<i>S,S,S</i>)-2-25	70	96	95
6	(<i>R,S,S</i>)-2-25	70	N.R.	–

Great yield of 97% and enantioselectivity of 97% were observed in the palladium-catalyzed allylic alkylation of chalcone derivative with SDP ligand. (Table 2.3) Similarly, (*S,S,S*)-**SPIRAP 2-25** was also an exceptional ligand that 94% yield and 97% ee were easily

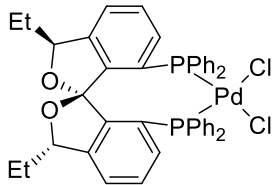
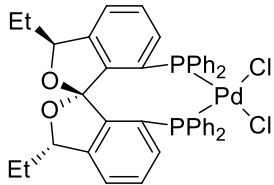
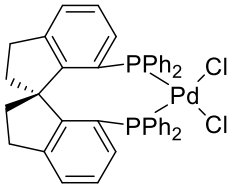
achieved. (*R,S,S*)-SPIRAP 2-25 provided the enantiomer of the product in this reaction, which indicated that the stereocontrol for the reaction was controlled by the center carbon chirality. Considering difficulties during the preparation of SPINOL-derived ligands, our SPIROL-derived diphosphine ligand should be the optimal choice as the same enantioselectivity and easier synthesis are advantages to consider.

Table 2.3 Studies of asymmetric allylic alkylation



entry	ligand	yield [%]	ee [%]
1	(<i>S</i>)-SDP	97	97
2	(<i>S,S,S</i>)-2-25	94	97
3	(<i>R,S,S</i>)-2-25	98	-83

Table 2.4 Comparison of 3D structures of SPIRAP diastereomers and SDP

entry	complex	natural charge at Pd(II)	τ_4	τ_4'	bite angle (°)
1	 (S,S,S)-SPIRAP complex 2-26	0.425	0.113	0.125	94.4
2	 (R,S,S)-SPIRAP complex 2-27	0.425	0.086	0.092	95.3
3	 (S)-SDP complex 2-28	0.427	0.112	0.129	94.2

To explain different reactivities and selectivities between two pseudoenantiomeric ligands, Alonso did computational studies with their 3D structures.²⁷ (Table 2.4) He also calculated these parameters for the SPINOL-derived ligand to compare with SPIRAP ligands. τ_4 and τ_4' are geometry index parameters describe two largest angles at Pd center, and similar values were found between **(S,S,S)-2-25** and **(S)-SDP**, which indicated they are structurally similar. On the other hand, **(R,S,S)-2-25** possess significantly different numbers from **(S,S,S)-2-25** and **(S)-SDP** implying a different structure for the metal-ligand complex.

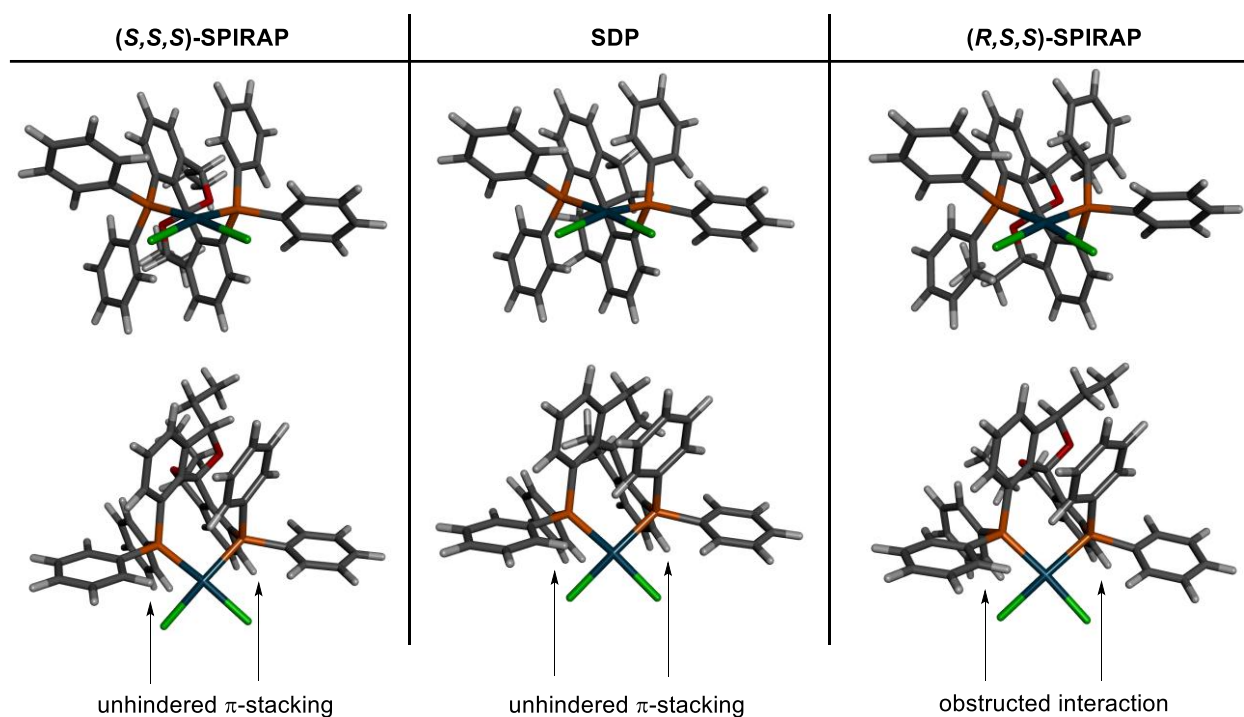


Figure 2.7 Comparison of (R,S,S)-SPIRAP, (S,S,S)-SPIRAP, and SDP complexes of PdCl₂

Additionally, computational studies of 3D structures (Figure 2.7²⁷) of these complexes showed disturbed π -stacking between the aryl groups in (R,S,S)-SPIRAP **2-25** resulting from the ethyl group, which agreed with our geometry index parameters calculations illustrated above.

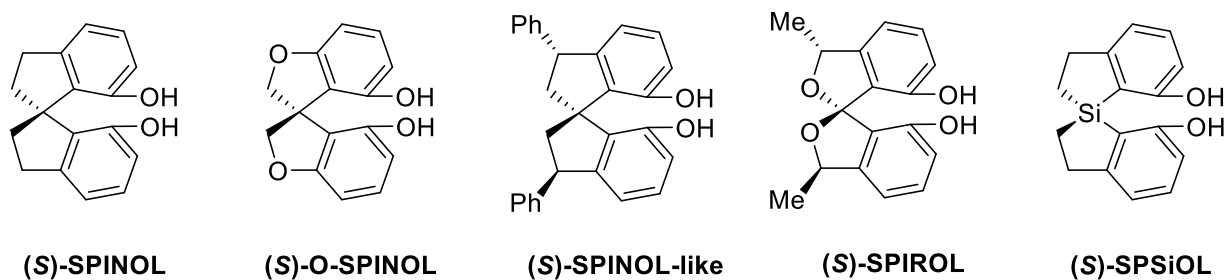


Figure 2.8 Recent developments of spirocyclic scaffold

After the publication of our work discussed above,¹⁰ several other studies targeted the synthesis of SPINOL analogs with the modified core, which are described in Chapter 1. Some of the new chiral scaffolds that emerged from these studies are depicted in Figure 2.8 and include O-SPINOL,²⁸ 3,3'-arylated SPINOL,^{29–32} Me-variant of the SPIROL³³ ligands and Si-analog

SPSiOL.³⁴ Although most of them demonstrated comparable or improved ligand and catalyst characteristics as described in the previous chapter, there are still plenty room of improvements regarding the efficiency in their ligand synthesis.

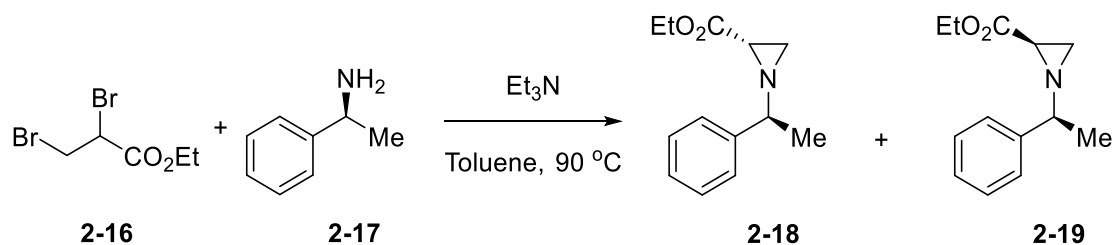
2.6. Experimental information

General information

Unless otherwise stated, all reagents were purchased from commercial suppliers and used without further purification. All reactions were carried out under an atmosphere of nitrogen in flame-dried glassware with magnetic stirring, unless otherwise noted. Air-sensitive reagents and solutions were transferred via syringe or cannula and were introduced to the apparatus through rubber septa. Reactions were cooled via external cooling baths: ice water (0°C), dry ice-acetone (-78°C), or Neslab CB 80 immersion cooler (0 to -60°C). Heating was achieved using a silicone oil bath with regulated by an electronic contact thermometer. Deionized water was used in the preparation of all aqueous solutions and for all aqueous extractions. Solvents used for extraction and column chromatography were ACS or HPLC grade. Dry tetrahydrofuran (THF), dichloromethane (DCM), toluene (PhMe), and diethyl ether (Et₂O) was prepared by filtration through a column (Innovative Technologies) of activated alumina under nitrogen atmosphere. Reactions were monitored by nuclear magnetic resonance (NMR, see below) or thin layer chromatography (TLC) on silica gel precoated glass plates (0.25 mm, SiliCycle, SiliaPlate). TLC plate visualization was accomplished by irradiation with UV light at 254 nm or by staining with a potassium permanganate (KMnO₄) or cerium ammonium molybdate (CAM) solution. Flash chromatography was performed using SiliCycle SiliaFlash P60 (230-400 mesh) silica gel. Powdered 4 Å molecular sieves were pre-activated by flame-drying under vacuum before use.

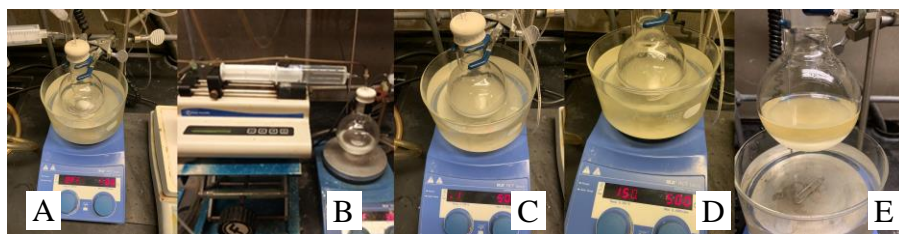
Proton (^1H), deuterium (D), carbon (^{13}C), fluorine (^{19}F), and phosphorus (^{31}P) NMR spectra were recorded on Varian VNMRS-700 (700 MHz), Varian VNMRS-500 (500 MHz), Varian INOVA 500 (500 MHz), or Varian MR400 (400 MHz). ^1H , ^{13}C , and ^{31}P NMR spectra are referenced on a unified scale, where the single reference is the frequency of the residual solvent peak in the ^1H NMR spectrum. Chemical shifts (δ) are reported in parts per million (ppm) relative to tetramethylsilane for ^1H and ^{13}C NMR, trichlorofluoromethane for ^{19}F , and 85% phosphoric acid for ^{31}P . Data is reported as (br = broad, s = singlet, d = doublet, t = triplet, q = quartet, m = multiplet; coupling constant(s) in Hz; integration). Slight shape deformation of the peaks in some cases due to weak coupling (e.g., aromatic protons) is not explicitly mentioned. High resolution mass spectra (HRMS) were recorded on Micromass AutoSpec Ultima or VG (Micromass) 70-250-S Magnetic sector mass. The enantiomeric excesses were determined by HPLC analysis employing a chiral stationary phase column and conditions specified in the individual experiment. HPLC experiments were performed using a Waters Alliance e2695 Separations Module instrument. Optical rotations were measured at room temperature in a solvent of choice on a JASCO P-2000 digital polarimeter at 589 nm (D-line). Fourier-transform infrared spectroscopy (FT-IR) were performed at room temperature on a Thermo-Nicolet IS-50 and converted into inverse domain (wavenumbers in cm^{-1}).

Synthesis of SPIROL scaffolds



An oven-dried 250-mL single-neck round bottom flask (24/40 joint) is equipped with a Teflon coated magnetic stir bar (16x32 mm, egg-shape). The flask is sealed with a rubber septum, connected to a Schlenk line with a needle adapter and subsequently cooled to room temperature. (*S*)-(-)-1-phenylethanamine **2-17** (2.97 mL, 23.0 mmol, 1.00 equiv.), triethylamine (6.41 mL, 46.0 mmol, 2.00 equiv.) and toluene (46.0 mL) are added to the flask via syringes under nitrogen atmosphere.

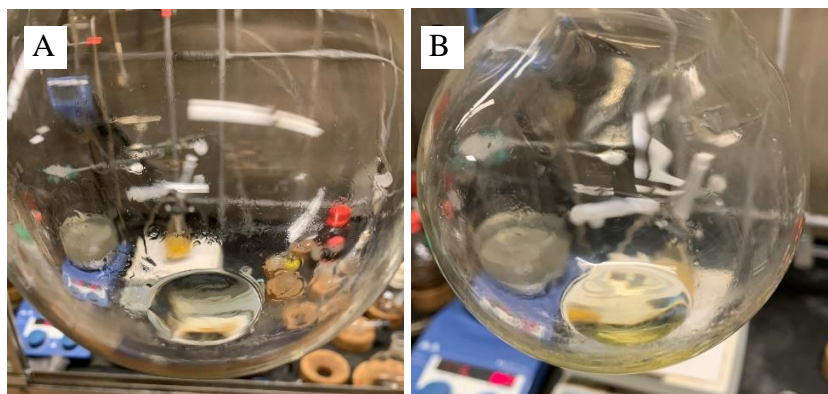
An oven-dried 100-mL single-neck round bottom flask (14/20 joint) is sealed with a rubber septum, connected to a Schlenk line with a needle adapter, and subsequently cooled to room temperature. Ethyl 2,3-dibromopropanoate **2-16** (3.34 mL, 23.0 mmol, 1.00 equiv.) and toluene (46.0 mL) are added to the flask via syringes under nitrogen atmosphere. The 100-mL flask is sonicated for 30 seconds, and the resulting clear solution is added to the 250-mL flask with syringe pump with a 60-mL syringe over 60 minutes. The suspension is stirred for 5 min at room temperature and then heated to 90 °C in an oil bath. After 6 hours, the reaction mixture is removed from the oil bath, cooled to room temperature, and naturally separated into two layers.



A) Reaction flask set-up after the addition of toluene and 2-17; B) addition of 2-18; C) reaction mixture at the beginning of heating; D) reaction mixture after 6 hours of heating; E) reaction mixture after settling

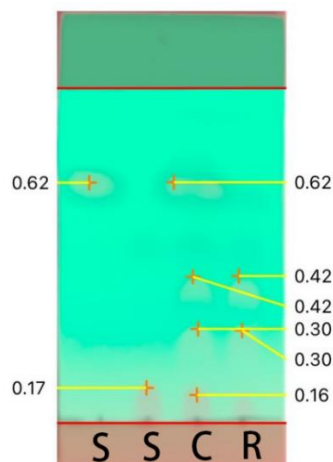
Deionized water (50.0 mL) is added to the reaction, the stir bar is removed, and the biphasic mixture is transferred to a 250-mL separatory funnel. An additional portion of ethyl acetate (50.0 mL) is used to rinse the reaction flask and then poured into the separatory funnel

and capped with a stopper. The organic layer is collected, and the aqueous layer is extracted with ethyl acetate (2x50.0 mL). The combined organic extracts are washed with saturated sodium chloride solution (50.0 mL) and dried with sodium sulfate (25.0 g). The solution is filtered into a 500-mL single-neck round bottom flask (24/40 joint) with ethyl acetate washings (3x10.0 mL) and then concentrated with the aid of a rotary evaporator to afford a crude, yellow oily mixture. The crude material is purified by chromatography on silica to afford ethyl (*S*)-1-((*S*)-1-phenylethyl)aziridine-2-carboxylate **2-18** (2.19 g, 43%, 98% purity) as a yellow oil and ethyl (*R*)-1-((*S*)-1-phenylethyl)aziridine-2-carboxylate **2-19** (1.91 g, 38%, 99% purity) as a yellow oil.



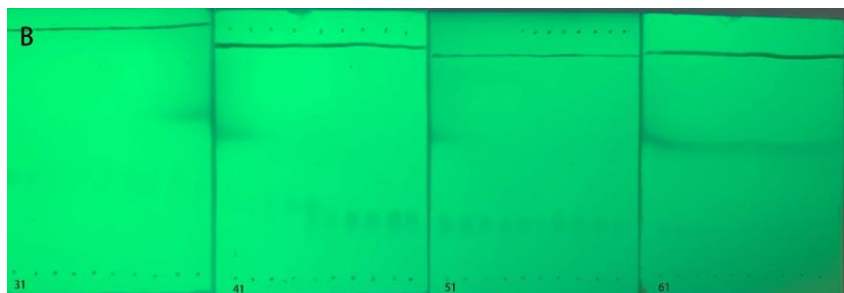
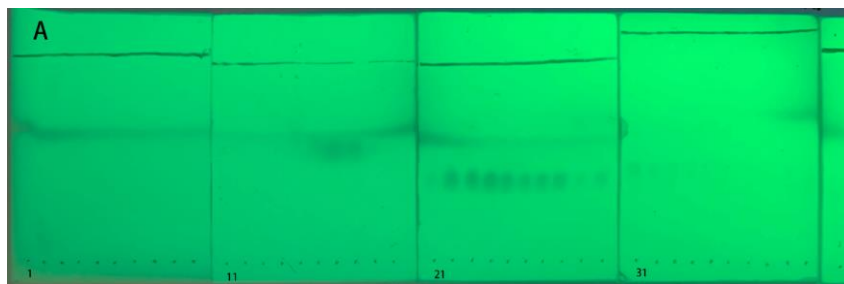
A) Product 2-18; B) Product 2-19.

The reaction can be monitored by TLC (SiO₂, Hexane/EtOAc 4/1, starting material **2-17**: R_f 0.17, starting material **2-16**: R_f 0.62, product **2-18**: R_f 0.42, product **2-19**: R_f 0.30; UV-C 254 nm) to observe complete consumption of starting material **2-16** (S refers to starting materials **2-16** and **2-17**. C refers to co-spot of reaction mixture and starting materials. R refers to the reaction mixture.).



TLC monitoring of the reaction

The crude material was loaded onto a slurry-packed (hexane) column (ID 42 mm) containing SiO₂ (150 g, 40-63 μm, 60 Å silica gels purchased from SiliCycle Inc.), and the flask was then rinsed with hexanes (7 mL) which was loaded afterwards. After loading, solvents were eluted under positive nitrogen pressure and fractions were taken in 25-mL tubes. The solvent system was switched to 900 mL of 8/1 hexane/EtOAc (ACS grade purchased from Fisher Scientific which was used as received) and product **2-18** (R_f 0.42, hexane/EtOAc 4/1, v/v) eluted first and was typically removed with this mixture. Fractions 21 through 35 were combined, concentrated on a rotary evaporator (30 °C, 780 to 20 mmHg), and dried in vacuo (1-2 mmHg) at ambient temperature for 12 h. After elution of product **2-18**, the solvent system was switched to 800 mL of 5/1 hexane/EtOAc, and elution of the product **2-19** (R_f 0.30, hexane/EtOAc 4/1, v/v) was completed this solvent mixture. Fractions 45 through 60 were combined, concentrated on a rotary evaporator (30 °C, 780 to 20 mmHg), and dried in vacuo (1-2 mmHg) at ambient temperature for 12 h.



TLC analysis of the fractions. (Visualization with UV-C 254 nm) A) fractions 1 through 40; B) fractions 31 through 70

The product **2-18** exhibited the following properties:

$[\alpha]_D^{23}$ -80.43 (*c* 0.50, CHCl₃)

R_f 0.42 (4/1, hexane/EtOAc, v/v)

bp 206.6 °C

IR (film): 3062, 2978, 2929, 1741, 1725, 1601, 1494, 1448, 1410, 1384, 1281, 1233, 1182, 1086, 1028, 959, 763, 698 cm⁻¹

¹H NMR (500 MHz, Chloroform-d) δ 7.41 (dd, *J* = 7.3, 1.5 Hz, 2H), 7.38 – 7.31 (m, 2H), 7.29 – 7.24 (m, 1H), 4.32 – 4.16 (m, 2H), 2.56 (q, *J* = 6.6 Hz, 1H), 2.21 (dd, *J* = 6.4, 3.2 Hz, 1H), 2.14 (dd, *J* = 3.2, 1.1 Hz, 1H), 1.61 (dd, *J* = 6.4, 1.1 Hz, 1H), 1.49 (dd, *J* = 6.6, 0.9 Hz, 3H), 1.32 (td, *J* = 7.1, 0.9 Hz, 3H).

¹³C NMR (126 MHz, Chloroform-d) δ 171.0, 143.6, 128.5, 127.4, 127.0, 70.1, 61.2, 38.3, 34.1, 23.3, 14.3

HRMS (ESI) m/z calcd for $C_{13}H_{17}NO_2Na$ $[M+Na]^+$ 242.1151, found 242.1148.

Purity was determined by quantitative 1H NMR spectroscopic analysis using dibromomethane as an internal standard to be 98% by weight. (The enantiomeric excess (ee) of this product could not be determined by the available HPLC or SFC techniques, and the product ee is reported based on the ee of precursor measured after the Grignard reaction step.)

The product **2-19** exhibited the following properties:

$[\alpha]_D^{23}$ +41.70 (c 0.35, $CHCl_3$)

R_f 0.28 (4/1, hexanes/EtOAc, v/v)

bp 181.7 °C

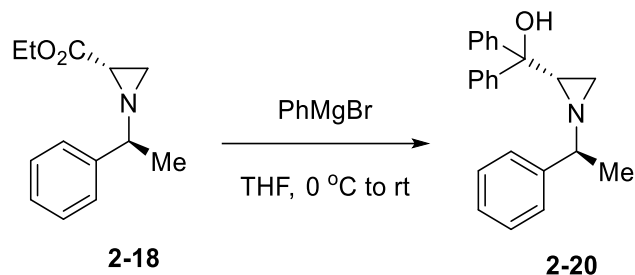
IR (film): 3061, 2976, 2928, 17439, 1493, 1447, 1412, 1282, 1235, 1184, 1089, 1028, 960, 759, 699 cm^{-1}

1H NMR (500 MHz, Chloroform- d) δ 7.40 – 7.32 (m, 3H), 7.35 – 7.30 (m, 1H), 7.30 – 7.23 (m, 1H), 4.17 (qd, $J = 7.1, 2.6$ Hz, 2H), 2.59 (q, $J = 6.6$ Hz, 1H), 2.35 (dd, $J = 3.2, 1.2$ Hz, 1H), 2.07 (dd, $J = 6.5, 3.1$ Hz, 1H), 1.80 (dd, $J = 6.5, 1.2$ Hz, 1H), 1.48 (dd, $J = 6.6, 1.1$ Hz, 3H), 1.23 (td, $J = 7.1, 1.1$ Hz, 3H).

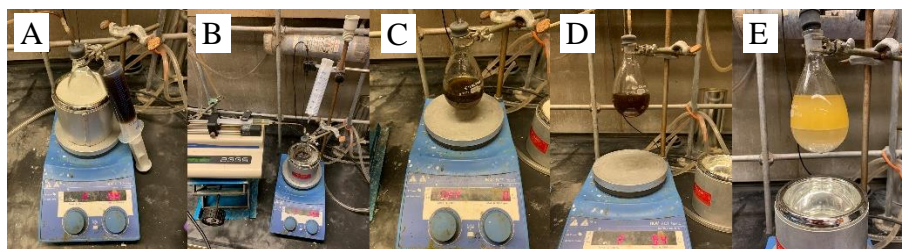
^{13}C NMR (126 MHz, Chloroform- d) δ 170.7, 143.9, 128.5, 127.2, 126.6, 69.9, 61.1, 37.3, 35.0, 23.7, 14.3

HRMS (ESI) m/z calcd for $C_{13}H_{17}NO_2Na$ $[M+Na]^+$ 242.1151, found 242.1150.

Purity was determined by quantitative 1H NMR spectroscopic analysis using dibromomethane as an internal standard to be 99% by weight.



An oven-dried 100-mL single-neck round bottom flask (14/20 joint) is equipped with a Teflon coated magnetic stir bar (9x12 mm, octagon). The flask is sealed with a rubber septum, connected to a Schlenk line with a needle adapter and subsequently cooled to room temperature. Phenylmagnesium chloride solution (26.9 mL, 39.8 mmol, 4.00 equiv) is added via a syringe under nitrogen atmosphere and then cooled to 0 °C while stirring.



A) Reaction flask set-up after addition of PhMgCl solution; B) addition of 2-18; C) reaction solution after the addition; D) reaction solution before work-up; E) reaction mixture after work-up

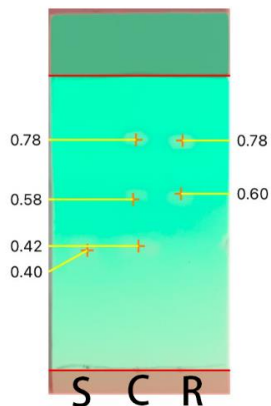
An oven-dried 50-mL single-neck round bottom flask (14/20 joint) is sealed with a rubber septum, connected to a Schlenk line with a needle adapter, and subsequently cooled to room temperature. Ethyl 1-((*S*)-1-phenylethyl)aziridine-2-carboxylate **1-18** (2.18 g, 9.94 mmol, 1.00 equiv.) and THF (26.0 mL) are added via syringes under nitrogen atmosphere. The 50-mL flask is sonicated for 30 seconds and resulting yellow solution is added to the 100-mL flask with the syringe pump at 0 °C over 40 minutes. The solution is slowly warmed to room temperature and stirred for 12 hours. The reaction flask is cooled to 0 °C and saturated ammonium chloride solution (20.0 mL) and 1N HCl solution (30.0 mL) are added slowly. The biphasic mixture is

transferred to a 250-mL separatory funnel. The organic layer is collected, and the aqueous layer is extracted with ethyl acetate (4x40.0 mL). The combined organic phases are dried with sodium sulfate (30.0 g), filtered into a 500-mL single-neck round bottom flask (24/40 joint) with ethyl acetate washings (3 x 15.0 mL). The solution is concentrated with the aid of a rotary evaporator to afford crude, light yellow solids. The crude product is purified by chromatography on silica to afford diphenyl((*S*)-1-((*S*)-1-phenylethyl)aziridin-2-yl)methanol **2-20** (2.97 g, 91%, 99% ee, 99% purity) as a white solid .



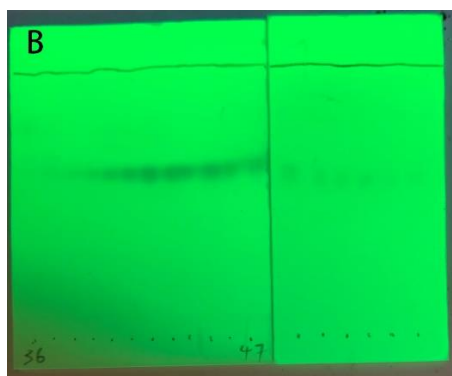
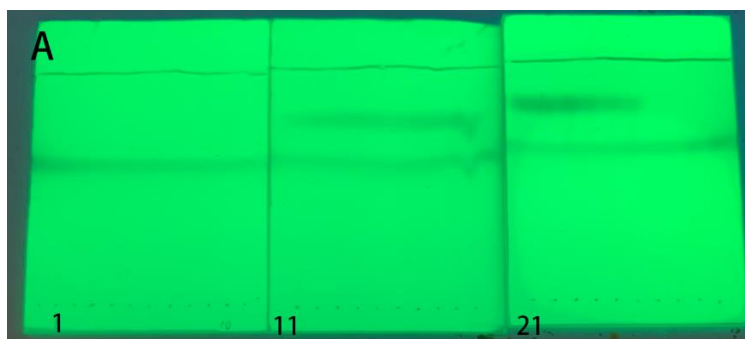
Product 2-20

The reaction can be monitored by TLC (SiO₂, Hexane/EtOAc 4/1, starting material **2-18**: R_f 0.42, product **2-20**: R_f 0.78; UV-C 254 nm) to observe complete consumption of starting material **2-18** (S refers to starting material **2-18**. C refers to co-spot of reaction mixture and starting material. R refers to the reaction mixture.).



TLC monitoring of the reaction

The crude was loaded onto a slurry-packed (hexane) column (ID 42 mm) containing SiO₂ (150 g, 40-63 μm, 60 Å silica gels purchased from SiliCycle Inc.), and the flask was then rinsed with hexanes (10 mL) which was loaded afterwards. After loading, solvents were eluted under positive nitrogen pressure and fractions were taken in 25-mL tubes. The solvent system was switched to 420 mL of 20/1 hexane/EtOAc (ACS grade purchased from Fisher Scientific which was used as received) and followed by 450 mL of 15/1 hexane/EtOAc. Product **2-20** (R_f 0.78, hexane/EtOAc 4/1, v/v) eluted, fractions 36 through 52 were combined, concentrated on a rotary evaporator (30 °C, 780 to 20 mmHg), and dried in vacuo (1-2 mmHg) at ambient temperature for 12 h.



TLC analysis of the fractions. (Visualization with UV-C 254 nm) A) fractions 1 through 30; B) fractions 36 through 53

The product **2-20** exhibited the following properties:

99% ee (HPLC (Chiralpak IA column, 90:10 hexanes/isopropanol, 1.0 ml/min), *tr* = 5.7 min (*S*), 6.6 min (*R*))

$[\alpha]_D^{23}$ -68.20 (*c* 0.10, CHCl₃)

R_f 0.66 (4/1, hexanes/EtOAc, v/v)

mp 125.2–125.6 °C

IR (powder): 3351 (br), 3059, 3027, 2981, 2966, 2926, 1599, 1492, 1449, 1354, 1342, 1301, 1188, 1167, 1066, 1029, 1014, 981, 931, 768, 747, 691, 644, 637, 612 cm⁻¹

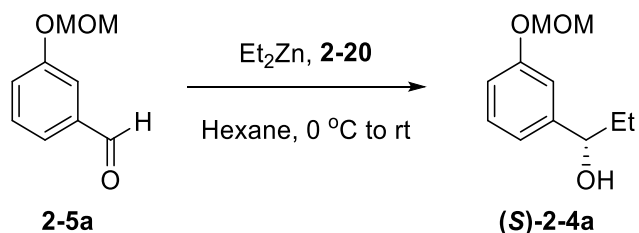
¹H NMR (500 MHz, Chloroform-*d*) δ 7.60 – 7.51 (m, 4H), 7.42 – 7.30 (m, 8H), 7.33 – 7.24 (m, 3H), 4.15 (s, 1H), 2.76 (q, *J* = 6.5 Hz, 1H), 2.56 (dd, *J* = 6.4, 3.6 Hz, 1H), 1.99 (d, *J* = 3.5 Hz, 1H), 1.59 (d, *J* = 6.2 Hz, 1H), 0.91 (d, *J* = 6.5 Hz, 3H).

¹³C NMR (176 MHz, Chloroform-*d*) δ 147.9, 144.9, 144.2, 128.4, 128.2, 128.0, 127.2, 127.2, 126.8, 126.7, 126.0, 73.9, 68.1, 47.4, 30.7, 23.6

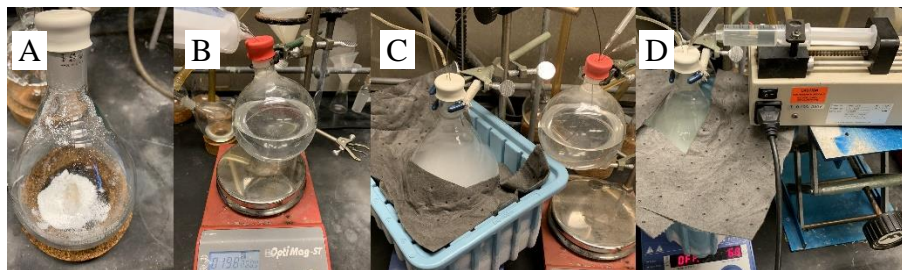
HRMS (ESI) *m/z* calcd for C₂₃H₂₃NONa [M+Na]⁺ 352.1672, found 352.1669.

Purity was determined by quantitative ¹H NMR spectroscopic analysis using dibromomethane as an internal standard to be 99% by weight.

The ee was determined by HPLC analysis with a Waters Alliance e2695 Separations Module HPLC system equipped with a CHIRALPAK IA column (length 250 mm, I.D. 4.6 mm). Optical rotations were measured at room temperature in a solvent of choice on a JASCO P-2000 digital polarimeter at 589 nm (D-line).

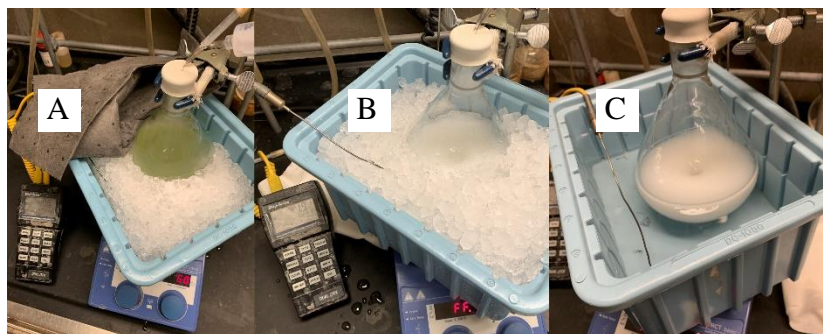


An oven-dried 1000-mL single-neck round bottom flask (24/40 joint) equipped with a Teflon coated magnetic stir bar (16x32 mm, egg-shape) is cooled to room temperature in a desiccator. Diphenyl((*S*)-1-((*S*)-1-phenylethyl) aziridin-2-yl)methanol **2-20** (1.98 g, 6.00 mmol, 5.0 mol%) is added to the flask and then sealed with a rubber septum, connected to a Schlenk line with a needle adapter, and purged to a nitrogen atmosphere. Hexane (265.0 mL) is then added to the flask via a syringe and the solution is stirred and cooled to 0 °C.



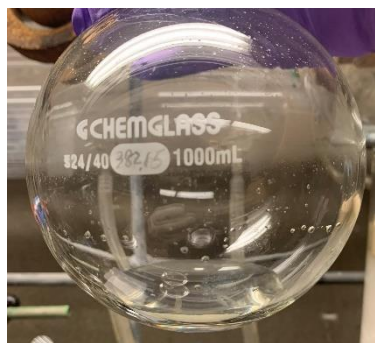
A) Reaction flask set-up after addition of catalyst (a); B) self-made Et₂Zn solution; C) reaction set-up for Et₂Zn transfer; D) reaction set-up for addition of 3-(methoxymethoxy)benzaldehyde

An oven-dried 500-mL single-neck round bottom flask (14/20 joint) is sealed with a rubber septum, connected to a Schlenk line with a needle adapter, and subsequently cooled to room temperature. Hexane (264.8 mL) followed by diethylzinc (27.2 mL, 264.8 mmol, 2.20 equiv.) are added to the flask via syringes under nitrogen atmosphere. The resulting clear solution is transferred to the 1000-mL flask dropwise over 60 minutes via the cannula 0 °C. The reaction mixture is stirred at 0 °C for 90 minutes. 3-(Methoxymethoxy)benzaldehyde **2-5a** (20.0 g, 120.4 mmol, 1.00 equiv.) is added to the reaction dropwise over 60 minutes via the syringe pump. The reaction mixture is maintained at 0 °C for 10 hours, then slowly warmed to room temperature and stirred for 20 hours.



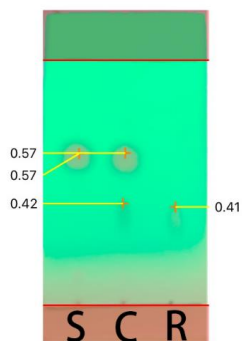
A) Reaction solution after addition of 2-5a; B) reaction mixture after 10 hours at 0 °C; C) reaction mixture after 20 hours at room temperature

The reaction is stopped by the slow addition of 1N HCl solution (150.0 mL) at 0 °C and then filtered into a 1000-mL round bottom flask (24/40 joint) with DCM washings (2x50.0 mL). Deionized water (400.0 mL) is added to the filtrate, and the biphasic mixture is transferred to a 2000-mL separatory funnel. The organic layer is collected, and the aqueous layer is extracted with DCM (4x100.0 mL). The combined organic phases are dried with MgSO₄ (100.0 g), filtered into a 2000-mL single-neck round bottom flask (24/40 joint) with DCM washings (3x50.0 mL). The solution is concentrated by the aid of a rotary evaporator to afford a crude yellow oil. The crude product is purified by chromatography to afford (*S*)-1-(3-(methoxymethoxy)phenyl)propan-1-ol (**S**)-2-4a (23.41 g, 99%, 99% ee, 99% purity) as a pale yellow oil.



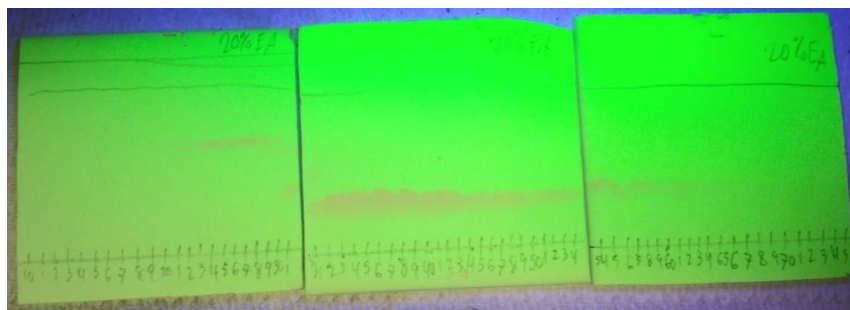
Product (*S*)-2-4a

The reaction can be monitored by TLC (SiO₂, Hexane/EtOAc 4/1, starting material **2-5a**: R_f 0.57, product (**S**)-**2-4a**: R_f 0.41; UV-C 254 nm) to observe complete consumption of starting material (S refers to starting material. C refers to co-spot of reaction mixture and starting materials. R refers to the reaction mixture.).



TLC monitoring of the reaction

The crude material was loaded onto a slurry-packed (hexane) column (ID 72 mm) containing SiO₂ (400 g, 40 - 63 μm, 60 Å silica gels purchased from SiliCycle Inc.), and the flask was then rinsed with DCM (20 mL) (Note 36) which was loaded afterwards. After loading, solvents were eluted under positive nitrogen pressure and fractions were taken in 50-mL tubes. The solvent system was switched to 5000 mL of 4/1 hexane/EtOAc (ACS grade purchased from Fisher Scientific which was used as received). Product (**S**)-**2-4a** (R_f 0.41, hexane/EtOAc 4/1, v/v) eluted, and fractions 31 through 98 were combined, concentrated on a rotary evaporator (30 °C, 780 to 20 mmHg), and dried in vacuo (1-2 mmHg) at ambient temperature for 12 h.



TLC analysis of fractions. (Visualization with UV-C 254 nm)

The product (**S**)-**2-4a** exhibited the following properties:

99% ee (HPLC (Chiralpak IA column, 97:3 hexanes/isopropanol, 1.0 ml/min), *tr* = 15.4 min (*R*), 17.0 min (*S*))

$[\alpha]_{\text{D}}^{23}$ -27.35 (*c* 0.30, CHCl₃)

R_f 0.41 (4/1, hexanes/EtOAc, v/v)

bp 89.5 °C (8.5 mmHg);

IR (film): 3411 (br), 2961, 2932, 1586, 1486, 1451, 1242, 1149, 1077, 1011, 993, 923 cm⁻¹

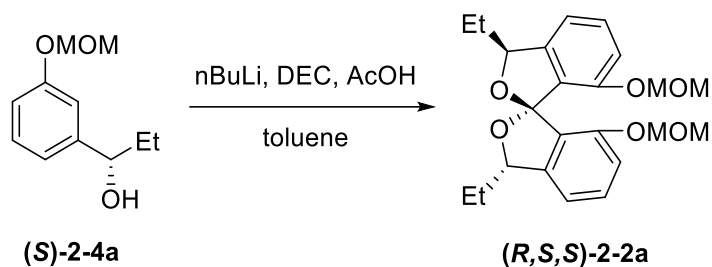
¹H NMR (500 MHz, Chloroform-*d*) δ 7.30 – 7.23 (m, 1H), 7.03 (dt, *J* = 2.6, 1.5 Hz, 1H), 6.97 (dddt, *J* = 17.6, 8.2, 2.5, 0.9 Hz, 2H), 5.18 (d, *J* = 1.1 Hz, 2H), 4.57 (t, *J* = 6.6 Hz, 1H), 3.48 (d, *J* = 1.2 Hz, 3H), 1.86 – 1.68 (m, 2H), 0.93 (td, *J* = 7.4, 1.2 Hz, 3H).

¹³C NMR (100 MHz, Chloroform-*d*) δ 157.4, 146.5, 129.5, 119.6, 115.3, 114.0, 94.5, 75.9, 56.1, 31.9, 10.2

HRMS (ESI) *m/z* calcd for C₁₁H₁₇O₃ [M+H]⁺ 197.1171, found 197.1175.

Purity was determined by quantitative ¹H NMR spectroscopic analysis using dibromomethane as an internal standard to be 99% by weight.

The ee was determined by HPLC analysis with a Waters Alliance e2695 Separations Module HPLC system equipped with a CHIRALPAK IA column (length 250 mm, I.D. 4.6 mm). Optical rotations were measured at room temperature in a solvent of choice on a JASCO P-2000 digital polarimeter at 589 nm (D-line).



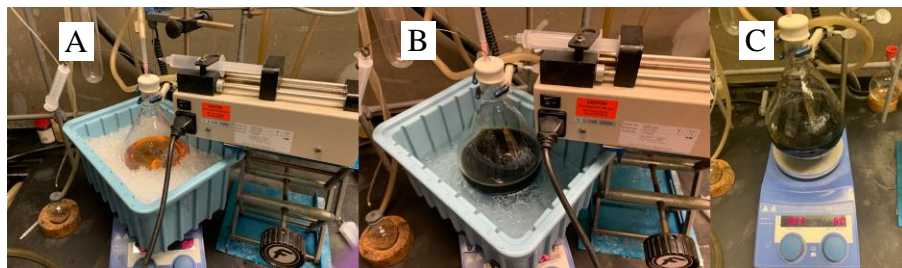
An oven-dried 1000-mL single-neck round bottom flask (24/40 joint) is equipped with a Teflon coated magnetic stir bar (16x32 mm, egg-shape). The flask is sealed with a rubber septum, connected to a Schlenk line via a needle adapter and subsequently cooled to room temperature. (*S*)-1-(3-(methoxymethoxy)phenyl)propan-1-ol **2-4a** (23.0 g, 117.1 mmol, 1.00 equiv.) and toluene (330.0 mL) are added to the flask via syringes and the solution is cooled to 0 °C. Upon which, n-butyllithium solution (97.7 mL, 236.5 mmol, 2.02 equiv.) is added dropwise to the solution over 90 minutes with the syringe pump.



A) Reaction flask set-up after addition of starting material (1) and toluene; B) reaction solution before the *n*BuLi addition; C) reaction solution during the *n*BuLi addition

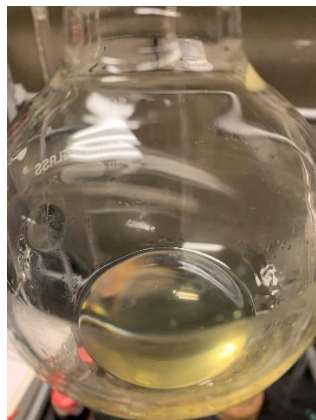
Reaction mixture is then allowed to slowly warm to room temperature. After 3 hours 12.0 mL of THF is added to the resulting suspension and then cooled again to 0 °C. Diethyl carbonate (7.52 mL, 62.1 mmol, 0.53 equiv.) is incorporated over 2 hours at 0 °C with the syringe pump. The reaction mixture is allowed to warm slowly to room temperature overnight. Glacial acetic acid (100.0 mL) is then added to the solution slowly over 10 minutes. After 4 hours deionized

water (400.0 mL) is added to the reaction mixture and the biphasic mixture is transferred to 2000-mL wide-mouth Erlenmeyer flask.



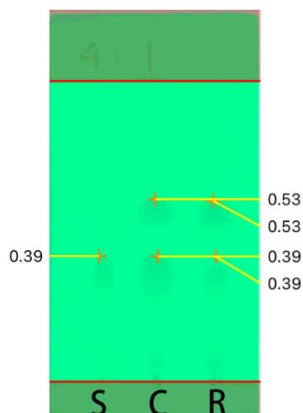
A) Reaction solution before addition of diethyl carbonate; B) reaction solution after addition of diethyl carbonate; C) reaction solution after overnight stirring at room temperature

NaHCO_3 (100.0 g) is added to the solution in small portions and the flask is swirled between additions. The biphasic mixture is transferred to a 2000-mL separatory funnel. The organic layer is collected, and the aqueous layer is extracted with DCM (4x100.0 mL). The combined organic phases are dried with MgSO_4 (100.0 g), filtered into a 2000-mL single-neck round bottom flask (24/40 joint) with DCM washings (3x50.0 mL). The solution is concentrated with the aid of a rotary evaporator to afford a crude yellow oil. The crude product is purified by chromatography on silica to afford (*1R,3S,3'S*)-3,3'-diethyl-7,7'-bis(methoxymethoxy)-3*H,3'H*-1,1'-spirobi-[isobenzofuran] **2** (19.03 g, 80.4%, 99% ee, 98% purity) as a bright yellow oil.



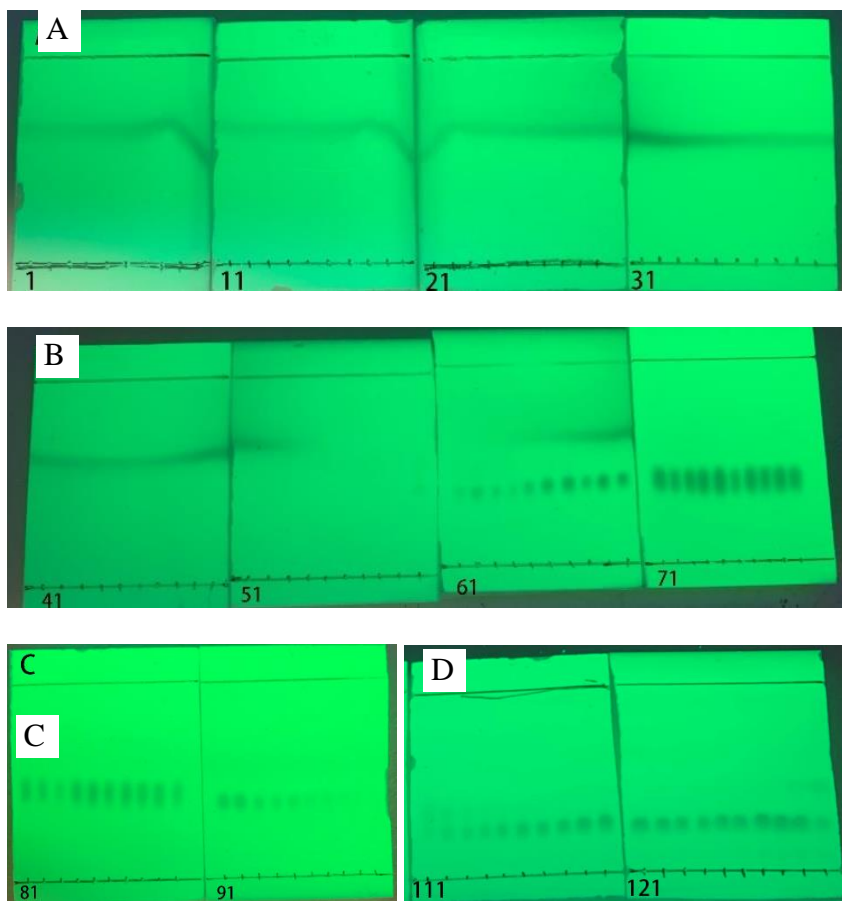
Product 2-2a

The reaction can be monitored by TLC (SiO₂, Hexane/EtOAc 4/1, starting material **2-4a**: R_f 0.39, product **2-2a**: R_f 0.53; UV-C 254 nm) (S refers to starting material. C refers to co-spot of reaction mixture and starting materials. R refers to the reaction mixture.).



TLC monitoring of the reaction

The crude material was loaded onto a slurry-packed (hexane) column (ID 72 mm) containing SiO₂ (500 g, 40 - 63 μ m, 60 Å silica gels purchased from SiliCycle Inc.), and the flask was then rinsed with 9/1 hexane/EtOAc (40 mL) which was loaded afterwards. After loading, solvents were eluted under positive nitrogen pressure and fractions were taken in 50-mL tubes. The solvent system was switched to 1000 mL of 9/1 hexane/EtOAc (ACS grade purchased from Fisher Scientific which was used as received), then 1800 mL of 8/1 hexane/EtOAc, followed by 800 mL of 7/1 hexane/EtOAc, and finished by 1500 mL of 6/1 hexane/EtOAc. Product **2-2a** (R_f 0.53, hexane/EtOAc 4/1, v/v) eluted first and fractions 60 through 99 were combined, concentrated on a rotary evaporator (30 °C, 780 to 20 mmHg), and dried in vacuo (1-2 mmHg) at ambient temperature for 12 h. Starting material **2-4a** (R_f 0.39, hexane/EtOAc 4/1, v/v) eluted later and fractions 111 through 130 were combined, concentrated on a rotary evaporator (30 °C, 780 to 20 mmHg), and dried in vacuo (1-2 mmHg) at ambient temperature for 12 h.



TLC analysis of the fractions. (Visualization with UV-C 254 nm) A) fractions 1 through 40; B) fractions 41 through 80; C) fractions 81 through 100; D) fractions 111 through 130

The product **2-2a** exhibited the following properties:

99% ee (HPLC (Chiralpak IA column, 99:1 hexanes/isopropanol, 1.0 ml/min), $t_r = 12.9$ min (*R*), 15.2 min (*S*))

$[\alpha]_D^{23} +4.76$ (c 2.30, CHCl_3)

R_f 0.53 (4/1, hexanes/EtOAc, v/v)

bp 161.4 °C

IR (film): 2962, 2934, 1614, 1599, 1479, 1256, 1152, 1002, 960, 928, 734 cm^{-1}

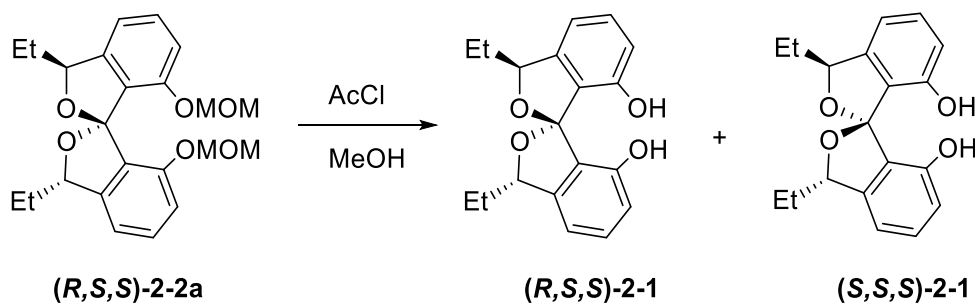
¹H NMR (500 MHz, Chloroform-d) δ 7.28 (dd, $J = 15.6, 7.5$ Hz, 2H), 6.88 (ddd, $J = 7.6, 3.1, 2.2$ Hz, 4H), 5.40 (dd, $J = 7.4, 4.0$ Hz, 2H), 4.94 (d, $J = 6.6$ Hz, 2H), 4.82 (d, $J = 6.6$ Hz, 2H), 3.07 (s, 6H), 2.04 – 1.92 (m, 2H), 1.91 – 1.80 (m, 2H), 1.04 (t, $J = 7.4$ Hz, 6H).

¹³C NMR (101 MHz, Chloroform-d) δ 152.4, 145.6, 130.5, 127.8, 115.8, 113.9, 112.1, 93.3, 83.1, 55.5, 28.0, 9.7

HRMS (ESI) m/z calcd for C₂₃H₂₉O₆ [M+H]⁺ 401.1958, found 401.1964.

Purity was determined by quantitative ¹H NMR spectroscopic analysis using 1,3,5-trimethoxybenzene as an internal standard to be 98% by weight.

The ee was determined by HPLC analysis with a Waters Alliance e2695 Separations Module HPLC system equipped with a CHIRALPAK IA column (length 250 mm, I.D. 4.6 mm). Optical rotations were measured at room temperature in a solvent of choice on a JASCO P-2000 digital polarimeter at 589 nm (D-line).



The deprotection of the MOM group using AcCl in MeOH was mild enough that after 6h at room temperature the contra-thermodynamic diol (**(R,S,S)-2-1**) is the major compound. However, SiO₂ and other acidic conditions epimerize it into (**(S,S,S)-2-1**). These results agree with the calculated ΔG of 1.0 kcal/mol favoring (**(R,S,S)-2-1**). Consequently, neutralizing the acidic conditions after 6h of reaction yields (**(R,S,S)-2-1**) selectively, while performing chromatography after the reaction time gives (**(S,S,S)-2-1**) enriched material, as exemplified below.

(*R,S,S*)-selective deprotection

Spiroketal (***R,S,S***)-**2-2a** (21.9mg, 0.055mmol) and MeOH (0.5mL) were added to a vial. Solution was cooled to 0°C, and then acetyl chloride (8.0μL, 0.11mmol) was added slowly. Reaction mixture was warmed to room temperature. After 6h, reaction mixture was quenched with a saturated solution of NaHCO₃. Extracted three times with DCM, and then combined organic was dried with Na₂SO₄, and concentrated *in vacuo* to afford diol **2-1** (17.0mg, 99% yield, dr ~1:3.1:11.7 of (***S,R,S***)-**2-1**:(***S,S,S***)-**2-1**:(***R,S,S***)-**2-1**).

¹H NMR (500 MHz, Chloroform-*d*) δ 7.34 (t, *J* = 7.7 Hz, 1H), 6.86 (d, *J* = 7.5, 1H), 6.77 (d, *J* = 8.0, 1H), 5.41 (dd, *J* = 6.7, 4.1 Hz, 1H), 4.73 (s, 1H), 2.07 (m, 1H), 1.83 (m, 1H), 1.01 (t, *J* = 7.4 Hz, 3H).

¹³C NMR (126 MHz, Chloroform-*d*) δ 151.8, 145.3, 132.3, 123.2, 115.4, 113.6, 83.0, 27.7, 9.1.

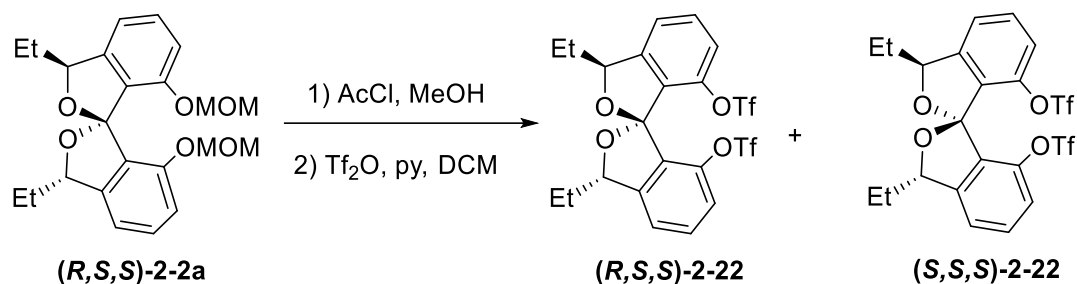
ESI-HRMS Calcd. for C₁₉H₂₁O₄⁺ 314.1440 [M+H]⁺, found 314.1435.

(*S,S,S*)-selective deprotection

Spiroketal (***R,S,S***)-**2-2a** (2.82g, 7.04mmol) and MeOH (35mL) were added to a round bottom flask. Solution was cooled to 0°C, and then acetyl chloride (1.0mL, 14.1mmol) was added slowly. Reaction mixture was warmed to room temperature. After 6h, reaction mixture was concentrated *in vacuo*, and purified by FCC (SiO₂, 30%→40% EtOAc in hexanes) to obtain diol **2-1** (2.15g, 97.5% yield 1:5.7:11.0 dr (***S,R,S***)-**2-1**:(***R,S,S***)-**2-1**:(***S,S,S***)-**2-1**).

¹H NMR (500 MHz, Chloroform-*d*) δ 7.31 (t, *J* = 7.8 Hz, 1H), 6.86 (d, *J* = 7.5 Hz, 1H), 6.75 (d, *J* = 8.0 Hz, 1H), 5.27 (dd, *J* = 7.6, 4.4 Hz, 1H), 4.60 (s, 1H), 1.99 – 1.85 (m, 2H), 1.07 (t, *J* = 7.3 Hz, 3H).

¹³C NMR (126 MHz, Chloroform-*d*) δ 151.6, 145.2, 131.9, 123.3, 115.4, 113.8, 84.8, 30.6, 9.7.



The $(R,S,S)\text{-}2\text{-}22:(S,S,S)\text{-}2\text{-}22$ ratio was mostly conserved during the triflation, so the product ratio depended on the d.r. of the diol used. An $(S,S,S)\text{-}2\text{-}22$ -selective preparation is described next. Spiroketal $(R,S,S)\text{-}2\text{-}2a$ (12.57g, 7.0mmol) and methanol (160mL) were cooled to 0°C before dropwise addition of acetyl chloride (1.0mL, 14.1mmol). Reaction mixture was then warmed to room temperature. After for 6h, the volatiles were removed *in vacuo*, and the crude was purified by FCC (SiO_2 , 30%→40% EtOAc in hexanes). Purified diol, DCM (150mL), and pyridine (12.5mL, 165.3mmol) were cooled to 0°C before addition of trifluoromethanesulfonic anhydride (12.0mL, 71.5mmol) over 30min. Reaction mixture was then warmed to room temperature. After 1h, a saturated aqueous solution of NaHCO_3 (150mL) was added. After separating the layers, the aqueous phase extracted with DCM twice. Combined organic was dried over Na_2SO_4 and concentrated *in vacuo*. Crude was purified by a short column (SiO_2 , 10% EtOAc in hexanes) to afford a mixture of triflates as an oil which solidified on cooling (15.8g, 1:2.6:4.7 d.r. of $(S,R,S)\text{-}2\text{-}22:(R,S,S)\text{-}2\text{-}22:(S,S,S)\text{-}2\text{-}22$, 49.6% yield of desired $(S,S,S)\text{-}2\text{-}22$, 27.1% yield of $(R,S,S)\text{-}2\text{-}22$).

The ditriflates can be separated by FCC (SiO_2 , 4% EtOAc in hexanes), but for convenience we chose to do a chemical resolution (*vide infra*). The spectral characteristics of the isolated ditriflates are shown below:

(*1R,3S,3'S*)-3,3'-diethyl-3*H,3'H*-1,1'-spirobi[isobenzofuran]-7,7'-diyl

bis(trifluoromethanesulfonate) (***R,S,S***)-**2-22**

¹H NMR (400 MHz, Chloroform-*d*) δ 7.53 (t, $J = 7.9$ Hz, 2H), 7.30 (d, $J = 8.5$ Hz, 4H), 5.36 (dd, $J = 8.5, 4.0$ Hz, 2H), 2.05 (m, $J = 15.0, 7.5, 4.0$ Hz, 2H), 1.97 – 1.82 (m, 2H), 1.11 (t, $J = 7.4$ Hz, 6H).

¹⁹F NMR (376 MHz, Chloroform-*d*) δ -74.57.

¹³C NMR (100 MHz, Chloroform-*d*) δ 147.8, 144.9, 132.2, 129.8, 122.9, 120.8, 119.7, 119.1, 116.5, 113.3, 83.6, 27.3, 10.0.

ESI-HRMS Calcd. for C₂₁H₁₉F₆O₈S₂⁺ 577.0426 [M+H]⁺, found 577.0415.

IR (powder): $\nu_{\max} = 2975, 2878, 1470, 1419, 1204, 1137, 936, 896, 848$ cm⁻¹

(*1S,3S,3'S*)-3,3'-diethyl-3*H,3'H*-1,1'-spirobi[isobenzofuran]-7,7'-diyl

bis(trifluoromethanesulfonate) (***S,S,S***)-**2-22**

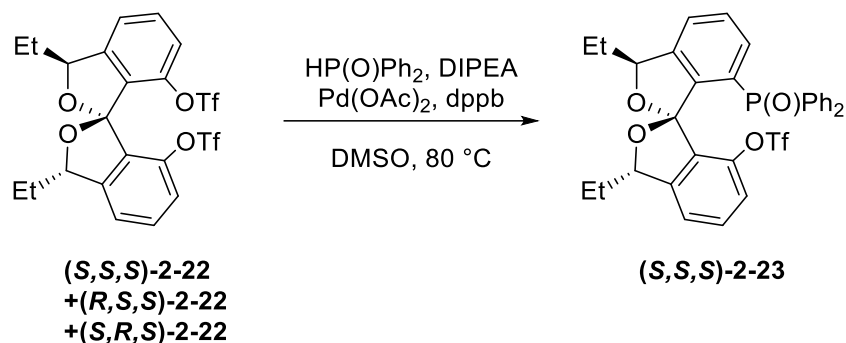
¹H NMR (400 MHz, Chloroform-*d*) δ 7.51 (t, $J = 7.9$ Hz, 2H), 7.29 (d, $J = 7.5$ Hz, 2H), 7.23 (d, $J = 8.2$ Hz, 2H), 5.38 (dd, $J = 7.2, 4.5$ Hz, 2H), 2.07 – 1.81 (m, 4H), 1.06 (t, $J = 7.4$ Hz, 6H)

¹⁹F NMR (376 MHz, Chloroform-*d*) δ -74.58.

¹³C NMR (100 MHz, Chloroform-*d*) δ 147.3, 144.7, 132.0, 130.3, 122.9, 121.2, 119.7, 119.6, 119.6, 116.5, 114.5, 113.3, 84.7, 30.0, 9.4.

ESI-HRMS Calcd. for C₂₁H₁₉F₆O₈S₂⁺ 577.0426 [M+H]⁺, found 577.0418.

IR (powder): $\nu_{\max} = 2973, 2880, 1470, 1422, 1207, 1137, 935, 852, 749$ cm⁻¹



A flask in the glovebox was charged with a 1:2.6:4.7 mixture of ditriflates (**(S,R,S)-2-22**:**(R,S,S)-2-22**:**(S,S,S)-2-22**) (12.624g, 21.86mmol), palladium(II) acetate (245mg, 1.09mmol), 1,4-Bis(diphenylphosphino)butane (466mg, 1.09mmol), and diphenylphosphine oxide (4.861g, 24.04mmol). The flask was taken outside the glovebox, and DMSO (85mL) and N,N-Diisopropylethylamine (9.5mL, 54.64mmol) were added. Reaction mixture was then stirred at room temperature for 1h, before being heated to 80°C. After 8h, reaction mixture was cooled to room temperature and partitioned between EtOAc (260mL) and a half saturated aqueous solution of NaHCO₃ (260mL). After separating the layers, the aqueous phase was extracted with EtOAc twice. Combined organic was washed with brine, dried over Na₂SO₄, and concentrated *in vacuo*. Crude was purified by FCC (SiO₂, 10 → 50% EtOAc in hexanes) to yield two fractions. At 10% EtOAc in hexanes, a mixture of **(S,R,S)-2-22** and **(R,S,S)-2-22** was obtained (1:4.2 d.r., 3.88g of useful **(R,S,S)-2-22**, 99.0% recovery based on starting **(R,S,S)-2-22**). At 50% EtOAc in hexanes, a mixture of epimeric product **(S,R,S)-2-23** and desired phosphine oxide **(S,S,S)-2-23** was obtained (1:12.6 d.r., 7.34g of desired **(S,S,S)-2-23**, 93.8% yield based on starting **(S,S,S)-2-22**). The desired product was further purified by two recrystallizations from cyclohexane with excellent recovery. The first recrystallization of 5.71g of the product mixture gave 5.33g of a 1:26 mixture of epimeric product **(S,R,S)-2-22** and desired phosphine oxide **(S,S,S)-2-23**, respectively (97% recovery of product). Chiral HPLC analysis showed that the desired product

was enantioenriched to >99% ee. A second recrystallization of 5.02g of this mixture produced 4.58g of almost pure (*S,S,S*)-**2-23** (1:65 with respect to (*S,R,S*)- **2-23**) (93% recovery of product), as a white foam.

¹H NMR (500 MHz, Chloroform-*d*) δ 7.52 – 7.42 (m, 4H), 7.42 – 7.31 (m, 4H), 7.27 – 7.21 (m, 2H), 7.21 – 7.10 (m, 4H), 7.02 (dd, $J = 13.9, 7.5$ Hz, 1H), 6.41 (dd, $J = 7.1, 1.5$ Hz, 1H), 5.56 (dd, $J = 7.1, 4.7$ Hz, 1H), 5.28 (dd, $J = 7.2, 5.0$ Hz, 1H), 1.92 (m, $J = 13.5, 6.3$ Hz, 3H), 1.83 (m, $J = 14.3, 7.2$ Hz, 1H), 1.06 (t, $J = 7.4$ Hz, 3H), 0.99 (t, $J = 7.4$ Hz, 3H).

¹³C NMR (126 MHz, Chloroform-*d*) δ 148.8, 146.4, 146.4, 144.1, 141.6, 141.6, 133.8, 133.7, 133.7, 132.9, 132.51, 132.14, 132.07, 131.68, 131.55, 131.53, 131.31, 131.25, 131.20, 131.1, 131.0, 130.9, 128.5, 128.4, 128.2, 128.1, 128.1, 128.0, 127.4, 125.3, 125.3, 121.8, 120.4, 119.3, 118.4, 116.8, 116.2, 85.2, 83.4, 30.6, 29.7, 26.9, 9.8, 9.6.

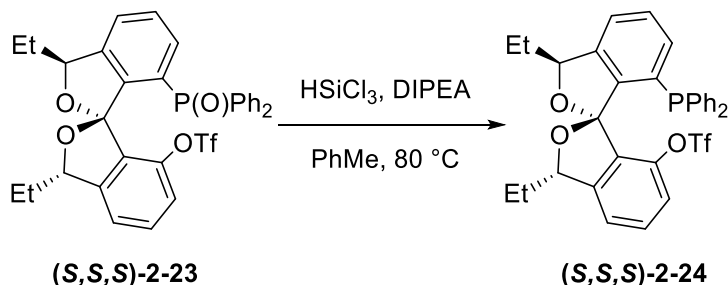
¹⁹F NMR (471 MHz, Chloroform-*d*) δ -75.05.

³¹P NMR (202 MHz, Chloroform-*d*) δ 28.57.

ESI-HRMS Calcd. for C₃₂H₂₉F₃O₆PS⁺ 629.1375 [M+H]⁺, found 629.1366.

IR (powder): $\nu_{\max} = 2934, 1419, 1210, 1194, 1140, 931$ cm⁻¹

$[\alpha]_D$: -70.8 ($c = 1.0$ in DCM)



Phosphine oxide (*S,S,S*)-**2-23** (4.95g, 7.88mmol), PhMe (80mL), and Diisopropylethylamine (55mL, 316.8mmol) were cooled to 0°C before addition of trichlorosilane (12.5mL, 126.1mmol)

over 10min. The flask was sealed with a glass stopper and heated to 80°C. After 20h, the mixture was cooled to room temperature and quenched carefully by transferring it to a flask containing a saturated aqueous solution of NaHCO₃ (120mL) at 0°C, with diethyl ether washings. Crude was filtered through Celite with diethyl ether washings, and the filtrate was dried over Na₂SO₄ and concentrated *in vacuo*. Crude was purified by FCC (SiO₂, 5% EtOAc in hexanes) to afford (*S,S,S*)-**2-24** (3.89g, 80.7% yield) as white foam.

¹H NMR (500 MHz, Chloroform-d) δ 7.32 (t, *J* = 7.5 Hz, 1H), 7.29 – 7.20 (m, 6H), 7.17 (d, *J* = 7.5 Hz, 1H), 7.13 (td, *J* = 7.5, 1.5 Hz, 2H), 7.07 (td, *J* = 7.5, 2.0 Hz, 2H), 6.89 (dd, *J* = 7.4, 4.6 Hz, 1H), 6.85 (td, *J* = 7.9, 1.4 Hz, 2H), 6.62 (d, *J* = 8.1 Hz, 1H), 5.35 (td, *J* = 6.8, 4.6 Hz, 2H), 1.96 (m, *J* = 16.9, 14.0, 5.9 Hz, 2H), 1.87 (m, *J* = 14.2, 7.2, 4.6 Hz, 2H), 1.06 (t, *J* = 7.3 Hz, 3H), 1.00 (t, *J* = 7.3 Hz, 3H).

¹³C NMR (126 MHz, Chloroform-d) δ 147.3, 147.3, 144.5, 143.6, 143.6, 142.5, 142.3, 137.0, 136.9, 135.4, 135.4, 133.9, 133.9, 133.6, 133.4, 133.4, 133.3, 132.5, 132.5, 132.4, 131.4, 129.5, 128.4, 128.2, 128.1, 128.1, 128.0, 127.9, 122.0, 120.5, 119.3, 118.8, 116.8, 116.5, 116.4, 84.6, 84.6, 84.0, 30.4, 29.7, 9.6, 9.4.

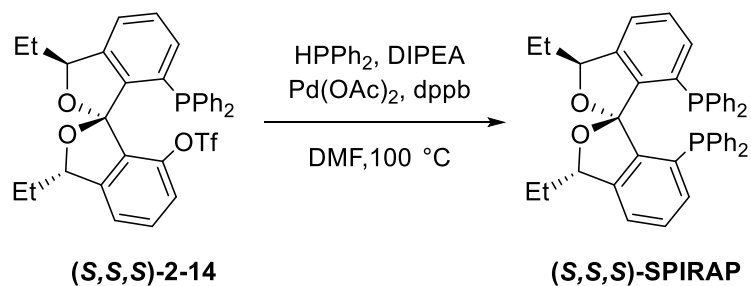
¹⁹F NMR (471 MHz, Chloroform-d) δ -74.90.

³¹P NMR (202 MHz, Chloroform-d) δ -18.88.

ESI-HRMS Calcd. for C₃₂H₂₉F₃O₅PS⁺ 613.1425 [M+H]⁺, found 613.1419.

IR (powder): ν_{max} = 2970, 1738, 1421, 1211, 1140, 943 cm⁻¹

[α]_D: -44.0 (c = 1.0 in DCM)



A Schlenk flask was charged with palladium(II) acetate (36.6mg, 0.163mmol) and 1,4-Bis(diphenylphosphino)butane (76.6mg, 0.180mmol). DMF (3.0mL) and diisopropylethylamine (1.8mL, 10.3mmol) were added. Solution was stirred at room temperature. After 1h, diphenyl phosphine (850 μ L, 4.89mmol) was added. After 5min, phosphine **(S,S,S)-2-24** (1.000g, 1.632mmol) was added as a solution in DMF (3.5mL, including washings). The sealed flask was heated to 100 $^\circ$ C. After 24h, volatiles were removed under N₂ flow. Crude was purified by FCC (SiO₂, 0 \rightarrow 15% \rightarrow 30% DCM in hexanes), and the product was then washed with hexanes to yield **(S,S,S)-SPIRAP 2-25** (977mg, 92.3% yield) as white solid.

¹H NMR (700 MHz, Chloroform-d) δ 7.30 (t, $J = 7.5$ Hz, 2H), 7.23 (tq, $J = 13.7, 7.6$ Hz, 10H), 7.17 – 7.10 (m, 4H), 7.06 (td, $J = 7.5, 1.8$ Hz, 4H), 6.89 (dd, $J = 7.5, 4.5$ Hz, 2H), 6.83 (t, $J = 7.4$ Hz, 4H), 4.96 (dd, $J = 6.8, 4.3$ Hz, 2H), 1.86 (m, $J = 14.6, 7.3, 4.1$ Hz, 2H), 1.76 (m, $J = 14.3, 7.2$ Hz, 2H), 0.87 (t, $J = 7.3$ Hz, 6H).

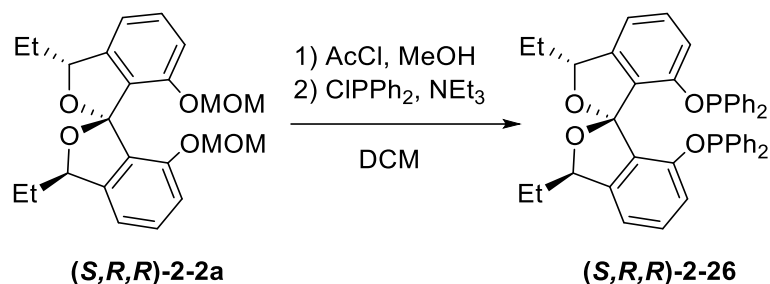
¹³C NMR (176 MHz, Chloroform-d) δ 145.5, 145.4, 145.3, 145.3, 144.0, 144.0, 144.0, 144.0, 138.2, 138.1, 136.8, 136.7, 134.1, 133.9, 133.7, 133.7, 133.1, 133.0, 132.5, 132.4, 129.1, 128.2, 128.0, 127.9, 127.9, 127.8, 127.8, 127.7, 121.5, 118.5, 83.2, 83.2, 29.7, 9.3.

³¹P NMR (283 MHz, Chloroform-d) δ -18.71.

ESI-HRMS Calcd. for C₄₃H₃₉O₂P₂⁺ 649.2425 [M+H]⁺, found 649.2417.

IR (powder): $\nu_{\text{max}} = 2970, 1739, 1433, 1365, 1217, 696\text{ cm}^{-1}$

$[\alpha]_{\text{D}}$: -227.4 ($c = 1.0$ in CHCl₃)



Spiroketal **(S,R,R)-2-2a** (40mg, 0.10mmol) and methanol (1.0mL) were cooled to 0°C before dropwise addition of acetyl chloride (14μL, 0.20mmol). Reaction mixture was then warmed to room temperature. After for 6h, the volatiles were removed in vacuo. The crude diol and 4-Dimethylaminopyridine (1.2mg, 0.01mmol) were dissolved into DCM (1.0mL) at room temperature before addition of triethylamine (0.13mL, 1.0mmol) and chlorodiphenylphosphine (46μL, 0.25mmol) over 30min. After 12h, volatiles were removed *in vacuo*, and the crude was purified by FCC (SiO₂ treated with 5% TEA, 4%→ 9% EtOAc in hexanes) to afford **(S,R,R)-SPIRAPO** (34mg, 56% yield) and **(R,R,R)-SPIRAPO** (17mg, 26% yield) as white foams.

For purified **(S,R,R)-2-26**

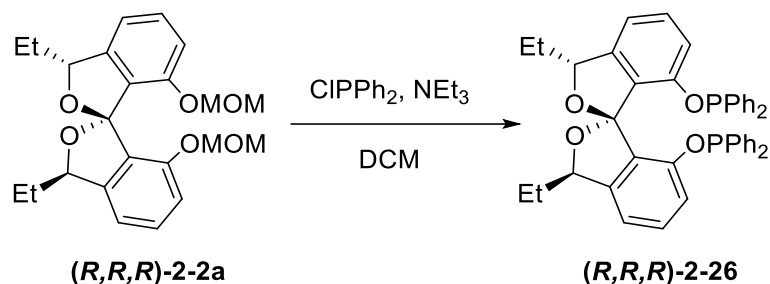
¹H NMR (399.54 MHz, Chloroform-d) δ 7.31-7.21 (m, 12H), 7.14 (t, *J* = 7.4 Hz, 2H), 7.06 (m, 6H), 6.97 – 6.90 (m, 4H), 6.86 – 6.81 (m, 2H), 5.26 (dd, *J* = 8.2, 4.2 Hz, 2H), 1.57 (m, 2H), 1.41 (m, 2H), 0.87 (t, *J* = 7.4 Hz, 6H)

¹³C NMR (100 MHz, Chloroform-d) δ 152.3, 152.2, 146.3, 140.1, 139.9, 139.8, 139.7, 130.7, 130.5, 130.4, 129.7, 129.6, 129.5, 128.8, 128.3, 128.3, 128.2, 128.1, 115.3, 115.1, 115.0, 114.6, 82.9, 28.0, 10.2

³¹P NMR (161.75 MHz, Chloroform-d) δ 105.24

ESI-HRMS Calcd. for C₄₃H₃₉O₄P₂⁺ 681.2317 [M+H]⁺, found 681.2316.

[α]_D: -80.7 (c = 1.25 in THF)



For purified **(*R,R,R*)-2-26**

¹H NMR (500 MHz, Chloroform-*d*) δ 7.34 – 7.19 (m, 12H), 7.15 (t, $J = 7.7$ Hz, 2H), 7.13 – 6.99 (m, 6H), 6.97 (t, $J = 7.4$ Hz, 4H), 6.71 (d, $J = 7.5$ Hz, 2H), 4.78 (dd, $J = 7.2, 4.5$ Hz, 2H), 1.89 – 1.72 (m, 4H), 0.99 (t, $J = 7.4$ Hz, 6H).

¹³C NMR (126 MHz, Chloroform-*d*) δ 145.8, 130.8, 130.6, 130.4, 130.4, 129.7, 129.6, 129.5, 129.0, 128.2, 128.1, 115.1, 114.7, 84.2, 30.0, 9.7.

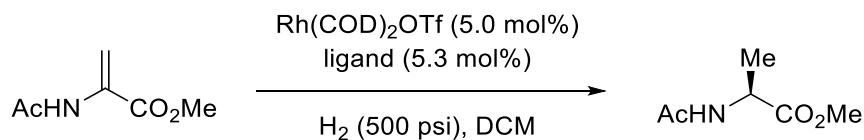
³¹P NMR (202 MHz, Chloroform-*d*) δ 104.37.

$[\alpha]_D$: -14.8 ($c = 5.25$ in THF)

Asymmetric catalysis with SPIROL-based ligands

Asymmetric hydrogenation of acrylate derivatives

Methyl acetyl-*L*-alaninate



The asymmetric hydrogenation of acetamidoacrylic esters was based on a reported procedure.³⁵

(*S,R,R*)-SPIRAPO (11.2mg, 0.016mmol) and $\text{Rh(COD)}_2\text{OTf}$ (7.0mg, 0.015mmol) were measured and packed into a Schlenk tube in the glovebox before the addition of dry DCM (3.0mL) to make a stock solution. Methyl 2-acetamidoacrylate (28.6mg, 0.20mmol) was added to the flask before addition of the stock solution (2.0mL). The reaction flask was placed into the

hydrogenation apparatus before purging with N₂ and H₂, and the reaction was stirred under 500 psi H₂ for 3h. Volatiles were removed *in vacuo*, and the crude was purified by FCC (SiO₂, 20% EtOAc in hexanes) to afford methyl acetyl-L-alaninate (25.3mg, 87% yield, 91% ee) as clear oil.

¹H NMR (400 MHz, Chloroform-d) δ 6.02 (s, 1H), 4.58 (p, *J* = 7.3 Hz, 1H), 3.74 (s, 3H), 2.00 (s, 3H), 1.38 (d, *J* = 7.1 Hz, 3H).

¹³C NMR (100 MHz, Chloroform-d) δ 173.6, 169.5, 52.4, 48.0, 23.1, 18.5.

IR (film): ν_{\max} = 3282, 2955, 1739, 1652, 1533, 1436, 1372, 1207, 1160, 1058, 733, 607 cm⁻¹

GC conditions 1:

Rt- bDExsm column (df = 0.25 μm, 0.25 mm i.d. × 30 m, fused silica capillary column); carrier gas, He (flow 1.5 mL/min); injection temp, 230 °C; initial column temperature, 70 °C; progress rate, 2 °C /min; final column temperature, 90 °C); t_r = 28.9 min (minor, *R*), 29.3 min (major, *S*)

GC conditions 2

Rt- bDExsm column (df = 0.25 μm, 0.25 mm i.d. × 30 m, fused silica capillary column); carrier gas, He (flow 1.5 mL/min); injection temp, 230 °C; initial column temperature, 70 °C; progress rate, 2 °C /min; final column temperature, 110 °C); t_r = 48.7 min (major, *R*), 51.2 min (minor, *S*)

For (*S*)-SDPO – 85% yield, 94% ee for (*S*)

For (*S*)-BINAPO – 84% yield, -91% ee for (*R*)

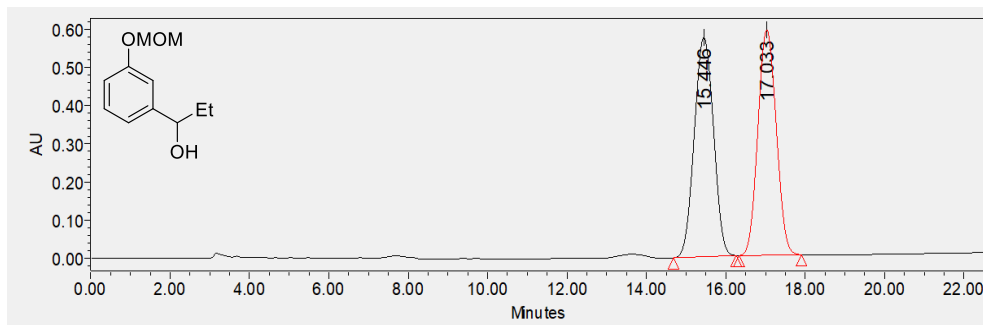
For (*R,R,R*)-SPIRAPO – 85% yield, -93% ee for (*R*)

Data for iridium-catalyzed hydroarylation and palladium-catalyzed allylic alkylation could be found in the supplement information section in our paper.¹⁰

HPLC and GC traces

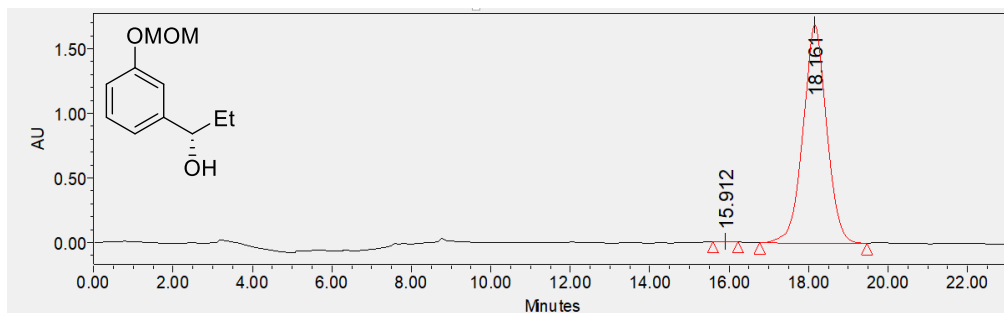
1-(3-(methoxymethoxy)phenyl)propan-1-ol **2-4a**

Racemic



Retention Time [min]	% Area
15.446	50.56
17.033	49.44

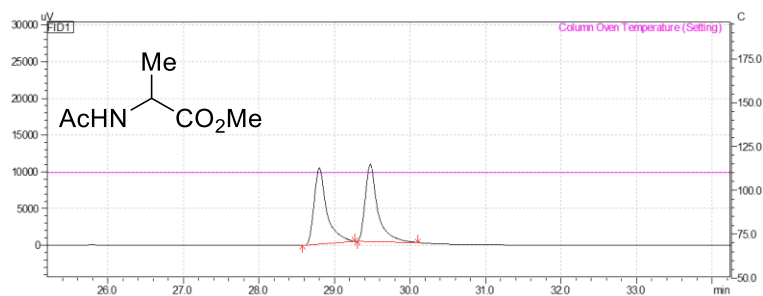
(S)-2-4a



Retention Time [min]	% Area
15.912	0.09
18.161	99.91

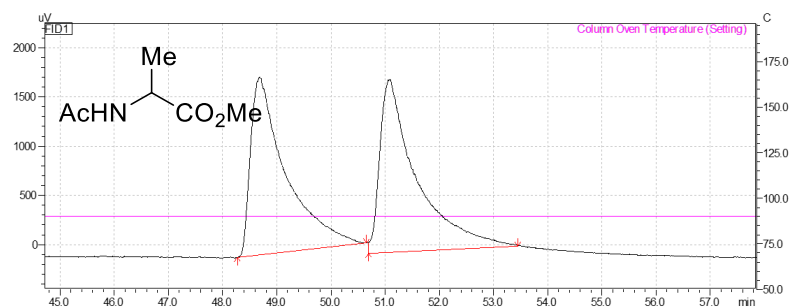
Methyl acetylalaninate

Racemic (GC conditions 1)



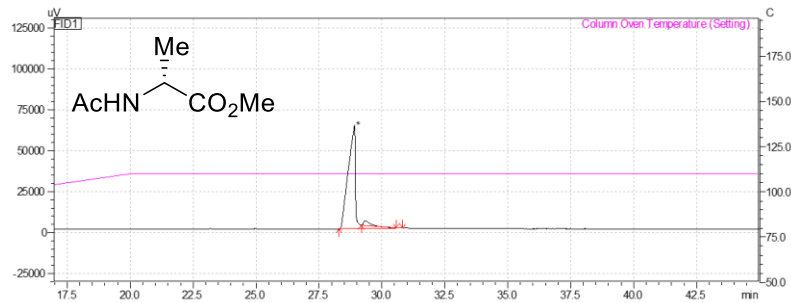
Retention Time [min]	% Area
28.800	50.176
29.476	49.824

Racemic (GC conditions 2)



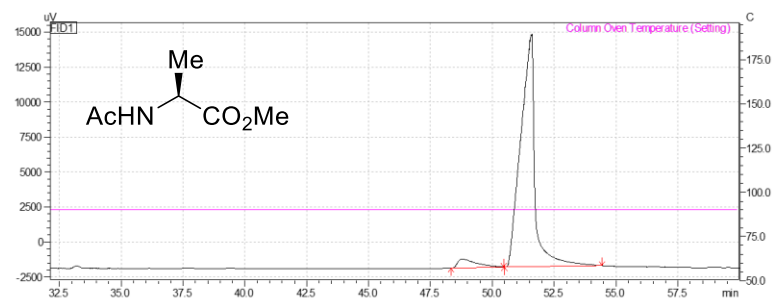
Retention Time [min]	% Area
48.687	49.415
51.078	50.585

With (*R,R,R*)-SPIRAPO (GC conditions 1)



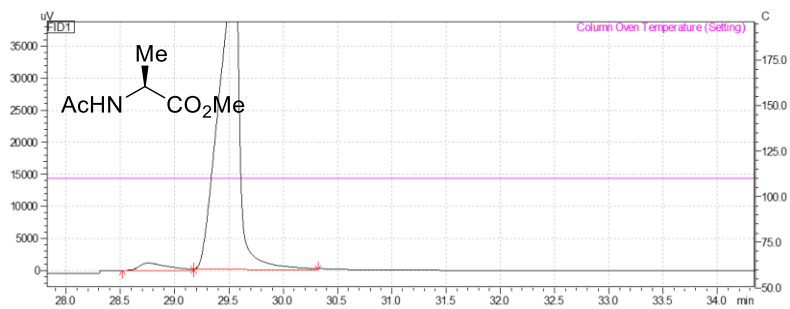
Retention Time [min]	% Area
28.914	96.449
29.344	3.551

With (*S,R,R*)-SPIRAPO (GC conditions 2)



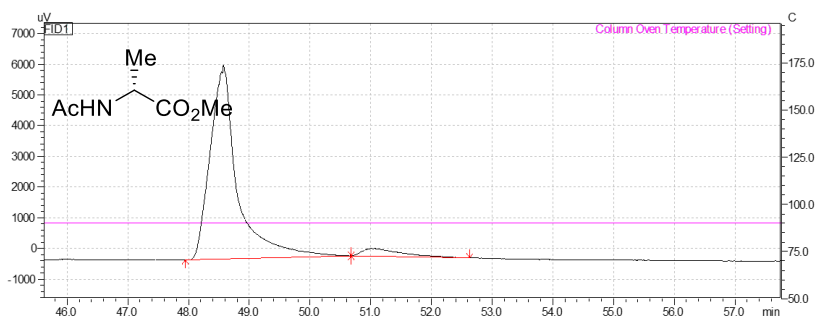
Retention Time [min]	% Area
48.776	4.785
51.595	95.215

With (*S*)-SDPO (GC conditions 1)



Retention Time [min]	% Area
28.753	3.256
29.553	96.744

With (*S*)-BINAPO (GC conditions 2)



Retention Time [min]	% Area
48.576	94.717
51.020	5.283

2.7. References

- (1) Xie, J.-H.; Zhou, Q.-L. Chiral Diphosphine and Monodentate Phosphorus Ligands on a Spiro Scaffold for Transition-Metal-Catalyzed Asymmetric Reactions. *Acc. Chem. Res.* **2008**, *41* (5), 581–593. <https://doi.org/10.1021/ar700137z>.
- (2) Rahman, A.; Lin, X. Development and Application of Chiral Spirocyclic Phosphoric Acids in Asymmetric Catalysis. *Org. Biomol. Chem.* **2018**, *16* (26), 4753–4777. <https://doi.org/10.1039/C8OB00900G>.
- (3) Ding, K.; Han, Z.; Wang, Z. Spiro Skeletons: A Class of Privileged Structure for Chiral Ligand Design. *Chem. – Asian J.* **2009**, *4* (1), 32–41. <https://doi.org/10.1002/asia.200800192>.
- (4) Xie, J.-H.; Wang, L.-X.; Fu, Y.; Zhu, S.-F.; Fan, B.-M.; Duan, H.-F.; Zhou, Q.-L. Synthesis of Spiro Diphosphines and Their Application in Asymmetric Hydrogenation of Ketones. *J. Am. Chem. Soc.* **2003**, *125* (15), 4404–4405. <https://doi.org/10.1021/ja029907i>.
- (5) Guo, X.-X.; Xie, J.-H.; Hou, G.-H.; Shi, W.-J.; Wang, L.-X.; Zhou, Q.-L. Asymmetric Palladium-Catalyzed Hydrosilylation of Styrenes Using Efficient Chiral Spiro Phosphoramidite Ligands. *Tetrahedron Asymmetry* **2004**, *15* (14), 2231–2234. <https://doi.org/10.1016/j.tetasy.2004.05.038>.
- (6) Zhu, S.-F.; Yang, Y.; Wang, L.-X.; Liu, B.; Zhou, Q.-L. Synthesis and Application of Chiral Spiro Phospholane Ligand in Pd-Catalyzed Asymmetric Allylation of Aldehydes with Allylic Alcohols. *Org. Lett.* **2005**, *7* (12), 2333–2335. <https://doi.org/10.1021/ol050556x>.
- (7) Birman, V. B.; L. Rheingold, A.; Lam, K.-C. 1,1'-Spirobiindane-7,7'-Diol: A Novel, C₂-Symmetric Chiral Ligand. *Tetrahedron Asymmetry* **1999**, *10* (1), 125–131. [https://doi.org/10.1016/S0957-4166\(98\)00481-9](https://doi.org/10.1016/S0957-4166(98)00481-9).
- (8) Zhang, J.-H.; Liao, J.; Cui, X.; Yu, K.-B.; Zhu, J.; Deng, J.-G.; Zhu, S.-F.; Wang, L.-X.; Zhou, Q.-L.; Chung, L. W.; Ye, T. Highly Efficient and Practical Resolution of 1,1'-Spirobiindane-7,7'-Diol by Inclusion Crystallization with N-Benzylcinchonidinium

- Chloride. *Tetrahedron Asymmetry* **2002**, *13* (13), 1363–1366. [https://doi.org/10.1016/S0957-4166\(02\)00360-9](https://doi.org/10.1016/S0957-4166(02)00360-9).
- (9) Li, S.; Zhang, J.-W.; Li, X.-L.; Cheng, D.-J.; Tan, B. Phosphoric Acid-Catalyzed Asymmetric Synthesis of SPINOL Derivatives. *J. Am. Chem. Soc.* **2016**, *138* (50), 16561–16566. <https://doi.org/10.1021/jacs.6b11435>.
- (10) Argüelles, A. J.; Sun, S.; Budaitis, B. G.; Nagorny, P. Design, Synthesis, and Application of Chiral C_2 -Symmetric Spiroketal-Containing Ligands in Transition-Metal Catalysis. *Angew. Chem. Int. Ed.* **2018**, *57* (19), 5325–5329. <https://doi.org/10.1002/anie.201713304>.
- (11) Kohler, M. C.; Wengryniuk, S. E.; Coltart, D. M. ASYMMETRIC A-ALKYLATION OF ALDEHYDES, KETONES, AND CARBOXYLIC ACIDS. **2013**.
- (12) Pu, L.; Yu, H.-B. Catalytic Asymmetric Organozinc Additions to Carbonyl Compounds. *Chem. Rev.* **2001**, *101* (3), 757–824. <https://doi.org/10.1021/cr000411y>.
- (13) Lumbroso, A.; Cooke, M. L.; Breit, B. Catalytic Asymmetric Synthesis of Allylic Alcohols and Derivatives and Their Applications in Organic Synthesis. *Angew. Chem. Int. Ed.* **2013**, *52* (7), 1890–1932. <https://doi.org/10.1002/anie.201204579>.
- (14) Lemire, A.; Côté, A.; Charette, A. B. Synthesis and Applications of Diorganozinc Reagents: Beyond Diethylzinc. 1.
- (15) Binder, C. M.; Singaram, B. Asymmetric Addition of Diorganozinc Reagents to Aldehydes and Ketones. *Org. Prep. Proced. Int.* **2011**, *43* (2), 139–208. <https://doi.org/10.1080/00304948.2011.564538>.
- (16) Oguni, N.; Omi, T. Enantioselective Addition of Diethylzinc to Benzaldehyde Catalyzed by a Small Amount of Chiral 2-Amino-1-Alcohols. *Tetrahedron Lett.* **1984**, *25* (26), 2823–2824. [https://doi.org/10.1016/S0040-4039\(01\)81300-9](https://doi.org/10.1016/S0040-4039(01)81300-9).
- (17) Kitamura, Masato.; Suga, Seiji.; Kawai, Koji.; Noyori, Ryoji. Catalytic Asymmetric Induction. Highly Enantioselective Addition of Dialkylzincs to Aldehydes. *J. Am. Chem. Soc.* **1986**, *108* (19), 6071–6072. <https://doi.org/10.1021/ja00279a083>.
- (18) Yoshioka, M.; Kawakita, T.; Ohno, M. Asymmetric Induction Catalyzed by Conjugate Bases of Chiral Proton Acids as Ligands: Enantioselective Addition of Dialkylzinc-Orthotitanate Complex to Benzaldehyde with Catalytic Ability of a Remarkable High Order. *Tetrahedron Lett.* **1989**, *30* (13), 1657–1660. [https://doi.org/10.1016/S0040-4039\(00\)99546-7](https://doi.org/10.1016/S0040-4039(00)99546-7).

- (19) Schmidt, B.; Seebach, D. Catalytic and Stoichiometric Enantioselective Addition of Diethylzinc to Aldehydes Using a Novel Chiral Spirotitanate. *Angew. Chem. Int. Ed. Engl.* **1991**, *30* (1), 99–101. <https://doi.org/10.1002/anie.199100991>.
- (20) (2S)-(-)-3-Exo-(DIMETHYLAMINO)ISOBORNEOL [(2S)-(-)-DAIB]. *Org. Synth.* **2002**, *79*, 130. <https://doi.org/10.15227/orgsyn.079.0130>.
- (21) Nugent, W. A. MIB: An Advantageous Alternative to DAIB for the Addition of Organozinc Reagents to Aldehydes. *Chem. Commun.* **1999**, No. 15, 1369–1370. <https://doi.org/10.1039/A904042K>.
- (22) Watanabe, M.; Soai, K. Catalytic Asymmetric Synthesis of γ -Hydroxy Ketones and Aromatic Hydroxy Ketones by the Chemo- and Enantio-Selective Alkylation of Keto Aldehydes with Dialkylzincs. *J. Chem. Soc. Perkin 1* **1994**, No. 21, 3125–3128. <https://doi.org/10.1039/P19940003125>.
- (23) Soai, K.; Yokoyama, S.; Hayasaka, T. Chiral N,N-Dialkylnorephedrine as Catalysts of the Highly Enantioselective Addition of Dialkylzincs to Aliphatic and Aromatic Aldehydes. The Asymmetric Synthesis of Secondary Aliphatic and Aromatic Alcohols of High Optical Purity. *J. Org. Chem.* **1991**, *56* (13), 4264–4268. <https://doi.org/10.1021/jo00013a035>.
- (24) Nugent, W. A. An Amino Alcohol Ligand for Highly Enantioselective Addition of Organozinc Reagents to Aldehydes: Serendipity Rules. *Org. Lett.* **2002**, *4* (13), 2133–2136. <https://doi.org/10.1021/ol0259488>.
- (25) Song, X.; Hua, Y.-Z.; Shi, J.-G.; Sun, P.-P.; Wang, M.-C.; Chang, J. Diastereomeric Aziridine Carbinol Catalyzed Enantioselective Arylation Reaction: Toward the Asymmetric Synthesis of Both Enantiomers of Chiral 3-Aryl Phthalide. *J. Org. Chem.* **2014**, *79* (13), 6087–6093. <https://doi.org/10.1021/jo500796w>.
- (26) Wang, M.-C.; Wang, Y.-H.; Li, G.-W.; Sun, P.-P.; Tian, J.-X.; Lu, H.-J. Applications of Conformational Design: Rational Design of Chiral Ligands Derived from a Common Chiral Source for Highly Enantioselective Preparations of (R)- and (S)-Enantiomers of Secondary Alcohols. *Tetrahedron Asymmetry* **2011**, *22* (7), 761–768. <https://doi.org/10.1016/j.tetasy.2011.04.013>.

- (27) Argüelles, A. J. Mechanistic Studies on Phosphoric Acid Catalyzed Acetalizations and Development of Acetal-Containing Ligands for Transition Metal Catalysis, University of Michigan, 2019.
- (28) Chen, G.-Q.; Lin, B.-J.; Huang, J.-M.; Zhao, L.-Y.; Chen, Q.-S.; Jia, S.-P.; Yin, Q.; Zhang, X. Design and Synthesis of Chiral Oxa-Spirocyclic Ligands for Ir-Catalyzed Direct Asymmetric Reduction of Bringmann's Lactones with Molecular H₂. *J. Am. Chem. Soc.* **2018**, *140* (26), 8064–8068. <https://doi.org/10.1021/jacs.8b03642>.
- (29) Shan, H.; Pan, R.; Lin, X. Synthesis and Application of a New Chiral Monodentate Spiro Phosphoramidite Ligand Based on Hexamethyl-1,1'-Spirobiindane Backbone in Asymmetric Hydroamination/Arylation of Alkenes. *Org. Biomol. Chem.* **2018**, *16* (34), 6183–6186. <https://doi.org/10.1039/C8OB01785A>.
- (30) Zheng, Z.; Cao, Y.; Chong, Q.; Han, Z.; Ding, J.; Luo, C.; Wang, Z.; Zhu, D.; Zhou, Q.-L.; Ding, K. Chiral Cyclohexyl-Fused Spirobiindanes: Practical Synthesis, Ligand Development, and Asymmetric Catalysis. *J. Am. Chem. Soc.* **2018**, *140* (32), 10374–10381. <https://doi.org/10.1021/jacs.8b07125>.
- (31) Zheng, Z.; Cao, Y.; Zhu, D.; Wang, Z.; Ding, K. Development of Chiral Spiro Phosphoramidites for Rhodium-Catalyzed Enantioselective Reactions. *Chem. – Eur. J.* **2019**, *25* (40), 9491–9497. <https://doi.org/10.1002/chem.201900486>.
- (32) Yin, L.; Xing, J.; Wang, Y.; Shen, Y.; Lu, T.; Hayashi, T.; Dou, X. Enantioselective Synthesis of 3,3'-Diaryl-SPINOLs: Rhodium-Catalyzed Asymmetric Arylation/BF₃-Promoted Spirocyclization Sequence. *Angew. Chem. Int. Ed.* **2019**, *58* (8), 2474–2478. <https://doi.org/10.1002/anie.201812266>.
- (33) Huang, J.; Hong, M.; Wang, C.-C.; Kramer, S.; Lin, G.-Q.; Sun, X.-W. Asymmetric Synthesis of Chiral Spiroketal Bisphosphine Ligands and Their Application in Enantioselective Olefin Hydrogenation. *J. Org. Chem.* **2018**, *83* (20), 12838–12846. <https://doi.org/10.1021/acs.joc.8b01693>.
- (34) Chang, X.; Ma, P.-L.; Chen, H.-C.; Li, C.-Y.; Wang, P. Asymmetric Synthesis and Application of Chiral Spirosilabiindanes. *Angew. Chem. Int. Ed.* **2020**, *59* (23), 8937–8940. <https://doi.org/10.1002/anie.202002289>.
- (35) Guo, R.; Au-Yeung, T. T. L.; Wu, J.; Choi, M. C. K.; Chan, A. S. C. Modified BINAPO Ligands for Rh-Catalysed Enantioselective Hydrogenation of Acetamidoacrylic Acids and

Esters. *Tetrahedron Asymmetry* **2002**, *13* (23), 2519–2522. [https://doi.org/10.1016/S0957-4166\(02\)00650-X](https://doi.org/10.1016/S0957-4166(02)00650-X).

Chapter 3

Exploration of Chiral Diastereomeric Spiroketal (SPIROL)-Based Phosphinite

Ligands in Asymmetric Hydrogenation of Heterocycles

(Excerpts of this chapter were adapted from:

Sun, S. and Nagorny, P. *Chem. Commun.*, **2020**,56, 8432-8435.)

3.1. Introduction of iridium-catalyzed hydrogenation of aromatic heterocycles

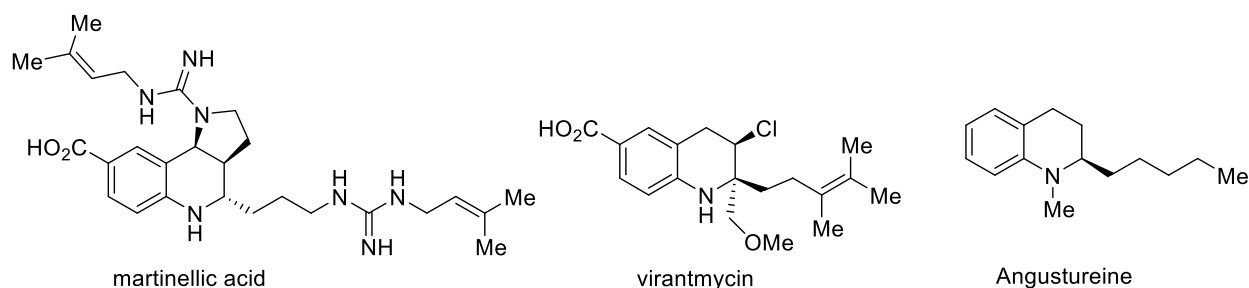


Figure 3.1 Examples of bioactive tetrahydroquinoline-containing alkaloids

Chiral nitrogen-containing heterocyclic motifs are commonly found in natural products^{1,2} and pharmaceuticals such as martinelliacid, virantmycin and alkaloid angustureine depicted in Figure 3.1.³⁻⁶ Over the years, chemists have been exploring various methods, including but not limited to biocatalysis,⁷ chiral pool synthesis,⁸ organocatalysis,⁹ and asymmetric catalysis,¹⁰ to access these high-value alkaloids. Among all available options, transition metal-catalyzed, asymmetric hydrogenation and CPA-catalyzed transfer hydrogenation of heteroarenes have emerged as the robust, convenient and general approaches for the synthesis of saturated chiral heterocycles.¹¹⁻¹⁴ To date, many transition metal complexes including Ru, Rh, Pd, and Ir-based complexes have been successfully utilized for the asymmetric hydrogenation reactions. Due to

its uniquely high catalytic activity and good compatibility with numerous chiral ligands,¹⁵ iridium based catalysts are by far among the most frequently used metals for the asymmetric hydrogenation reactions. Thus, iridium-based catalysts have been extensively used for asymmetric hydrogenations of heteroarenes, including quinolines,^{10,16–47} isoquinolines,^{33,37,38,40,41,43,44,48} quinoxalines,^{30,34,49–54} pyridines,^{43,55–59} indoles,^{60–62} furans,^{63,64} benzofurans,^{63–66} and benzoxazines.^{67,68} However, these transformations are often limited by the required forcing reaction conditions (high pressure, temperature, etc.), high catalyst loading, and limited substrate scope. The structural features of the chiral ligands in Ir-catalyzed hydrogenation reactions may significantly impact both the reaction rate and selectivities, and many of the aforementioned challenges could be addressed by improving the chiral ligand design. Below we provide a brief overview of the iridium-catalyzed asymmetric hydrogenation of various heterocyclic compounds and highlight some of the most successful chiral ligands that have been developed to date to accomplish these reductions.

Asymmetric hydrogenation of furans and benzofurans

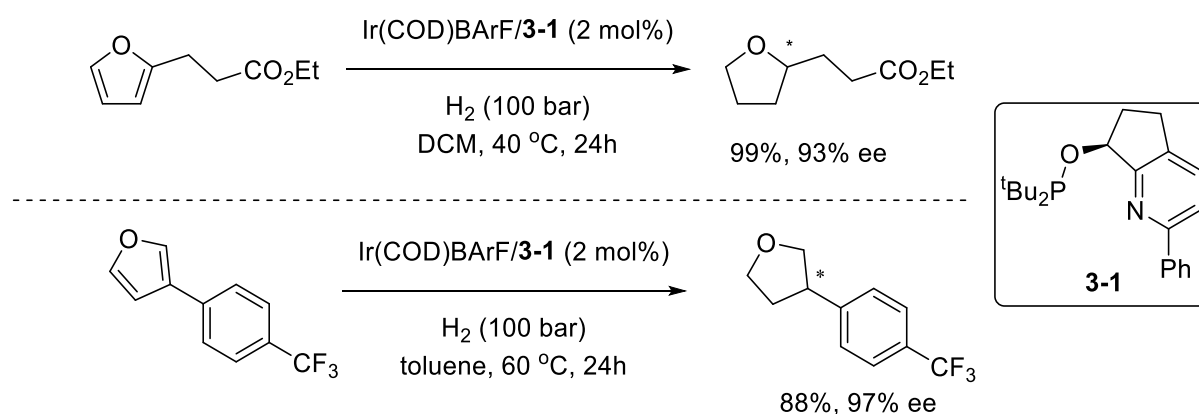
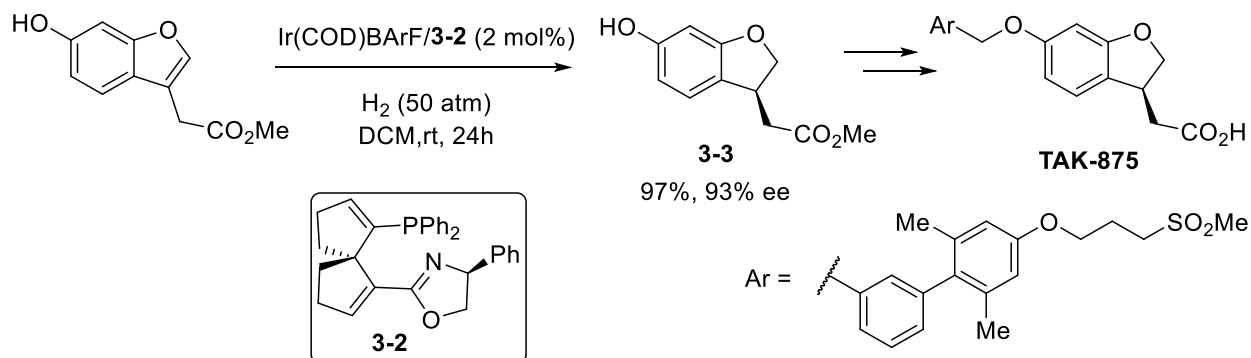


Figure 3.2 Asymmetric hydrogenation of furans

Furans are five-membered aromatic rings with four carbon atoms and one oxygen atom, and they could be reduced to high-value unfunctionalized or functionalized tetrahydrofurans via hydrogenations. However, there are only few efficient protocols to asymmetrically reduce sole furans with iridium catalysts due to the low reactivity of furans' π system.⁶³ In 2006, Pfaltz and coworkers developed a pyridine-phosphinite ligand **3-1**, which could be synthesized in 6 steps and 30% overall yield from acetophenone. These ligands were used in combination with [Ir(COD)]BArF catalyst at slightly elevated temperatures (40–60 °C) and high hydrogen pressures (100 bar) to produce 2-substituted furans were reduced in 84-99% yield and 78-93% ee. These reaction conditions were further extended to the reduction of benzofuran to provide valuable chiral products 2-methyl-2,3-dihydrobenzofuran (93% yield, 98% ee) and ethyl 2,3-dihydrobenzofuran-2-carboxylate (47% yield, >99% ee). In their subsequent studies, several 3-alkyl or 3-aryl substituted furans were reduced with excellent enantioselectivities (>95%) and high conversions. In addition, the described above catalytic system demonstrated great performances in the asymmetric reduction 2- or 3-alkyl substituted benzofurans.⁶⁴ (Figure 3.2)

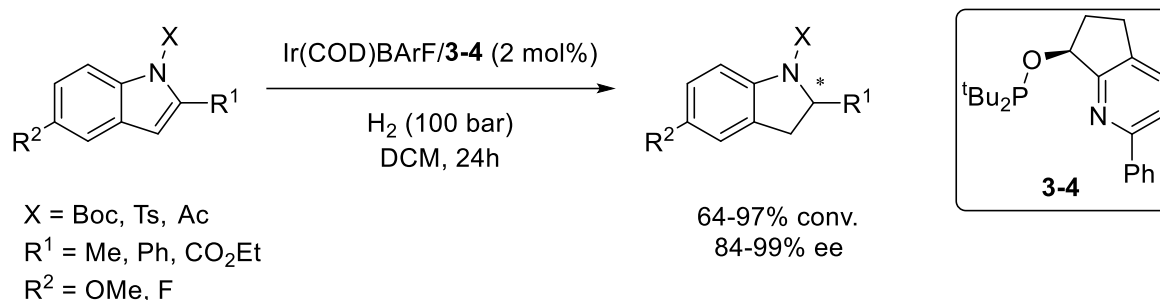


Scheme 3.1 Asymmetric hydrogenation of benzofurans by Ding and Coworkers

Recently, Ding and coworkers utilized the SpinPHOX ligand **3-2** for the asymmetric reduction of 8 benzofurans and benzopyrans.⁶⁵ (Scheme 3.1) All products were obtained with more than 90% ee, and the key precursor **3-3** subsequently converted into the antidiabetic agent

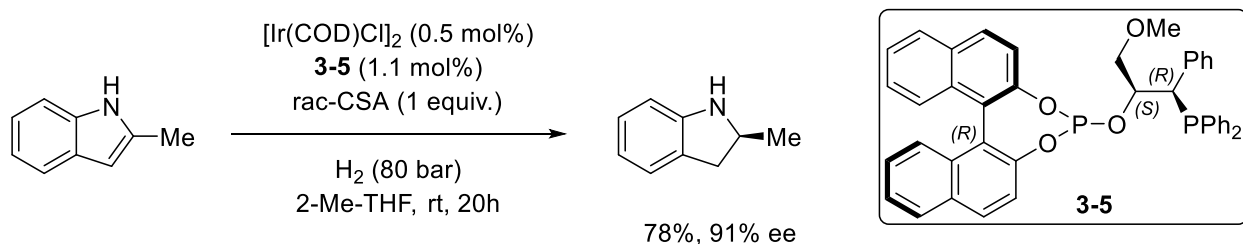
TAK-875⁶⁶ was produced with 97% yield and 93% ee. In the same report they also described the reduction of more than 21 *N*-protected indole derivatives bearing 2- or 3-substituents in 73-99% yield and 93-99% ee.

Asymmetric hydrogenation of indoles



Scheme 3.2 Asymmetric hydrogenation of protected indoles

Pfaltz and Baeza probed Ir-catalyzed hydrogenations to access chiral indolines with their pyridine-phosphinite ligand **3-4** back in 2010.⁶⁰ (Scheme 3.2) They found that either the C-2 or C-3 substituent in *N*-protected indoles did not have a significant impact on the enantioselectivity (84-99% ee), and that elevating the temperature was key to the success reduction of the other, less reactive, substrates.



Scheme 3.3 Asymmetric hydrogenation of unprotected indoles

In 2014, Vidal-Ferran and coworkers developed a new Ir/phosphine-phosphinite **3-5** complex to asymmetrically reduce unprotected indoles (Scheme 3.3).⁶¹ Up to 91% ee was observed in the stepwise C=C bond isomerization mediated by reusable Brønsted acid, followed

by the Ir-catalyzed asymmetric hydrogenation. However, the assembly for the ligand itself would require a 6-step synthesis with hard-to-obtain starting materials along with multiple chiral reagents. Soon after, the Lyubimov group tested similar, but much simpler phosphite ligands, available in only 1 step from the chiral BINOL, in the hydrogenation of 2-methyl indole.⁶² Acceptable results (up to 80% ee) were produced from their study only when iodine was used as the additive.

Asymmetric hydrogenation of pyridine, pyrazine and their derivatives

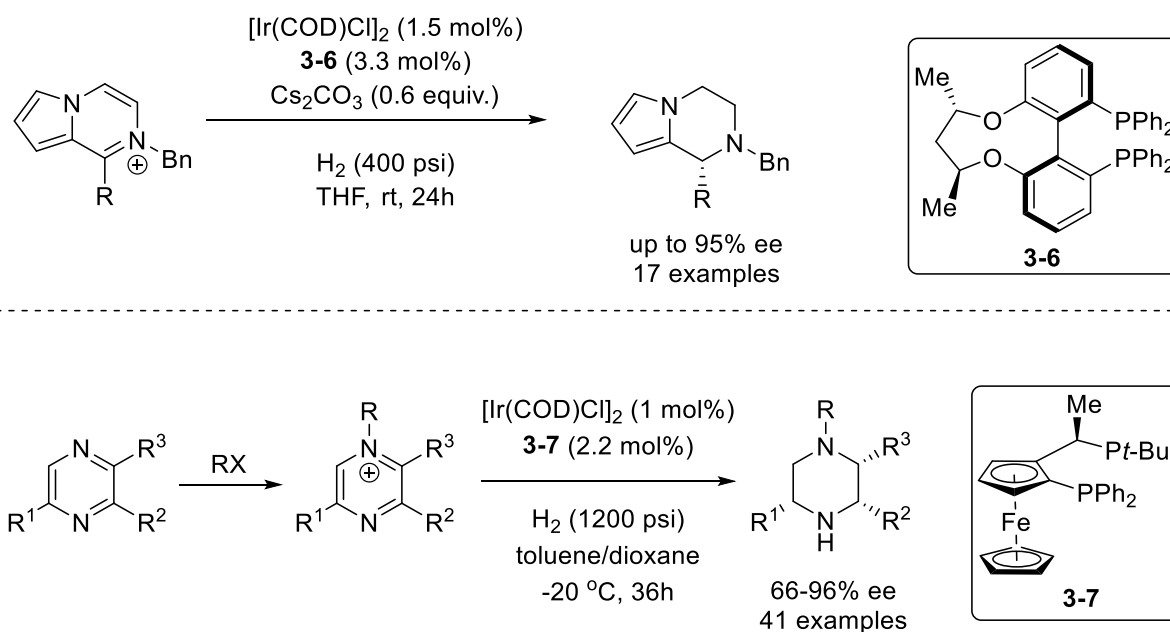
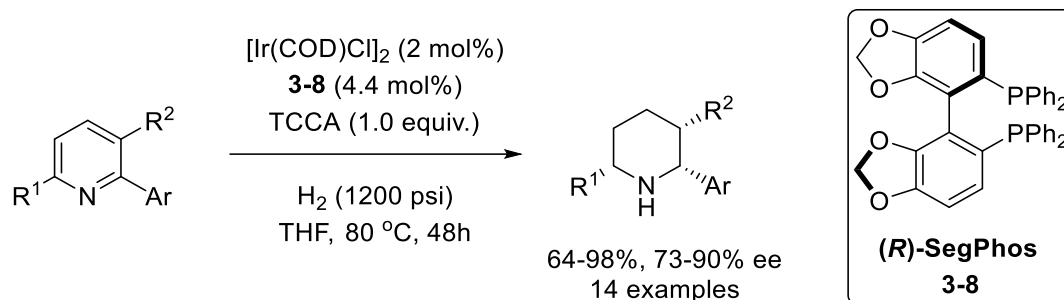


Figure 3.3 Asymmetric hydrogenation of pyrazine and derivatives

Pyrazines⁵⁵ and pyrazinium salts⁶⁹ could be fully reduced to piperazine derivatives, which could be key chiral intermediates in drug synthesis. A recent study utilized C₃-TunePhos **3-6**, derived from Biphep, in the reduction of prochiral pyrrolo[1,2-*a*]pyrazinium salts (Figure 3.3).⁶⁹ Interestingly, cesium carbonate was the key reagent to stop the racemization pathway in product formation. At the same time, most studies had shown that pyrazines should be converted to

pyrazinium salts by reaction with alkyl halides prior to hydrogenation in order to weaken aromaticity with the pyrazine. With no exception for activation to pyrazinium salts, JosiPhos **3-7** were successfully used for 41 substrates with 66 to 96% ee obtained, but the drawback with this condition was that the reaction required ultra-high hydrogen pressure in order to reach high conversion.⁵⁵



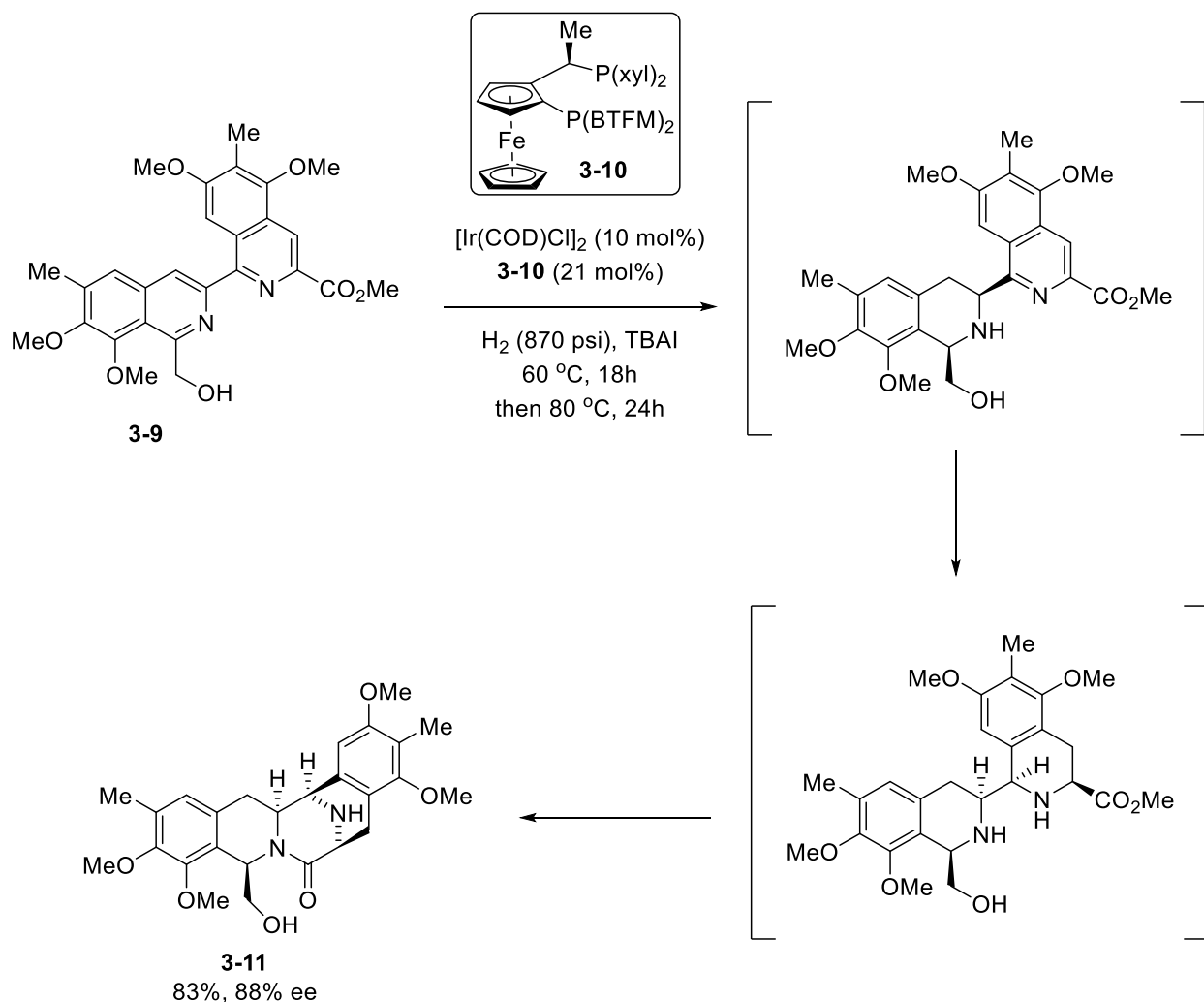
Scheme 3.4 Asymmetric hydrogenation of pyridine

Also due to the stabilized resonance on the nitrogen atom in pyridine, asymmetric hydrogenations had only been extensively studied on activated pyridine derivatives.⁵⁶⁻⁵⁹ However, a recent study disclosed that additional activating groups would be no longer required as in situ generated hydrogen halides could be used as the activators.⁴³ With 1 equivalent of trichloroisocyanuric acid in THF as the traceless activator, 14 trisubstituted pyridines were successfully reduced to chiral substituted piperidines (64-98% yield and 73-90% ee) with commercially available SegPhos **3-8** as the ligand at 80°C. (Scheme 3.4)

Asymmetric hydrogenation of isoquinolines

The asymmetric reduction of isoquinolines had been extensively studied in many recent publications.^{33,37,38,40,41,43,48} An important milestone with Ir-catalyzed asymmetric reduction of isoquinolines **3-9** was featured in the concise total synthesis of (-)-Jorumycin **3-11**.⁴⁴ The key to the success was the chelation between the hydroxymethyl group in the substrate and iridium

catalyst; hence, a double asymmetric hydrogenation for the bis-isoquinoline provided the product as the single diastereomer with 83% yield and 88% ee. (Scheme 3.5)



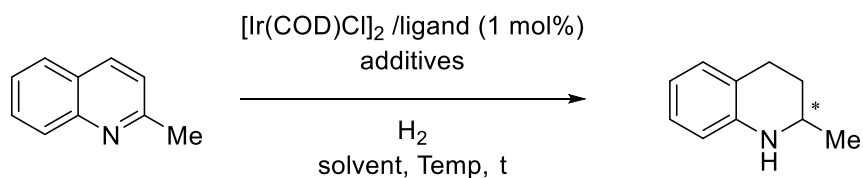
Scheme 3.5 Asymmetric hydrogenation of isoquinolines in total synthesis of (-)-Jorumycin by Stoltz and coworkers

Asymmetric hydrogenation of quinolines

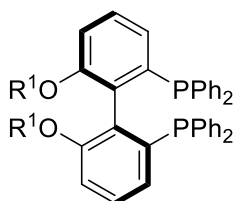
Quinaldine is the simplest pro-chiral quinoline with 2-methyl substituent, and it quickly became the standard substrate to test ligand performance in asymmetric reduction of C2-alkyl substituted quinolines. The family of Biphep diphosphine ligands were extensively studied by

the Zhou group, and they found different reactivities with different backbone substituents such as OMe^{16,28} **3-12**, OTf³² **3-13**, and CF₃³⁶ **3-14**. In another early study, Zhou and coworkers reported that chiral ferrocenyloxazoline-derived P-N ligand **3-15** demonstrated great selectivities for this reaction with up to 90% ee obtained.¹⁷ A C₃-TunePhos derived from Biphep with modified sterics on the phosphine was observed with a similar reactivity under slightly reduced hydrogen pressure.²⁹ Vidal-Ferran and coworkers tested their phosphine-phosphinite ligand **3-5** in the hydrogenation, but slightly diminished enantioselectivity even with higher hydrogen pressure was obtained.³⁰ Rueping *et al* reported the H8-BINOL-derived Brønsted acid **3-18**-differentiated metal-catalyzed hydrogenation, and 94% ee was observed even at -10 °C.⁷⁰ Recently, Chan and coworkers prepared H8-BINAPO¹⁸ **3-16** and SPINOL-based diphosphinites²¹ ligands **3-17**, both of which were just obtained in 1 synthetic step from chiral H8-BINOL and SPINOL. Both **3-16** and **3-17** could serve as excellent ligands for the iridium-catalyzed hydrogenation allowing to achieve high S/C ratios and excellent enantioselectivities for narrow range of isoquinolines as substrates. However, the reaction would require a bi-phasic solvent system, DMPEG-hexane, to achieve good enantioselectivities. (Table 3.1)

Table 3.1 Asymmetric hydrogenation of 2-methyl quinoline



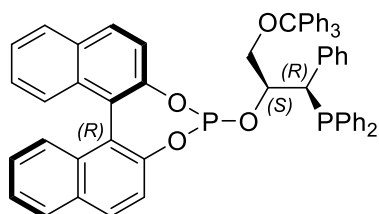
Ligand	additives	H ₂ (psi)	solvent	Temp(°C)	t(h)	ee(%)
3-12	I ₂ (10 mol%)	700	toluene	25	15	94
3-13	I ₂ (10 mol%)	700	THF	25	22	95
3-14	I ₂ (10 mol%)	700	toluene	25	22	98
3-5	HCl (10 mol%)	1160	toluene	25	65	91
3-15	-	600	toluene	25	12	90
3-16	I ₂ (10 mol%)	700	DMPEG-hexane	25	20	97
3-17	I ₂ (10 mol%)	700	DMPEG-hexane	25	20	92
3-18	-	1450	o-xylene	-10	24	94



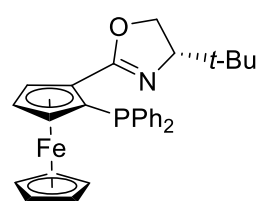
3-12: R¹=Me

3-13: R¹=Tf

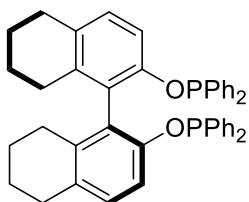
3-14: R¹=CF₃



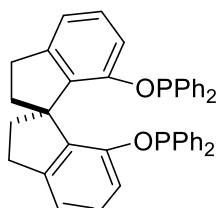
3-5



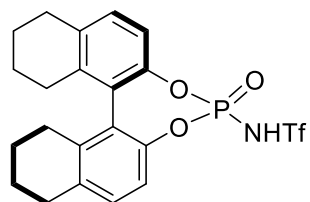
3-15



3-16



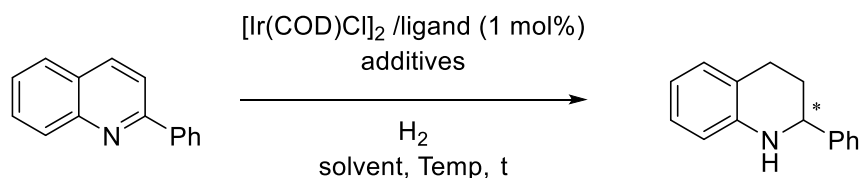
3-17



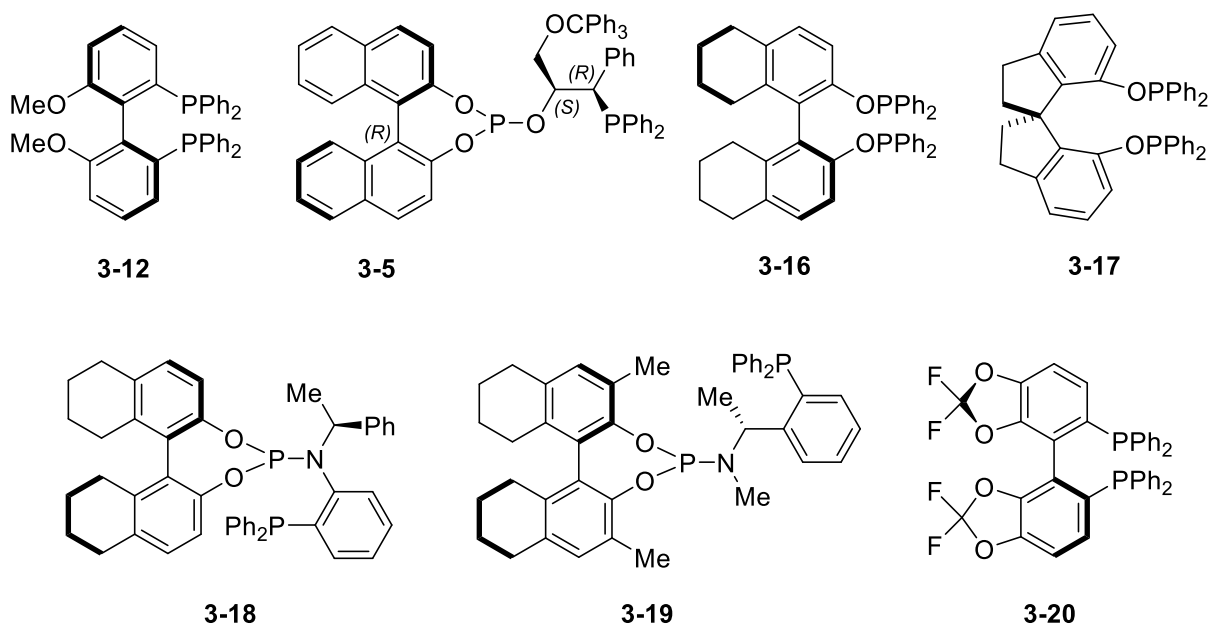
3-18

On the other hand, switching from alkyl to aromatic for C2-substituent could change catalysts' enantioselectivities significantly. Although ligand **3-16** was exceptional in many other studies, Zhou group found it could only provide 72% ee for this substrate.¹⁶ Despite 84% ee obtained with **3-5**, extended reaction time and high hydrogen pressure would be limiting factors to expand its applications.³⁰ Enantioselectivity with either H8-BINAPO **3-16**¹⁸ or SDPO **3-17**²¹ decreased significantly comparing with the result from 2-methyl quinoline. Although both catalysts **3-18**²⁶ and **3-19**⁴⁶ had outstanding performances comparing to the rest of table, the synthetic challenges to access these H8-BINOL-based phosphine–phosphoramidite skeletons still poses. The drawback with (*S*)-difluoroSegPhos **3-20** complex was from the usage of HBr, which might not be compatible with more complex molecules.²⁷ (Table 3.2)

Table 3.2 Asymmetric hydrogenation of 2-phenyl quinoline



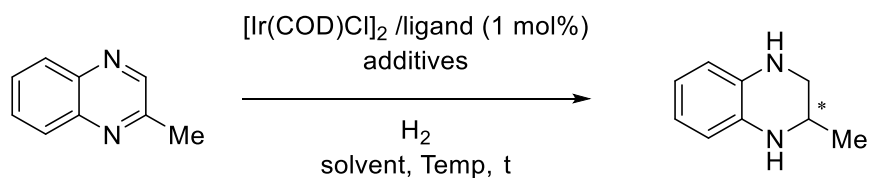
Ligand	additives	H ₂ (psi)	solvent	Temp(°C)	t(h)	ee(%)
3-12	I ₂ (10 mol%)	700	toluene	25	15	72
3-5	HCl (10 mol%)	1160	toluene	25	65	84
3-16	I ₂ (10 mol%)	700	DMPEG-hexane	25	20	87
3-17	I ₂ (10 mol%)	700	DMPEG-hexane	25	20	65
3-18	-	580	toluene	25	16	95
3-19	-	145	1,4-dioxane	25	24	93
3-20	HBr	435	1,4-dioxane/MeOH	30	16	91



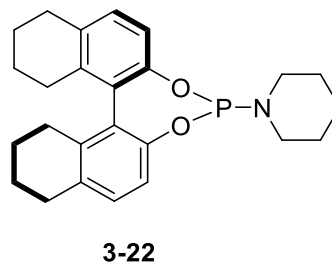
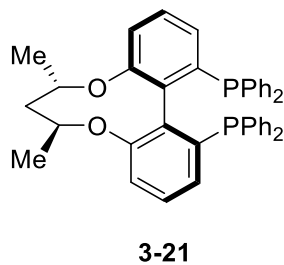
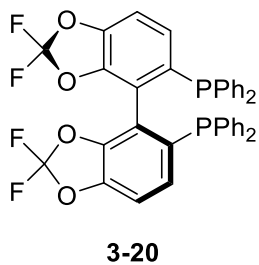
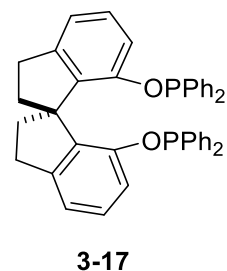
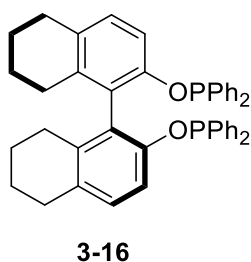
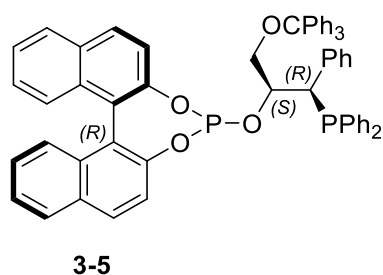
Asymmetric hydrogenation of quinoxaline

3-5 was again could be used in asymmetric hydrogenation of quinoxaline, but only moderate 72% ee was observed even in their optimized reaction condition.³⁰ Impressively, H8-BINAPO **3-16** catalyzed the reaction at -5 °C and provided product with 93% ee in 90 minutes, while SDPO **3-17** struggled with only 83% ee with the optimized reaction condition.⁵⁰ (*S*)-difluoroSegPhos **3-20** provided comparable enantioselectivity (94% ee) with HCl as the activator under lower hydrogen pressure,⁵¹ but the following study regarding the same ligand with slightly modified condition only provided 89% ee.⁵⁴ **3-21** was a good ligand candidate for quinoline reductions, but it could only provide up to 80% ee for quinoxalines.⁷¹ Finally, H8-BINOL-derived monodentate phosphoramidite ligand **3-22** seemed to be the best one in this category with 96% ee of the desired product.⁴⁹ However, with high reaction temperature and piperidine/HCl coactivator, less functional groups would be tolerated in a more complex system. (Table 3.3)

Table 3.3 Asymmetric hydrogenation of 2-methyl quinoxaline



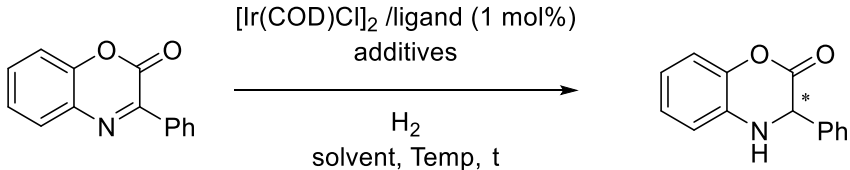
Ligand	additives	H ₂ (psi)	solvent	Temp(°C)	t(h)	ee(%)
3-5	HCl (10 mol%)	1160	toluene	25	65	70
3-16	I ₂ (10 mol%)	700	THF	-5	1.5	93
3-17	I ₂ (10 mol%)	700	THF	25	20	83
3-20	HCl	435	1,4-dioxane	30	20	94
3-21	-	700	THF	25	20	80
3-22	HCl-piperidine (10 mol%)	350	DCM	60	24	96



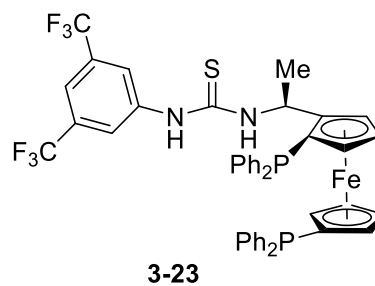
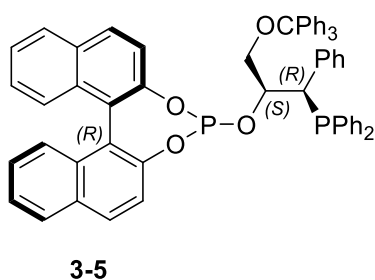
Asymmetric hydrogenation of bezoxazinones

The reduction of bezoxazinones has been well studied with transfer hydrogenation and Ru-catalyzed reductions. However, there were only two asymmetric examples with iridium-based catalysts. In 2013, Vidal-Ferran and Núñez-Rico found that **3-5** had excellent performance with 95% ee but requiring more than 1000 psi of hydrogen.⁶⁷ Zhang and coworkers reported an impressive 98% ee with ZhaoPhos **3-23** under only 650 psi of hydrogen with the presence of HCl activator in their study.⁶⁸ (Table 3.4) However, it would be hard to ignore that both ligands were difficult to synthesize and acid cocatalysts were required in both studies. Hence, a mild reaction condition with an easily accessible ligand would greatly improve the efficiency in this reaction, and possibly would be applied into more complex syntheses.

Table 3.4 Asymmetric hydrogenation of bezoxazinone



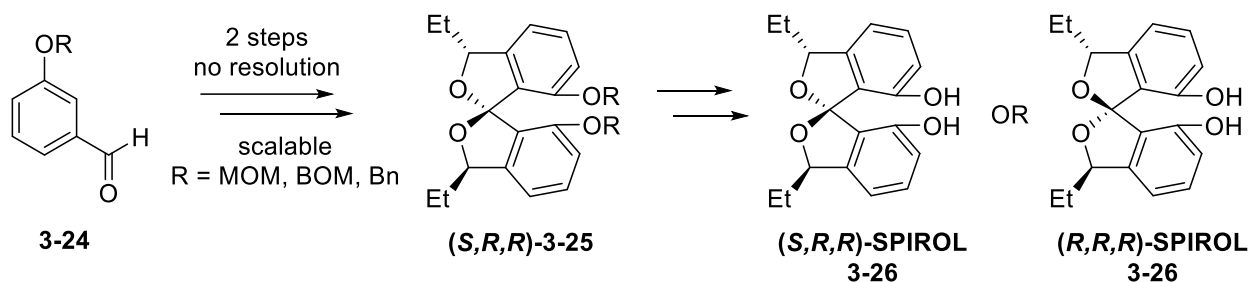
Ligand	additives	H ₂ (psi)	solvent	Temp(°C)	t(h)	ee(%)
3-5	HCl (10 mol%)	1160	toluene	25	65	95
3-23	HCl	650	1,4-dioxane	25	24	98



Easily accessible H8-BINOL derived phosphinites were useful in most cases, while catalyst **3-5** not only hard to prepare but also required harsh reaction conditions to achieve high

selectivities with limited number of selected substrates. With these aforementioned developments in mind, our studies described in this chapter were focused on exploring the easily accessible and highly tunable SPIROL-derived ligands in Ir-catalyzed asymmetric hydrogenations of different aromatic heterocycles.

3.2. Background of SPIROL-based phosphinite ligands



Scheme 3.6 Development of SPIROL-based ligands

Previously,⁷² we observed that SPIROL scaffolds are almost unmatched in terms of their ease of preparation and unique structural features that allow the ligand properties to be tuned.^{73–76} These ligands could be easily generated from inexpensive aldehydes **3-24** through a two-step protocol that gives rise to the protected (*S,R,R*)-diastereomer **3-25** (or its (*R,S,S*)-counterpart) in good yields and selectivities. The (*S,R,R*)-**3-25** was further elaborated to various (*S,R,R*)- and (*R,R,R*)- (or enantiomeric(*R,S,S*)- and (*S,S,S*)-) diols **3-26**.⁷² The subsequent experimental evaluation of both diastereomeric scaffolds demonstrated that ligands with (*R,R,R*)-SPIROL **3-26** configuration are similar to (*S*)-SPINOL-based ligands in terms of their performance and structural parameters. In contrary, diastereomeric (*S,R,R*)-SPIROL ligands behaved as pseudo enantiomers of (*R,R,R*)-SPIROL and provided opposite enantiomers with lower enantioselectivities. The computational studies were consistent with these observations and indicated that (*S,R,R*)-SPIROL and (*R,R,R*)-SPIROL ligands possessed considerably different geometry index parameters τ_4 and τ_4' and the calculated bite angles. The subsequent analysis by

Alongside of the computed three-dimensional structures indicated that the Et-side chain in (*S,R,R*)-complexes disturbs the π -stacking between the aryl groups of the backbone, leading to a different overall geometry. (Figure 3.4)

Structurally similar to (*S*)-SPINOL-based complexes

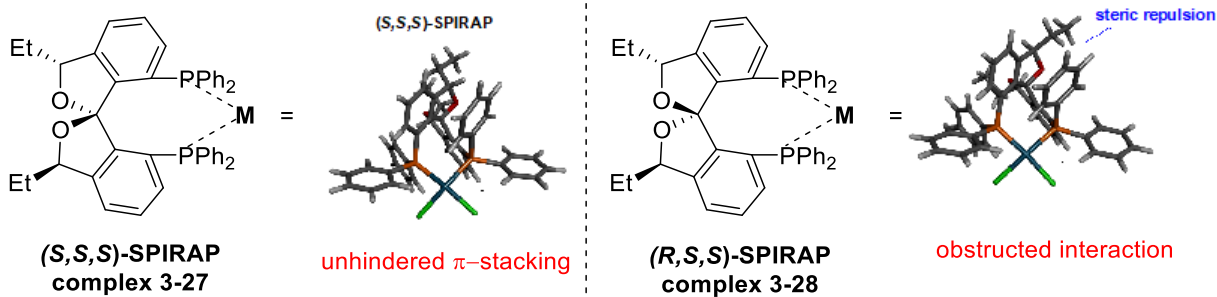
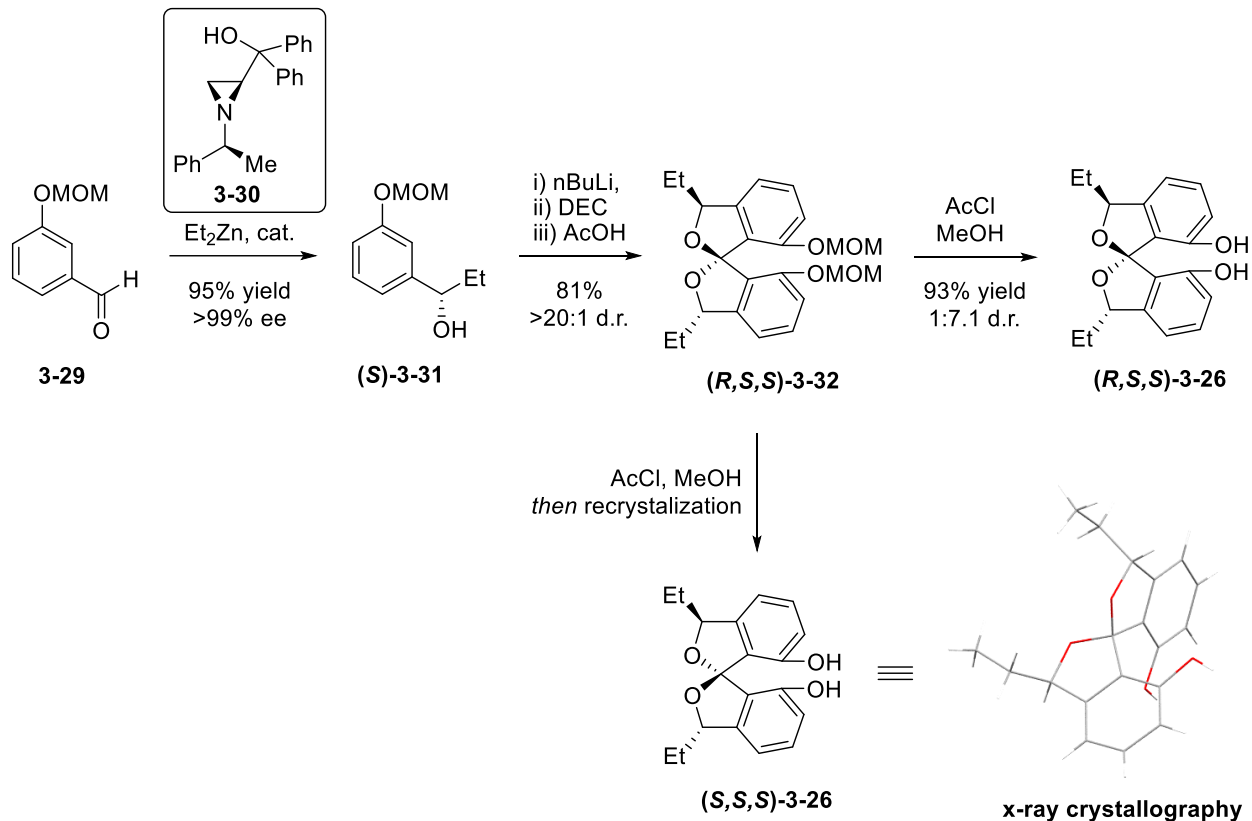


Figure 3.4 Effect of spiroketal and substituent configuration on diastereomeric SPIROL ligands

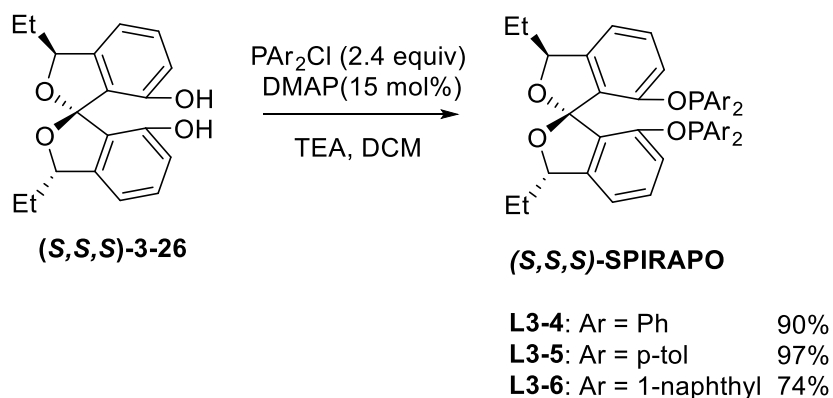
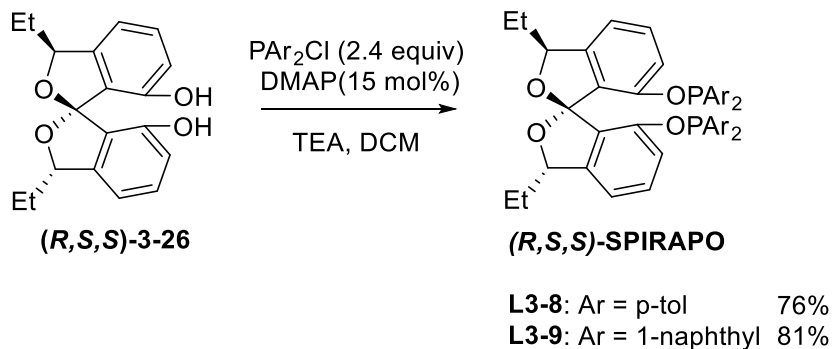
The structural dissimilarities between the (*S,R,R*)-spiroketal manifold and the SPINOL core led us to believe that the (*S,R,R*)-based catalytic platform could provide a unique solution to new asymmetric methodologies of importance while the (*R,R,R*)-based platform provides a more readily available alternative to SPINOL. This study focused on the use of (*S,R,R*)-SPIROL phosphinites in asymmetric dearomatizative hydrogenation reactions leading to the formation of chiral heterocyclic frameworks. It is noteworthy that (*S,R,R*)-SPIROL phosphinites outperform (*R,R,R*)-SPIROL and (*R*)-SPINOL-based ligands and demonstrate great substrate tolerance to the changes in the heterocycle substitutions and frameworks.

3.3. Design and synthesis of SPIRAPO ligands



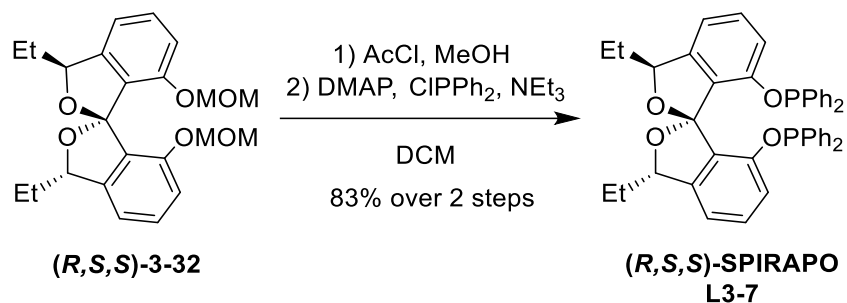
Scheme 3.7 Efficient synthesis towards SPIROL diastereomers

The synthesis of **(R,S,S)**- and **(S,S,S)**-SPIROL **3-26** followed our previously disclosed protocol with some modifications.⁷² Asymmetric alkylation with diethyl zinc and chiral aziridine catalyst **3-30** provided **(S)-3-31** with 95% yield and 99.8% ee. The following spirocyclization from 23.3 g of **(S)-3-31** produced **(R,S,S)-3-32** with 81% yield and more than 20:1 in d.r. which was improved from our early studies. The following selective deprotection with AcCl and methanol followed by sodium bicarbonate work up yielded **(R,S,S)**-SPIROL **3-26** with 93% yield and at least 7:1 in d.r. To our surprise, a recrystallization from the DCM/hexane system after selective deprotection of **(R,S,S)-3-32** gave us the access to enantiopure single diastereomer **(S,S,S)**-SPIROL **3-32** which was also confirmed by X-ray crystallography. (Scheme 3.7)



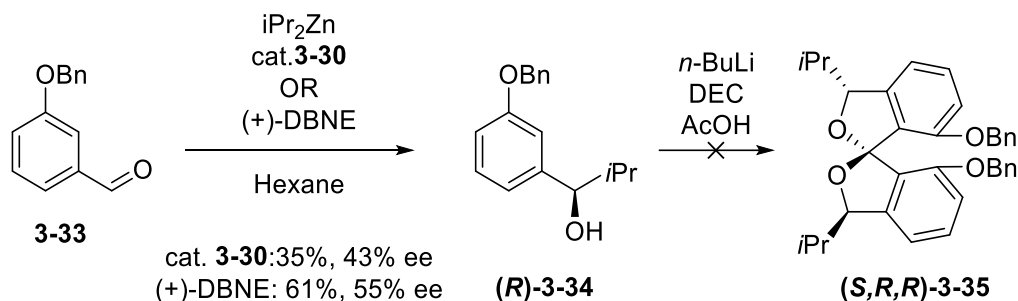
Scheme 3.8 Syntheses of diphosphinite ligands

With different diarylphosphine chlorides, **(R,S,S)-SPIRAPO** ligands **L3-8** and **L3-9** were synthesized from **(R,S,S)-SPIROL 3-26** with 76% and 81% yield, respectively. Similarly, **(S,S,S)-SPIRAPO** ligands **L3-3** to **L3-6** were accessed in 1 step from the recrystallized enantiopure **(S,S,S)-SPIROL 3-26**, and excellent yields were obtained as 90%, 97% and 74%, respectively. the ligand synthesis from **(S,R,R)-SPIROL 3-32** could be optimized to the one-pot deprotection/substitution method, and comparable yields were observed.



Scheme 3.9 One-pot synthesis of diphosphinite from 3-32

Surprising, we had also developed the one-pot protocol to access **(R,S,S)-SPIRAPO L3-7**. The direct access started with 77 mg of **(R,S,S)-3-32**, and a quick MOM deprotection followed by a substitution with PPh₂Cl yield the ligand **(R,S,S)-SPIRAPO**. Up to 83% yield was obtained while the diastereomeric **(S,S,S)-SPIRAPO** was removed with column chromatography. (Scheme 3.9)

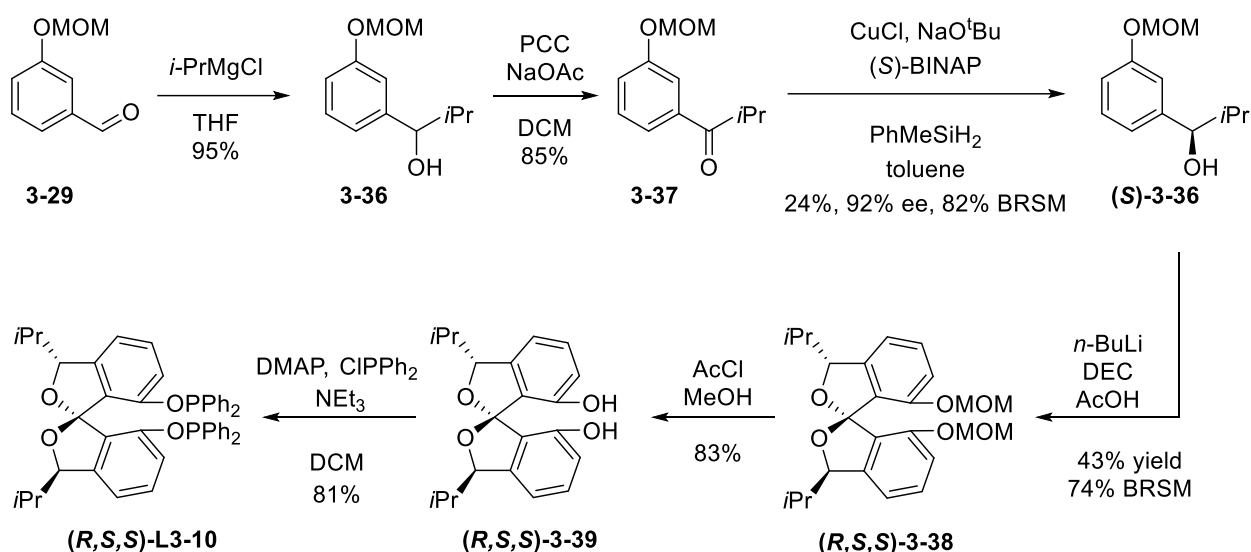


Scheme 3.10 Initial synthetic attempt towards 3-35

In this study, we also investigated the effect with different substituents on the SPIROL backbone, which led us to a new ligand **L3-10**. In our previous study, asymmetric alkylation of Bn-protected aldehyde **3-33** with diethyl zinc proceed smoothly with either DBNE or aziridine catalysts, followed by a successful spirocyclization to afford desired spirocyclic product. Deprotection of Bn group only required 1 atm of H₂ in the presence of Pd/C, and the non-acidic reaction condition would not epimerize the product opposed to what we observed with MOM deprotection. The diol obtained was in the form of single diastereomer as the same of which we

would expect with (*S,R,R*)-**3-26**. Hence, we commenced our investigation of asymmetric addition with Bn-protected aldehyde **3-33**. However, the results went unsatisfactory as only 35% yield and 43% ee obtained with the aziridine catalyst **3-30**, which was perfect in our previous studies. We next made a bid with (+)-DBNE catalyst, and only tiny improvements in yield and enantioselectivity was observed. Although (*R*)-**3-34** was surprisingly enriched to 75% ee after additional purifications, our experience suggested that spirocyclization with low enantiopurity material would be a disaster. So, we betted on the 75% ee (*R*)-**3-34**, and our attempt failed miserably with unexpected extremely low overall yield along with multiple inseparable products.

(Scheme 3.10)



Scheme 3.11 Synthesis of ligand L3-10

Therefore, we decided to take additional steps to pursue enantiopure **3-36**, and with MOM-protected **3-29**, we hoped to avoid the same problem from spiroketalization with (*R*)-**3-34**. Grignard reaction for **3-29** with *i*-PrMgCl yielded racemic **3-36** with 95% yield. A direct chiral resolution with *L*-menthyl chloroformate for **3-36** did not produce separable diastereomers, and then the racemic **3-36** was oxidized to ketone **3-37** with PCC and 85% yield was obtained. The

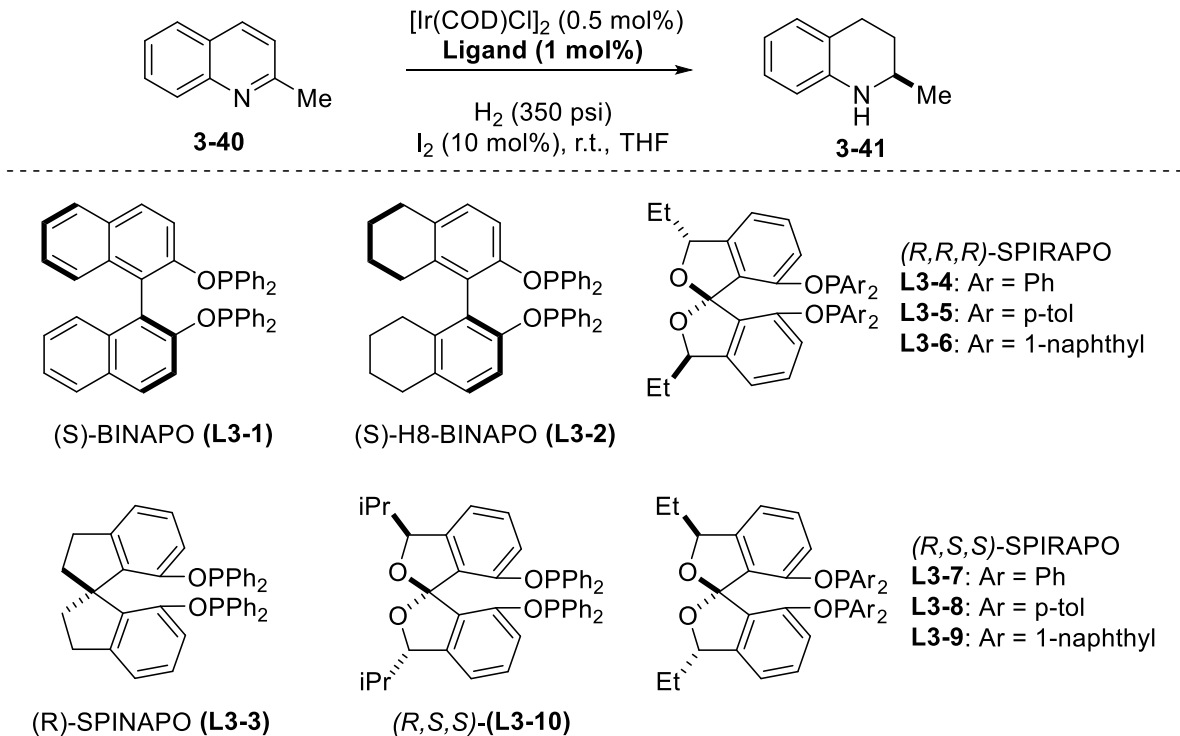
following asymmetric reduction catalyzed by Cu(I)-(S)-BINAP with PhMeSiH₂ finally produced (S)-**3-36** with 24% yield (82% BRSM) and 92% ee. The enantiopurity of (S)-**3-9** could be increased via cocrystallization with the salt of chiral amine and benzoic acid.⁶² Spiroketalization with (S)-**3-36** provided (R,S,S)-**3-38** with a moderate yield (43%, 74% BRSM), but the following deprotection and substitution allowed us to obtain the final ligand (R,S,S)-**L3-10** with 67% yield over two steps. (Scheme 3.11)

3.4. Evaluation of all ligands in asymmetric hydrogenation of quinaldine

We then commenced our investigation of asymmetric iridium-catalyzed reductions of quinaldine **3-40** using (R,R,R)-SPIROL and (R,S,S)-SPIROL-derived diphosphinites (**L3-4** to **L3-10**, Table 3.5). As it was observed by Chan and coworkers,²¹ BINAPO ligand **L3-1** may serve as good ligand for the reduction of **3-40** providing **3-41** in 81% ee; however, high pressures (700 psi) and long reaction times (20 h) were required to achieve full conversion and selectivity (entry 1). In our studies, we decided to optimize these conditions so that the reduction of **3-40** could be carried at lower and safer pressure (350 psi) and shorter reaction time (10 h). However, when **L3-1** was used under such conditions, **3-41** was formed in only 42% ee (entry 2). At the same time, the reaction with related (S)-H8-BINAPO ligand **L3-2** (entry 3) resulted in 87% ee and full conversion, and SPINAPO ligand **L3-3** demonstrated even better performance (99% conversion, 90% ee, entry 4). Having this as a benchmark for our further studies, we subsequently evaluated various SPIRAPHO ligands **L3-4** to **L3-10** (entries 5-11). As expected, (R,R,R)-SPIRAPHO ligand **L3-4** (Ar = Ph), performed similarly to SPINAPO affording **3-41** in 88% ee. The increase of the steric of the Ar group on phosphorus(III) in **L3-5** and **L3-6** resulted in inferior enantioselectivities (33% ee and 12% ee correspondingly, entries 6 and 7). At the same time, the diastereomeric counterparts of ligands **L3-4**, (R,S,S)-ligand **L3-7** demonstrated

significantly better performance affording **3-41** in 94% ee (entry 8), and could be further raised to 96% ee if run at higher pressure (600 psi) and 0 °C (entry 9). Remarkably, this transformation could be run for the same lapse of time with only 0.01 mol% of the catalyst (S/C = 10 000) without significant reduction in conversion and selectivity (93%, 91% ee, entry 9). In addition, we observed that the reduction time could be cut tenfold (1 h instead of 10 h) without significant impact on conversion (entry 10). In further attempts to optimize the selectivity using (*R,S,S*)-counterparts of **L3-5** and **L3-6**, (*R,S,S*)-ligands **L3-8**, and **L3-9**, were tested (entries 11 and 12). Although these ligands demonstrated significantly better performance than **L3-5** and **L3-6** affording **3-41** in 87% ee and 55% ee, correspondingly, they were inferior to **L3-7**. Finally, an *i*-Pr, rather than Et-group substituted (*R,S,S*)-SPIRAPO ligand **L3-10** was synthesized and tested (entry 13). This ligand demonstrated performance comparable to (*R,R,R*)- SPIRAPO ligand **L3-4**, but inferior to (*R,S,S*)-SPIRAPO ligand **L3-7**.

Table 3.5 Evaluation of ligands for the iridium(I)-catalyzed reduction of quinaldine



entry	ligand	H ₂ (psi)	time (h)	conv. (%) ^b	ee (%)
1 ^c	L3-1	700	20	99	81
2	L3-1	350	10	99	42
3	L3-2	350	10	99	87
4	L3-3	350	10	99	90
5	L3-4	350	10	99	88
6	L3-5	350	10	99	33
7	L3-6	350	10	99	12
8	L3-7	350	10	99	94
9 ^d	L3-7	600	3	99	96
10 ^e	L3-7	350	10	93	91
11	L3-7	350	1	95	94
12	L3-8	350	10	99	87
13	L3-9	350	10	99	55
14	L3-10	350	10	99	90

^aReactions were carried out at 25°C with 0.1 mmol **3-40** using Ir(I) complex generated in situ from [Ir(COD)Cl]₂ (0.5 mol%), ligand (1.1 mol%), and I₂ (10 mol%) under pressurized H₂ in 1 ml of THF. ^bThe conversion was determined by ¹H NMR and the ee was determined by HPLC analysis with Chiralpak OJ-H column. ^cFrom the literature. ^dPerformed at 0°C and 600 psi for 3h. ^e Performed with 0.01 mol% of catalyst

3.5. Results and discussion

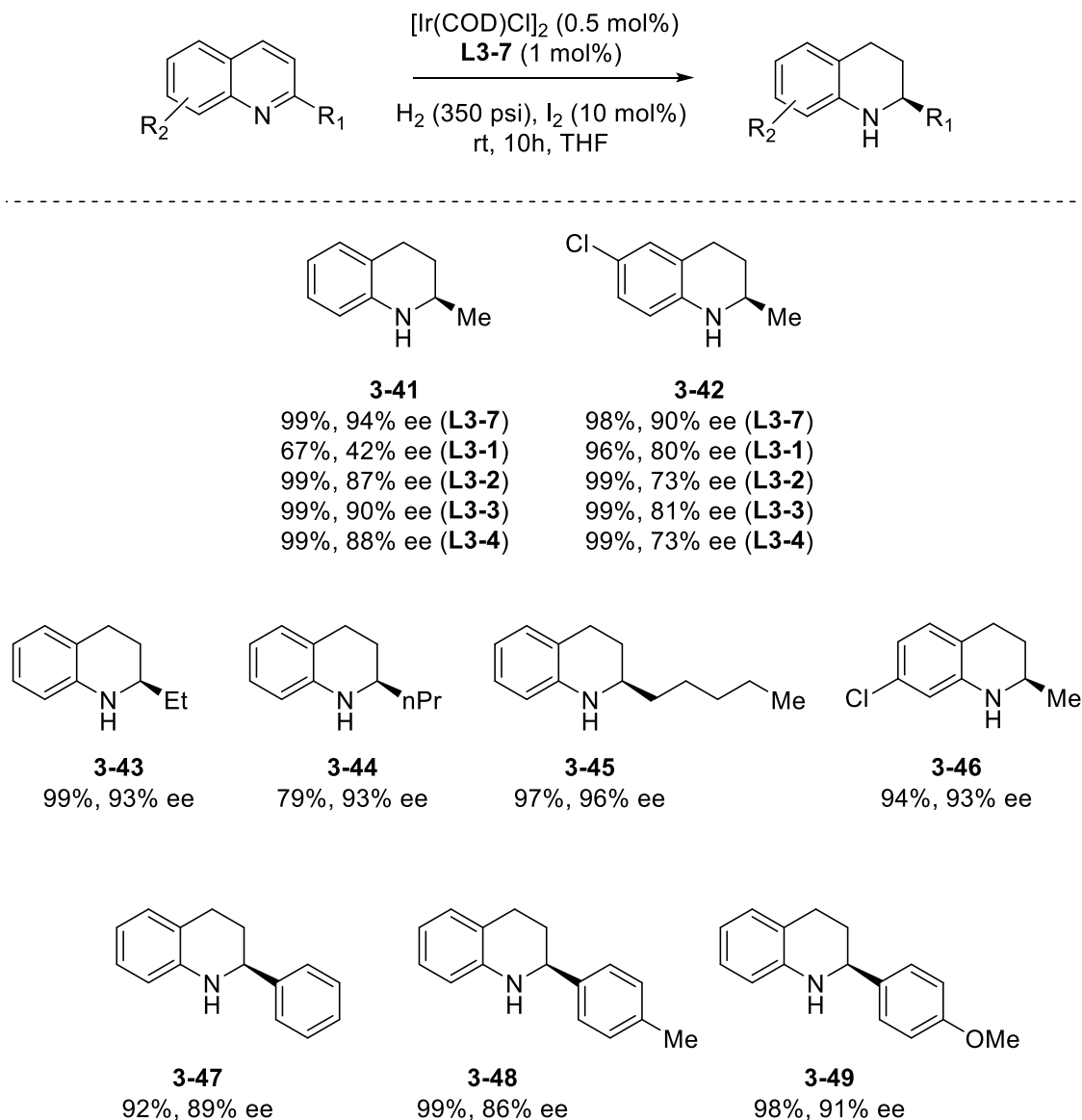
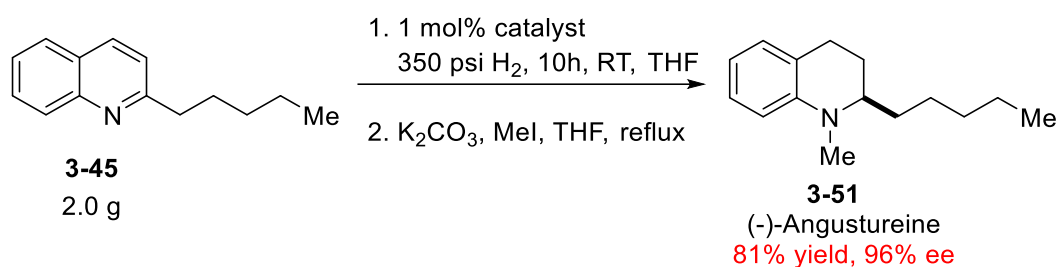


Figure 3.5 Asymmetric reduction of 2-substituted quinolines

After careful evaluations of all ligands and reaction conditions, our study identified **L3-7** as the best ligand for the lower pressure (350 psi) hydrogenation of **3-40**. In addition, the generally better performance of **L3-7** relative to ligands **L3-1** and **L3-4** was tested and observed for other substrates such as **3-42** and **3-51**. Thus, **L3-7** was selected and used for the reduction of other substituted quinolines. The changes in the size of the C2-substituent were well tolerated,

and chiral products **3-43** to **3-45** were obtained in excellent yields and selectivities (93–96% ee). In addition, the substitution in the benzene ring was tolerated, and chlorinated products **3-42** and **3-46** were produced in 90% ee and 93% ee, correspondingly. While the C2-alkyl to C2-aromatic substituent switch often results in significant erosion of selectivity and necessity to re-optimize the ligand,^{15,16,21,22,24,28,30,35,39,46,50,55,56,59,67–69,78–80} (*R,S,S*)-SPIROL-based ligand **L3-7** demonstrated great performance for the reduction of 2-aryl substituted quinolines resulting in products **3-47**, **3-48** and **3-49** in 89% ee, 86% ee and 91% ee, correspondingly.



Scheme 3.12 Synthesis of (-)-(R)-angustureine 3-50

Finally, to demonstrate that these transformations are amenable to scale up, the reduction of quinoline with C2-*n*-pentyl was performed on 2.0 g-scale. The resultant product **3-45** was obtained without erosion in the yield and selectivity. This compound was subsequently methylated to provide natural alkaloid (-)-(R)-angustureine **3-50** in 81% yield and 96% ee. (Scheme 3.12)

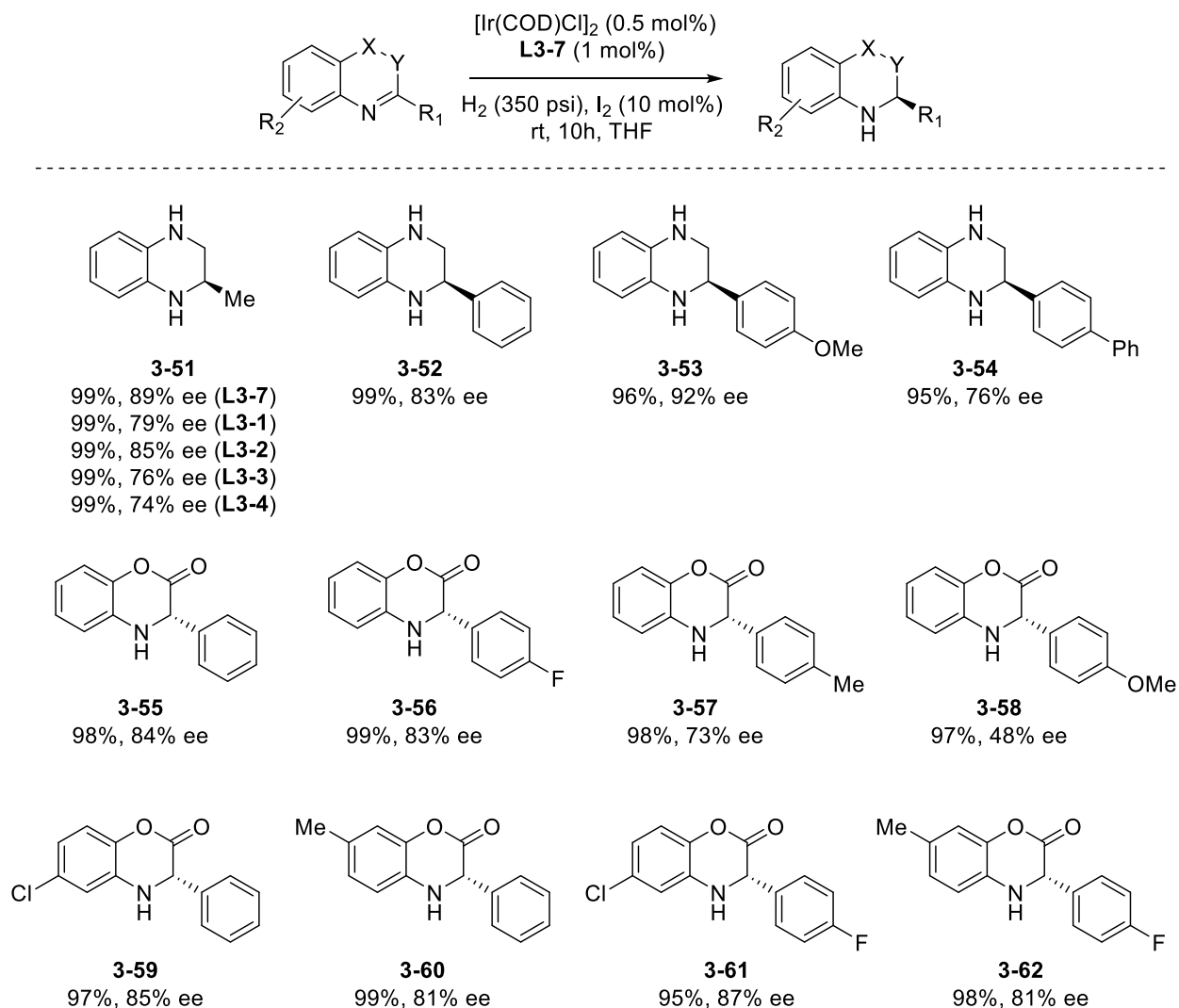


Figure 3.6 Asymmetric reduction of quinoxalines and bezoxazinones

Our subsequent studies were focused on evaluating the scope of other related heterocyclic systems that could be reduced by iridium complexes with **L3-7**. In particular, we were interested in examining the reduction of 2-substituted quinoxalines and 3-substituted 2*H*-1,4-bezoxazin-2-ones.^{30,67} The products arising from the reduction of these heterocyclic compounds often display bioactivity and are of great importance to drug discovery. With the optimized reaction condition, the reduction of 2-substituted quinoxalines was also accomplished in good enantioselectivities and resulted in chiral products **3-51** to **3-54**. This transformation was

tolerant to the nature of the C2-substituent, and Me-substituted product **3-51** and Ph-substituted product **3-52** were obtained in 89% ee and 83% ee, correspondingly. Importantly, when tested, other common ligands **L3-1** to **L3-3**⁵⁰ demonstrated inferior performance relative to **L3-7**. The substitution at the Ph ring was found to affect the selectivities as the 4-methoxyphenyl-substituted substrate **3-53** was obtained in 92% ee and 4-biphenyl-substituted substrate **3-54** was obtained in 76% ee. The reactions of 3-aryl substituted 2*H*-1,4-bezoxazin-2-ones were examined next (**3-55** to **3-62**) using (*S,R,R*)-enantiomer of ligand **L3-7**. These substrates were hydrogenated with good levels of enantiocontrol. As for quinoxalines, additional substitution at the C4 position of the aromatic group was found to affect the stereoselectivity of the reduction. While the C2-phenyl-substituted product **3-55** was obtained in 84% ee, the reduction of 4-fluorophenyl- and 4-tolyl-substituted substrates lead to products **3-56** and **3-57** in 83% ee and 73% ee, correspondingly. At the same time, substitution at the 6- or 7-positions of the heterocyclic skeleton did not lead to significant changes in selectivity, and products **3-59** and **3-60** were obtained in 85% ee and 80% ee, correspondingly. Similarly, additional substitution at both the C2-aryl group or the 6- or 7-positions of the heterocyclic skeleton could be tolerated as substrates **3-61** and **3-62** were obtained in 85% ee and 81% ee.

3.6. Conclusions

In summary, this work showcases the use of readily available by a 3-step synthesis chiral SPIROL-based diphosphinite ligands (SPIRAPO) for iridium-catalyzed asymmetric hydrogenations of quinolines, quinoxalines and 2*H*-1,4-bezoxazin-2-ones. The asymmetric hydrogenations with (*R,S,S*)-SPIRAPO ligand **L3-7** were accomplished at reduced pressures (350 psi) and could be run for the reaction times as short as 1-10 h with the S/C ratio as low as 10 000. Under these conditions, the (*R,S,S*)-diastereomer of SPIRAPO **L3-7** was found to be

highly effective ligand with generally better performance than more common ligands **L3-1** to **L3-3** or (*R,R,R*)-SPIRAPO diastereomer **L3-4**. This dearomatizative hydrogenation provided direct access to optically active tetrahydroquinolines in high enantioselectivities (up to 94% ee) and excellent yields (up to 99%) and was used to carry a 2-step synthesis of natural alkaloid (-)-(*R*)-angustureine on a 2.0-gram scale. This protocol was subsequently extended to achieve an asymmetric hydrogenation of quinoxalines and 2*H*-1,4-benzoxazin-2-ones in good to excellent enantioselectivities. Our future direction with SPIROL-derived ligands would focus on asymmetric reduction of pyrrole and furan derivatives, with which only limited number of efficient methods had been attempted.

3.7. Experimental information

General Information

Unless otherwise stated, all reagents were purchased from commercial suppliers and used without further purification. All reactions were carried out under an atmosphere of nitrogen in flame-dried glassware with magnetic stirring, unless otherwise noted. Air-sensitive reagents and solutions were transferred via syringe or cannula and were introduced to the apparatus through rubber septa. Reactions were cooled via external cooling baths: ice water (0°C), dry ice-acetone (-78°C), or Neslab CB 80 immersion cooler (0 to -60°C). Heating was achieved using a silicone oil bath with regulated by an electronic contact thermometer. Deionized water was used in the preparation of all aqueous solutions and for all aqueous extractions. Solvents used for extraction and column chromatography were ACS or HPLC grade. Dry tetrahydrofuran (THF), dichloromethane (DCM), toluene (PhMe), and diethyl ether (Et₂O) were prepared by filtration through a column (Innovative Technologies) of activated alumina under nitrogen atmosphere. Reactions were monitored by nuclear magnetic resonance (NMR, see below) or thin layer

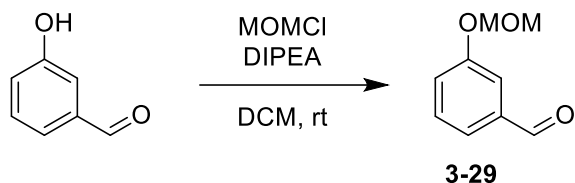
chromatography (TLC) on silica gel precoated glass plates (0.25 mm, SiliCycle, SiliaPlate). TLC plate visualization was accomplished by irradiation with UV light at 254 nm or by staining with a potassium permanganate (KMnO₄) or cerium ammonium molybdate (CAM) solution. Flash chromatography was performed using SiliCycle SiliaFlash P60 (230-400 mesh) silica gel. Powdered 4 Å molecular sieves were pre-activated by flame-drying under vacuum before use.

Proton (¹H), deuterium (D), carbon (¹³C), fluorine (¹⁹F), and phosphorus (³¹P) NMR spectra were recorded on Varian VNMRS-700 (700 MHz), Varian VNMRS-500 (500 MHz), Varian INOVA 500 (500 MHz), or Varian MR400 (400 MHz). ¹H, ¹³C, and ³¹P NMR spectra are referenced on a unified scale, where the single reference is the frequency of the residual solvent peak in the ¹H NMR spectrum. Chemical shifts (δ) are reported in parts per million (ppm) relative to tetramethylsilane for ¹H and ¹³C NMR, trichlorofluoromethane for ¹⁹F, and 85% phosphoric acid for ³¹P. Data is reported as (br = broad, s = singlet, d = doublet, t = triplet, q = quartet, m = multiplet; coupling constant(s) in Hz; integration). Slight shape deformation of the peaks in some cases due to weak coupling (e.g., aromatic protons) is not explicitly mentioned. High resolution mass spectra (HRMS) were recorded on Micromass AutoSpec Ultima or VG (Micromass) 70-250-S Magnetic sector mass. The enantiomeric excesses were determined by HPLC analysis employing a chiral stationary phase column and conditions specified in the individual experiment. HPLC experiments were performed using a Waters Alliance e2695 Separations Module instrument. Optical rotations were measured at room temperature in a solvent of choice on a JASCO P-2000 digital polarimeter at 589 nm (D-line). Fourier-transform infrared spectroscopy (FT-IR) were performed at room temperature on a Thermo-Nicolet IS-50 and converted into inverse domain (wavenumbers in cm⁻¹).

Synthesis of SPIRAPO ligands

Compounds **3-29** and **3-31** were prepared in according to the literature procedures⁴⁷.

3-(methoxymethoxy)benzaldehyde (**3-29**)



3-Hydroxybenzaldehyde (16.00 g, 131.0 mmol), DCM (150 mL), and *N,N*-diisopropylethylamine (67.0 mL, 393.0 mmol) were cooled to 0 °C before adding chloromethyl methyl ether (16.7 mL, 196.0 mmol) over 1 hour with a venting needle to handle the fumes. Reaction mixture was then warmed to room temperature. After 17 hours at room temperature, reaction mixture was quenched with a saturated aqueous solution of NaHCO₃ (170 mL). After separating the phases, the aqueous layer was extracted with DCM twice. Combined organic was washed with brine, dried over Na₂SO₄, and concentrated *in vacuo*. Crude was purified by FCC (SiO₂, 10-20% EtOAc in hexanes) to obtain the desired product **3-29** as pale-yellow liquid (20.78 g, 96.2% yield).

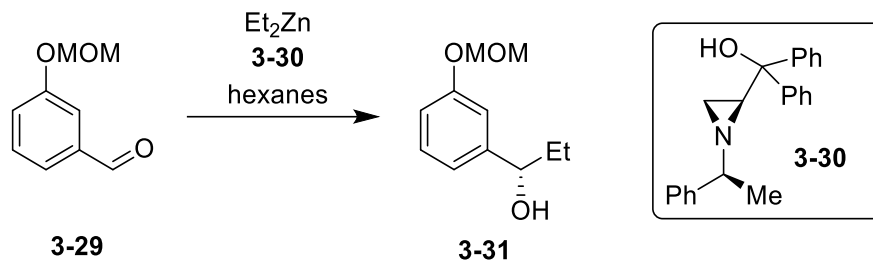
¹H NMR (700 MHz, Chloroform-d) δ 9.98 (s, 1H), 7.57–7.51 (m, 2H), 7.46 (t, *J* = 7.8 Hz, 1H), 7.32–7.28 (m, 1H), 5.24 (s, 2H), 3.49 (s, 3H).

¹³C NMR (176 MHz, Chloroform-d) δ 191.9, 157.7, 137.8, 130.1, 123.8, 122.8, 115.9, 94.3, 56.1.

IR (film): ν_{\max} = 2956, 2923, 2849, 2730, 1699, 1585, 1463, 1454, 1389, 1248, 1152, 1077, 1008, 789 cm⁻¹

The use of aziridine catalyst **3-30** was based on another report⁷².

(*S*)-1-(3-(methoxymethoxy)phenyl)propan-1-ol (**3-31**)



Hexanes (100 mL), and diphenyl((*R*)-1-((*S*)-1-phenylethyl)aziridin-2-yl)methanol **3-30** (2.47 g, 7.50 mmol) were cooled to 0 °C before adding a 1 M solution of diethylzinc in hexanes (275.0 mL, 275.0 mmol) dropwise. Reaction mixture was stirred at 0 °C before the addition of aldehyde **3-29** (20.78 g, 125.0 mmol) dropwise. After 20 hours at 0°C and 20 hours at room temperature, reaction mixture was quenched with a saturated solution of NH_4Cl (200 mL). After separating the layers, the aqueous fraction was washed with EtOAc (3x100 mL). Combined organic was washed with brine, dried over Na_2SO_4 , and concentrated *in vacuo*. Crude was purified by FCC (SiO_2 , 20% EtOAc in hexanes) to obtain (*S*)-**3-31** (23.31 g, 95.0 % yield, 99.8% ee) as pale-yellow oil.

^1H NMR (700 MHz, Chloroform-*d*) δ 7.29 – 7.24 (m, 1H), 7.03 (t, $J = 2.0$ Hz, 1H), 6.99 (dt, $J = 7.4, 1.2$ Hz, 1H), 6.96 (ddd, $J = 8.2, 2.6, 1.0$ Hz, 1H), 5.19 (s, 2H), 4.60 – 4.55 (m, 1H), 3.49 (s, 3H), 1.85 – 1.71 (m, 2H), 0.94 (t, $J = 7.4$ Hz, 3H).

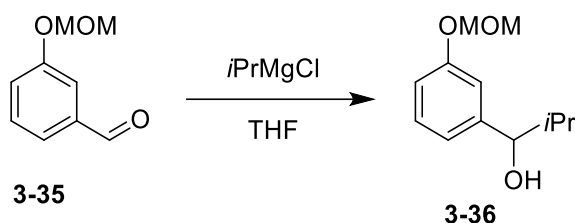
^{13}C NMR (176 MHz, Chloroform-*d*) δ 157.3, 146.4, 129.4, 119.4, 115.1, 113.9, 94.4, 75.8, 56.0, 31.8, 10.1.

ESI-HRMS Calcd. for $\text{C}_{11}\text{H}_{17}\text{O}_3^+$ 197.1171 $[\text{M}+\text{H}]^+$, found 197.1175.

IR (film): $\nu_{\text{max}} = 3411$ (br), 2961, 2932, 1586, 1486, 1451, 1242, 1149, 1077, 1011, 993, 923 cm^{-1}

HPLC (Chiralpak IA column, 96:4 hexanes/isopropanol, 1.0 ml/min), $t_r = 15.4$ min (minor, *R*),
17.0 min (major, *S*)

(*rac*)-1-(3-(benzyloxy)phenyl)-2-methylpropan-1-ol (**3-36**)



1.6 M solution isopropylmagnesium chloride in THF (5.3 mL, 8.48 mmol) and THF (5mL) were cooled to -20 °C before slow addition of the aldehyde **3-29** (697 mg, 4.20 mmol) over 20 minutes. After 5 hours at -20 °C the reaction mixture was quenched with a saturated solution of NH_4Cl (20 mL). After separating the layers, the aqueous fraction was with EtOAc three times. Combined organic was washed with brine, dried over Na_2SO_4 , and concentrated *in vacuo*. Crude was purified by FCC (SiO_2 , 15% EtOAc in hexanes) to obtain **3-36** (841 mg, 95.2% yield) as pale yellow oil.

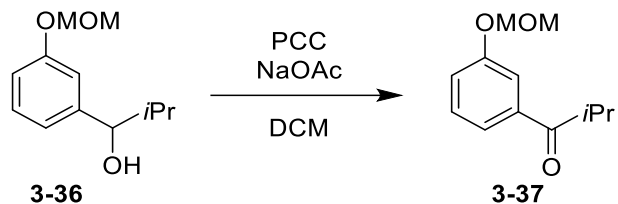
^1H NMR (400 MHz, Chloroform-*d*) δ 7.21 (m, 1H), 6.98 (m, 1H), 6.96 – 6.86 (m, 2H), 5.16 (d, $J = 0.7$ Hz, 2H), 4.33 (dd, $J = 6.8, 3.4$ Hz, 1H), 3.47 (s, 3H), 1.93 (h, $J = 6.8$ Hz, 1H), 1.78 (br s, 1H), 0.98 (d, $J = 6.7$ Hz, 3H), 0.80 (d, $J = 6.8$ Hz, 3H).

^{13}C NMR (100 MHz, Chloroform-*d*) δ 157.2, 145.4, 129.2, 120.1, 115.0, 114.5, 94.4, 79.8, 56.0, 35.1, 19.0, 18.1.

IR (film): $\nu_{\text{max}} = 3431$ (br), 2957, 2898, 2872, 2826, 1585, 1485, 1450, 1404, 1382, 1243, 1207, 1147, 1076, 834 cm^{-1}

ESI-HRMS Calcd. for $\text{C}_{12}\text{H}_{19}\text{O}_3^+$ 211.1329 $[\text{M}+\text{H}]^+$, found 211.1328.

1-(3-(methoxymethoxy)phenyl)-2-methylpropan-1-one (**3-37**)



Pyridinium chlorochromate (1.29 g, 6.00 mmol) and sodium acetate (393 mg, 4.8 mmol) were dissolved into dry DCM (25 mL) at the room temperature under the nitrogen. The mixture was stirred for 10 minutes before adding the DCM solution (8 mL) of 1-(3-(benzyloxy)phenyl)-2-methylpropan-1-ol **3-36** (840 mg, 4.0 mmol). After 5 hours at room temperature diethyl ether (10 mL) was added to the mixture and then filtered by a fritted funnel. Black insoluble solids were washed with Et₂O three times. Combined organic was washed with brine, dried over Na₂SO₄, and concentrated *in vacuo*. Crude was purified by FCC (SiO₂, 10% EtOAc in hexanes) to obtain **3-37** (711 mg, 85.0 % yield) as colorless oil.

¹H NMR (400 MHz, Chloroform-d) δ 7.67 – 7.53 (m, 2H), 7.36 (t, *J* = 7.9 Hz, 1H), 7.21 (m, 1H), 5.20 (s, 2H), 3.56 – 3.48 (m, 1H), 3.47 (s, 3H), 1.20 (d, *J* = 6.8 Hz, 6H).

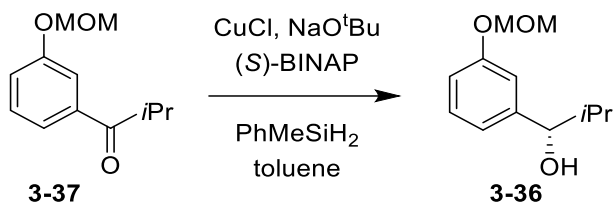
¹³C NMR (100 MHz, Chloroform-d) δ 204.1, 157.4, 137.6, 129.6, 121.8, 120.7, 115.8, 94.4, 56.1, 35.4, 19.1.

IR (film): ν_{\max} = 2970, 2933, 2904, 2826, 1682, 1581, 1485, 1467, 1435, 1247, 1149, 1078, 1017, 999, 979, 745cm⁻¹

ESI-HRMS Calcd. for C₁₂H₁₇O₃⁺ 209.1172 [M+H]⁺, found 209.1176.

The enantioselective hydrosilylation was practiced according to the literature procedure⁴⁹.

(*S*)-1-(3-(benzyloxy)phenyl)-2-methylpropan-1-ol (**3-36**)



A dry flask was charged with CuCl (17.0 mg, 0.17 mmol), NaO^tBu (16.3 mg, 0.17 mmol) and (S)-BINAP (105.8mg, 0.17 mmol) in the glove box. Dry toluene (15 mL) was added under nitrogen and the bright yellow solution was stirred for 20 minutes at room temperature. After cooling to -78 °C PhMeSiH₂ (0.93 mL, 6.80 mmol) was added dropwise over 5 minutes followed by dropwise addition of 1-(3-(methoxymethoxy)phenyl)-2-methylpropan-1-one **3-37** (710 mg, 3.40 mmol). After 15 hours at -78 °C, a saturated solution K₂CO₃ in methanol (12 mL) was added and the resulting solution was stirred for 1 h at room temperature. The organic solvents were concentrated *in vacuo*, and the crude was purified by FCC (SiO₂, 15% EtOAc in hexanes) to obtain (S)-**3-36** (175 mg, 24% yield, 92% ee, 82% BRSM) as pale yellow oil.

¹H NMR (400 MHz, Chloroform-d) δ 7.21 (m, 1H), 6.98 (m, 1H), 6.96 – 6.86 (m, 2H), 5.16 (d, *J* = 0.7 Hz, 2H), 4.33 (dd, *J* = 6.8, 3.4 Hz, 1H), 3.47 (s, 3H), 1.93 (h, *J* = 6.8 Hz, 1H), 1.78 (br s, 1H), 0.98 (d, *J* = 6.7 Hz, 3H), 0.80 (d, *J* = 6.8 Hz, 3H).

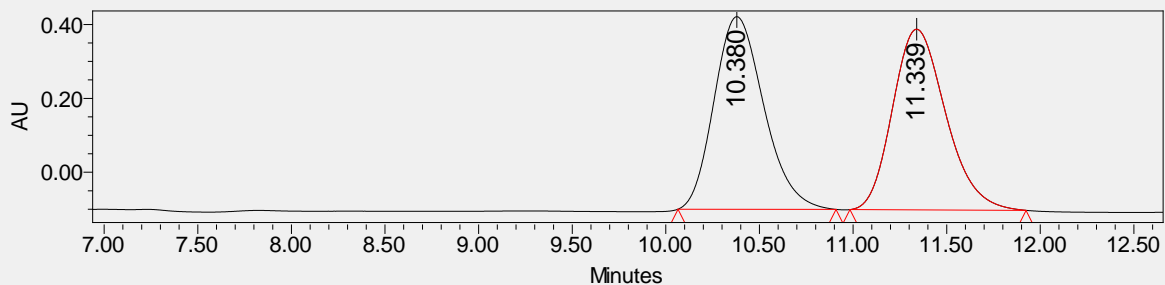
¹³C NMR (100 MHz, Chloroform-d) δ 157.2, 145.4, 129.2, 120.1, 115.0, 114.5, 94.4, 79.8, 56.0, 35.1, 19.0, 18.1.

IR (film): ν_{max} = 3431 (br), 2957, 2898, 2872, 2826, 1585, 1485, 1450, 1404, 1382, 1243, 1207, 1147, 1076, 834 cm⁻¹

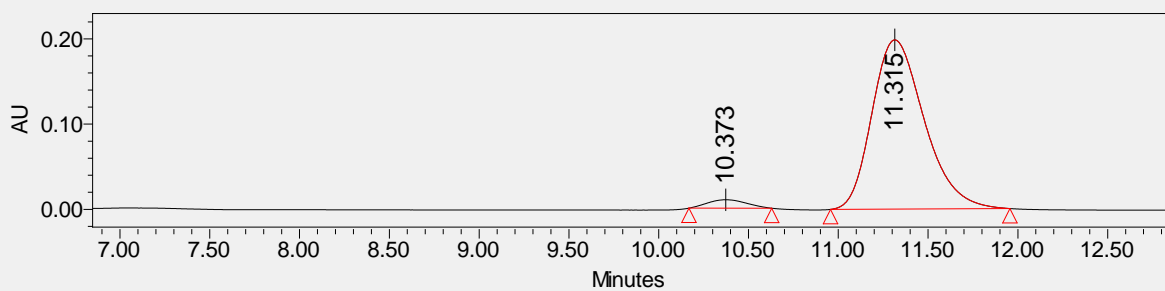
[α]_D: -22.8 (c = 4.00 in CH₂Cl₂)

ESI-HRMS Calcd. for C₁₂H₁₉O₃⁺ 211.1329 [M+H]⁺, found 211.1328.

HPLC (Chiralpak IA column, 95:5 hexanes/isopropanol, 1.0 ml/min), t_r = 10.3 min (*R*), 11.3 min (*S*)

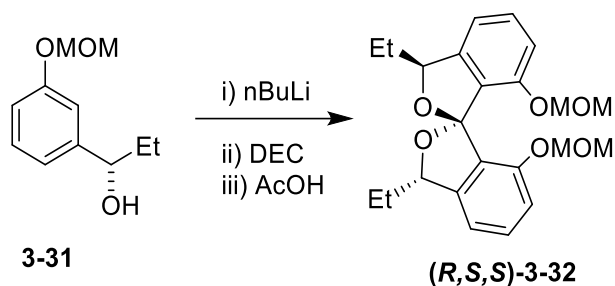


	Retention Time	Area	% Area	Height
1	10.380	9695842	50.17	523058
2	11.339	9629520	49.83	488982



	Retention Time	Area	% Area	Height
1	10.373	148692	3.57	9899
2	11.315	4012474	96.43	198536

(1R,3S,3'S)-3,3'-diethyl-7,7'-bis(methoxymethoxy)-3H,3'H-1,1'-spirobi[isobenzofuran] (*(R,S,S)*-
3-32)



Alcohol **3-31** (23.30 g, 118.7 mmol) and PhMe (250 mL) were cooled to 0 °C before addition of a 2.5 M solution *n*-butyllithium in hexanes (45 mL over 15 minutes, then 51 mL over 1.2 hours, 239.8 mmol). Reaction mixture was then warmed to room temperature. After 3 hours the resulting suspension was dissolved using 10.0 mL of THF and cooled again to 0 °C. Diethyl carbonate (7.85 mL, 64.8 mmol) was incorporated over 2 hours at 0 °C. Reaction mixture was allowed to warm slowly to room temperature overnight (12 hours). Glacial acetic acid (100 mL) was then added slowly at room temperature. After 4 hours at room temperature, reaction mixture was quenched with 80 mL of water, followed by careful addition of 20 g of NaHCO₃. After separating the layers, the aqueous fraction was with DCM three times. Combined organic was washed with brine, dried over Na₂SO₄, and concentrated *in vacuo*. The mixture components were purified by FCC (SiO₂, 10-25% EtOAc in hexanes), 19.33 g of desired (*R,S,S*)- **3-32** (81.3 % yield) were isolated as pale yellow oil and 1.30 g (5.7%) of starting material **3-31** was recovered.

¹H NMR (500 MHz, Chloroform-*d*) δ 7.29 (t, *J* = 7.8 Hz, 2H), 6.88 (dd, *J* = 7.9, 3.6 Hz, 4H), 5.40 (dd, *J* = 7.4, 3.9 Hz, 2H), 4.95 (d, *J* = 6.6 Hz, 2H), 4.82 (d, *J* = 6.6 Hz, 2H), 3.07 (s, 6H), 1.98 (dtd, *J* = 14.8, 7.3, 3.9 Hz, 2H), 1.86 (dq, *J* = 14.3, 7.3 Hz, 2H), 1.04 (t, *J* = 7.4 Hz, 6H).

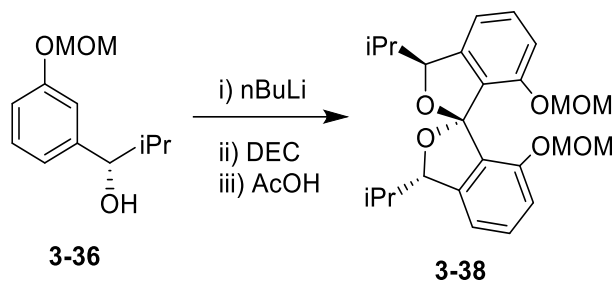
¹³C NMR (126 MHz, Chloroform-*d*) δ 152.4, 145.6, 130.5, 127.7, 115.8, 113.9, 112.1, 93.2, 83.1, 55.6, 28.0, 9.7.

IR (film): ν_{\max} = 2962, 2934, 1614, 1599, 1479, 1256, 1152, 1002, 960, 928, 734 cm⁻¹

ESI-HRMS Calcd. for C₂₃H₂₉O₆⁺ 401.1964 [M+H]⁺, found 401.1958.

(1*R*,3*S*,3'*S*)-3,3'-diisopropyl-7,7'-bis(methoxymethoxy)-3*H*,3'*H*-1,1'-spirobi[isobenzofuran]

((*R,S,S*)-**3-38**)



Alcohol **3-36** (175 mg, 0.83 mmol) and PhMe (3.0 mL) were cooled to 0 °C before addition of a 2.5 M solution *n*-butyllithium in hexanes (0.67 mL over 35 min, 1.67 mmol). Reaction mixture was then warmed to room temperature. After 4 hours the solution was cooled again to 0 °C. Diethyl carbonate (55 μ L, 0.45 mmol) was incorporated over 40 minutes at 0 °C. Reaction mixture was allowed to warm slowly to room temperature overnight (11 hours). Glacial acetic acid (1.0 mL) was then added slowly at room temperature. After 4 hours at room temperature, reaction mixture was quenched with 3 mL of saturated NaHCO₃ solution. After separating the layers, the aqueous fraction was with DCM three times. Combined organic was washed with brine, dried over Na₂SO₄, and concentrated *in vacuo*. The mixture components were purified by FCC (SiO₂, 10-25% EtOAc in hexanes), 81 mg of desired (*R,S,S*)-**3-38** (43.4 % yield, 73.5 % BRSM) were isolated as pale yellow oil and 72 mg (41%) of starting material **3-36** was recovered.

¹H NMR (500 MHz, Chloroform-*d*) δ 7.30 (t, J = 7.8 Hz, 2H), 6.96 – 6.91 (m, 4H), 5.32 (d, J = 3.3 Hz, 2H), 4.95 (d, J = 6.6 Hz, 2H), 4.80 (d, J = 6.7 Hz, 2H), 3.14 (s, 6H), 2.23 (pd, J = 6.9, 3.4 Hz, 2H), 1.11 (d, J = 6.9 Hz, 6H), 0.92 (d, J = 6.9 Hz, 6H).

¹³C NMR (176 MHz, Chloroform-*d*) δ 152.9, 145.1, 130.3, 128.3, 114.4, 112.0, 93.7, 85.9, 55.7, 32.1, 18.9, 16.7.

[α]_D: -32.9 (*c* = 1.00 in CH₂Cl₂)

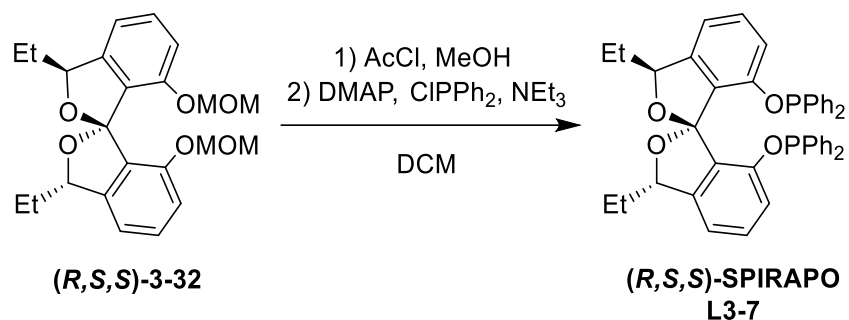
IR (film): ν_{max} = 2962, 2930, 2849, 1653, 1465, 1209, 1151, 1079, 995, 969 cm⁻¹

ESI-HRMS Calcd. for C₂₅H₃₃O₆⁺ 429.2272 [M+H]⁺, found 429.2268.

One-pot synthesis for the diphosphinite ligand

(((*1R,3S,3'S*)-3,3'-diethyl-3H,3'H-1,1'-spirobi[isobenzofuran]-7,7'-

diyl)bis(oxy))bis(diphenylphosphane) ((*R,S,S*)-**L3-7**)



Spiroketal (**(*R,S,S*)-3-32**) (77.0 mg, 0.18 mmol) and MeOH (1.5 mL) were added to a round bottom flask at room temperature. Solution was cooled to 0 °C, and then acetyl chloride (24 μ L, 0.36 mmol) was added slowly. Reaction mixture was warmed to room temperature. After complete consumption of the starting material indicated by TLC, the solution was concentrated *in vacuo*. Dimethylaminopyridine (6.4 mg, 0.05 mmol) and dry DCM (6.0 mL) were added to the flask at room temperature before addition of triethylamine (0.51 mL, 3.9 mmol) and chlorodiarylpophine (0.77 mmol) over 30min. After 12h, volatiles were removed *in vacuo*, and the crude was purified by FCC (SiO₂ treated with 5% TEA, 4% → 9% EtOAc in hexanes) to afford (**(*R,S,S*)-L3-7**) (51.1 mg, 83% yield) as white solids.

¹H NMR (399.54 MHz, Chloroform-*d*) δ 7.31-7.21 (m, 12H), 7.14 (t, *J* = 7.4 Hz, 2H), 7.06 (m, 6H), 6.97 – 6.90 (m, 4H), 6.86 – 6.81 (m, 2H), 5.26 (dd, *J* = 8.2, 4.2 Hz, 2H), 1.57 (m, 2H), 1.41 (m, 2H), 0.87 (t, *J* = 7.4 Hz, 6H)

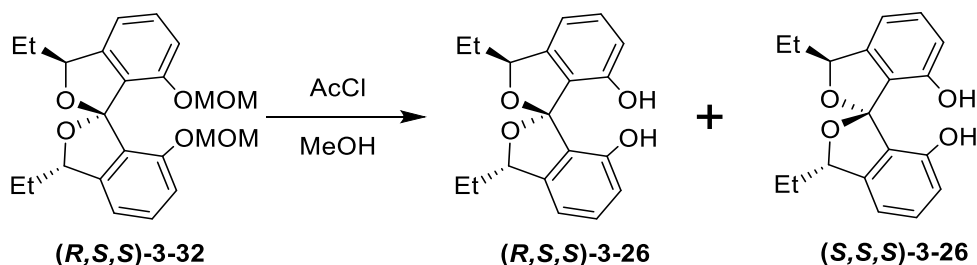
^{13}C NMR (100 MHz, Chloroform-*d*) δ 152.3, 152.2, 146.3, 140.1, 139.9, 139.8, 139.7, 130.7, 130.5, 130.4, 129.7, 129.6, 129.5, 128.8, 128.3, 128.3, 128.2, 128.1, 115.3, 115.1, 115.0, 114.6, 82.9, 28.0, 10.2

^{31}P NMR (161.75 MHz, Chloroform-*d*) δ 105.25

ESI-HRMS Calcd. for $\text{C}_{43}\text{H}_{39}\text{O}_4\text{P}_2^+$ 681.2317 $[\text{M}+\text{H}]^+$, found 681.2316.

Two-step synthesis for diphosphinite ligands

(*1R,3S,3'S*)-3,3'-diethyl-3H,3'H-1,1'-spirobi[isobenzofuran]-7,7'-diol (*R,S,S*)-**3-26** and (*S,S,S*)-**3-26** diastereomer from (*R,S,S*)-**3-32**



The deprotection of the MOM group using AcCl in MeOH was mild enough that after 6h at room temperature the contrathermodynamic diol (*R,S,S*)-**3-26** is the major compound. However, SiO_2 and other acidic conditions epimerize it into (*S,S,S*)-**3-26**. These results agree with the calculated ΔG of 1.0 kcal/mol favoring (*R,S,S*)-**3-26**. Consequently, neutralizing the acidic conditions after 6h of reaction yields (*R,S,S*)-**3-26** selectively, while performing chromatography after the reaction time gives (*S,S,S*)-**3-26** enriched material, as exemplified below.

(*R,S,S*)-selective deprotection

Spiroketal (*R,S,S*)-**3-26** (1.38 g, 3.44 mmol) and MeOH (15 mL) were added to a vial. Solution was cooled to 0 °C, and then acetyl chloride (480 μL , 6.90 mmol) was added slowly.

Reaction mixture was warmed to room temperature. After 6 hours, reaction mixture was quenched with a saturated solution of NaHCO₃. Extracted three times with DCM, and then combined organic was dried with Na₂SO₄, and concentrated *in vacuo* to afford diol **3-26** (400.9 mg, 93% yield, dr ~1:7.1 of *(S,S,S)*-**3-26**:*(R,S,S)*-**3-26**).

¹H NMR (500 MHz, Chloroform-*d*) δ 7.34 (t, *J* = 7.7 Hz, 2H), 6.86 (d, *J* = 7.5, 2H), 6.77 (d, *J* = 8.0, 2H), 5.41 (dd, *J* = 6.7, 4.1 Hz, 2H), 4.73 (s, 2H), 2.07 (m, 2H), 1.83 (m, 2H), 1.01 (t, *J* = 7.4 Hz, 6H).

¹³C NMR (126 MHz, Chloroform-*d*) δ 151.8, 145.3, 132.3, 123.2, 115.4, 113.6, 83.0, 27.7, 9.1

ESI-HRMS Calcd. for C₁₉H₂₁O₄⁺ 314.1440 [M+H]⁺, found 314.1435.

***(S,S,S)*-selective deprotection**

Spiroketal *(R,S,S)*-**3-26** (2.82 g, 7.04 mmol) and MeOH (35 mL) were added to a round bottom flask. Solution was cooled to 0 °C, and then acetyl chloride (1.0 mL, 14.1 mmol) was added slowly. Reaction mixture was warmed to room temperature. After 6 hours, reaction mixture was concentrated *in vacuo*, and purified by FCC (SiO₂, 30%→40% EtOAc in hexanes) to obtain diol **3-26** (2.15 g, 97.5% yield 1:5.7:11.0 dr *(S,R,S)*:*(R,S,S)*-**3-26**:*(S,S,S)*-**3-26**).

¹H NMR (500 MHz, Chloroform-*d*) δ 7.31 (t, *J* = 7.8 Hz, 2H), 6.86 (d, *J* = 7.5 Hz, 2H), 6.75 (d, *J* = 8.0 Hz, 2H), 5.27 (dd, *J* = 7.6, 4.4 Hz, 2H), 4.60 (s, 2H), 1.99 – 1.85 (m, 4H), 1.07 (t, *J* = 7.3 Hz, 6H).

¹³C NMR (126 MHz, Chloroform-*d*) δ 151.6, 145.2, 131.9, 123.3, 115.4, 113.8, 84.8, 30.6, 9.7.

ESI-HRMS Calcd. for C₁₉H₂₁O₄⁺ 314.1440 [M+H]⁺, found 314.1435.

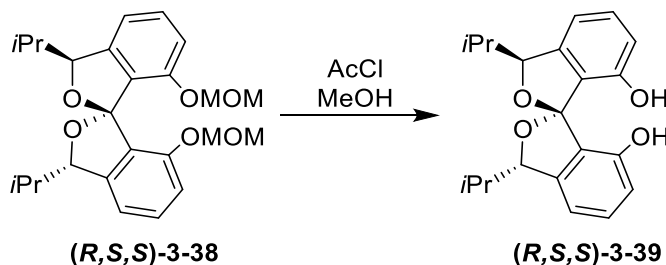
IR (powder): ν_{max} = 3299 (br), 2971, 2961, 2928, 1625, 1604, 1476, 1350, 1251, 1202, 1162, 1058, 1004, 959, 828 cm⁻¹

The purified (*S,S,S*)-**3-26** can be further enantio-enriched by recrystallization.

2.0 g of diol **3-26** after the purification step was placed into a dry 50-mL erlenmeyer flask and hot DCM was quickly added dropwise by a pipette to the flask while constant swaying movement was maintained. Once all solids were dissolved in hot DCM, the flask was then transferred and placed into a glass jar prefilled with hexanes. The jar was capped and hexanes were allowed to slowly diffuse into the flask. After 5 days, colorless hexagonal crystals were grown in the solution. The mother liquid was filter off and crystals were washed by ice-cold hexanes and dried *in vacuo* to afford diol (*S,S,S*)-**3-26**.

[α]_D: -42.2 (c = 0.20 in CH₂Cl₂)

(*1R,3S,3'S*)-3,3'-diisopropyl-3H,3'H-1,1'-spirobi[isobenzofuran]-7,7'-diol (*R,S,S*)-**3-39**



Spiroketal (*R,S,S*)-**3-38** (77.0 mg, 0.18 mmol) and MeOH (1.5 mL) were added to a round bottom flask at room temperature. Solution was cooled to 0 °C, and then acetyl chloride (24 μ L, 0.36 mmol) was added slowly. Reaction mixture was warmed to room temperature. After 14 hours, reaction mixture was quenched with a saturated solution of NaHCO₃. Extracted three times with DCM, and then combined organic was dried with Na₂SO₄, and concentrated *in vacuo* to afford diol (*R,S,S*)-**3-39** (51.1 mg, 83% yield) as white solids.

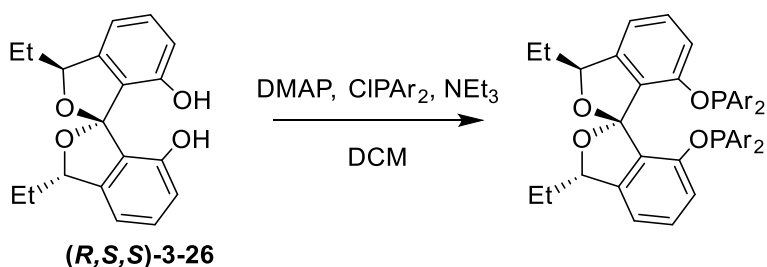
¹H NMR (401 MHz, Methanol-*d*₄) δ 7.18 (t, *J* = 7.7 Hz, 2H), 6.73 (d, *J* = 7.5 Hz, 2H), 6.62 (d, *J* = 8.0 Hz, 2H), 5.17 (d, *J* = 3.3 Hz, 2H), 2.17 (pd, *J* = 6.8, 3.4 Hz, 2H), 1.07 (d, *J* = 6.9 Hz, 6H), 0.86 (d, *J* = 6.9 Hz, 6H).

¹³C NMR (100 MHz, Methanol-*d*₄) δ 153.4, 144.8, 130.0, 125.3, 113.8, 111.4, 85.9, 32.1, 18.3, 15.5.

[α]_D: -32.4 (c = 0.50 in CH₂Cl₂)

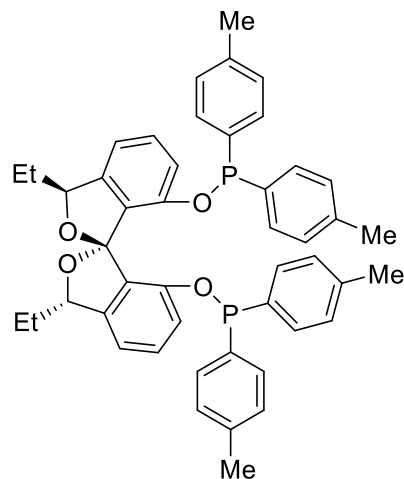
IR (film): ν_{max} = 3408 (br), 2961, 2930, 2873, 1743, 1715, 1601, 1457, 1343, 985, 836 cm⁻¹

ESI-HRMS Calcd. for C₂₁H₂₅O₄⁺ 341.1747 [M+H]⁺, found 341.1743.



Dimethylaminopyridine (6.4 mg, 0.05 mmol) and the **(R,S,S)-3-26** (100 mg, 0.32 mmol, 1:7.1 of **(S,S,S)-3-26:(R,S,S)-3-26**) were dissolved into dry DCM (6.0 mL) at room temperature before addition of triethylamine (0.51 mL, 3.9 mmol) and chlorodiaryolphosphine (0.77 mmol) over 30min. After 12h, volatiles were removed *in vacuo*, and the crude was purified by FCC (SiO₂ treated with 5% TEA, 4%→9% EtOAc in hexanes) to afford products.

(((*1R,3S,3'S*)-3,3'-diethyl-3H,3'H-1,1'-spirobi[isobenzofuran]-7,7'-diyl)bis(oxy))bis(di-p-tolylphosphane) **(R,S,S)-L3-8**



(R,S,S)-L3-8

white foam, 180.0 mg, 76% yield

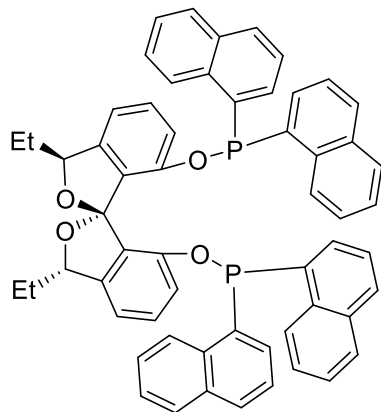
¹H NMR (500 MHz, Benzene-*d*₆) δ 7.31 (t, *J* = 7.9 Hz, 6H), 7.09 (t, *J* = 7.6 Hz, 4H), 7.03 (t, *J* = 7.8 Hz, 2H), 6.80 (dd, *J* = 14.4, 7.7 Hz, 8H), 6.57 (d, *J* = 7.5 Hz, 2H), 5.32 (dd, *J* = 8.2, 4.5 Hz, 2H), 1.93 (d, *J* = 3.8 Hz, 12H), 1.57 – 1.45 (m, 4H), 0.92 (t, *J* = 7.3 Hz, 6H).

¹³C NMR (126 MHz, Benzene-*d*₆) δ 146.9, 139.3, 138.5, 130.9, 130.7, 130.1, 130.0, 129.8, 129.1, 129.0, 129.0, 115.3, 115.2, 114.3, 82.7, 28.2, 20.8, 10.4.

³¹P NMR (202 MHz, *c*₆*d*₆) δ 106.24.

ESI-HRMS Calcd. for C₄₇H₄₇O₄P₂⁺ 737.2944 [M+H]⁺, found 737.2941.

(((*1R,3S,3'S*)-3,3'-diethyl-3H,3'H-1,1'-spirobi[isobenzofuran]-7,7'-diyl)bis(oxy))bis(di(naphthalen-1-yl)phosphane) **(R,S,S)-L3-9**



(R,S,S)-L3-9

white foam, 230.0 mg, 81% yield

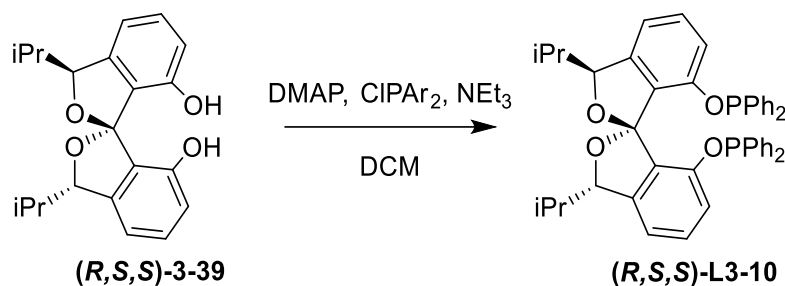
¹H NMR (400 MHz, Benzene-*d*₆) δ 8.43 (ddd, *J* = 17.8, 8.1, 3.4 Hz, 4H), 7.48 – 7.43 (m, 8H), 7.41 (d, *J* = 8.2 Hz, 4H), 7.25 – 7.15 (m, 4H), 7.07 – 6.94 (m, 8H), 6.90 (t, *J* = 7.6 Hz, 2H), 6.70 (t, *J* = 7.8 Hz, 2H), 6.22 (d, *J* = 7.5 Hz, 2H), 5.09 (dd, *J* = 9.6, 3.5 Hz, 2H), 1.21 – 1.04 (m, 4H), 0.65 (t, *J* = 7.4 Hz, 6H).

¹³C NMR (100 MHz, Benzene-*d*₆) δ 152.4, 146.4, 145.5, 136.6, 135.3, 134.6, 133.5, 131.6, 130.4, 130.1, 128.5, 128.2, 126.5, 126.4, 125.7, 125.7, 125.3, 125.0, 121.0, 115.5, 114.2, 113.8, 83.1, 28.0, 10.5.

³¹P NMR (202 MHz, *c*₆*d*₆) δ 92.46.

ESI-HRMS Calcd. for C₅₉H₄₇O₄P₂⁺ 881.2944 [M+H]⁺, found 881.2938.

(((*1R,3S,3'S*)-3,3'-diisopropyl-3H,3'H-1,1'-spirobi[isobenzofuran]-7,7'-diyl)bis(oxy))bis(diphenylphosphane) **(R,S,S)-L3-10**



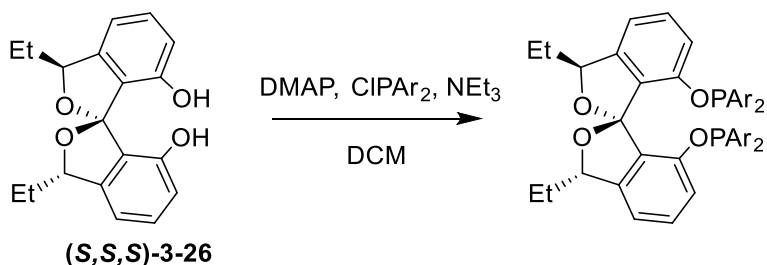
Dimethylaminopyridine (2.9 mg, 0.022 mmol) and the *(R,S,S)*-**3-39** (49 mg, 0.14 mmol) were dissolved into dry DCM (2.0 mL) at room temperature before addition of triethylamine (0.23 mL, 1.8 mmol) and chlorodiphenylphosphine (66 μ L, 0.36 mmol) over 30min. After 12h, volatiles were removed *in vacuo*, and the crude was purified by FCC (SiO_2 treated with 5% TEA, 1% TEA in hexanes) to afford *(R,S,S)*-**L3-10** (84 mg, 84% yield) as white solids.

$^1\text{H NMR}$ (500 MHz, Benzene- d_6) δ 7.47 – 7.40 (m, 4H), 7.20 (q, $J = 10.9, 9.3$ Hz, 6H), 7.02 – 6.95 (m, 8H), 6.91 (d, $J = 5.5$ Hz, 6H), 6.66 (d, $J = 7.5$ Hz, 2H), 5.32 (d, $J = 4.4$ Hz, 2H), 1.88 (dq, $J = 11.1, 6.7$ Hz, 2H), 0.96 (d, $J = 6.8$ Hz, 6H), 0.77 (d, $J = 6.8$ Hz, 6H).

$^{13}\text{C NMR}$ (126 MHz, Benzene- d_6) δ 153.2, 146.7, 141.2, 141.0, 140.7, 130.9, 130.7, 130.7, 130.5, 129.7, 129.2, 128.7, 128.7, 128.6, 128.5, 116.3, 116.1, 115.6, 86.0, 32.5, 19.7, 17.6.

$^{31}\text{P NMR}$ (202 MHz, c_6d_6) δ 107.75.

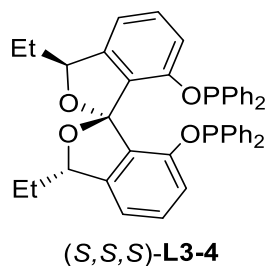
ESI-HRMS Calcd. for $\text{C}_{45}\text{H}_{43}\text{O}_4\text{P}_2^+$ 709.2631 $[\text{M}+\text{H}]^+$, found 709.2636.



Dimethylaminopyridine (6.4 mg, 0.05 mmol) and the recrystallized *(S,S,S)*-**3-26** (100 mg, 0.32 mmol) were dissolved into dry DCM (6.0 mL) at room temperature before addition of

triethylamine (0.51 mL, 3.9 mmol) and chlorodiaryolphosphine (0.77 mmol) over 30min. After 12h, volatiles were removed *in vacuo*, and the crude was purified by FCC (SiO₂ treated with 5% TEA, 4%→ 9% EtOAc in hexanes) to afford the corresponding product.

(((*1R,3S,3'S*)-3,3'-diethyl-3H,3'H-1,1'-spirobi[isobenzofuran]-7,7'-diyl)bis(oxy))bis(diphenylphosphane) ((*S,S,S*)-**L3-4**)



white foam, 197.0 mg, 90% yield

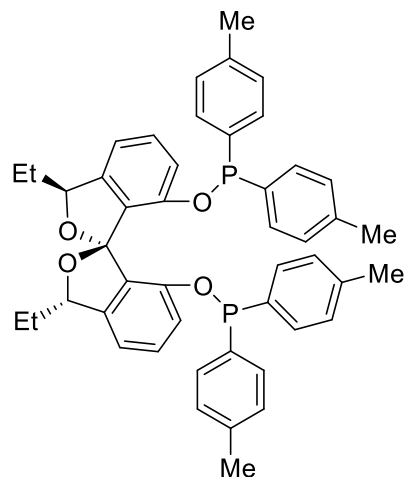
¹H NMR (500 MHz, Chloroform-*d*) δ 7.34 – 7.19 (m, 12H), 7.15 (t, *J* = 7.7 Hz, 2H), 7.13 – 6.99 (m, 6H), 6.97 (t, *J* = 7.4 Hz, 4H), 6.71 (d, *J* = 7.5 Hz, 2H), 4.78 (dd, *J* = 7.2, 4.5 Hz, 2H), 1.89 – 1.72 (m, 4H), 0.99 (t, *J* = 7.4 Hz, 6H).

¹³C NMR (126 MHz, Chloroform-*d*) δ 145.8, 130.8, 130.6, 130.4, 130.4, 129.7, 129.6, 129.5, 129.0, 128.2, 128.1, 115.1, 114.7, 84.2, 30.0, 9.7.

³¹P NMR (202 MHz, Chloroform-*d*) δ 104.21.

ESI-HRMS Calcd. for C₄₃H₃₉O₄P₂⁺ 681.2317 [M+H]⁺, found 681.2318.

(((*1S,3S,3'S*)-3,3'-diethyl-3H,3'H-1,1'-spirobi[isobenzofuran]-7,7'-diyl)bis(oxy))bis(di-*p*-tolylphosphane) ((*S,S,S*)-**L3-5**)



(S,S,S)-L3-5

white foam, 230.0 mg, 97% yield

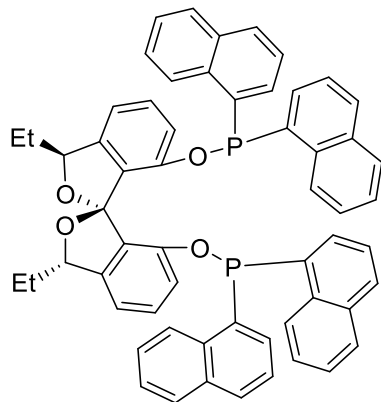
¹H NMR (500 MHz, Benzene-*d*₆) δ 7.35 (dd, *J* = 8.1, 3.5 Hz, 2H), 7.31 (t, *J* = 7.8 Hz, 4H), 7.03 (t, *J* = 7.7 Hz, 6H), 6.84 (d, *J* = 7.7 Hz, 4H), 6.77 (d, *J* = 7.6 Hz, 4H), 6.55 (d, *J* = 7.5 Hz, 2H), 4.94 (t, *J* = 5.7 Hz, 2H), 1.95 (d, *J* = 6.8 Hz, 12H), 1.88 – 1.77 (m, 4H), 1.05 (t, *J* = 7.3 Hz, 6H),

¹³C NMR (126 MHz, Benzene-*d*₆) δ 152.9, 152.8, 146.2, 139.4, 138.7, 137.8, 137.7, 137.5, 137.4, 131.1, 130.9, 130.1, 130.1, 129.9, 129.0, 129.0, 128.9, 114.9, 114.8, 114.4, 83.9, 30.0, 20.8, 20.8, 9.6.

³¹P NMR (202 MHz, *c*₆*d*₆) δ 105.47.

ESI-HRMS Calcd. for C₄₇H₄₇O₄P₂⁺ 737.2944 [M+H]⁺, found 737.2943.

(((*1S,3S,3'S*)-3,3'-diethyl-3H,3'H-1,1'-spirobi[isobenzofuran]-7,7'-diyl)bis(oxy))bis(di(naphthalen-1-yl)phosphane) ((*S,S,S*)-**L3-6**)



(S,S,S)-L3-6

white foam, 211.0 mg, 74% yield

¹H NMR (500 MHz, Benzene-*d*₆) δ 8.54 (dd, *J* = 8.3, 3.4 Hz, 2H), 8.40 (dd, *J* = 8.4, 3.5 Hz, 2H), 7.53 – 7.45 (m, 10H), 7.28 (t, *J* = 6.2 Hz, 2H), 7.12 (m, 4H), 7.05 (td, *J* = 7.6, 3.9 Hz, 6H), 6.95 (td, *J* = 7.5, 4.7 Hz, 4H), 6.66 (t, *J* = 7.8 Hz, 2H), 6.08 (d, *J* = 7.5 Hz, 2H), 4.40 (dd, *J* = 6.6, 4.7 Hz, 2H), 1.58 (qd, *J* = 12.5, 11.3, 6.7 Hz, 4H), 0.84 (t, *J* = 7.3 Hz, 8H).

¹³C NMR (126 MHz, Benzene-*d*₆) δ 152.8, 145.9, 136.2, 136.1, 135.9, 135.7, 135.2, 134.9, 133.9, 130.6, 130.6, 130.4, 130.3, 128.9, 126.9, 126.7, 126.2, 126.1, 126.1, 125.9, 125.8, 125.6, 125.4, 116.7, 114.8, 114.6, 114.3, 84.1, 29.9, 9.9.

³¹P NMR (202 MHz, *c*₆*d*₆) δ 94.52.

ESI-HRMS Calcd. for C₅₉H₄₇O₄P₂⁺ 881.2944 [M+H]⁺, found 881.2946.

Recrystallization of (1*S*,3*S*,3'*S*)-3,3'-diethyl-3*H*,3'*H*-1,1'-spirobi[isobenzofuran]-7,7'-diol ((*S,S,S*)-3-26)

Colorless hexagonal crystals of **ssspiro** were grown from a dichloromethane/hexanes solution of the compound at 22 deg. C. A crystal of dimensions 0.22 x 0.20 x 0.18 mm was mounted on a Rigaku AFC10K Saturn 944+ CCD-based X-ray diffractometer equipped with a low temperature

device and Micromax-007HF Cu-target micro-focus rotating anode ($\lambda = 1.54187 \text{ \AA}$) operated at 1.2 kW power (40 kV, 30 mA). The X-ray intensities were measured at 85(1) K with the detector placed at a distance 42.00 mm from the crystal. A total of 2028 images were collected with an oscillation width of 1.0° in ω . The exposure times were 1 sec. for the low angle images, 4 sec. for high angle. Rigaku d*trek images were exported to CrysAlisPro for processing and corrected for absorption. The integration of the data yielded a total of 61312 reflections to a maximum 2θ value of 138.33° of which 4949 were independent and 4874 were greater than $2s(I)$. The final cell constants (Table 1) were based on the xyz centroids of 33076 reflections above $10s(I)$. Analysis of the data showed negligible decay during data collection. The structure was solved and refined with the Bruker SHELXTL (version 2018/3) software package, using the space group $P3(1)21$ with $Z = 9$ for the formula $C_{19}H_{20}O_4$. All non-hydrogen atoms were refined anisotropically with the hydrogen atoms placed in a combination of refined and idealized positions. Full matrix least-squares refinement based on F^2 converged at $R1 = 0.0470$ and $wR2 = 0.1248$ [based on $I > 2\sigma(I)$], $R1 = 0.0474$ and $wR2 = 0.1253$ for all data. Additional details are presented in Table 1 and are given as Supporting Information in a CIF file. Acknowledgement is made for funding from NSF grant CHE-0840456 for X-ray instrumentation.

G.M. Sheldrick (2015) "Crystal structure refinement with SHELXL", *Acta Cryst.*, C71, 3-8 (Open Access).

CrystalClear Expert 2.0 r16, Rigaku Americas and Rigaku Corporation (2014), Rigaku Americas, 9009, TX, USA 77381-5209, Rigaku Tokyo, 196-8666, Japan.

CrysAlisPro 1.171.38.41 (Rigaku Oxford Diffraction, 2015).

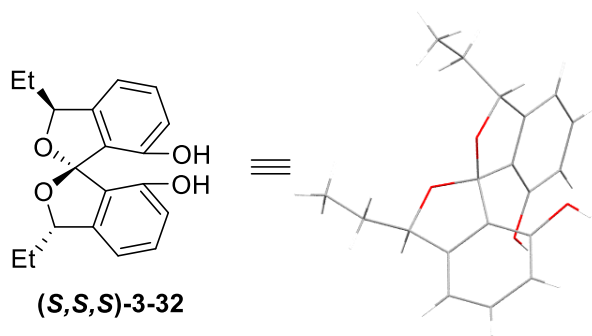


Table 1. Crystal data and structure refinement for ssspiro.

Identification code	ssspiro
Empirical formula	C ₁₉ H ₂₀ O ₄
Formula weight	312.35
Temperature	85(2) K
Wavelength	1.54184 Å
Crystal system, space group	Trigonal, P3(1)21
Unit cell dimensions	a = 12.81980(10) Å alpha = 90 deg. b = 12.81980(10) Å beta = 90 deg. c = 27.9907(5) Å gamma = 120 deg.
Volume	3983.88(9) Å ³
Z, Calculated density	9, 1.172 Mg/m ³
Absorption coefficient	0.664 mm ⁻¹
F(000)	1494
Crystal size	0.220 x 0.200 x 0.180 mm
Theta range for data collection	3.982 to 69.164 deg.

Limiting indices $-15 \leq h \leq 15, -15 \leq k \leq 15, -33 \leq l \leq 32$

Reflections collected / unique 61312 / 4949 [R(int) = 0.0435]

Completeness to theta = 67.684 99.9 %

Absorption correction Semi-empirical from equivalents

Max. and min. transmission 1.00000 and 0.75742

Refinement method Full-matrix least-squares on F^2

Data / restraints / parameters 4949 / 0 / 328

Goodness-of-fit on F^2 1.062

Final R indices [$I > 2\sigma(I)$] R1 = 0.0470, wR2 = 0.1248

R indices (all data) R1 = 0.0474, wR2 = 0.1253

Absolute structure parameter -0.11(6)

Extinction coefficient 0.0043(4)

Largest diff. peak and hole 0.372 and -0.258 e. \AA^{-3}

Representative procedure for asymmetric hydrogenation of quinoline derivatives

Hydrogenations were carried out according to the procedure in a reported literature⁷⁴. Bis(1,5-cyclooctadiene)diiridium(I) dichloride (3.4 mg, 0.005 mmol) and (*R,S,S*)-SPIRAPO **L3-7** (7.6 mg, 0.011 mmol) [or (*S,R,R*)-SPIRAPO **L3-7** (7.6 mg, 0.011 mmol)] were added to a Schlenk tube with a stir bar strictly under nitrogen in the glovebox. After the Schlenk tube taken out of the glovebox, dry THF (1000 μ L) was added, and the mixture was stirred under the nitrogen atmosphere at room temperature for 2 hours. In an oven-dried 1-dram vial was charged a stir bar, the corresponding substrate (0.1 mmol), I₂ (2.5 mg, 0.01 mmol) and dry THF (0.9 mL) under the nitrogen, and then 100 μ L of the pre-mixed catalyst solution was transferred into the vial via a syringe. The vial was then brought into the high-pressure reactor and an 18G needle was left in the vial septa. The inner atmosphere of the reactor was purged by charging and carefully releasing 100 psi of H₂ for 5 times before setting to 350 psi of H₂. The reaction was stirred at 350 psi of H₂ for 10 hours. After the reaction, the vial was taken out of the reactor and concentrated *in vacuo*. Crude was purified by FCC (SiO₂, 10% EtOAc in hexanes) to obtain the desired product. The purified product was analyzed by NMR, ESI-HRMS and the ee was analyzed by HPLC.

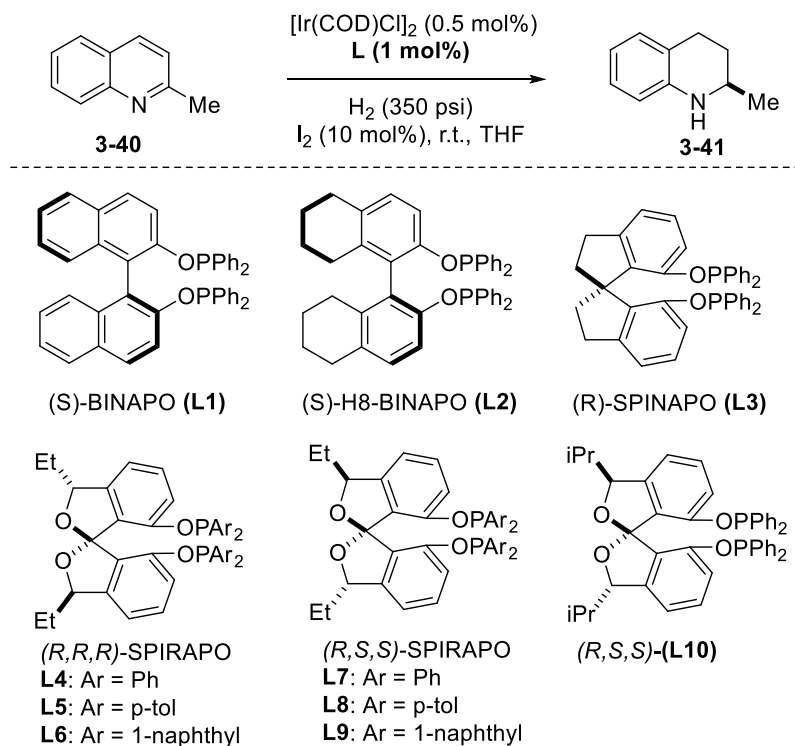
Determination of Configuration:

The absolute (*R*)-configuration of the 2-alkyl tetrahydroquinolines and (*S*)-configuration of 2-aryl tetrahydroquinolines are assigned by analogy based on the optical rotation of the X-ray crystal structure of 2-(3-Bromophenyl)-tetrahydroquinoline previously reported in the literature⁷⁵.

The absolute (*R*)-configuration of tetrahydroquinoxalines are assigned by analogy based on the optical rotation of the X-ray crystal structure of (*R*)-7-chloro-2-phenyl-1,2,3,4-tetrahydroquinoxaline previously reported in the literature⁷⁶.

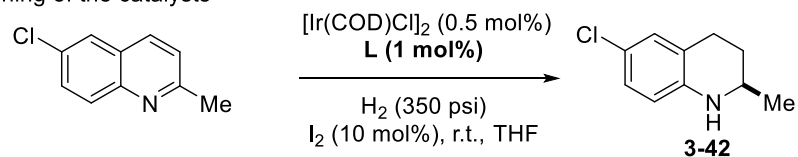
The absolute (*S*)-configuration of 3,4-dihydro-2*H*-1,4-benzoxazin-2-ones are assigned by analogy based on the optical rotation of the X-ray crystal structure of (*S*)-3-(2-thienyl)-3,4-dihydro-2*H*-1,4-benzoxazin-2-one previously reported in the literature⁷⁷.

Table S1. Screening of the catalysts

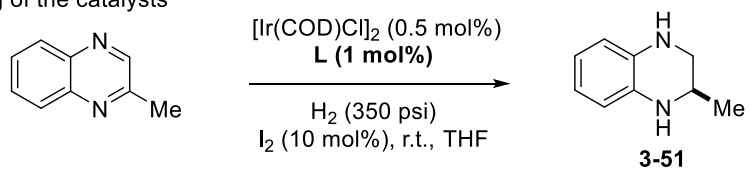


entry	ligand	H ₂ (psi)	time (h)	conv. (%)	ee (%)
1 ^c	L1	700	20	99	81
2	L1	350	10	99	42
3	L2	350	10	67	51
4	L3	350	10	99	90
5	L4	350	10	99	88
6	L5	350	10	99	33
7	L6	350	10	99	12
8	L7	350	10	99	94
9	L8	350	10	99	87
10	L9	350	10	99	55
11	L10	350	10	99	90
12 ^d	L7	350	10	93	91

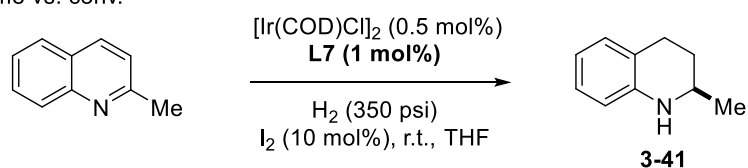
^a All reactions were carried out at room temperature with 0.1 mmol quinaldine **3-40** using Ir complex generated in situ from [Ir(COD)Cl]₂ (0.5 mol%), ligand L1 to L10 (1.1 mol%), and I₂ (10 mol%) under pressurized H₂ in 1 ml of solvent. ^b The conversion was determined by ¹H NMR and the enantioselectivity was determined by HPLC analysis with a Chiralpak OJ-H column. The product was in R-configuration. ^c From the literature. ^d S/C = 10,000.

Table S2. Screening of the catalysts

entry	ligand	H ₂ (psi)	time (h)	conv. (%)	ee (%)
1	L1	350	10	99	80
2	L2	350	10	99	1
3	L3	350	10	99	89
4	L4	350	10	99	69
5	L7	350	10	99	90

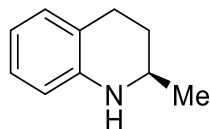
Table S3. Screening of the catalysts

entry	ligand	H ₂ (psi)	time (h)	conv. (%)	ee (%)
1	L1	350	10	99	79
2	L2	350	10	99	23
3	L3	350	10	99	76
4	L4	350	10	99	74
5	L7	350	10	99	89

Table S4. Study of time vs. conv.

Time	1 hr	2 hr	4 hr	7 hr	10 hr
conv.	95%	96%	97%	98%	99%

^a All reactions were carried out at room temperature with 0.1 mmol substrate using Ir complex generated in situ from $[\text{Ir}(\text{COD})\text{Cl}]_2$ (0.5 mol%), ligand L1 to L7 (1.1 mol%), and I_2 (10 mol%) under pressurized H_2 in 1 ml of solvent. ^b The conversion was determined by ¹H NMR and the enantioselectivity was determined by HPLC analysis with a Chiralpak OJ-H column. The product was in R-configuration.



(*R*)-2-methyl-1,2,3,4-tetrahydroquinoline (**3-41**)

Known compound⁷⁸; colorless oil, 14.5 mg, 99% yield, 95% ee

$[\alpha]_D$: +79.8 ($c = 1.00$ in CHCl_3); literature $[\alpha]_D$: +84.3 ($c = 0.20$ in CHCl_3) for 99% ee

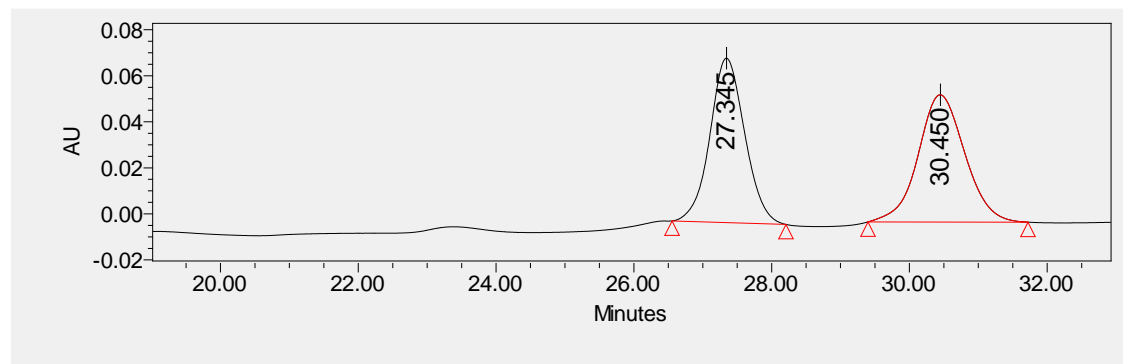
$^1\text{H NMR}$ (700 MHz, Chloroform-*d*) δ 7.09 – 6.95 (m, 2H), 6.84 – 6.62 (m, 2H), 4.13 – 3.99 (br s, 1H), 3.50 (ddq, $J = 9.8, 6.4, 3.5$ Hz, 1H), 2.86 (ddd, $J = 16.9, 11.2, 5.8$ Hz, 1H), 2.77 (ddd, $J = 16.5, 5.0, 3.6$ Hz, 1H), 2.03 – 1.96 (m, 1H), 1.70 (dddd, $J = 13.2, 11.2, 9.9, 5.4$ Hz, 1H), 1.32 (d, $J = 6.3$ Hz, 3H).

$^{13}\text{C NMR}$ (176 MHz, Chloroform-*d*) δ 141.9, 129.4, 126.8, 122.7, 119.1, 115.7, 47.9, 29.5, 26.1, 21.7.

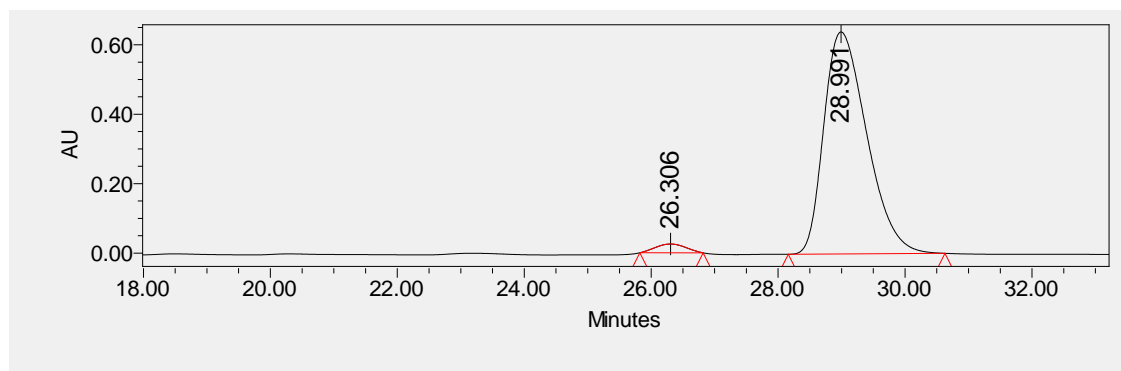
ESI-HRMS Calcd. for $\text{C}_{10}\text{H}_{14}\text{N}^+$ 148.1120 $[\text{M}+\text{H}]^+$, found 148.1118

IR (powder): $\nu_{\text{max}} = 3283, 3037, 2955, 2923, 2858, 1597, 1543, 1424, 1383, 1211, 1036, 958, 888, 825 \text{ cm}^{-1}$

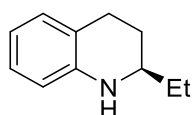
HPLC (Chiralpak OJ-H column, 95:5 hexanes/isopropanol, 0.5 ml/min), $t_r = 26.3$ min (minor, S), 28.9 min (major, R)



	Retention Time	Area	% Area	Height
1	27.345	2509966	49.10	71451
2	30.450	2601958	50.90	55287



	Retention Time	Area	% Area	Height
1	26.306	838726	2.72	25352
2	28.991	30024126	97.28	639683



(*R*)-2-ethyl-1,2,3,4-tetrahydroquinoline (**3-43**)

Known compound⁷⁸; colorless oil, 15.9 mg, 99% yield, 93% ee

$[\alpha]_D$: +72.4 ($c = 1.02$ in CHCl_3); literature $[\alpha]_D$: +80.3 ($c = 0.19$ in CHCl_3) for 99% ee

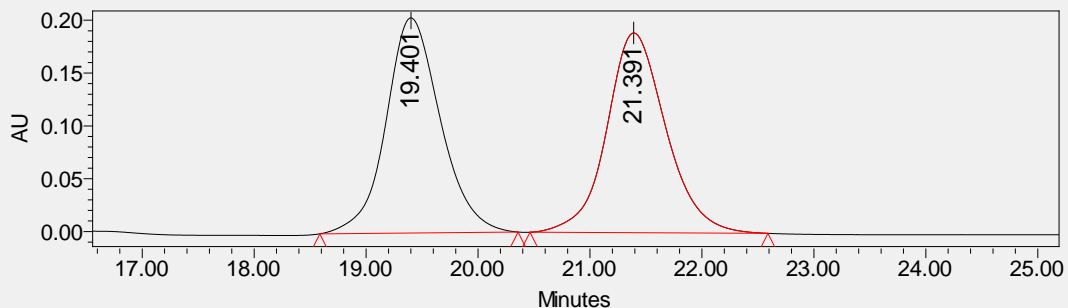
$^1\text{H NMR}$ (700 MHz, Chloroform-*d*) δ 6.98 – 6.93 (m, 2H), 6.59 (td, $J = 7.3, 1.2$ Hz, 1H), 6.49 – 6.47 (m, 1H), 3.77 (br s, 1H), 3.17 (dtd, $J = 9.5, 6.4, 2.9$ Hz, 1H), 2.81 (ddd, $J = 16.6, 11.2, 5.6$ Hz, 1H), 2.73 (dt, $J = 16.2, 4.6$ Hz, 1H), 1.97 (dddd, $J = 12.6, 5.6, 3.9, 2.9$ Hz, 1H), 1.59 (dddd, $J = 12.8, 11.2, 9.7, 5.2$ Hz, 1H), 1.54 – 1.50 (m, 2H), 0.99 (t, $J = 7.5$ Hz, 3H).

$^{13}\text{C NMR}$ (176 MHz, Chloroform-*d*) δ 144.7, 129.2, 126.6, 121.3, 116.8, 113.9, 53.0, 29.3, 27.5, 26.4, 10.0.

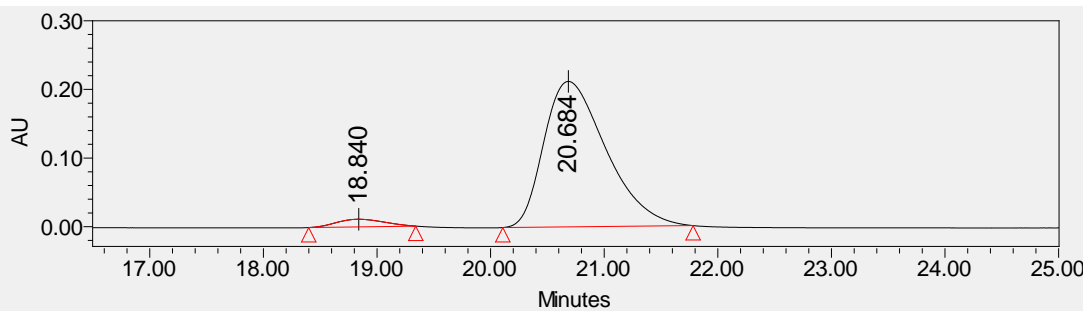
ESI-HRMS Calcd. for $\text{C}_{11}\text{H}_{16}\text{N}^+$ 162.1277 $[\text{M}+\text{H}]^+$, found 162.1278

IR (film): $\nu_{\text{max}} = 3393, 2956, 2923, 2872, 2853, 1603, 1502, 1308, 1122, 745$ cm^{-1}

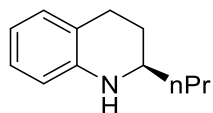
HPLC (Chiralpak OJ-H column, 90:10 hexanes/isopropanol, 0.5 ml/min), $t_r = 18.8$ min (minor, S), 20.7 min (major, R)



	Retention Time	Area	% Area	Height
1	19.401	18166484	49.86	533752
2	21.391	18269512	50.14	494848



	Retention Time	Area	% Area	Height
1	18.840	324513	3.47	11151
2	20.684	9027447	96.53	211944



(*R*)-2-propyl-1,2,3,4-tetrahydroquinoline (**3-44**)

Known compound⁷⁸; colorless oil, 16.6 mg, 95% yield, 93% ee

$[\alpha]_D$: +74.3 (c = 1.21 in CHCl₃); literature $[\alpha]_D$: +89.0 (c = 0.16 in CHCl₃) for 99% ee

¹H NMR (400 MHz, Chloroform-*d*) δ 7.06 – 6.89 (m, 2H), 6.58 (td, *J* = 7.4, 1.2 Hz, 1H), 6.46 (dd, *J* = 8.4, 1.3 Hz, 1H), 3.74 (br s, 1H), 3.24 (dtd, *J* = 9.4, 6.1, 2.9 Hz, 1H), 2.92 – 2.59 (m,

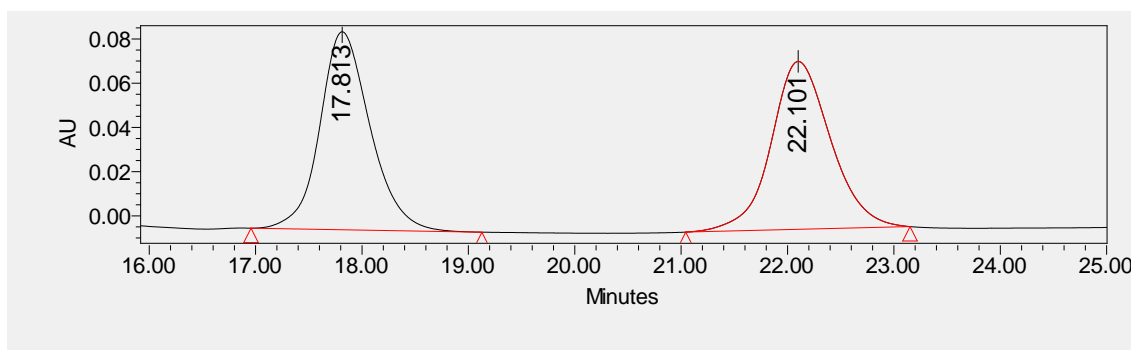
2H), 1.95 (dddd, $J = 12.7, 5.6, 4.0, 2.9$ Hz, 1H), 1.64 – 1.55 (m, 1H), 1.51 – 1.37 (m, 4H), 0.95 (t, $J = 6.5$ Hz, 3H).

^{13}C NMR (100 MHz, Chloroform- d) δ 144.6, 129.2, 126.6, 121.3, 116.8, 113.9, 51.2, 38.8, 28.0, 26.4, 18.8, 14.1.

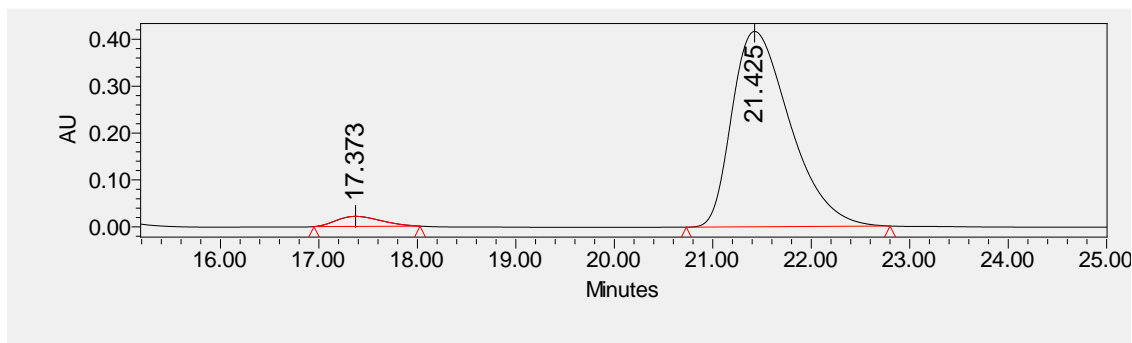
ESI-HRMS Calcd. for $\text{C}_{12}\text{H}_{18}\text{N}^+$ 176.1433 $[\text{M}+\text{H}]^+$, found 176.1429

IR (film): $\nu_{\text{max}} = 3395, 3331, 2956, 2927, 2870, 1601, 1502, 1457, 1309, 825, 781, 745$ cm^{-1}

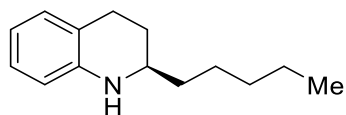
HPLC (Chiralpak OJ-H column, 90:10 hexanes/isopropanol, 0.5 ml/min), $t_r = 17.4$ min (minor, S), 21.4 min (major, R)



	Retention Time	Area	% Area	Height
1	17.813	2945186	49.93	89523
2	22.101	2953952	50.07	75940



	Retention Time	Area	% Area	Height
1	17.373	675866	3.37	21407
2	21.425	19379505	96.63	416736



(*R*)-2-pentyl-1,2,3,4-tetrahydroquinoline (**3-45**)

Known compound⁷⁵; pale yellow clear oil, 19.7 mg, 97% yield, 94% ee

$[\alpha]_D$: +47.6 ($c = 1.01$ in CH_2Cl_2); literature $[\alpha]_D$: +51.4 ($c = 1.0$ in CHCl_3) for 90% ee

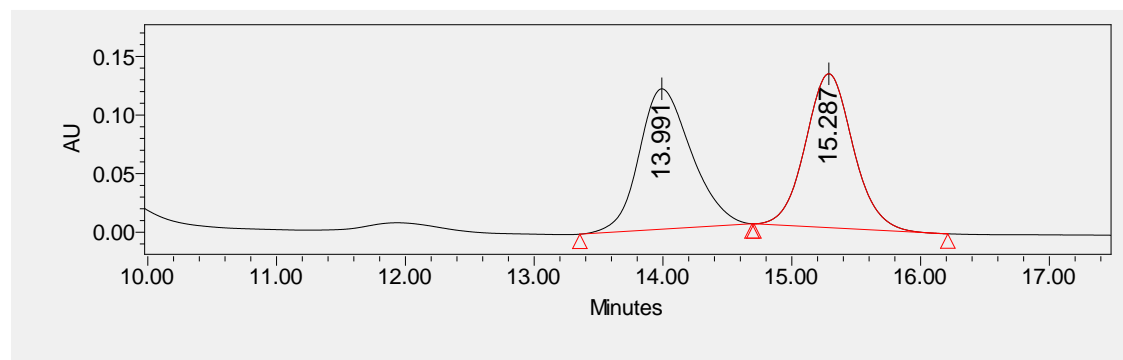
$^1\text{H NMR}$ (500 MHz, Chloroform-*d*) δ 6.96 (t, $J = 7.6$ Hz, 2H), 6.60 (td, $J = 7.3, 1.2$ Hz, 1H), 6.51 – 6.44 (m, 1H), 3.77 (br s, 1H), 3.24 (dtd, $J = 9.4, 6.3, 2.9$ Hz, 1H), 2.88 – 2.69 (m, 2H), 2.03 – 1.91 (m, 1H), 1.60 (dddd, $J = 13.0, 11.1, 9.5, 5.3$ Hz, 1H), 1.50 (dt, $J = 9.1, 5.8$ Hz, 2H), 1.45 – 1.29 (m, 6H), 0.92 (t, $J = 6.8$ Hz, 3H).

$^{13}\text{C NMR}$ (126 MHz, Chloroform-*d*) δ 144.7, 129.2, 126.6, 121.3, 116.8, 114.0, 51.5, 36.6, 31.9, 28.1, 26.4, 25.4, 22.6, 14.0.

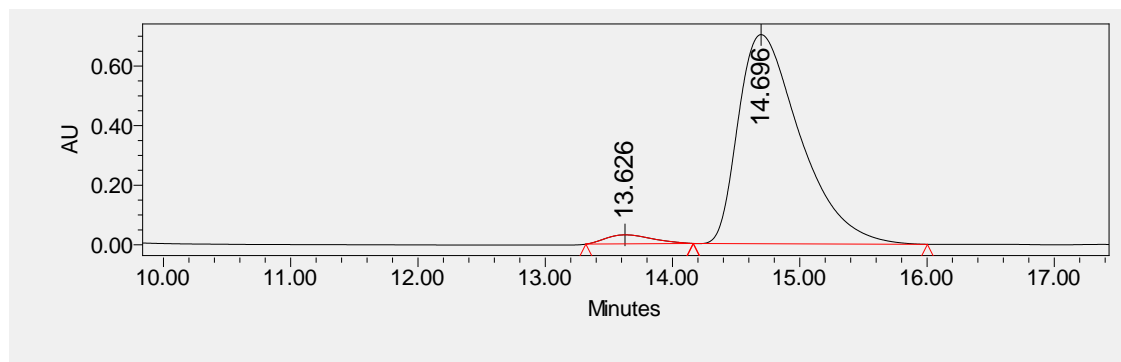
ESI-HRMS Calcd. for $\text{C}_{14}\text{H}_{22}\text{N}^+$ 204.1746 $[\text{M}+\text{H}]^+$, found 204.1747

IR (film): $\nu_{\text{max}} = 3369, 3059, 2956, 2926, 1463, 1340, 1113, 1076, 1018, 833$ cm^{-1}

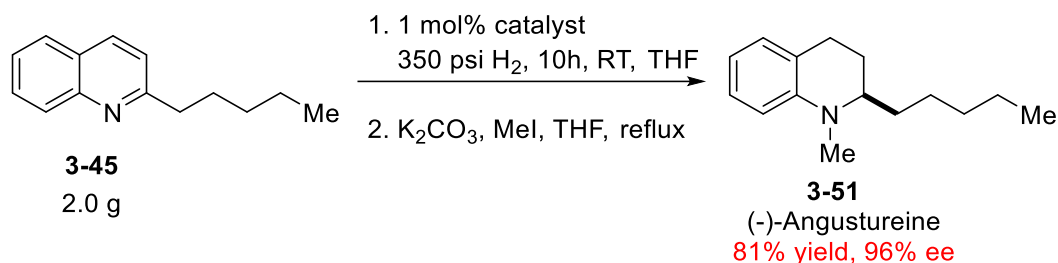
HPLC (Chiralpak OJ-H column, 90:10 hexanes/isopropanol, 0.5 ml/min), $t_r = 13.6$ min (minor, S), 14.7 min (major, R)



	Retention Time	Area	% Area	Height
1	13.991	2324435	49.95	83191
2	15.287	2328896	50.05	91094

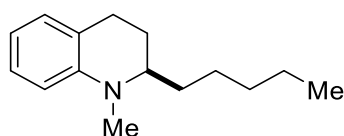


	Retention Time	Area	% Area	Height
1	13.626	768900	3.13	30345
2	14.696	23758927	96.87	702236



Bis(1,5-cyclooctadiene)diiridium(I) dichloride (34 mg, 0.05 mmol) and (*R,S,S*)-SPIRAPO **L3-7** (76 mg, 0.11 mmol) were added to an oven-dried flask with a stir bar and sealed in the glovebox strictly under the nitrogen. After the flask taken out of the glovebox, dry THF (1 mL) was added and the mixture was stirred under the nitrogen atmosphere at room temperature for 2 hours. Dry THF (19 mL) solution of 2-pentylquinoline (2.0g, 10.0 mmol) and I₂ (254.0 mg, 1.0 mmol) was transferred to the flask with pre-mixed catalyst solution via a syringe. The flask was then brought into the high-pressure reactor and an 18G needle was left in the vial septa. The inner atmosphere of the reactor was purged by charging and carefully releasing 100 psi of hydrogen for 5 times before setting to 350 psi of hydrogen. The reaction was stirred at 350 psi of hydrogen for 10 hours. After the reaction time the flask was taken out of the reactor and to the crude mixture was added K₂CO₃ (4.10 g, 30.0 mmol) and MeI (1.25 mL, 20.0 mmol) and the

flask was fitted with a reflux condenser. After 17h at reflux, reaction mixture was quenched with a DI water (50 mL). After separating the phases, the aqueous layer was extracted with DCM twice. Combined organic was washed with brine, dried over Na₂SO₄, and concentrated *in vacuo*. Crude was purified by FCC (SiO₂, 5-10% EtOAc in hexanes) to obtain the desired product as pale yellow oil.



(*R*)-1-Methyl-2-pentyl-1,2,3,4-tetrahydroquinoline (**3-51**)

Known compound⁷⁵; pale yellow clear oil, 1.75 g, 81% yield (2 steps), 96% ee

[α]_D: -9.6 (c = 1.32 in CHCl₃); literature [α]_D: -6.9 (c = 1.0 in CHCl₃) for 90% ee

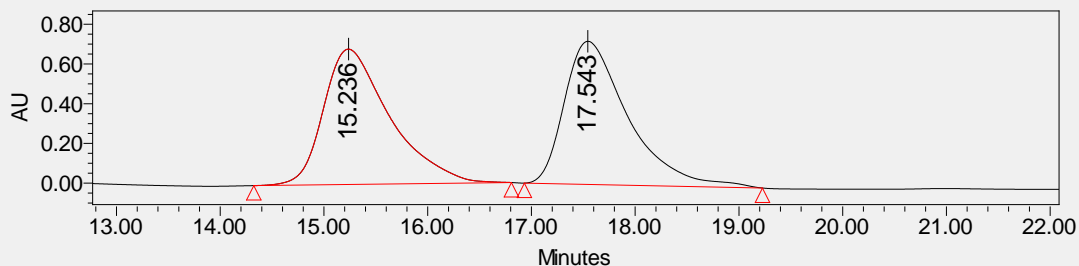
¹H NMR (500 MHz, Chloroform-*d*) δ 7.12 – 7.04 (m, 1H), 6.96 (dd, *J* = 7.1, 1.7 Hz, 1H), 6.57 (td, *J* = 7.3, 1.1 Hz, 1H), 6.52 (d, *J* = 8.2 Hz, 1H), 3.23 (dq, *J* = 8.7, 4.2 Hz, 1H), 2.92 (s, 3H), 2.80 (ddd, *J* = 17.5, 11.4, 6.8 Hz, 1H), 2.65 (dt, *J* = 16.1, 4.3 Hz, 1H), 1.88 (ddt, *J* = 10.8, 7.4, 4.1 Hz, 2H), 1.64 – 1.55 (m, 1H), 1.46 – 1.23 (m, 7H), 0.89 (t, *J* = 6.9 Hz, 3H).

¹³C NMR (126 MHz, Chloroform-*d*) δ 145.3, 128.6, 127.0, 121.8, 115.1, 110.3, 58.9, 37.9, 32.0, 31.1, 25.7, 24.3, 23.5, 22.6, 14.0.

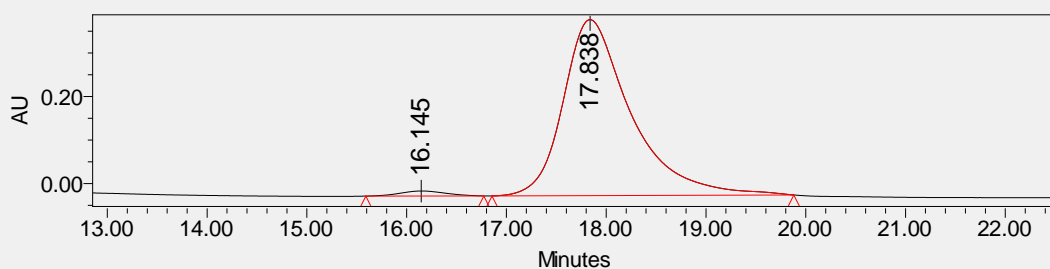
ESI-HRMS Calcd. for C₁₅H₂₄N⁺ 218.1902 [M+H]⁺, found 218.1899

IR (film): ν_{\max} = 2953, 2926, 2869, 2855, 2795, 1602, 1575, 1499, 1335, 1214, 742cm⁻¹

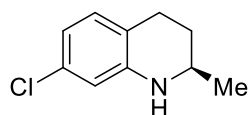
HPLC (Chiralpak OJ-H column, 99:1 hexanes/isopropanol, 0.4 ml/min), tr = 18.8 min (minor, S), 20.6 min (major, R)



	Retention Time	Area	% Area	Height
1	15.236	17439959	49.31	398804
2	17.543	17925412	50.69	422565



	Retention Time	Area	% Area	Height
1	16.145	364883	1.88	11521
2	17.838	19068464	98.12	403966



(*R*)-7-chloro-2-methyl-1,2,3,4-tetrahydroquinoline (**3-46**)

Known compound⁷⁴; white solids, 17.1 mg, 94% yield, 93% ee

$[\alpha]_D$: +61.1 ($c = 0.25$ in CHCl_3); literature $[\alpha]_D$: -68.5 ($c = 0.5$ in CHCl_3) for 90% ee (*S*)

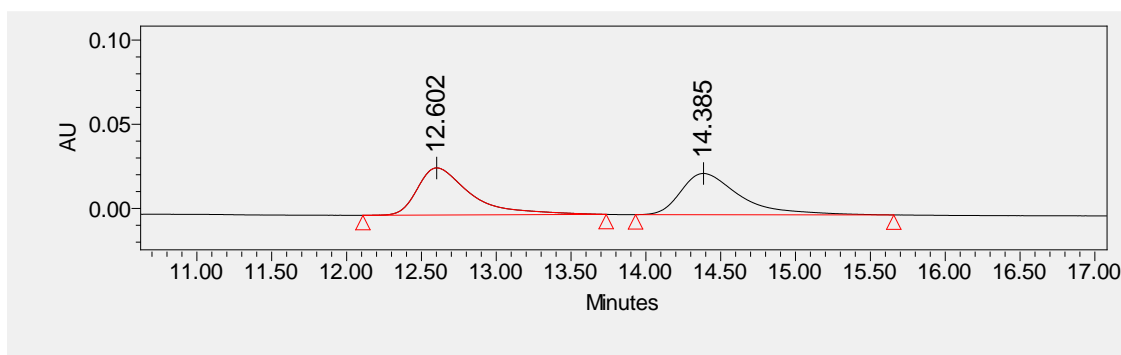
$^1\text{H NMR}$ (400 MHz, Chloroform-*d*) δ 6.85 (dt, $J = 8.0, 1.0$ Hz, 1H), 6.54 (dd, $J = 8.0, 2.1$ Hz, 1H), 6.43 (d, $J = 2.1$ Hz, 1H), 3.75 (br s, 1H), 3.39 (dq, $J = 9.4, 6.3, 3.0$ Hz, 1H), 2.85 – 2.62 (m, 2H), 1.96 – 1.87 (m, 1H), 1.62 – 1.49 (m, 1H), 1.20 (d, $J = 6.3$ Hz, 3H).

^{13}C NMR (100 MHz, Chloroform-*d*) δ 145.6, 131.8, 130.1, 119.2, 116.5, 113.2, 46.9, 29.7, 26.0, 22.4.

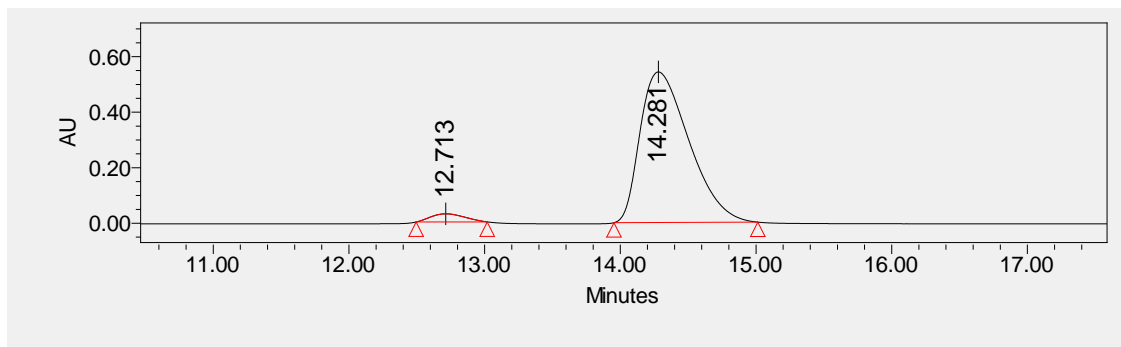
ESI-HRMS Calcd. for $\text{C}_{10}\text{H}_{13}\text{ClN}^+$ 182.0731 $[\text{M}+\text{H}]^+$, found 182.0733

IR (powder): ν_{max} = 3411, 3055, 2912, 1607, 1596, 1494, 1405, 1332, 1218, 1066, 1035, 970, 912, 901, 837 cm^{-1}

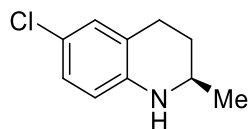
HPLC (Chiralpak OJ-H column, 92:8 hexanes/isopropanol, 1 ml/min), t_r = 12.7 min (minor, S), 14.3 min (major, R)



	Retention Time	Area	% Area	Height
1	12.602	1888746	50.49	86618
2	14.385	1851983	49.51	75260



	Retention Time	Area	% Area	Height
1	12.713	505853	3.59	29294
2	14.281	13572112	96.41	542294



(*R*)-6-chloro-2-methyl-1,2,3,4-tetrahydroquinoline (**3-42**)

Known compound⁷⁴; colorless oil, 17.8 mg, 98% yield, 90% ee

$[\alpha]_D$: +77.6 ($c = 0.50$ in CHCl_3); literature $[\alpha]_D$: -81.8 ($c = 0.5$ in CHCl_3) for 90% ee (*S*)

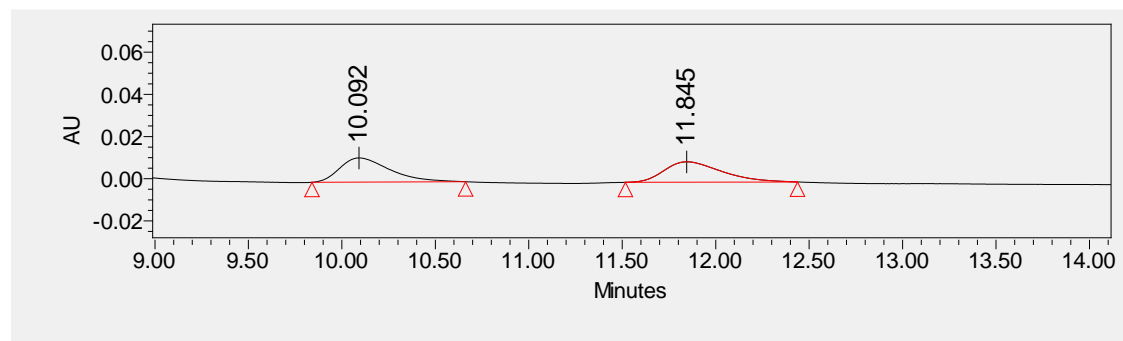
$^1\text{H NMR}$ (400 MHz, Chloroform-*d*) δ 6.94 – 6.84 (m, 2H), 6.36 (d, $J = 8.4$ Hz, 1H), 3.67 (br s, 1H), 3.36 (dq, $J = 9.3, 6.3, 2.9$ Hz, 1H), 2.87 – 2.62 (m, 2H), 1.95 – 1.84 (m, 1H), 1.60 – 1.46 (m, 1H), 1.19 (d, $J = 6.3$ Hz, 3H).

$^{13}\text{C NMR}$ (100 MHz, Chloroform-*d*) δ 143.2, 128.8, 126.4, 122.5, 121.2, 114.8, 47.1, 29.6, 26.4, 22.4.

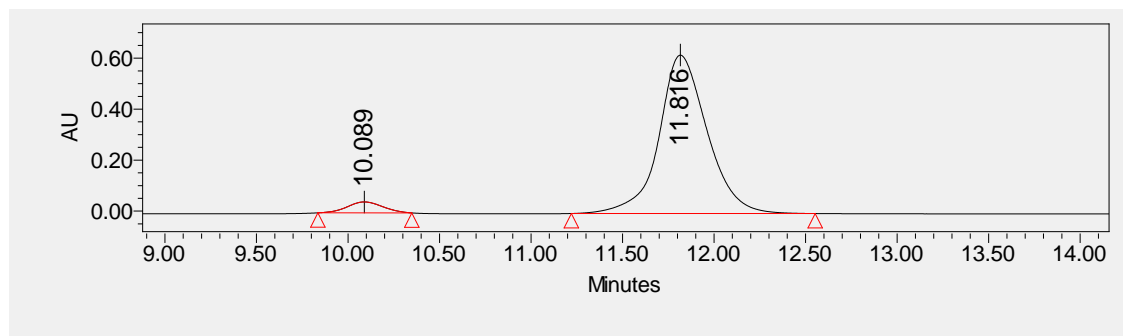
ESI-HRMS Calcd. for $\text{C}_{10}\text{H}_{13}\text{ClN}^+$ 182.0731 $[\text{M}+\text{H}]^+$, found 182.0729

IR (film): $\nu_{\text{max}} = 3404, 2964, 2926, 2849, 1604, 1492, 1298, 805 \text{ cm}^{-1}$

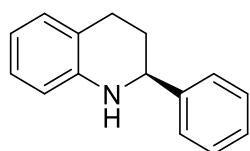
HPLC (Chiralpak OJ-H column, 92:8 hexanes/isopropanol, 1 ml/min), $t_r = 10.1$ min (minor, *S*), 11.8 min (major, *R*)



	Retention Time	Area	% Area	Height
1	10.092	213628	50.77	11483
2	11.845	207115	49.23	9680



	Retention Time	Area	% Area	Height
1	10.089	577708	4.83	42946
2	11.816	11395334	95.17	621347



(*S*)-2-phenyl-1,2,3,4-tetrahydroquinoline (**3-47**)

Known compound⁷⁵; colorless oil, 19.2 mg, 92% yield, 89% ee

$[\alpha]_D$: -31.3 ($c = 0.73$ in CHCl_3); literature $[\alpha]_D$: -37.7 ($c = 1.0$ in CHCl_3) for 97% ee

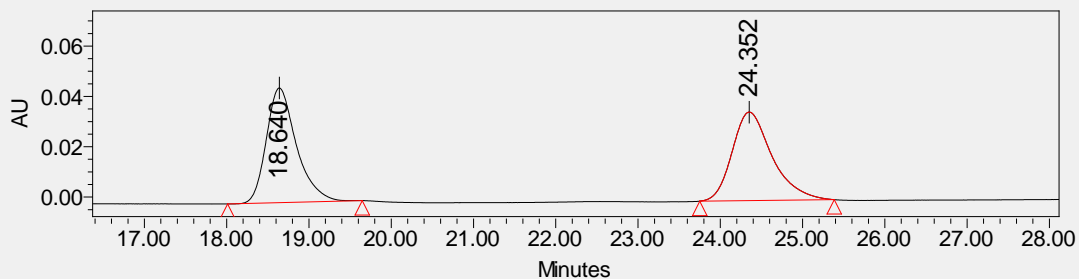
$^1\text{H NMR}$ (400 MHz, Chloroform-*d*) δ 7.42 – 7.32 (m, 4H), 7.31 – 7.27 (m, 1H), 7.00 (dd, $J = 7.4, 1.1$ Hz, 2H), 6.65 (td, $J = 7.4, 1.2$ Hz, 1H), 6.56 – 6.50 (m, 1H), 4.43 (dd, $J = 9.4, 3.3$ Hz, 1H), 4.03 (br s, 1H), 2.92 (ddd, $J = 16.2, 10.7, 5.5$ Hz, 1H), 2.73 (dt, $J = 16.3, 4.8$ Hz, 1H), 2.12 (dq, $J = 13.2, 4.5$ Hz, 1H), 1.99 (dddd, $J = 12.9, 10.6, 9.3, 5.1$ Hz, 1H).

$^{13}\text{C NMR}$ (100 MHz, Chloroform-*d*) δ 144.7, 144.7, 129.2, 128.5, 127.4, 126.8, 126.5, 120.8, 117.1, 113.9, 56.2, 30.9, 26.3.

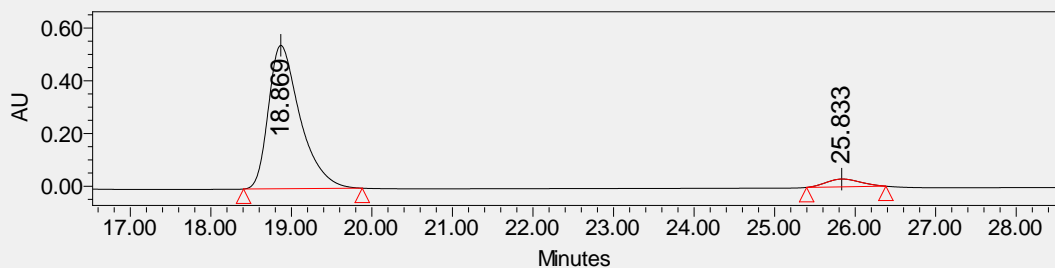
ESI-HRMS Calcd. for $\text{C}_{15}\text{H}_{16}\text{N}^+$ 210.1277 $[\text{M}+\text{H}]^+$, found 210.1278

IR (film): $\nu_{\text{max}} = 3393, 3383, 3053, 2971, 2944, 2840, 1606, 1584, 1479, 1431, 1308, 1251, 1110, 1005, 924, 830, 815$ cm^{-1}

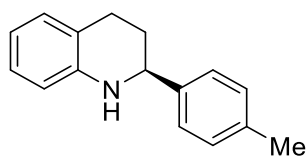
HPLC (Chiralpak OD-H column, 95:5 hexanes/isopropanol, 0.6 ml/min), $t_r = 18.8$ min (major, *S*), 25.8 min (minor, *R*)



	Retention Time	Area	% Area	Height
1	18.640	1158602	49.43	45569
2	24.352	1185130	50.57	35183



	Retention Time	Area	% Area	Height
1	18.869	14861297	94.43	544071
2	25.833	875809	5.57	29625



(*S*)-2-(*p*-tolyl)-1,2,3,4-tetrahydroquinoline (**3-48**)

Known compound⁷⁹; colorless oil, 22.2 mg, 99% yield, 86% ee

[α]_D: -15.7 (c = 0.68 in CHCl₃); literature [α]_D: -24.3 (c = 1.0 in CHCl₃) for 90% ee

¹H NMR (700 MHz, Chloroform-*d*) δ 7.29 (d, *J* = 7.9 Hz, 2H), 7.17 (d, *J* = 7.7 Hz, 2H), 7.01 (t, *J* = 7.6 Hz, 2H), 6.65 (td, *J* = 7.4, 1.2 Hz, 1H), 6.54 (d, *J* = 7.8 Hz, 1H), 4.41 (dd, *J* = 9.5, 3.2

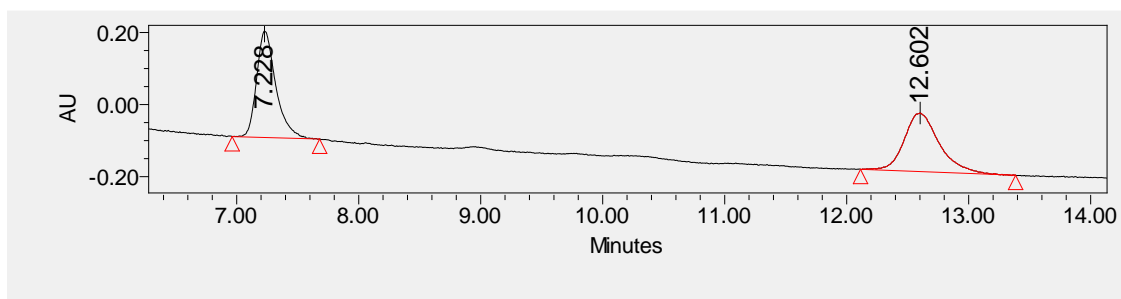
Hz, 1H), 4.00 (br s, 1H), 2.93 (ddd, $J = 16.3, 10.9, 5.5$ Hz, 1H), 2.75 (dt, $J = 16.3, 4.7$ Hz, 1H), 2.36 (s, 3H), 2.14 – 2.08 (m, 1H), 1.99 (dddd, $J = 13.0, 10.9, 9.6, 5.0$ Hz, 1H).

^{13}C NMR (176 MHz, Chloroform-*d*) δ 144.8, 141.8, 137.0, 129.2, 129.2, 126.8, 126.4, 120.8, 117.0, 113.9, 56.0, 31.0, 26.4, 21.0.

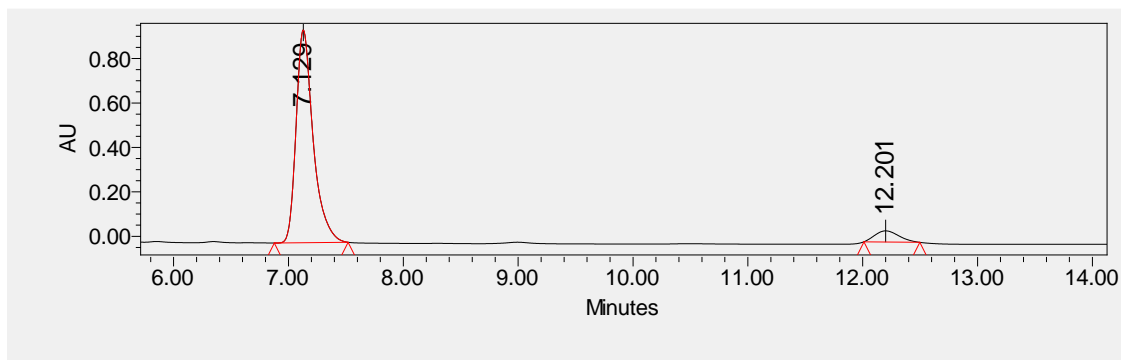
ESI-HRMS Calcd. for $\text{C}_{16}\text{H}_{18}\text{N}^+$ 224.1434 $[\text{M}+\text{H}]^+$, found 224.1436

IR (film): $\nu_{\text{max}} = 3377, 3014, 2973, 2922, 2853, 1606, 1598, 1543, 1498, 1309, 1114, 1046, 971, 813$ cm^{-1}

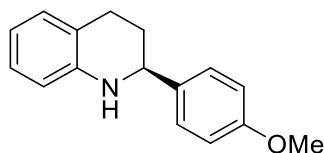
HPLC (Chiralpak OD-H column, 90:10 hexanes/isopropanol, 1 ml/min), $t_r = 7.1$ min (major, S), 12.2 min (minor, R)



	Retention Time	Area	% Area	Height
1	7.228	3232020	49.88	295451
2	12.602	3248172	50.12	162613



	Retention Time	Area	% Area	Height
1	7.129	9904243	93.17	957304
2	12.201	726272	6.83	50146



(*S*)-2-(4-Methoxyphenyl)-1,2,3,4-tetrahydroquinoline (**3-49**)

Known compound⁷⁵; white solids, 23.4 mg, 98% yield, 91% ee

[α]_D: -24.7 (c = 0.22 in CH₂Cl₂); literature [α]_D: -18.6 (c = 1.0 in CHCl₃) for 98% ee

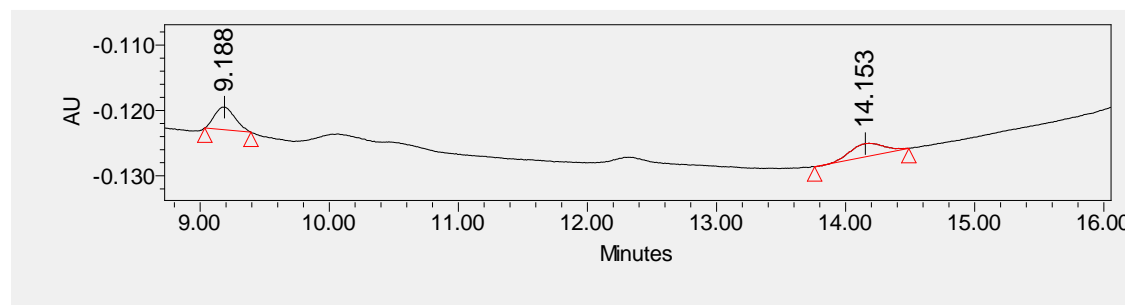
¹H NMR (700 MHz, Chloroform-*d*) δ 7.33 – 7.29 (m, 2H), 7.00 (t, *J* = 7.0 Hz, 2H), 6.91 – 6.86 (m, 2H), 6.64 (td, *J* = 7.4, 1.2 Hz, 1H), 6.54 – 6.50 (m, 1H), 4.40 – 4.36 (m, 1H), 3.98 (s, 1H), 3.81 (s, 3H), 2.92 (ddd, *J* = 16.4, 11.0, 5.5 Hz, 1H), 2.74 (dt, *J* = 16.3, 4.6 Hz, 1H), 2.08 (dd, *J* = 13.1, 4.3 Hz, 1H), 1.97 (dddd, *J* = 13.0, 11.0, 9.6, 5.0 Hz, 1H).

¹³C NMR (176 MHz, Chloroform-*d*) δ 158.9, 144.8, 136.8, 129.2, 127.6, 126.8, 120.8, 117.0, 113.9, 113.9, 55.7, 55.3, 31.0, 26.5.

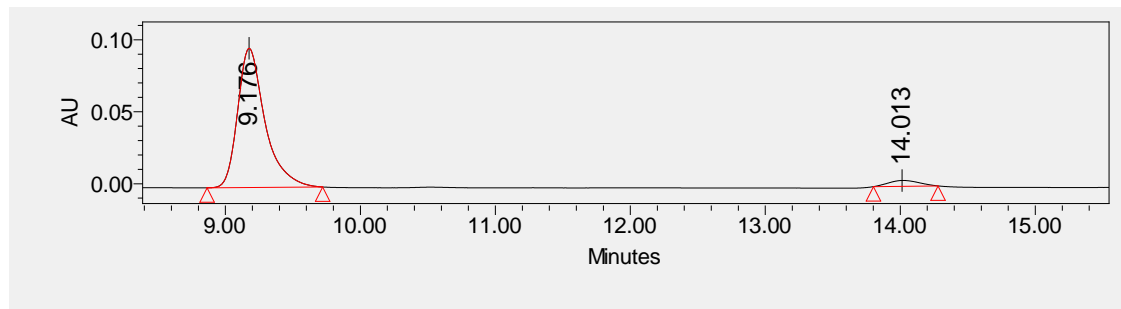
ESI-HRMS Calcd. for C₁₆H₁₈NO⁺ 240.1383 [M+H]⁺, found 240.1388

IR (film): ν_{\max} = 3381, 3012, 2959, 2839, 1604, 1551, 1248, 1175, 1028, 833cm⁻¹

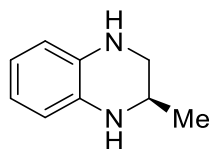
HPLC (Chiralpak OD-H column, 90:10 hexanes/isopropanol, 1 ml/min), *t*_r = 9.2 min (major, *S*), 14.0 min (minor, *R*)



	Retention Time	Area	% Area	Height
1	9.188	37815	50.96	3462
2	14.153	36388	49.04	2037



	Retention Time	Area	% Area	Height
1	9.176	1357374	95.54	96644
2	14.013	63407	4.46	4064



(*R*)-2-methyl-1,2,3,4-tetrahydroquinoxaline (**3-51**)

Known compound⁸⁰; yellow solids, 14.7 mg, 99% yield, 89% ee

$[\alpha]_D$: +18.2 ($c = 0.80$ in CHCl_3); literature $[\alpha]_D$: +3.7 ($c = 0.5$ in CH_2Cl_2) for 98% ee

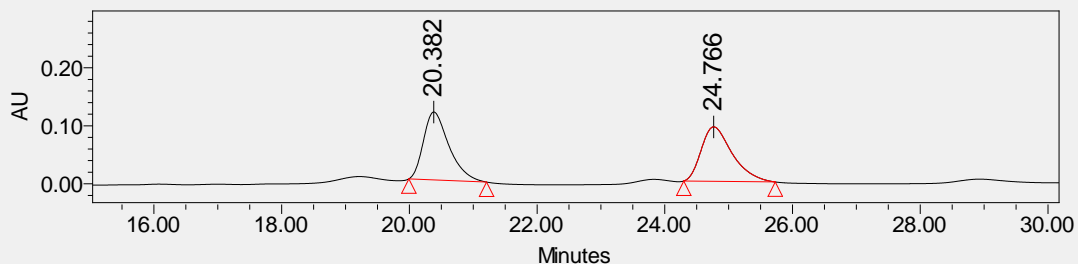
$^1\text{H NMR}$ (500 MHz, Chloroform-*d*) δ 6.59 (ddt, $J = 7.2, 3.9, 2.0$ Hz, 2H), 6.55 – 6.46 (m, 2H), 3.60 (br s, 2H), 3.51 (dtd, $J = 8.7, 6.3, 2.7$ Hz, 1H), 3.32 (dd, $J = 10.7, 2.8$ Hz, 1H), 3.04 (dd, $J = 10.7, 8.1$ Hz, 1H), 1.19 (dd, $J = 6.3, 0.9$ Hz, 3H).

$^{13}\text{C NMR}$ (126 MHz, Chloroform-*d*) δ 133.5, 133.1, 118.7, 118.6, 114.4, 114.4, 48.2, 45.7, 19.9.

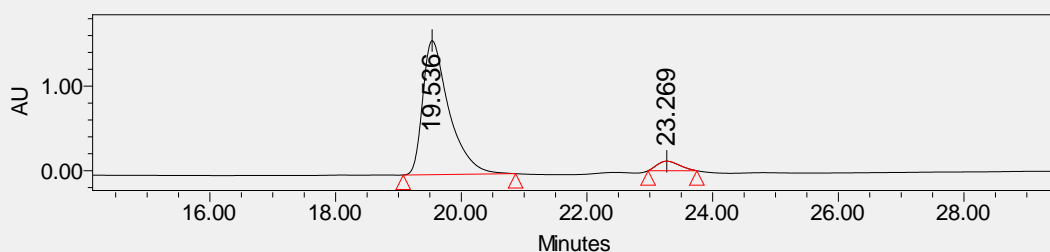
ESI-HRMS Calcd. for $\text{C}_9\text{H}_{13}\text{N}_2^+$ 149.1073 $[\text{M}+\text{H}]^+$, found 149.1070

IR (film): $\nu_{\text{max}} = 3350, 3049, 2963, 2925, 2850, 1602, 1502, 1360, 1301, 910, 736$ cm^{-1}

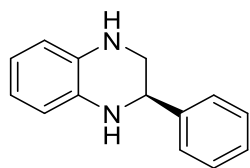
HPLC (Chiralpak OD-H column, 80:20 hexanes/isopropanol, 0.5 ml/min), $t_r = 19.5$ min (major, *R*), 23.3 min (minor, *S*)



	Retention Time	Area	% Area	Height
1	20.382	10455967	50.64	368952
2	24.766	10191463	49.36	297423



	Retention Time	Area	% Area	Height
1	19.536	46222166	94.32	1587006
2	23.269	2783025	5.68	112915



(R)-2-Phenyl-1,2,3,4-tetrahydroquinoxaline (3-52)

Known compound⁷⁶; yellow solids, 20.8mg, 99% yield, 83% ee

$[\alpha]_D$: -97.5 (c = 0.63 in CHCl₃); literature $[\alpha]_D$: -98.6 (c = 1.0 in CHCl₃) for 90% ee

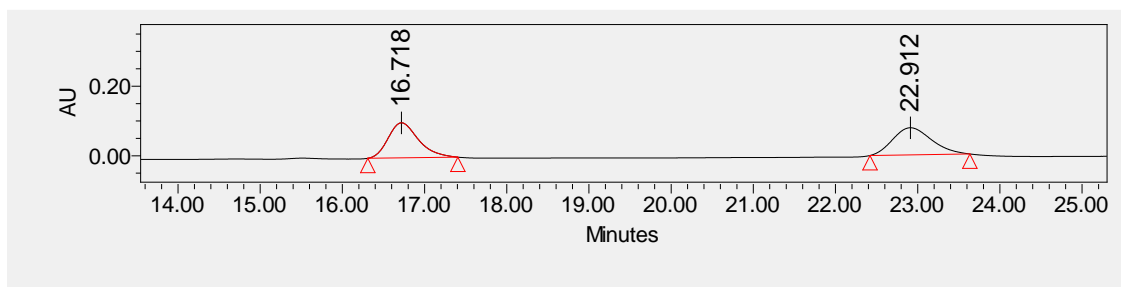
¹H NMR (700 MHz, Chloroform-*d*) δ 7.41 – 7.34 (m, 4H), 7.32 (ddt, *J* = 8.5, 6.3, 1.6 Hz, 1H), 6.67 – 6.61 (m, 2H), 6.61 – 6.55 (m, 2H), 4.48 (dd, *J* = 8.2, 3.1 Hz, 1H), 3.90 (br s, 1H), 3.81 (br s, 1H), 3.46 (dd, *J* = 11.1, 3.1 Hz, 1H), 3.33 (dd, *J* = 11.1, 8.2 Hz, 1H).

^{13}C NMR (176 MHz, Chloroform-*d*) δ 141.8, 134.1, 132.8, 128.6, 127.8, 126.9, 118.9, 118.7, 114.6, 114.4, 54.7, 49.1.

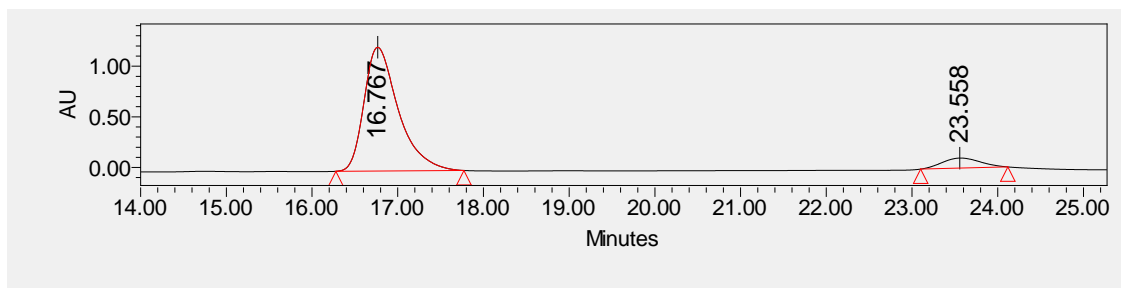
ESI-HRMS Calcd. for $\text{C}_{14}\text{H}_{15}\text{N}_2^+$ 211.1229 $[\text{M}+\text{H}]^+$, found 211.1227

IR (film): ν_{max} = 3362, 3025, 2849, 1594, 1502, 1451, 1342, 1299, 909, 737 cm^{-1}

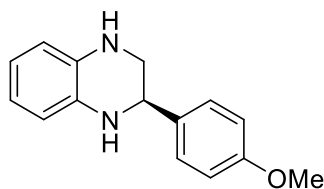
HPLC (Chiralpak OD-H column, 85:15 hexanes/isopropanol, 1.0 ml/min), t_r = 16.7 min (major, R), 23.5 min (minor, S)



	Retention Time	Area	% Area	Height
1	16.718	2579944	50.21	100693
2	22.912	2558058	49.79	78000



	Retention Time	Area	% Area	Height
1	16.767	34013063	91.74	1221730
2	23.558	3060572	8.26	99559



(R)-1,2,3,4-tetrahydro-2-(4-methoxyphenyl)quinoxaline (**3-53**)

Known compound⁷⁶; yellow solids; 23.2mg, 96% yield, 92% ee

$[\alpha]_D$: -51.9 (c = 0.78 in CHCl₃); literature $[\alpha]_D$: -83.2 (c = 1.0 in CHCl₃) for 94% ee

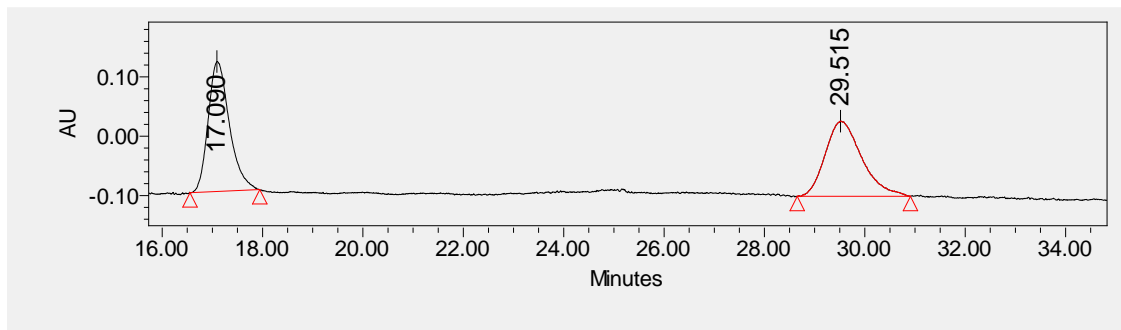
¹H NMR (700 MHz, Chloroform-*d*) δ 7.30 (d, *J* = 8.3 Hz, 2H), 6.92 – 6.88 (m, 2H), 6.63 (dt, *J* = 7.3, 3.7 Hz, 2H), 6.57 (td, *J* = 7.0, 5.9, 3.8 Hz, 2H), 4.43 (dd, *J* = 8.4, 3.0 Hz, 1H), 3.84 (br s, 2H), 3.81 (s, 3H), 3.42 (dd, *J* = 11.0, 3.1 Hz, 1H), 3.30 (dd, *J* = 11.0, 8.3 Hz, 1H).

¹³C NMR (176 MHz, Chloroform-*d*) δ 159.3, 134.1, 133.9, 132.8, 128.0, 118.8, 118.7, 114.6, 114.3, 114.0, 55.3, 54.1, 49.2.

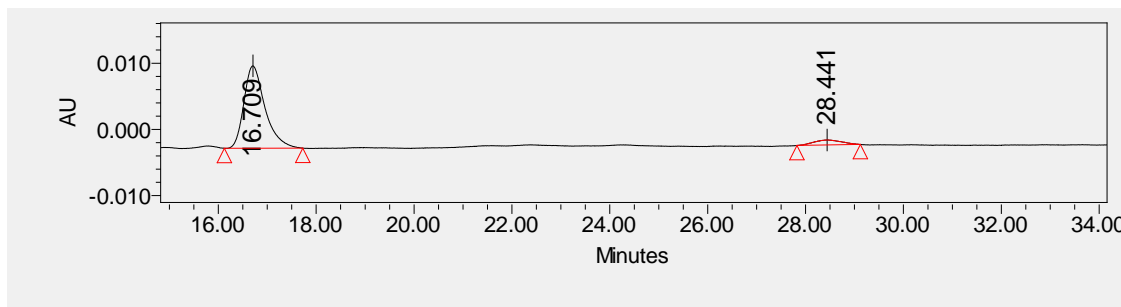
ESI-HRMS Calcd. for C₁₅H₁₇N₂O⁺ 241.1335 [M+H]⁺, found 241.1331

IR (film): ν_{\max} = 3364, 3018, 2955, 2925, 2850, 1602, 1510, 1443, 1339, 1245, 1105, 908, 737 cm⁻¹

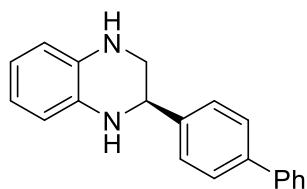
HPLC (Chiralpak OD-H column, 80:20 hexanes/isopropanol, 1.0 ml/min), *tr* = 16.7 min (major, R), 28.4 min (minor, S)



	Retention Time	Area	% Area	Height
1	17.090	6428801	50.17	219134
2	29.515	6385640	49.83	126889



	Retention Time	Area	% Area	Height
1	16.709	697477	95.89	12444
2	28.441	29895	4.11	768



(*R*)-2-([1,1'-Biphenyl]-4-yl)-1,2,3,4-tetrahydroquinoxaline (**3-54**)

Pale yellow solids; 95% yield, 76% ee;

$[\alpha]_D$: -11.3 ($c = 0.73$ in CH_2Cl_2)

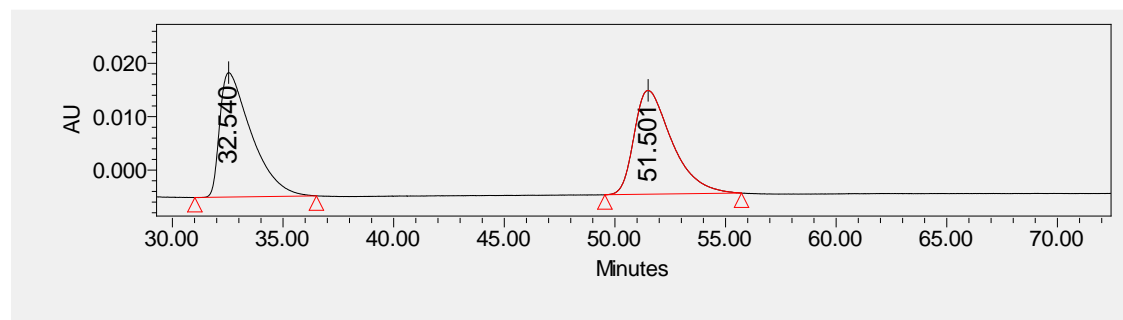
$^1\text{H NMR}$ (400 MHz, Chloroform-*d*) δ 7.63 – 7.55 (m, 4H), 7.50 – 7.41 (m, 4H), 7.40 – 7.31 (m, 1H), 6.69 – 6.63 (m, 2H), 6.63 – 6.57 (m, 2H), 4.55 (dd, $J = 8.1, 3.0$ Hz, 1H), 3.93 (br s, 2H), 3.51 (dd, $J = 11.1, 3.1$ Hz, 1H), 3.38 (dd, $J = 11.0, 8.0$ Hz, 1H).

$^{13}\text{C NMR}$ (100 MHz, Chloroform-*d*) δ 141.0, 140.8, 134.2, 132.8, 128.9, 127.5, 127.5, 127.5, 127.2, 119.1, 118.9, 114.9, 114.6, 54.5, 49.2.

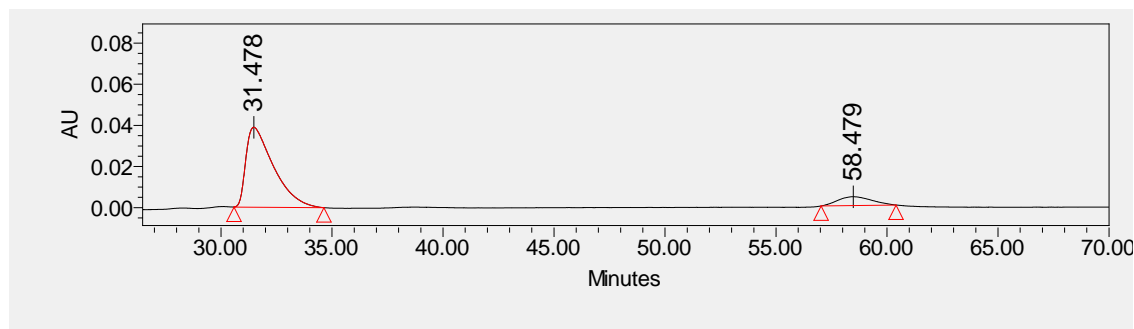
ESI-HRMS Calcd. for $\text{C}_{20}\text{H}_{19}\text{N}_2^+$ 287.1542 $[\text{M}+\text{H}]^+$, found 287.1534

IR (film): $\nu_{\text{max}} = 3347, 3058, 3033, 2923, 2852, 1682, 1603, 1540, 1464, 956, 845, 764$ cm^{-1}

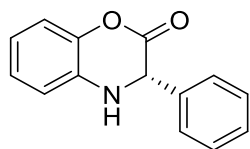
HPLC (Chiralpak OD-H column, 80:20 hexanes/isopropanol, 1.0 ml/min), $t_r = 31.5$ min (major, R), 58.5 min (minor, S)



	Retention Time	Area	% Area	Height
1	32.540	2316704	50.05	23313
2	51.501	2312280	49.95	19445



	Retention Time	Area	% Area	Height
1	31.478	3353930	88.06	38871
2	58.479	454916	11.94	4319



(*S*)-3-phenyl-3,4-dihydro-2H-benzo[*b*][1,4]oxazin-2-one (**3-55**)

Known compound⁷⁷; white solids, 22.1 mg, 98% yield, 84% ee

$[\alpha]_D$: +51.9 ($c = 0.75$ in CH_2Cl_2), literature $[\alpha]_D$: -46.3 ($c = 1.0$ in CHCl_3) for 99% ee (*R*)

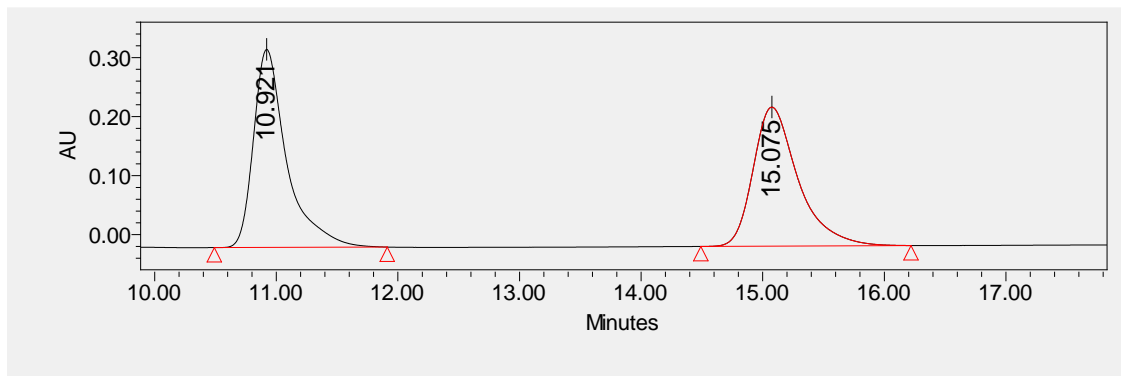
$^1\text{H NMR}$ (500 MHz, Chloroform-*d*) δ 7.45 – 7.34 (m, 5H), 7.08 – 7.00 (m, 2H), 6.87 (td, $J = 7.8$, 1.5 Hz, 1H), 6.82 (dd, $J = 7.8$, 1.5 Hz, 1H), 5.08 (d, $J = 1.9$ Hz, 1H), 4.22 (br s, 1H), .

$^{13}\text{C NMR}$ (126 MHz, Chloroform-*d*) δ 165.1, 140.9, 136.3, 132.3, 129.0, 129.0, 127.4, 125.1, 120.4, 117.0, 114.8, 59.3.

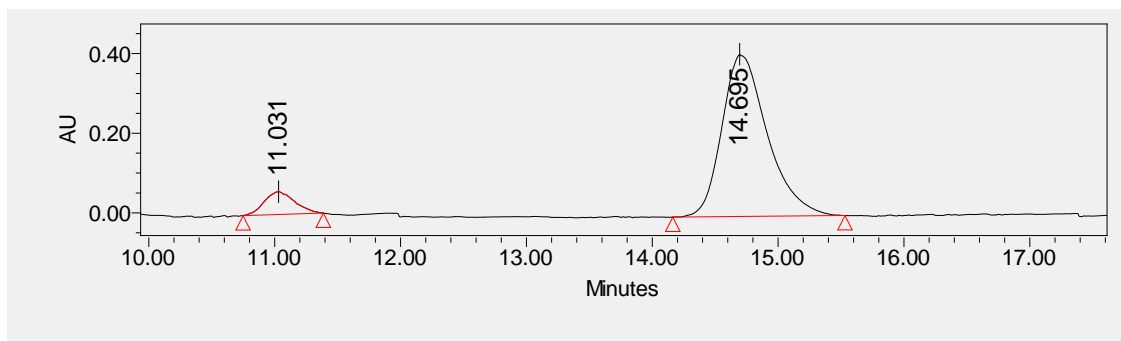
ESI-HRMS Calcd. for $\text{C}_{14}\text{H}_{12}\text{NO}_2^+$ 226.0863 $[\text{M}+\text{H}]^+$, found 226.0866

IR (powder): ν_{max} = 3352, 3056, 2919, 2850, 1736, 1621, 1500, 1453, 1429, 1183, 1151, 917, 810, 738, 720, 698 cm^{-1}

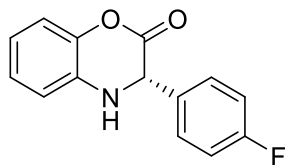
HPLC (Chiralpak OD-H column, 70:30 hexanes/isopropanol, 0.7 ml/min), $t_r = 11.0$ min (minor, R), 14.6 min (major, S)



	Retention Time	Area	% Area	Height
1	10.921	1273154	50.57	66163
2	15.075	1244373	49.43	47488



	Retention Time	Area	% Area	Height
1	11.031	900474	8.11	57637
2	14.695	10202786	91.89	407359



(*S*)-3-(4-fluorophenyl)-3,4-dihydro-2H-benzo[*b*][1,4]oxazin-2-one (**3-56**)

Known compound⁷⁹; white solids, 24.1 mg, 99% yield, 83% ee

$[\alpha]_D$: +81.9 ($c = 0.63$ in CHCl_3), literature $[\alpha]_D$: -98.4 ($c = 0.80$ in CHCl_3) for 95% ee (*R*)

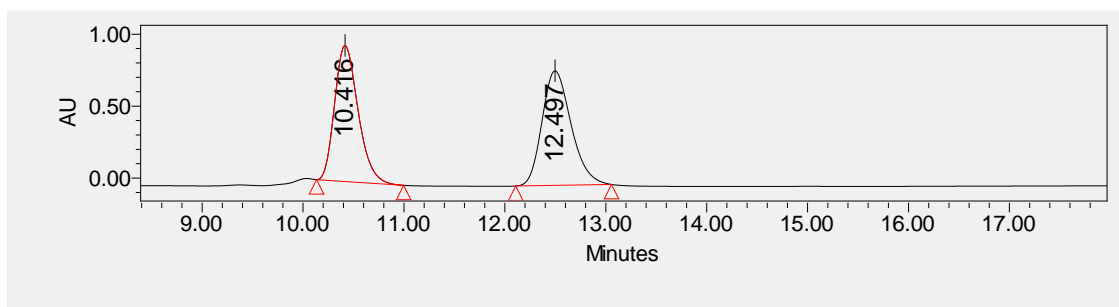
^1H NMR (500 MHz, Chloroform-*d*) δ 7.44 – 7.37 (m, 2H), 7.11 – 7.01 (m, 4H), 6.89 (td, $J = 7.8$, 1.5 Hz, 1H), 6.82 (dd, $J = 7.8$, 1.5 Hz, 1H), 5.04 (d, $J = 2.0$ Hz, 1H), 4.20 (s, 1H),

^{13}C NMR (126 MHz, Chloroform-*d*) δ 165.0, 163.0 (d, $J = 248.17$ Hz), 140.9, 132.2, 132.0 (d, $J = 3.07$ Hz), 129.4 (d, $J = 8.44$ Hz), 125.2, 120.6, 117.0, 115.9 (d, $J = 21.04$ Hz), 114.9, 58.7.

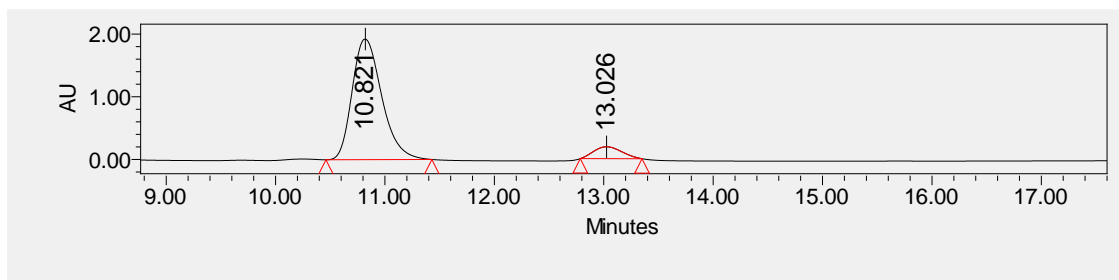
ESI-HRMS Calcd. for $\text{C}_{14}\text{H}_{11}\text{FNO}_2^+$ 244.0768 $[\text{M}+\text{H}]^+$, found 244.0762

IR (film): $\nu_{\text{max}} = 3354, 3068, 2954, 2924, 2853, 1758, 1650, 1617, 1499, 1411, 1292, 1193, 1156, 917, 802, 745 \text{ cm}^{-1}$

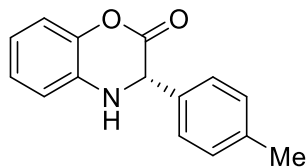
HPLC (Chiralpak IA column, 80:20 hexanes/isopropanol, 0.8 ml/min), $t_r = 10.8$ min (major, S), 13.0 min (minor, R)



	Retention Time	Area	% Area	Height
1	10.416	15276584	48.99	944985
2	12.497	15908081	51.01	795297



	Retention Time	Area	% Area	Height
1	10.821	36172403	91.42	1920678
2	13.026	3396497	8.58	189871



(*S*)-3-(*p*-tolyl)-3,4-dihydro-2*H*-1,4-benzoxazin-2-one (**3-57**)

Known compound⁷⁹; white solids, 23.4 mg, 98% yield, 73% ee

[α]_D: +67.2 (*c* = 0.78 in CHCl₃), literature [α]_D: -88.2 (*c* = 0.92 in CHCl₃) for 93% ee (*R*)

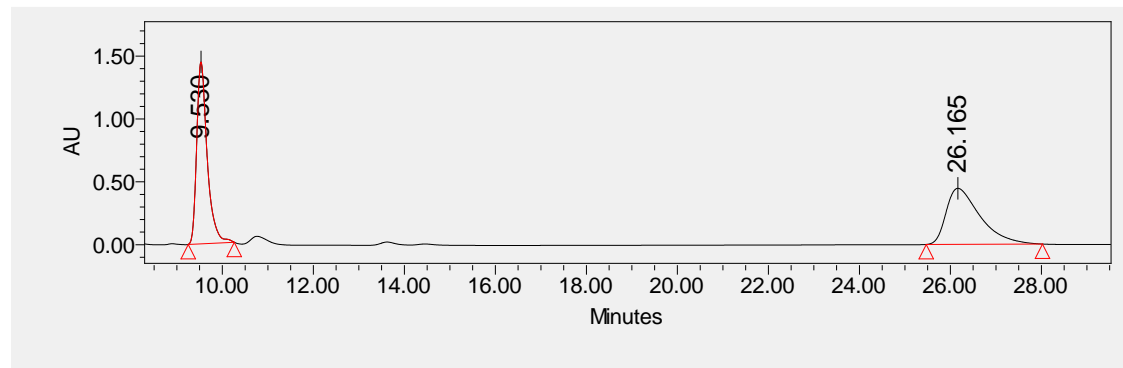
¹H NMR (700 MHz, Chloroform-*d*) δ 7.31 – 7.27 (m, 2H), 7.18 (d, *J* = 7.8 Hz, 2H), 7.07 – 7.03 (m, 1H), 7.02 (td, *J* = 7.7, 1.4 Hz, 1H), 6.86 (td, *J* = 7.7, 1.4 Hz, 1H), 6.80 (dd, *J* = 7.8, 1.4 Hz, 1H), 5.03 (d, *J* = 1.9 Hz, 1H), 4.19 (s, 1H), 2.34 (s, 3H).

¹³C NMR (176 MHz, Chloroform-*d*) δ 165.3, 140.9, 138.9, 133.3, 132.4, 129.6, 127.3, 125.1, 120.3, 116.9, 114.8, 77.2, 77.1, 77.0, 76.8, 59.0, 21.1.

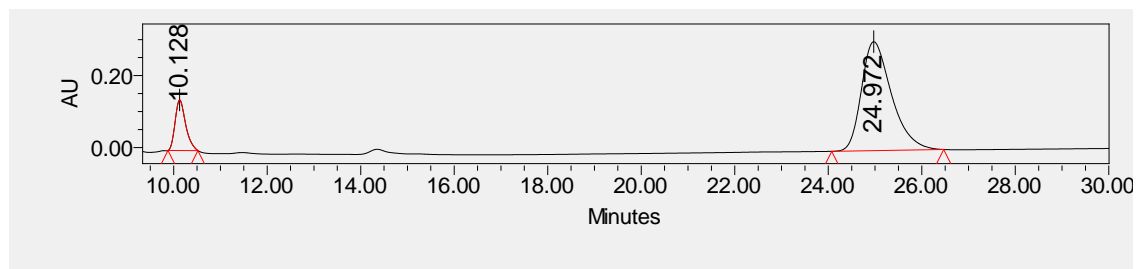
ESI-HRMS Calcd. for C₁₅H₁₄NO₂⁺ 240.1019 [M+H]⁺, found 240.1014

IR (film): ν_{max} = 3463, 3099, 2998, 2955, 2851, 1737, 1600, 1461, 1306, 1187, 1149, 970, 843, 760 cm⁻¹

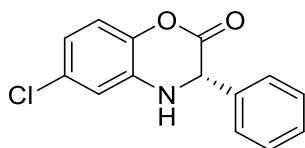
HPLC (Chiralpak OD-H column, 70:30 hexanes/isopropanol, 0.7 ml/min), *tr* = 10.1 min (minor, *R*), 24.9 min (major, *S*)



	Retention Time	Area	% Area	Height
1	9.530	23162022	50.08	1446243
2	26.165	23087060	49.92	445562



	Retention Time	Area	% Area	Height
1	10.128	2201323	13.30	140444
2	24.972	14349978	86.70	302463



(*S*)-6-Chloro-3-phenyl-3,4-dihydro-2*H*-1,4-benzoxazin-2-one (**3-59**)

Known compound⁷⁹; colorless solids, 25.1 mg, 97% yield, 88% ee

$[\alpha]_D$: +89.4 ($c = 0.80$ in CHCl_3), literature $[\alpha]_D$: -109.9 ($c = 0.90$ in CHCl_3) for 89% ee (*R*)

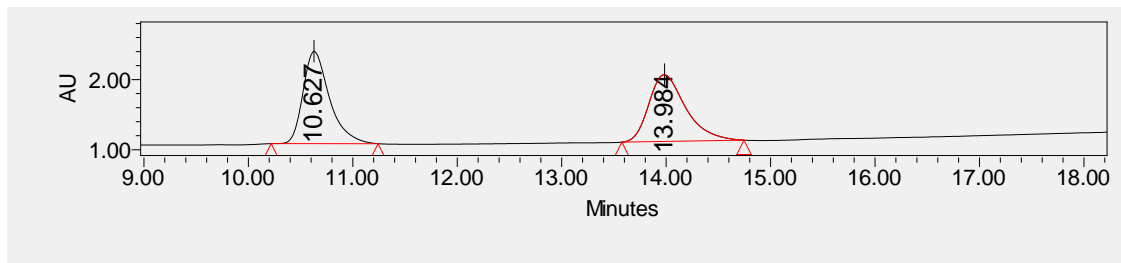
$^1\text{H NMR}$ (500 MHz, Chloroform-*d*) δ 7.38 (s, 5H), 6.96 (d, $J = 8.3$ Hz, 1H), 6.82 (dt, $J = 11.0$, 2.2 Hz, 2H), 5.09 (d, $J = 1.5$ Hz, 1H), 4.32 (s, 1H).

$^{13}\text{C NMR}$ (126 MHz, Chloroform-*d*) δ 164.3, 139.3, 135.9, 133.1, 130.1, 129.1, 129.1, 127.2, 120.1, 117.9, 114.6, 58.8.

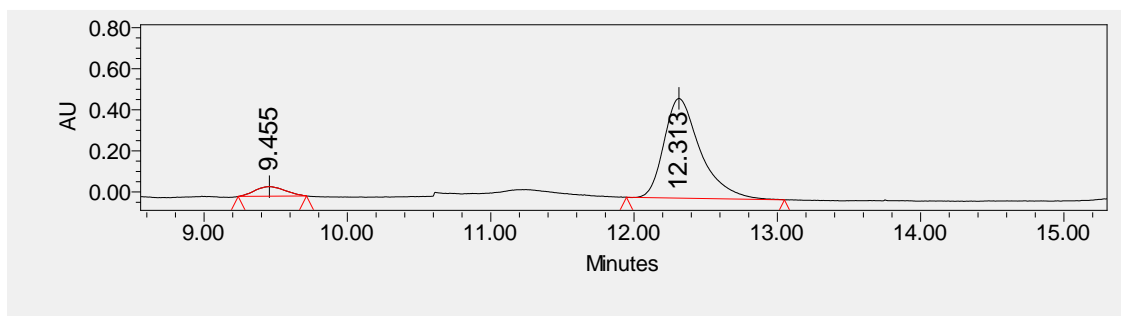
ESI-HRMS Calcd. for $\text{C}_{14}\text{H}_{11}\text{ClNO}_2^+$ 260.0473 $[\text{M}+\text{H}]^+$, found 260.0475

IR (powder): $\nu_{\text{max}} = 3465, 3098, 3073, 2958, 2924, 1741, 1581, 1443, 1290, 1137, 1073, 972, 823 \text{ cm}^{-1}$

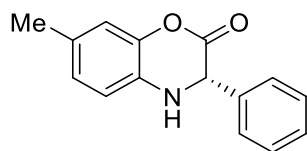
HPLC (Chiralpak OD-H column, 70:30 hexanes/isopropanol, 0.7 ml/min), $t_r = 9.5$ min (minor, *R*), 12.3 min (major, *S*)



	Retention Time	Area	% Area	Height
1	10.627	23194895	49.92	1317572
2	13.984	23265941	50.08	951680



	Retention Time	Area	% Area	Height
1	9.455	1793922	5.92	46753
2	12.313	28514976	94.08	485574



(*S*)-7-Methyl-3-phenyl-3,4-dihydro-2*H*-1,4-benzoxazin-2-one (**3-60**)

Known compound⁷⁹; colorless oil, 23.6 mg, 99% yield, 80% ee

$[\alpha]_D$: +66.7 ($c = 0.84$ in CHCl_3), literature $[\alpha]_D$: -80.6 ($c = 0.86$ in CHCl_3) for 93% ee (*R*)

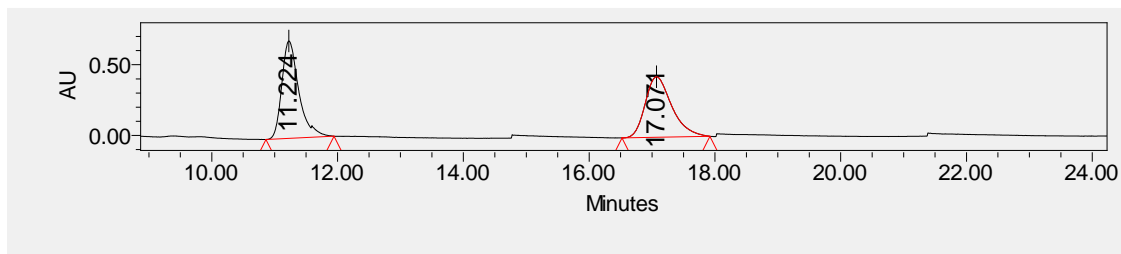
$^1\text{H NMR}$ (500 MHz, Chloroform-*d*) δ 7.44 – 7.33 (m, 5H), 6.86 (d, $J = 1.8$ Hz, 1H), 6.83 (dd, $J = 7.9, 1.9$ Hz, 1H), 6.71 (d, $J = 7.9$ Hz, 1H), 5.03 (d, $J = 2.1$ Hz, 1H), 4.13 (s, 1H), 2.29 (s, 3H).

$^{13}\text{C NMR}$ (126 MHz, Chloroform-*d*) δ 165.3, 140.9, 136.4, 130.4, 129.7, 128.9, 128.9, 127.4, 125.6, 117.3, 114.7, 59.4, 20.6.

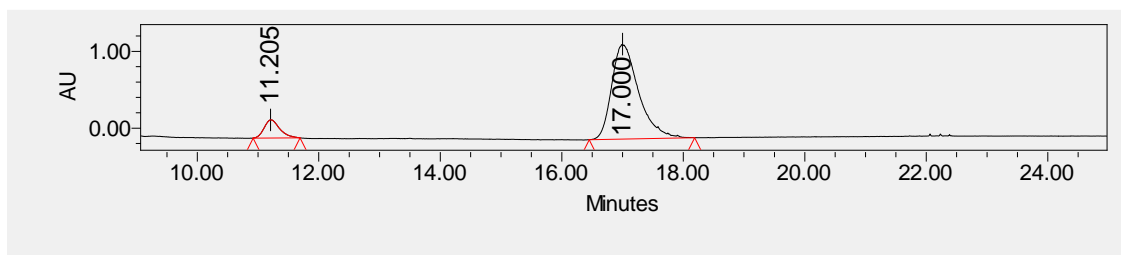
ESI-HRMS Calcd. for $\text{C}_{15}\text{H}_{14}\text{NO}_2^+$ 240.1019 $[\text{M}+\text{H}]^+$, found 240.1018

IR (powder): ν_{\max} = 3455, 3062, 2957, 2923, 2851, 1734, 1445, 1242, 1074, 946, 815 cm^{-1}

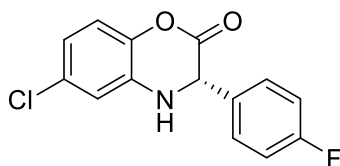
HPLC (Chiralpak OD-H column, 70:30 hexanes/isopropanol, 0.7 ml/min), t_r = 11.2 min (minor, R), 17.0 min (major, S)



	Retention Time	Area	% Area	Height
1	11.224	12953816	50.83	689034
2	17.071	12528629	49.17	428037



	Retention Time	Area	% Area	Height
1	11.205	4185537	9.92	236139
2	17.000	37993398	90.08	1234940



(S)-6-chloro-3-(4-fluorophenyl)-3,4-dihydro-2H-1,4-benzoxazin-2-one (**3-61**)

Colorless oil, 26.3 mg, 95% yield, 85% ee

$[\alpha]_D$: +71.7 (c = 0.82 in CHCl_3)

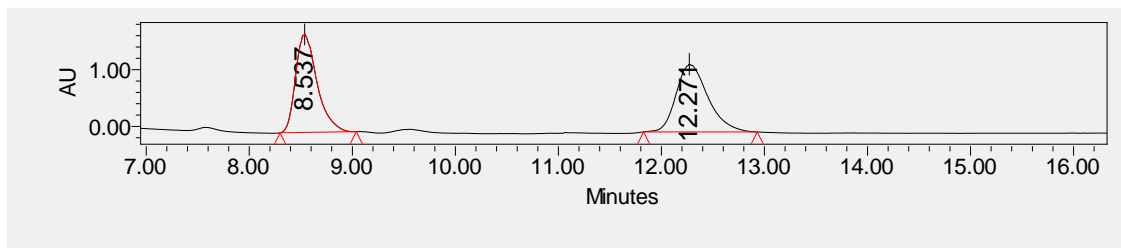
$^1\text{H NMR}$ (500 MHz, Chloroform-*d*) δ 7.41 – 7.35 (m, 2H), 7.12 – 7.05 (m, 2H), 6.98 (d, J = 8.5 Hz, 1H), 6.90 – 6.80 (m, 2H), 5.06 (d, J = 2.0 Hz, 1H), 4.28 – 4.24 (m, 1H).

^{13}C NMR (176 MHz, Chloroform-*d*) δ 164.1, 163.8, 162.3, 139.3, 132.9, 131.6, 130.2, 129.2, 129.2, 120.4, 118.0, 116.1(*d*, $J = 21.90$ Hz), 114.7, 58.2.

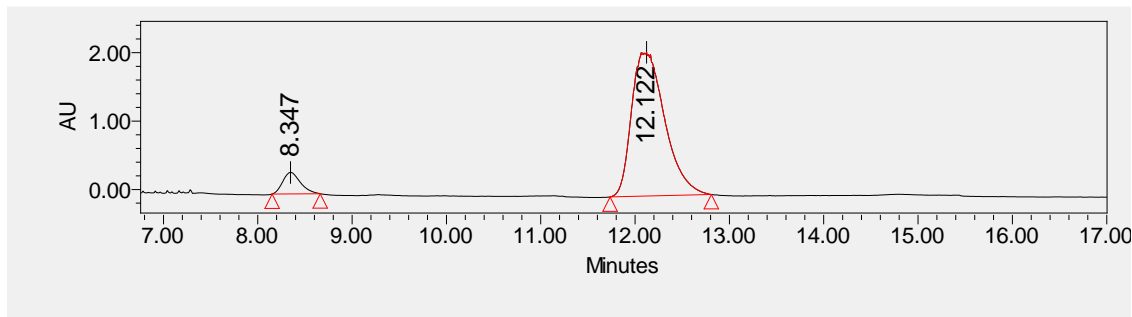
ESI-HRMS Calcd. for $\text{C}_{14}\text{H}_{10}\text{ClFNO}_2^+$ 278.0379 $[\text{M}+\text{H}]^+$, found 278.0374

IR (film): $\nu_{\text{max}} = 3400, 3383, 2976, 2875, 1741, 1598, 1506, 1224, 1155, 981, 837$ cm^{-1}

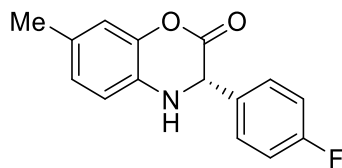
HPLC (Chiralpak OD-H column, 70:30 hexanes/isopropanol, 0.7 ml/min), $t_r = 8.3$ min (minor, R), 12.1 min (major, S)



	Retention Time	Area	% Area	Height
1	8.537	25031120	49.44	1735241
2	12.271	25598370	50.56	1191790



	Retention Time	Area	% Area	Height
1	8.347	4085561	7.37	313660
2	12.122	51349001	92.63	2100018



(*S*)-7-methyl-3-(4-fluorophenyl)-3,4-dihydro-2*H*-1,4-benzoxazin-2-one (**3-62**)

White solid, 25.1 mg, 98% yield, 81% ee

[α]_D: +58.8 (c = 0.84 in CHCl₃)

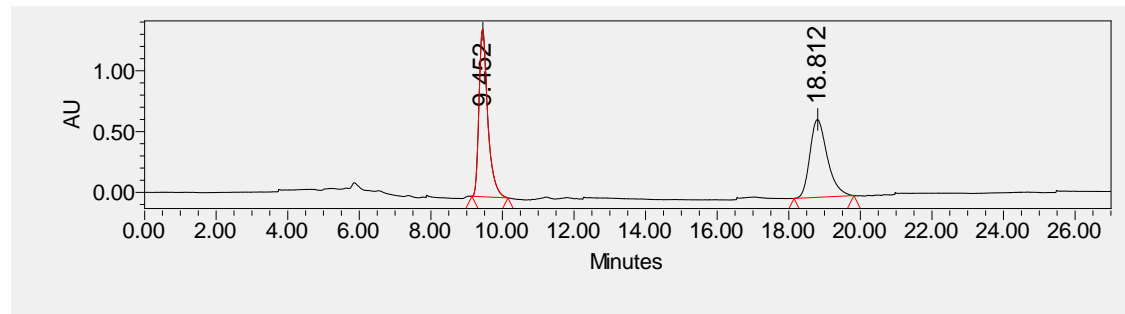
¹H NMR (401 MHz, Chloroform-*d*) δ 7.43 – 7.34 (m, 2H), 7.11 – 7.02 (m, 2H), 6.92 – 6.80 (m, 2H), 6.70 (d, *J* = 7.9 Hz, 1H), 4.99 (d, *J* = 2.2 Hz, 1H), 4.06 (s, 1H), 2.28 (s, 3H).

¹³C NMR (126 MHz, Chloroform-*d*) δ 165.3, 162.9 (d, *J* = 250.66 Hz), 140.9, 132.1 (d, *J* = 3.21 Hz), 130.6, 129.6, 129.4 (d, *J* = 8.43 Hz), 125.7, 117.4, 115.9 (d, *J* = 21.07 Hz), 114.8, 58.8, 20.6.

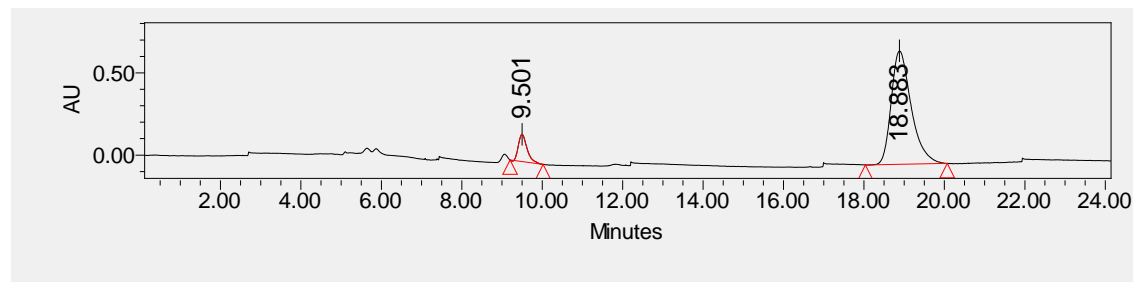
ESI-HRMS Calcd. for C₁₅H₁₃FNO₂⁺ 258.0925 [M+H]⁺, found 258.0924

IR (film): ν_{max} = 3345, 2924, 1735, 1603, 1299, 1221, 1157, 1101, 834 cm⁻¹

HPLC (Chiralpak OD-H column, 80:20 hexanes/isopropanol, 1.0 ml/min), tr = 9.5 min (minor, R), 18.8 min (major, S)



	Retention Time	Area	% Area	Height
1	9.452	23385297	51.94	1375036
2	18.812	21635546	48.06	641190



	Retention Time	Area	% Area	Height
1	9.501	2503371	9.53	166123
2	18.883	23763113	90.47	689490

3.8. References


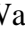
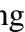
- (1) Walsh, C. T. Nature Loves Nitrogen Heterocycles. *Tetrahedron Lett.* **2015**, *56* (23), 3075–3081. <https://doi.org/10.1016/j.tetlet.2014.11.046>.
- (2) *Heterocycles in Natural Product Synthesis*, 1st ed.; John Wiley & Sons, Ltd. <https://doi.org/10.1002/9783527634880>.
- (3) Vitaku, E.; Smith, D. T.; Njardarson, J. T. Analysis of the Structural Diversity, Substitution Patterns, and Frequency of Nitrogen Heterocycles among U.S. FDA Approved Pharmaceuticals. *J. Med. Chem.* **2014**, *57* (24), 10257–10274. <https://doi.org/10.1021/jm501100b>.
- (4) Taylor, R. D.; MacCoss, M.; Lawson, A. D. G. Rings in Drugs. *J. Med. Chem.* **2014**, *57* (14), 5845–5859. <https://doi.org/10.1021/jm4017625>.
- (5) Roughley, S. D.; Jordan, A. M. The Medicinal Chemist's Toolbox: An Analysis of Reactions Used in the Pursuit of Drug Candidates. *J. Med. Chem.* **2011**, *54* (10), 3451–3479. <https://doi.org/10.1021/jm200187y>.
- (6) Meanwell, N. A. Chapter Five - A Synopsis of the Properties and Applications of Heteroaromatic Rings in Medicinal Chemistry. In *Advances in Heterocyclic Chemistry*; Scriven, E. F. V., Ramsden, C. A., Eds.; Academic Press, 2017; Vol. 123, pp 245–361. <https://doi.org/10.1016/bs.aihch.2016.11.002>.
- (7) Zumbrägel, N.; Merten, C.; Huber, S. M.; Gröger, H. Enantioselective Reduction of Sulfur-Containing Cyclic Imines through Biocatalysis. *Nat. Commun.* **2018**, *9* (1), 1949. <https://doi.org/10.1038/s41467-018-03841-5>.
- (8) Blaser, H. U. The Chiral Pool as a Source of Enantioselective Catalysts and Auxiliaries. *Chem. Rev.* **1992**, *92* (5), 935–952. <https://doi.org/10.1021/cr00013a009>.
- (9) Biswas, A.; Mondal, H.; Maji, M. S. Synthesis of Heterocycles by Isothiourea Organocatalysis. *J. Heterocycl. Chem.* **2020**, *57* (11), 3818–3844. <https://doi.org/10.1002/jhet.4119>.
- (10) Nomura, H.; Richards, C. J. Asymmetric Synthesis of Unsaturated Monocyclic and Bicyclic Nitrogen Heterocycles. *Org. Lett.* **2009**, *11* (13), 2892–2895. <https://doi.org/10.1021/ol900880w>.

- (11) Wang, D.-S.; Chen, Q.-A.; Lu, S.-M.; Zhou, Y.-G. Asymmetric Hydrogenation of Heteroarenes and Arenes. *Chem. Rev.* **2012**, *112* (4), 2557–2590. <https://doi.org/10.1021/cr200328h>.
- (12) Zheng, C.; You, S.-L. Catalytic Asymmetric Dearomatization by Transition-Metal Catalysis: A Method for Transformations of Aromatic Compounds. *Chem* **2016**, *1* (6), 830–857. <https://doi.org/10.1016/j.chempr.2016.11.005>.
- (13) Wiesenfeldt, M. P.; Nairoukh, Z.; Dalton, T.; Glorius, F. Selective Arene Hydrogenation for Direct Access to Saturated Carbo- and Heterocycles. *Angew. Chem. Int. Ed.* **2019**, *58* (31), 10460–10476. <https://doi.org/10.1002/anie.201814471>.
- (14) Kim, A. N.; Stoltz, B. M. Recent Advances in Homogeneous Catalysts for the Asymmetric Hydrogenation of Heteroarenes. *ACS Catal.* **2020**, *10* (23), 13834–13851. <https://doi.org/10.1021/acscatal.0c03958>.
- (15) Crabtree, R. H.; Chodosh, D. F.; Quirk, J. M.; Felkin, H.; Fillebeen-Khan, T.; Morris, G. E. Iridium Compounds in Homogeneous Hydrogenation. In *Fundamental Research in Homogeneous Catalysis*; Tsutsui, M., Ed.; Springer US: Boston, MA, 1979; pp 475–485. https://doi.org/10.1007/978-1-4613-2958-9_32.
- (16) Wang, W.-B.; Lu, S.-M.; Yang, P.-Y.; Han, X.-W.; Zhou, Y.-G. Highly Enantioselective Iridium-Catalyzed Hydrogenation of Heteroaromatic Compounds, Quinolines. *J. Am. Chem. Soc.* **2003**, *125* (35), 10536–10537. <https://doi.org/10.1021/ja0353762>.
- (17) Lu, S.-M.; Han, X.-W.; Zhou, Y.-G. Asymmetric Hydrogenation of Quinolines Catalyzed by Iridium with Chiral Ferrocenyloxazoline Derived N,P Ligands. *Adv. Synth. Catal.* **2004**, *346* (8), 909–912. <https://doi.org/10.1002/adsc.200404017>.
- (18) Lam, K. H.; Xu, L.; Feng, L.; Fan, Q.-H.; Lam, F. L.; Lo, W.; Chan, A. S. C. Highly Enantioselective Iridium-Catalyzed Hydrogenation of Quinoline Derivatives Using Chiral Phosphinite H8-BINAPO. *Adv. Synth. Catal.* **2005**, *347* (14), 1755–1758. <https://doi.org/10.1002/adsc.200505130>.
- (19) Rueping, M.; Antonchick, A. P.; Theissmann, T. A Highly Enantioselective Brønsted Acid Catalyzed Cascade Reaction: Organocatalytic Transfer Hydrogenation of Quinolines and Their Application in the Synthesis of Alkaloids. *Angew. Chem. Int. Ed.* **2006**, *45* (22), 3683–3686. <https://doi.org/10.1002/anie.200600191>.

- (20) Liu, S.; Fan, Y.; Peng, X.; Wang, W.; Hua, W.; Akber, H.; Liao, L. A Concise and Enantioselective Approach to the Total Synthesis of (–)-Lasubine I. *Tetrahedron Lett.* **2006**, *47* (44), 7681–7684. <https://doi.org/10.1016/j.tetlet.2006.08.137>.
- (21) Tang, W.-J.; Zhu, S.-F.; Xu, L.-J.; Zhou, Q.-L.; Fan, Q.-H.; Zhou, H.-F.; Lam, K.; Chan, A. S. C. Asymmetric Hydrogenation of Quinolines with High Substrate/Catalyst Ratio. *Chem. Commun.* **2007**, No. 6, 613–615. <https://doi.org/10.1039/B614446B>.
- (22) Wang, Z.-J.; Deng, G.-J.; Li, Y.; He, Y.-M.; Tang, W.-J.; Fan, Q.-H. Enantioselective Hydrogenation of Quinolines Catalyzed by Ir(BINAP)-Cored Dendrimers: Dramatic Enhancement of Catalytic Activity. *Org. Lett.* **2007**, *9* (7), 1243–1246. <https://doi.org/10.1021/ol0631410>.
- (23) Guo, Q.-S.; Du, D.-M.; Xu, J. The Development of Double Axially Chiral Phosphoric Acids and Their Catalytic Transfer Hydrogenation of Quinolines. *Angew. Chem. Int. Ed.* **2008**, *47* (4), 759–762. <https://doi.org/10.1002/anie.200703925>.
- (24) Wang, X.-B.; Zhou, Y.-G. Synthesis of Tunable Bisphosphine Ligands and Their Application in Asymmetric Hydrogenation of Quinolines. *J. Org. Chem.* **2008**, *73* (14), 5640–5642. <https://doi.org/10.1021/jo800779r>.
- (25) Zhou, H.; Li, Z.; Wang, Z.; Wang, T.; Xu, L.; He, Y.; Fan, Q.-H.; Pan, J.; Gu, L.; Chan, A. S. C. Hydrogenation of Quinolines Using a Recyclable Phosphine-Free Chiral Cationic Ruthenium Catalyst: Enhancement of Catalyst Stability and Selectivity in an Ionic Liquid. *Angew. Chem. Int. Ed.* **2008**, *47* (44), 8464–8467. <https://doi.org/10.1002/anie.200802237>.
- (26) Eggenstein, M.; Thomas, A.; Theuerkauf, J.; Franciò, G.; Leitner, W. Highly Efficient and Versatile Phosphine-Phosphoramidite Ligands for Asymmetric Hydrogenation. *Adv. Synth. Catal.* **2009**, *351* (5), 725–732. <https://doi.org/10.1002/adsc.200800653>.
- (27) Tadaoka, H.; Cartigny, D.; Nagano, T.; Gosavi, T.; Ayad, T.; Genêt, J.-P.; Ohshima, T.; Ratovelomanana-Vidal, V.; Mashima, K. Unprecedented Halide Dependence on Catalytic Asymmetric Hydrogenation of 2-Aryl- and 2-Alkyl-Substituted Quolinium Salts by Using Ir Complexes with Difluorophos and Halide Ligands. *Chem. – Eur. J.* **2009**, *15* (39), 9990–9994. <https://doi.org/10.1002/chem.200901477>.
- (28) Wang, D.-W.; Wang, X.-B.; Wang, D.-S.; Lu, S.-M.; Zhou, Y.-G.; Li, Y.-X. Highly Enantioselective Iridium-Catalyzed Hydrogenation of 2-Benzylquinolines and 2-

- Functionalized and 2,3-Disubstituted Quinolines. *J. Org. Chem.* **2009**, *74* (7), 2780–2787. <https://doi.org/10.1021/jo900073z>.
- (29) Gou, F.-R.; Li, W.; Zhang, X.; Liang, Y.-M. Iridium-Catalyzed Asymmetric Hydrogenation of Quinoline Derivatives with C3*-TunePhos. *Adv. Synth. Catal.* **2010**, *352* (14–15), 2441–2444. <https://doi.org/10.1002/adsc.201000485>.
- (30) Núñez-Rico, J. L.; Fernández-Pérez, H.; Benet-Buchholz, J.; Vidal-Ferran, A. Asymmetric Hydrogenation of Heteroaromatic Compounds Mediated by Iridium–(P-OP) Complexes. *Organometallics* **2010**, *29* (24), 6627–6631. <https://doi.org/10.1021/om100955t>.
- (31) Wang, T.; Zhuo, L.-G.; Li, Z.; Chen, F.; Ding, Z.; He, Y.; Fan, Q.-H.; Xiang, J.; Yu, Z.-X.; Chan, A. S. C. Highly Enantioselective Hydrogenation of Quinolines Using Phosphine-Free Chiral Cationic Ruthenium Catalysts: Scope, Mechanism, and Origin of Enantioselectivity. *J. Am. Chem. Soc.* **2011**, *133* (25), 9878–9891. <https://doi.org/10.1021/ja2023042>.
- (32) Zhang, D.-Y.; Wang, D.-S.; Wang, M.-C.; Yu, C.-B.; Gao, K.; Zhou, Y.-G. Synthesis of Electronically Deficient Atropisomeric Bisphosphine Ligands and Their Application in Asymmetric Hydrogenation of Quinolines. *Synthesis* **2011**, *2011* (17), 2796–2802. <https://doi.org/10.1055/s-0030-1260129>.
- (33) Shi, L.; Ye, Z.-S.; Cao, L.-L.; Guo, R.-N.; Hu, Y.; Zhou, Y.-G. Enantioselective Iridium-Catalyzed Hydrogenation of 3,4-Disubstituted Isoquinolines. *Angew. Chem. Int. Ed.* **2012**, *51* (33), 8286–8289. <https://doi.org/10.1002/anie.201203647>.
- (34) Chen, Q.-A.; Gao, K.; Duan, Y.; Ye, Z.-S.; Shi, L.; Yang, Y.; Zhou, Y.-G. Dihydrophenanthridine: A New and Easily Regenerable NAD(P)H Model for Biomimetic Asymmetric Hydrogenation. *J. Am. Chem. Soc.* **2012**, *134* (4), 2442–2448. <https://doi.org/10.1021/ja211684v>.
- (35) Xie, J.-H.; Yan, P.-C.; Zhang, Q.-Q.; Yuan, K.-X.; Zhou, Q.-L. Asymmetric Hydrogenation of Cyclic Imines Catalyzed by Chiral Spiro Iridium Phosphoramidite Complexes for Enantioselective Synthesis of Tetrahydroisoquinolines. *ACS Catal.* **2012**, *2* (4), 561–564. <https://doi.org/10.1021/cs300069g>.
- (36) Zhang, D.-Y.; Yu, C.-B.; Wang, M.-C.; Gao, K.; Zhou, Y.-G. A New Electronically Deficient Atropisomeric Diphosphine Ligand (S)-CF3O-BiPhep and Its Application in

- Asymmetric Hydrogenation. *Tetrahedron Lett.* **2012**, *53* (20), 2556–2559. <https://doi.org/10.1016/j.tetlet.2012.03.036>.
- (37) Iimuro, A.; Yamaji, K.; Kandula, S.; Nagano, T.; Kita, Y.; Mashima, K. Asymmetric Hydrogenation of Isoquinolinium Salts Catalyzed by Chiral Iridium Complexes: Direct Synthesis for Optically Active 1,2,3,4-Tetrahydroisoquinolines. *Angew. Chem. Int. Ed.* **2013**, *52* (7), 2046–2050. <https://doi.org/10.1002/anie.201207748>.
- (38) Ye, Z.-S.; Guo, R.-N.; Cai, X.-F.; Chen, M.-W.; Shi, L.; Zhou, Y.-G. Enantioselective Iridium-Catalyzed Hydrogenation of 1- and 3-Substituted Isoquinolinium Salts. *Angew. Chem. Int. Ed.* **2013**, *52* (13), 3685–3689. <https://doi.org/10.1002/anie.201208300>.
- (39) Dragan, V.; McWilliams, J. C.; Miller, R.; Sutherland, K.; Dillon, J. L.; O'Brien, M. K. Asymmetric Synthesis of Vabicaserin via Oxidative Multicomponent Annulation and Asymmetric Hydrogenation of a 3,4-Substituted Quinolinium Salt. *Org. Lett.* **2013**, *15* (12), 2942–2945. <https://doi.org/10.1021/ol401029k>.
- (40) Guo, R.-N.; Cai, X.-F.; Shi, L.; Ye, Z.-S.; Chen, M.-W.; Zhou, Y.-G. An Efficient Route to Chiral N-Heterocycles Bearing a C–F Stereogenic Center via Asymmetric Hydrogenation of Fluorinated Isoquinolines. *Chem. Commun.* **2013**, *49* (76), 8537–8539. <https://doi.org/10.1039/C3CC45341C>.
- (41) Kita, Y.; Yamaji, K.; Higashida, K.; Sathaiah, K.; Iimuro, A.; Mashima, K. Enhancing Effects of Salt Formation on Catalytic Activity and Enantioselectivity for Asymmetric Hydrogenation of Isoquinolinium Salts by Dinuclear Halide-Bridged Iridium Complexes Bearing Chiral Diphosphine Ligands. *Chem. – Eur. J.* **2015**, *21* (5), 1915–1927. <https://doi.org/10.1002/chem.201405408>.
- (42) Stopka, T.; Niggemann, M. Metal Free Carboamination of Internal Alkynes – an Easy Access to Polysubstituted Quinolines. *Chem. Commun.* **2016**, *52* (33), 5761–5764. <https://doi.org/10.1039/C5CC10460B>.
- (43) Chen, M.-W.; Ji, Y.; Wang, J.; Chen, Q.-A.; Shi, L.; Zhou, Y.-G. Asymmetric Hydrogenation of Isoquinolines and Pyridines Using Hydrogen Halide Generated in Situ as Activator. *Org. Lett.* **2017**, *19* (18), 4988–4991. <https://doi.org/10.1021/acs.orglett.7b02502>.
- (44) Welin, E. R.; Ngamnithiporn, A.; Klatte, M.; Lapointe, G.; Pototschnig, G. M.; McDermott, M. S. J.; Conklin, D.; Gilmore, C. D.; Tadross, P. M.; Haley, C. K.; Negoro,

- K.; Glibstrup, E.; Grünanger, C. U.; Allan, K. M.; Virgil, S. C.; Slamon, D. J.; Stoltz, B. M. Concise Total Syntheses of (–)-Jorunnamycin A and (–)-Jorumycin Enabled by Asymmetric Catalysis. *Science* **2019**, *363* (6424), 270–275. <https://doi.org/10.1126/science.aav3421>.
- (45) Xu, C.; Feng, Y.; Li, F.; Han, J.; He, Y.-M.; Fan, Q.-H. A Synthetic Route to Chiral Benzo-Fused N-Heterocycles via Sequential Intramolecular Hydroamination and Asymmetric Hydrogenation of Anilino-Alkynes. *Organometallics* **2019**, *38* (20), 3979–3990. <https://doi.org/10.1021/acs.organomet.9b00183>.
- (46) Hu, X.-H.; Hu, X.-P. Highly Diastereo- and Enantioselective Ir-Catalyzed Hydrogenation of 2,3-Disubstituted Quinolines with Structurally Fine-Tuned Phosphine–Phosphoramidite Ligands. *Org. Lett.* **2019**, *21* (24), 10003–10006. <https://doi.org/10.1021/acs.orglett.9b03925>.
- (47) Sun, S.; Nagorny, P. Exploration of Chiral Diastereomeric Spiroketal (SPIROL)-Based Phosphinite Ligands in Asymmetric Hydrogenation of Heterocycles. *Chem. Commun.* **2020**, *56* (60), 8432–8435. <https://doi.org/10.1039/D0CC03088K>.
- (48) Kim, A. N.; Ngamnthiporn, A.; Welin, E. R.; Daiger, M. T.; Grünanger, C. U.; Bartberger, M. D.; Virgil, S. C.; Stoltz, B. M. Iridium-Catalyzed Enantioselective and Diastereoselective Hydrogenation of 1,3-Disubstituted Isoquinolines. *ACS Catal.* **2020**, *10* (5), 3241–3248. <https://doi.org/10.1021/acscatal.0c00211>.
- (49) Mršić, N.; Jerphagnon, T.; Minnaard, A. J.; Feringa, B. L.; Vries, J. G. de. Asymmetric Hydrogenation of Quinoxalines Catalyzed by Iridium/PipPhos. *Adv. Synth. Catal.* **2009**, *351* (16), 2549–2552. <https://doi.org/10.1002/adsc.200900522>.
- (50) Tang, W.; Xu, L.; Fan, Q.-H.; Wang, J.; Fan, B.; Zhou, Z.; Lam, K.; Chan, A.    C. Asymmetric Hydrogenation of Quinoxalines with Diphosphinite Ligands: A Practical Synthesis of Enantioenriched, Substituted Tetrahydroquinoxalines. *Angew. Chem. Int. Ed.* **2009**, *48* (48), 9135–9138. <https://doi.org/10.1002/anie.200904518>.
- (51) Cartigny, D.; Nagano, T.; Ayad, T.; Genêt, J.-P.; Ohshima, T.; Mashima, K.; Ratovelomanana-Vidal, V. Iridium-Difluorophos-Catalyzed Asymmetric Hydrogenation of 2-Alkyl- and 2-Aryl-Substituted Quinoxalines: A General and Efficient Route into Tetrahydroquinoxalines. *Adv. Synth. Catal.* **2010**, *352* (11–12), 1886–1891. <https://doi.org/10.1002/adsc.201000513>.

- (52) Rueping, M.; Tato, F.; Schoepke, Fenja. R. The First General, Efficient and Highly Enantioselective Reduction of Quinoxalines and Quinoxalinones. *Chem. - Eur. J.* **2010**, *16* (9), 2688–2691. <https://doi.org/10.1002/chem.200902907>.
- (53) Qin, J.; Chen, F.; Ding, Z.; He, Y.-M.; Xu, L.; Fan, Q.-H. Asymmetric Hydrogenation of 2- and 2,3-Substituted Quinoxalines with Chiral Cationic Ruthenium Diamine Catalysts. *Org. Lett.* **2011**, *13* (24), 6568–6571. <https://doi.org/10.1021/ol2029096>.
- (54) Cartigny, D.; Berhal, F.; Nagano, T.; Phansavath, P.; Ayad, T.; Genêt, J.-P.; Ohshima, T.; Mashima, K.; Ratovelomanana-Vidal, V. General Asymmetric Hydrogenation of 2-Alkyl- and 2-Aryl-Substituted Quinoxaline Derivatives Catalyzed by Iridium-Difluorophos: Unusual Halide Effect and Synthetic Application. *J. Org. Chem.* **2012**, *77* (10), 4544–4556. <https://doi.org/10.1021/jo300455y>.
- (55) Huang, W.-X.; Liu, L.-J.; Wu, B.; Feng, G.-S.; Wang, B.; Zhou, Y.-G. Synthesis of Chiral Piperazines via Hydrogenation of Pyrazines Activated by Alkyl Halides. *Org. Lett.* **2016**, *18* (13), 3082–3085. <https://doi.org/10.1021/acs.orglett.6b01190>.
- (56) Legault, C. Y.; Charette, A. B. Catalytic Asymmetric Hydrogenation of N-Iminopyridinium Ylides: Expedient Approach to Enantioenriched Substituted Piperidine Derivatives. *J. Am. Chem. Soc.* **2005**, *127* (25), 8966–8967. <https://doi.org/10.1021/ja0525298>.
- (57) Cadu, A.; Upadhyay, P. K.; Andersson, P. G. Iridium-Catalyzed Asymmetric Hydrogenation of Substituted Pyridines. *Asian J. Org. Chem.* **2013**, *2* (12), 1061–1065. <https://doi.org/10.1002/ajoc.201300160>.
- (58) Ye, Z.-S.; Chen, M.-W.; Chen, Q.-A.; Shi, L.; Duan, Y.; Zhou, Y.-G. Iridium-Catalyzed Asymmetric Hydrogenation of Pyridinium Salts. *Angew. Chem. Int. Ed.* **2012**, *51* (40), 10181–10184. <https://doi.org/10.1002/anie.201205187>.
- (59) Qu, B.; Mangunuru, H. P. R.; Teyrulnikov, S.; Rivalti, D.; Zatulochnaya, O. V.; Kurouski, D.; Radomkit, S.; Biswas, S.; Karyakarte, S.; Fandrick, K. R.; Sieber, J. D.; Rodriguez, S.; Desrosiers, J.-N.; Haddad, N.; McKellop, K.; Pennino, S.; Lee, H.; Yee, N. K.; Song, J. J.; Kozlowski, M. C.; Senanayake, C. H. Enantioselective Synthesis of α -(Hetero)Aryl Piperidines through Asymmetric Hydrogenation of Pyridinium Salts and Its Mechanistic Insights. *Org. Lett.* **2018**, *20* (5), 1333–1337. <https://doi.org/10.1021/acs.orglett.8b00067>.

- (60) Baeza, A.; Pfaltz, A. Iridium-Catalyzed Asymmetric Hydrogenation of N-Protected Indoles. *Chem. – Eur. J.* **2010**, *16* (7), 2036–2039. <https://doi.org/10.1002/chem.200903105>.
- (61) Núñez-Rico, J. L.; Fernández-Pérez, H.; Vidal-Ferran, A. Asymmetric Hydrogenation of Unprotected Indoles Using Iridium Complexes Derived from P–OP Ligands and (Reusable) Brønsted Acids. *Green Chem.* **2014**, *16* (3), 1153–1157. <https://doi.org/10.1039/C3GC42132E>.
- (62) Lyubimov, S. E.; Ozolin, D. V.; Davankov, V. A. Asymmetric Iridium-Catalyzed Hydrogenation of 2-Methylindole Using Phosphite Ligands. *Tetrahedron Lett.* **2014**, *55* (26), 3613–3614. <https://doi.org/10.1016/j.tetlet.2014.04.113>.
- (63) Kaiser, S.; Smidt, S. P.; Pfaltz, A. Iridium Catalysts with Bicyclic Pyridine–Phosphinite Ligands: Asymmetric Hydrogenation of Olefins and Furan Derivatives. *Angew. Chem. Int. Ed.* **2006**, *45* (31), 5194–5197. <https://doi.org/10.1002/anie.200601529>.
- (64) Pauli, L.; Tannert, R.; Scheil, R.; Pfaltz, A. Asymmetric Hydrogenation of Furans and Benzofurans with Iridium–Pyridine–Phosphinite Catalysts. *Chem. – Eur. J.* **2015**, *21* (4), 1482–1487. <https://doi.org/10.1002/chem.201404903>.
- (65) Ge, Y.; Wang, Z.; Han, Z.; Ding, K. Iridium-Catalyzed Enantioselective Hydrogenation of Indole and Benzofuran Derivatives. *Chem. – Eur. J.* **2020**, *26* (67), 15482–15486. <https://doi.org/10.1002/chem.202002532>.
- (66) Negoro, N.; Sasaki, S.; Mikami, S.; Ito, M.; Tsujihata, Y.; Ito, R.; Suzuki, M.; Takeuchi, K.; Suzuki, N.; Miyazaki, J.; Santou, T.; Odani, T.; Kanzaki, N.; Funami, M.; Morohashi, A.; Nonaka, M.; Matsunaga, S.; Yasuma, T.; Momose, Y. Optimization of (2,3-Dihydro-1-Benzofuran-3-Yl)Acetic Acids: Discovery of a Non-Free Fatty Acid-Like, Highly Bioavailable G Protein-Coupled Receptor 40/Free Fatty Acid Receptor 1 Agonist as a Glucose-Dependent Insulinotropic Agent. *J. Med. Chem.* **2012**, *55* (8), 3960–3974. <https://doi.org/10.1021/jm300170m>.
- (67) Núñez-Rico, J. L.; Vidal-Ferran, A. [Ir(P–OP)]-Catalyzed Asymmetric Hydrogenation of Diversely Substituted C=N-Containing Heterocycles. *Org. Lett.* **2013**, *15* (8), 2066–2069. <https://doi.org/10.1021/ol400854a>.

- (68) Han, Z.; Liu, G.; Wang, R.; Dong, X.-Q.; Zhang, X. Highly Efficient Ir-Catalyzed Asymmetric Hydrogenation of Benzoxazinones and Derivatives with a Brønsted Acid Cocatalyst. *Chem. Sci.* **2019**, *10* (15), 4328–4333. <https://doi.org/10.1039/C8SC05797D>.
- (69) Huang, W.-X.; Yu, C.-B.; Shi, L.; Zhou, Y.-G. Iridium-Catalyzed Asymmetric Hydrogenation of Pyrrolo[1,2-a]Pyrazinium Salts. *Org. Lett.* **2014**, *16* (12), 3324–3327. <https://doi.org/10.1021/ol5013313>.
- (70) Rueping, M.; Koenigs, R. M. Brønsted Acid Differentiated Metal Catalysis by Kinetic Discrimination. *Chem. Commun.* **2010**, *47* (1), 304–306. <https://doi.org/10.1039/C0CC02167A>.
- (71) Qiu, L.; Kwong, F. Y.; Wu, J.; Lam, W. H.; Chan, S.; Yu, W.-Y.; Li, Y.-M.; Guo, R.; Zhou, Z.; Chan, A. S. C. A New Class of Versatile Chiral-Bridged Atropisomeric Diphosphine Ligands: Remarkably Efficient Ligand Syntheses and Their Applications in Highly Enantioselective Hydrogenation Reactions. *J. Am. Chem. Soc.* **2006**, *128* (17), 5955–5965. <https://doi.org/10.1021/ja0602694>.
- (72) Argüelles, A. J.; Sun, S.; Budaitis, B. G.; Nagorny, P. Design, Synthesis, and Application of Chiral C_2 -Symmetric Spiroketal-Containing Ligands in Transition-Metal Catalysis. *Angew. Chem. Int. Ed.* **2018**, *57* (19), 5325–5329. <https://doi.org/10.1002/anie.201713304>.
- (73) Sun, Z.; Winschel, G. A.; Borovika, A.; Nagorny, P. Chiral Phosphoric Acid-Catalyzed Enantioselective and Diastereoselective Spiroketalizations. *J. Am. Chem. Soc.* **2012**, *134* (19), 8074–8077. <https://doi.org/10.1021/ja302704m>.
- (74) Nagorny, P.; Sun, Z.; Winschel, G. A. Chiral Phosphoric Acid Catalyzed Stereoselective Spiroketalizations. *Synlett* **2013**, *24* (06), 661–665. <https://doi.org/10.1055/s-0032-1318098>.
- (75) Khomutnyk, Y. Ya.; Argüelles, A. J.; Winschel, G. A.; Sun, Z.; Zimmerman, P. M.; Nagorny, P. Studies of the Mechanism and Origins of Enantioselectivity for the Chiral Phosphoric Acid-Catalyzed Stereoselective Spiroketalization Reactions. *J. Am. Chem. Soc.* **2016**, *138* (1), 444–456. <https://doi.org/10.1021/jacs.5b12528>.
- (76) Wang, S.; Argüelles, A. J.; Tay, J.-H.; Hotta, M.; Zimmerman, P. M.; Nagorny, P. Experimental and Computational Studies on Regiodivergent Chiral Phosphoric Acid Catalyzed Cycloisomerization of Mupirocin Methyl Ester. *Chem. – Eur. J.* **2020**, *26* (20), 4583–4591. <https://doi.org/10.1002/chem.201905222>.

- (77) Kodama, K.; Kobayashi, Y.; Saigo, K. Two-Component Supramolecular Helical Architectures: Creation of Tunable Dissymmetric Cavities for the Inclusion and Chiral Recognition of the Third Components. *Chem. – Eur. J.* **2007**, *13* (7), 2144–2152. <https://doi.org/10.1002/chem.200601295>.
- (78) Chong, E.; Qu, B.; Zhang, Y.; Cannone, Z. P.; Leung, J. C.; Tcyrulnikov, S.; Nguyen, K. D.; Haddad, N.; Biswas, S.; Hou, X.; Kaczanowska, K.; Chwalba, M.; Tracz, A.; Czarnocki, S.; Song, J. J.; Kozlowski, M. C.; Senanayake, C. H. A Versatile Catalyst System for Enantioselective Synthesis of 2-Substituted 1,4-Benzodioxanes. *Chem. Sci.* **2019**, *10* (15), 4339–4345. <https://doi.org/10.1039/C8SC05612A>.
- (79) Feng, G.-S.; Shi, L.; Meng, F.-J.; Chen, M.-W.; Zhou, Y.-G. Iridium-Catalyzed Asymmetric Hydrogenation of 4,6-Disubstituted 2-Hydroxypyrimidines. *Org. Lett.* **2018**, *20* (20), 6415–6419. <https://doi.org/10.1021/acs.orglett.8b02723>.
- (80) Huang, W.-X.; Yu, C.-B.; Ji, Y.; Liu, L.-J.; Zhou, Y.-G. Iridium-Catalyzed Asymmetric Hydrogenation of Heteroaromatics Bearing a Hydroxyl Group, 3-Hydroxypyridinium Salts. *ACS Catal.* **2016**, *6* (4), 2368–2371. <https://doi.org/10.1021/acscatal.5b02625>.
- (81) Argüelles, A. J.; Sun, S.; Budaitis, B. G.; Nagorny, P. Design, Synthesis, and Application of Chiral C_2 -Symmetric Spiroketal-Containing Ligands in Transition-Metal Catalysis. *Angew. Chem. Int. Ed.* **2018**, *57* (19), 5325–5329. <https://doi.org/10.1002/anie.201713304>.
- (82) Wang, M.-C.; Wang, Y.-H.; Li, G.-W.; Sun, P.-P.; Tian, J.-X.; Lu, H.-J. Applications of Conformational Design: Rational Design of Chiral Ligands Derived from a Common Chiral Source for Highly Enantioselective Preparations of (R)- and (S)-Enantiomers of Secondary Alcohols. *Tetrahedron Asymmetry* **2011**, *22* (7), 761–768. <https://doi.org/10.1016/j.tetasy.2011.04.013>.
- (83) Issenhuth, J.-T.; Dagherne, S.; Bellemin-Laponnaz, S. Enantioselective Hydrosilylation of Prochiral Ketones Catalyzed by Chiral BINAP-Copper(I) Complexes. *Comptes Rendus Chim.* **2010**, *13* (3), 353–357. <https://doi.org/10.1016/j.crci.2009.11.002>.
- (84) Gou, F.-R.; Li, W.; Zhang, X.; Liang, Y.-M. Iridium-Catalyzed Asymmetric Hydrogenation of Quinoline Derivatives with C_3^* -TunePhos. *Adv. Synth. Catal.* **2010**, *352* (14–15), 2441–2444. <https://doi.org/10.1002/adsc.201000485>.
- (85) Rueping, M.; Antonchick, A. P.; Theissmann, T. A Highly Enantioselective Brønsted Acid Catalyzed Cascade Reaction: Organocatalytic Transfer Hydrogenation of Quinolines and

- Their Application in the Synthesis of Alkaloids. *Angew. Chem. Int. Ed.* **2006**, *45* (22), 3683–3686. <https://doi.org/10.1002/anie.200600191>.
- (86) Rueping, M.; Tato, F.; Schoepke, Fenja. R. The First General, Efficient and Highly Enantioselective Reduction of Quinoxalines and Quinoxalinones. *Chem. - Eur. J.* **2010**, *16* (9), 2688–2691. <https://doi.org/10.1002/chem.200902907>.
- (87) Rueping, M.; Antonchick, A. P.; Theissmann, T. Geringste Katalysatormengen in der Brønsted-Säure-katalysierten Transferhydrierung: enantioselective Reduktion von Benzoxazinen, Benzthiazinen und Benzoxazinonen. *Angew. Chem.* **2006**, *118* (40), 6903–6907. <https://doi.org/10.1002/ange.200601832>.
- (88) Wang, T.; Zhuo, L.-G.; Li, Z.; Chen, F.; Ding, Z.; He, Y.; Fan, Q.-H.; Xiang, J.; Yu, Z.-X.; Chan, A. S. C. Highly Enantioselective Hydrogenation of Quinolines Using Phosphine-Free Chiral Cationic Ruthenium Catalysts: Scope, Mechanism, and Origin of Enantioselectivity. *J. Am. Chem. Soc.* **2011**, *133* (25), 9878–9891. <https://doi.org/10.1021/ja2023042>.
- (89) Chen, Q.-A.; Gao, K.; Duan, Y.; Ye, Z.-S.; Shi, L.; Yang, Y.; Zhou, Y.-G. Dihydrophenanthridine: A New and Easily Regenerable NAD(P)H Model for Biomimetic Asymmetric Hydrogenation. *J. Am. Chem. Soc.* **2012**, *134* (4), 2442–2448. <https://doi.org/10.1021/ja211684v>.
- (90) Qin, J.; Chen, F.; Ding, Z.; He, Y.-M.; Xu, L.; Fan, Q.-H. Asymmetric Hydrogenation of 2- and 2,3-Substituted Quinoxalines with Chiral Cationic Ruthenium Diamine Catalysts. *Org. Lett.* **2011**, *13* (24), 6568–6571. <https://doi.org/10.1021/ol2029096>.

Chapter 4

Exploration of Chiral Spiroketal (SPIROL)-Based Oxazoline Ligands (SPIROX) in Asymmetric Insertion of α -Diazocarbonyl Compounds

4.1. Introduction of carbene insertion

Carbenes' history could be backdated back to the beginning of last century,¹ but nowadays the use of these carbon(II) derivatives has become routine in organic chemistry.² Carbenes could be generated via thermo- or photochemically-activated decomposition of diazo compounds. Most carbenes have short lifetimes after generation, while stable carbenes, such as *N*-Heterocyclic carbenes (NHC), are long-lived. Depending on the specific electronic structure in each case, carbene's may exist in a singlet (spin-paired) or a triplet (spin-non-paired) form. The lone pair of electrons in singlet carbenes occupies the σ orbital, while the electrons in triplet carbenes occupy one σ -orbital and one p-orbital. Therefore, spin-paired carbenes could be described as sp^2 -hybridized carbon-containing structures, in which the carbene center contains both carboanionic and carbocationic characters. According to the Valence Bond Theory, the triplet carbenes could possess either a linear or bent geometries, both of which behave like biradicals in the reactions. Electron paramagnetic resonance (EPR) spectroscopy also gave evidence of such proposed structures with measurements of the angle between R^1 and R^2 to be 100-110° in singlets and 125-140° for triplets.

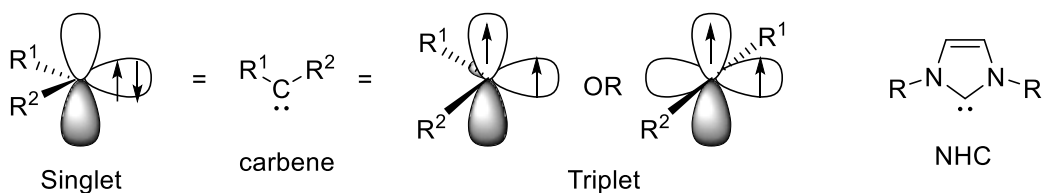
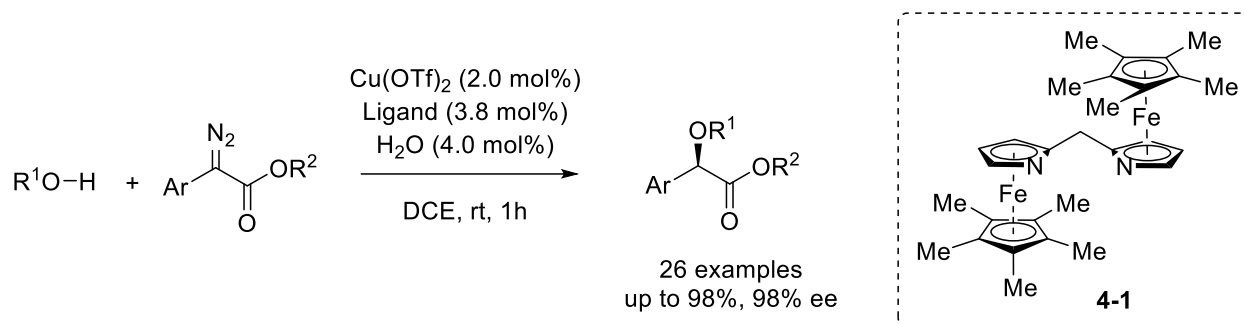


Figure 4.1 Example of different states of carbenes

Carbenoids represent the derivatives of carbenes with the carbene carbon bonded to a transition metal. Because of the extremely high reactivity of carbenes, the reactions with their ‘masked’ versions (i.e., carbenoids), proceed in a significantly more selective manner. Carbenoids could be easily generated by a reaction of carbene ligands or diazo compounds and metals such as Cu,³ Pd,⁴ Zn,^{5,6} and Rh.⁷ Early studies demonstrated that metal-carbenoids would be extraordinary catalysts with plentiful applications,^{3,8,9} especially in the heteroatom (N, O, S, Si)-H insertion reactions. Copper-carbenoids exhibit different selectivity profiles from the rhodium carbenoids, and copper-based catalysts have been recently utilized to achieve higher reactivities and selectivities with less expensive overall costs in chiral catalysis. Metal-catalyzed asymmetric insertion of α -diazocarbonyl compounds into X-H (X = C, N, O, S, Si) bonds is considered to be one of the most useful methods to construct C-X bonds.^{10,11} Since chiral α -alkyloxy, α -aryloxy or α -hydroxy esters and ketones, and oxygen containing heterocyclic compounds are important intermediates to access various biologically active compounds,^{12,13} the methods leading to the asymmetric formation of these motifs are of great value. In 2006, Fu and coworkers reported the first effective method for the catalytic enantioselective insertions into O-H bonds.¹⁴ They successfully utilized copper(II) trifluoromethanesulfonate with *bis*-azaferrocene ligand **4-1** to insert methyl α -diazo- α -phenylacetate into 10 different alcohols with up to 94% yield and 90% ee. The catalysts were also tested with a wide range of α -diazo esters with up to 98% ee obtained in selected substrates (*cf.* Scheme 4.1).



Scheme 4.1 Early study of asymmetric carbenoid insertion

4.2. Introduction of BOX ligands

Bisoxazoline (BOX) ligands represent a large family of the C_2 -symmetric chiral ligands that are often viewed as the most popular bidentate nitrogen ligands developed to date. The BOX ligands are conveniently generated in 3-5 step synthetic sequences, and the BOX scaffold is highly tunable and could be tailored to a variety of applications. Early efforts included copper-BOX-catalyzed enantioselective cyclopropanation of olefins¹⁵ and iridium-BOX-assisted enantioselective transfer hydrogenation of alkyl aryl ketones.¹⁶ At the same time, metal-BOX catalysts were also utilized in the asymmetric cyclopropanation of styrenes reported by the Evans group¹⁷ and enantioselective Diels-Alder reaction disclosed by Corey and coworkers¹⁸ in 1991. (Figure 4.2)

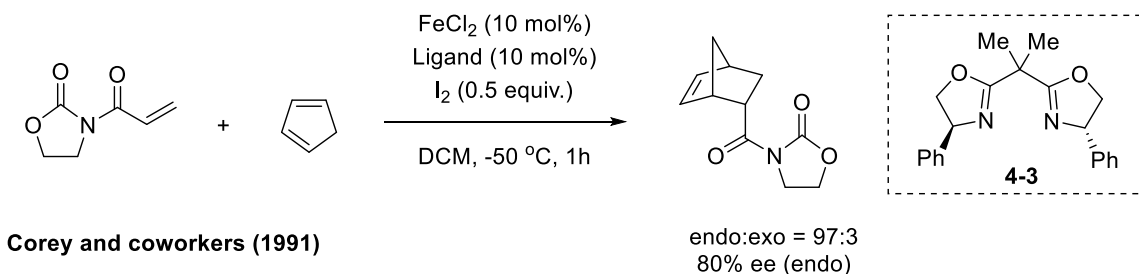
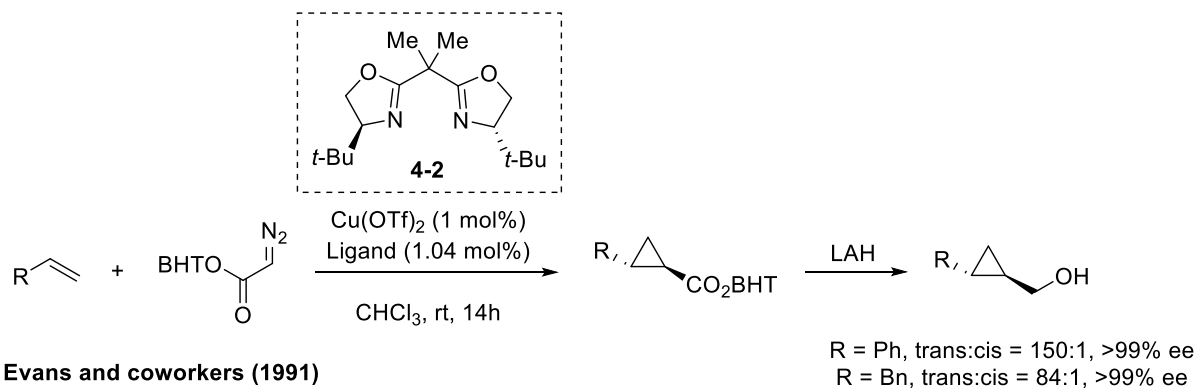


Figure 4.2 Early studies with BOX ligands

Nowadays, the synthesis of BOX ligands is well established and could be easily performed on large scale even by students in undergraduate-level courses. Cyclization of diethyl malonimidate or dicyanopyridine derivatives with various commercially available amino alcohols affords the corresponding BOX or PyBOX ligands (*cf.* Figure 4.3). Additionally, disubstituted BOX ligands could be also prepared from the reaction of diacyl chlorides and chiral amino alcohols, followed by a dehydrative cyclization.¹⁹ Due to their utility and easy access, a large number of BOX ligand variants is commercially available, and routinely used to promote a wide variety of fundamentally important transformations such as Aldol-like reactions,²⁰ ene reactions,²¹ Mannich reactions,²² and Michael reactions.²³ Nagorny group has long standing interest in exploring Cu(II) complexes of BOX ligands, and several recent studies demonstrated the utility of the copper-BOX catalysts in the Michael addition/intramolecular Aldol cyclizations leading to the formation of steroidal cores.^{24,25,26}

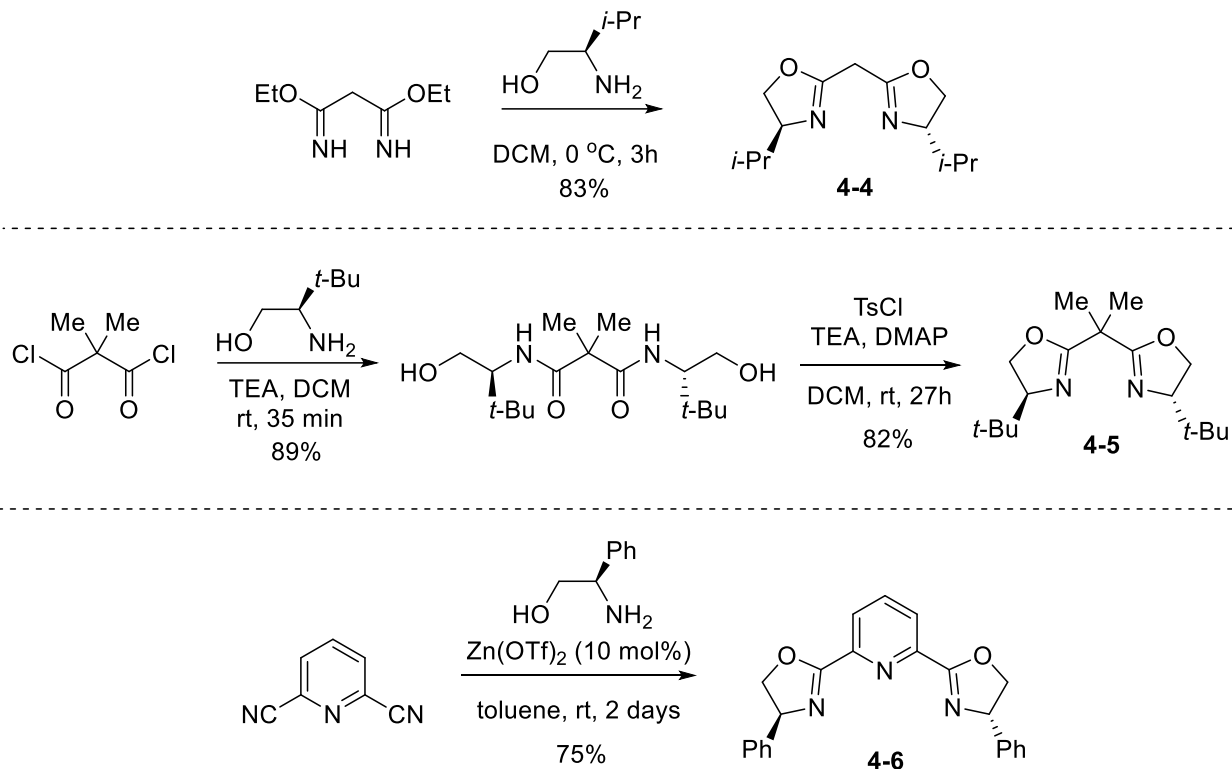
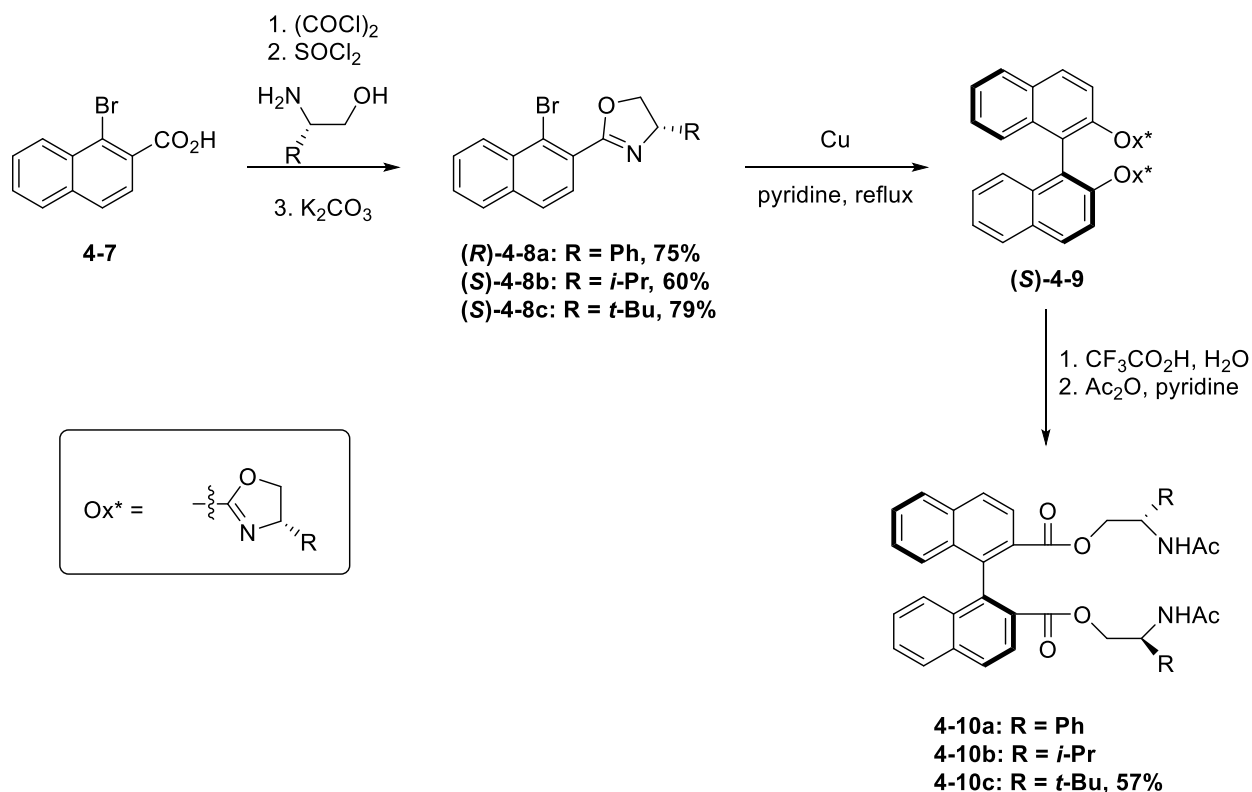


Figure 4.3 Selected examples of the BOX and PyBOX ligand syntheses

Due to the excellent performance of oxazoline-containing BOX and PyBOX ligands in thousands of reports, the possibility of installing oxazoline motifs into other C₂-symmetric privileged scaffolds has also been extensively investigated. In 1994, Meyers and Nelson first reported the synthesis of BINOL-based oxazoline ligands via Ullmann reaction.²⁷ Three different chiral oxazoline intermediates **4-8** were produced from the reaction with commercially available 1-bromo-2-naphthoic acid **4-7** and chiral amino alcohols, followed by the cyclization of the amide with 60-79% yield after 3 steps. Activated copper powder in pyridine at reflux catalyzed the Ullmann coupling, and the resulting oxazoline-containing binaphthyls **4-9** were successfully accessed. However, the original purpose of their study was to access enantiomerically pure C₂-symmetric binaphthyl skeletons, and they realized that the enantiomeric and diastereomeric ratio

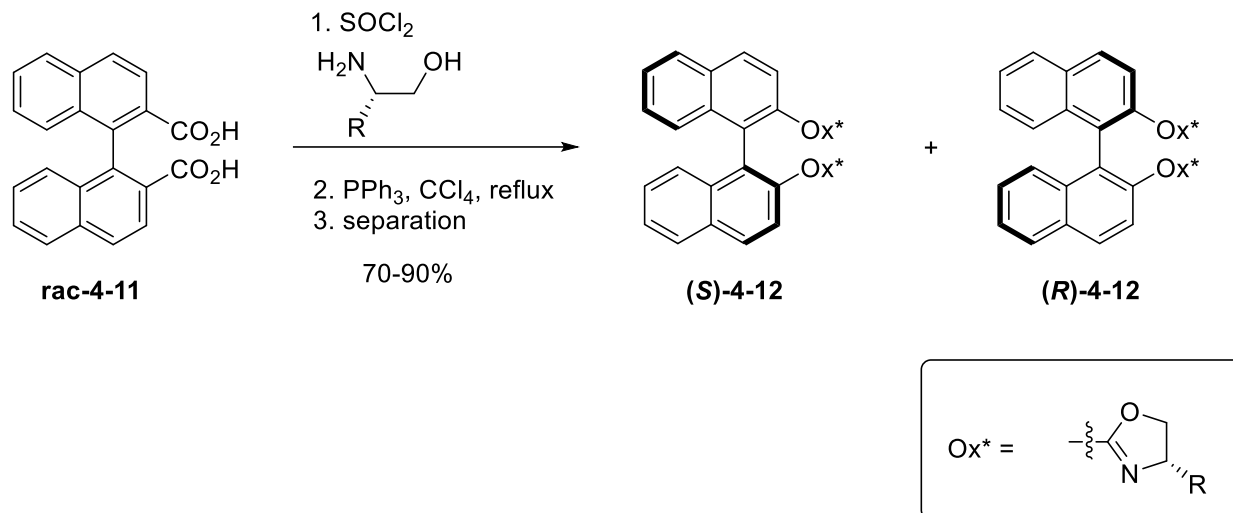
could be affected by the size of substituent in the oxazoline ring. Therefore, the oxazoline ring was opened, and the *t*-butyl group-containing **4-10c** was produced with 57% yield from **4-8c**.

(Scheme 4.2)



Scheme 4.2 Early development of BINOL-based oxazoline ligands

Later in 1996, Hayashi and coworkers reported their ligand synthesis starting with racemic BINOL-based carboxylic acids **4-11**.²⁸ Due to additional chiral centers introduced from the reaction with amino alcohol, two diastereomeric amides were produced, and the corresponding oxazoline products **4-12** after cyclization were separable by column chromatography. (Scheme 4.3)



Scheme 4.3 Optimized synthesis of BINOL-based oxazoline ligands

There have been some successful studies with BINOL-based oxazoline ligands in asymmetric catalysis. Hayashi and coworkers synthesized and applied **(S)-4-12a** in the Cu-catalyzed asymmetric cyclopropanation of styrene with diazoacetates, and they could achieve up to 97% ee and 60% yield with *l*-menthyl diazoacetate.²⁸ (Figure 4.4, reaction [1]) In the following year, they also discovered that Wacker-type cyclization could be catalyzed asymmetrically by palladium catalysts coordinated with BINOL-based bisoxazoline ligand **(S)-4-12b**.²⁹ 5 *ortho*-allyl phenols were tested and products were obtained with 90-97% ee. In their study, they also compared the performance with other BOX ligands which only provided much lower selectivities and yields. (Figure 4.4, reaction [2]) Later in 1999, they further optimized the reaction condition for the Wacker-type cyclization with a novel 3,3'-disubstituted BINOL-based oxazoline ligand.³⁰ **(S)-4-13** could achieve 96% ee with 80% yield at room temperature while non-substituted ligand **(S)-4-12b** only provided 9% ee and 90% yield at elevated 60°C. (Figure 4.4, reaction [3])

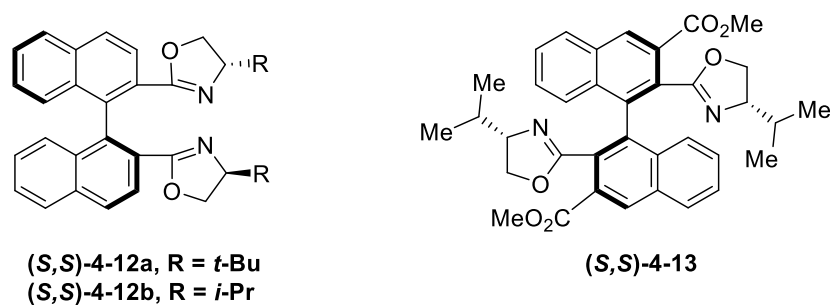
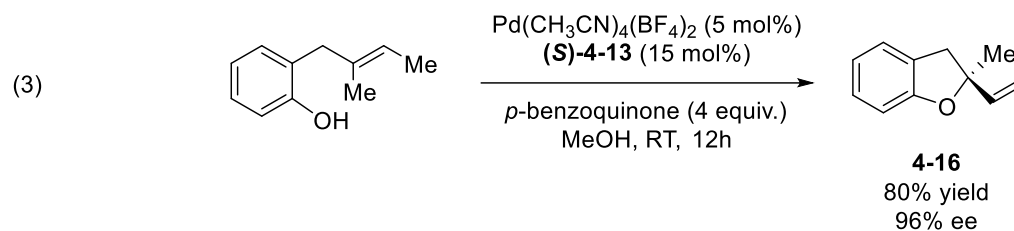
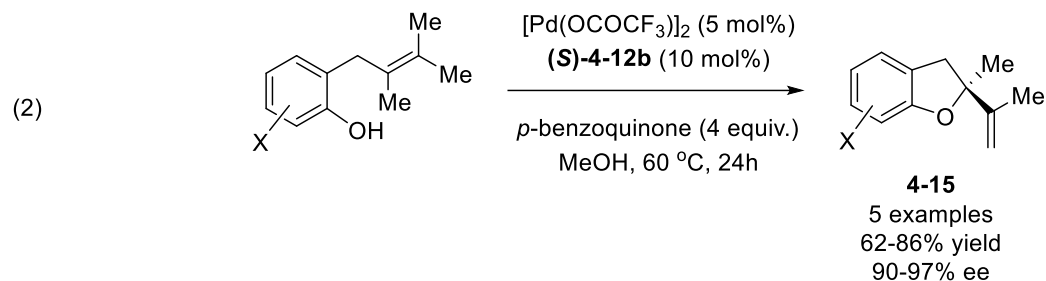
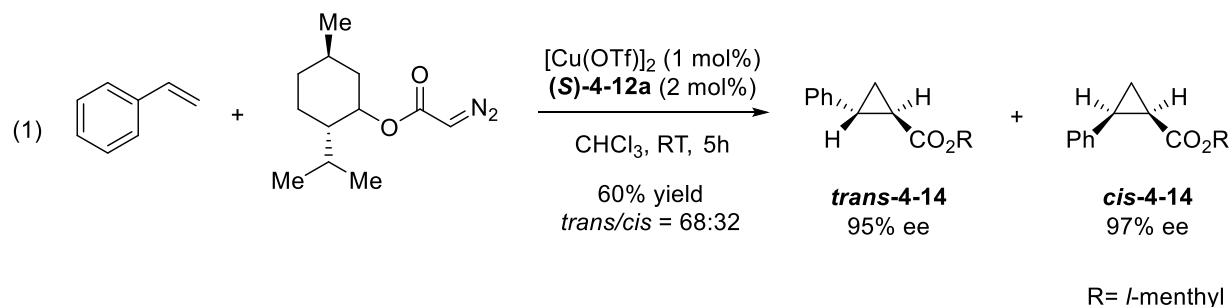
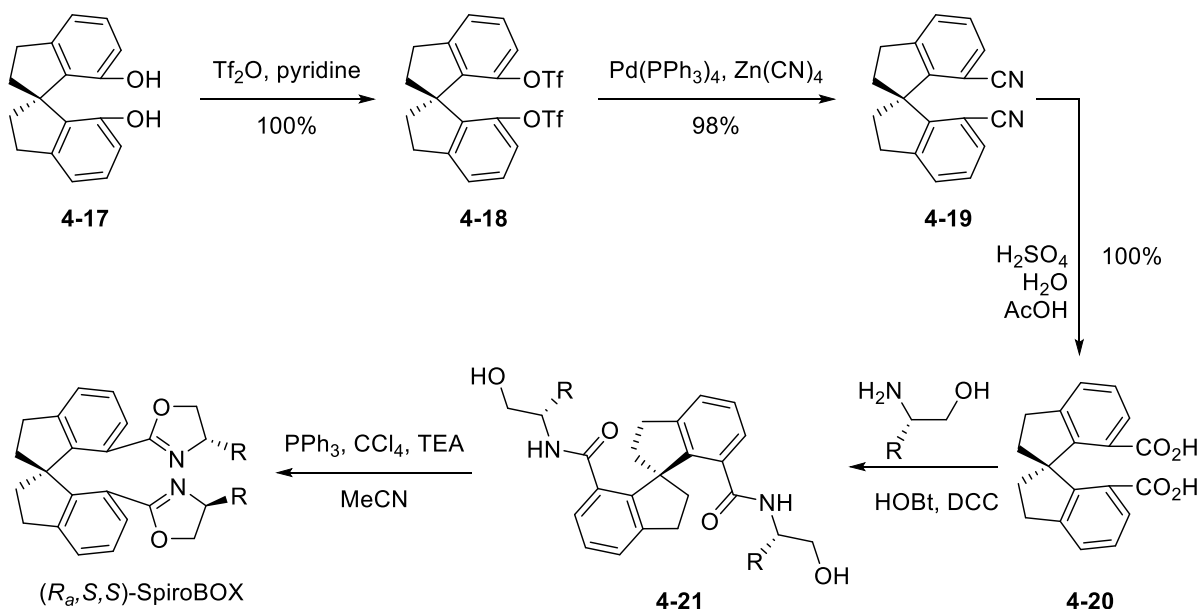


Figure 4.4 Examples of asymmetric catalysis with BINOL-based oxazoline ligands

In addition, the Tietze also explored the potentials of BINOL-based oxazoline ligands in total synthesis various natural products. A key intermediate in the synthesis of blennolide A was achieved through an enantioselective Wacker oxidation with 96 % ee.³¹ Later, in their synthesis of secalonic acid E, 99 % ee of a chiral chroman with a quaternary carbon center was obtained

from the Wacker-type cyclization.³² They recently reported the first enantioselective total synthesis of natural dimeric tetrahydroxanthenone dicerandrol C, of which core was constructed via a Wacker-type cyclization and 99% ee was observed.³³

In 2006 Zhou and coworkers investigated the use of oxazolines in conjunction with SPIROL-based scaffold, and disclosed a new family of chiral SPINOL-based oxazoline-containing ligands termed “SpiroBOX ligands” **4-22**.³⁴ (*cf.* Scheme 4.4) In that report, promising results were observed for both the asymmetric cyclopropanation of styrenes (up to 93% yield and 82% ee), and allylic oxidation of cyclic alkenes (up to 80% yield and 70% ee).

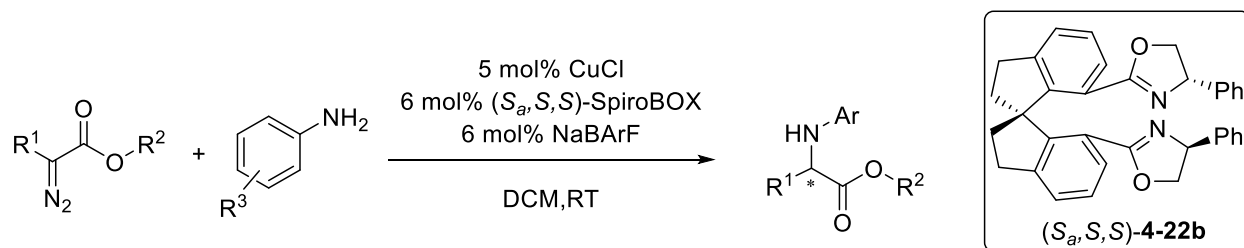


4-22a, R = *i*-Pr: 90% over 2 steps

4-22b, R = Ph : 94% over 2 steps

Scheme 4.4 Preparation of SpiroBOX ligand

These studies by Zhou and coworkers suggested that SpiroBOX catalyst might be useful for the transformations, for which poor performance of the BOX ligands is observed. Soon after, they were pleased to report that 20 chiral α -amino acid derivatives (up to 98% ee) were prepared via Cu-SpiroBOX catalyzed insertion of carbenoids into anilines.³⁵



R¹=Me, R²=Et, Ar=Ph: 94%, 98% ee

R¹=Me, R²=Me, Ar=Ph: 78%, 96% ee

R¹=Ph, R²=Et, Ar=Ph: 85%, 8% ee

Scheme 4.5 Asymmetric carbenoid insertion into N-H with SpiroBOX ligand

In 2007 Zhou group reported a new study with SpiroBOX ligand **4-22a** used for copper(I)-catalyzed carbenoid insertion into the O-H bonds of phenols.³⁶ More than 20 α -diazo esters were tested and the majority of them were obtained with at least 98% ee. The same strategy was employed in the intramolecular insertion to access various chiral 2-carboxy cyclic ethers bearing different ring sizes as well as substituents.³⁷ Impressively, the Zhou and coworkers were also able to demonstrate a successful insertion of Cu-based carbenoids into O-H bond of water.³⁸ With a different copper source, CuSO₄, at elevated reaction temperature (40 °C), more than 20 chiral α -hydroxyesters and acids were prepared in 36-94% ee and the reaction times < 30 min. In addition, iron(II) chloride complexes with SpiroBOX **4-22b** were found to catalyze the analogous reactions of α -diazo esters and alcohols or water with exceptionally high enantioselectivities (76-98% ee) and mild reaction conditions.³⁹

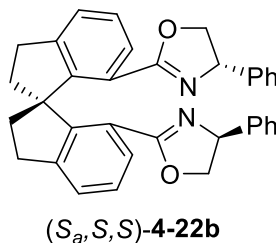
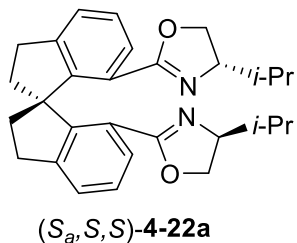
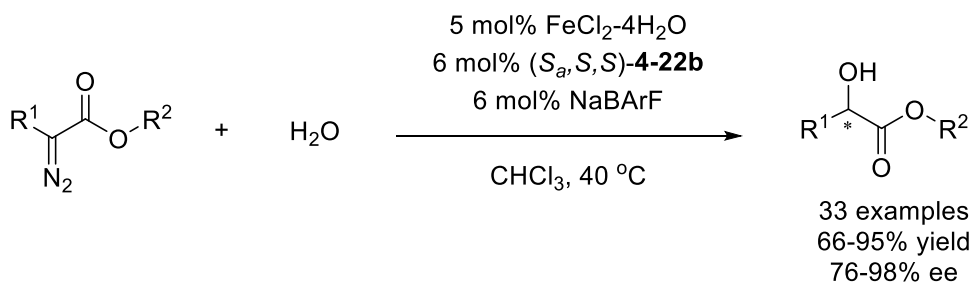
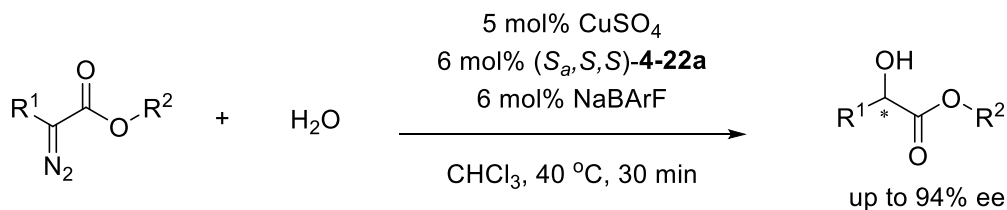
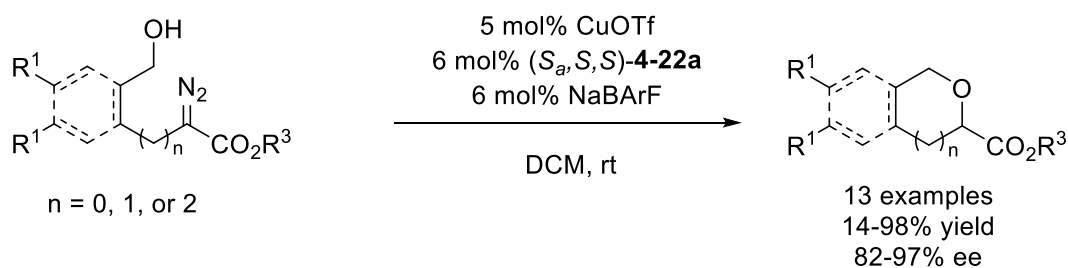
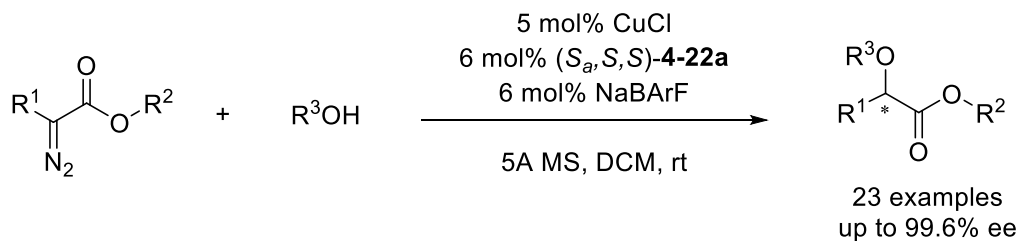
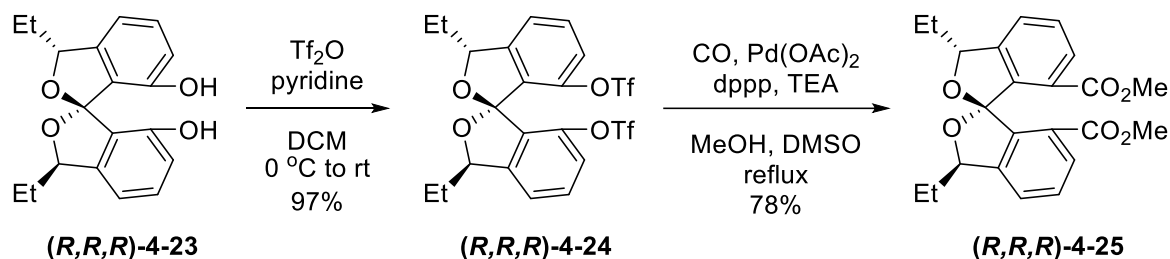


Figure 4.5 Asymmetric insertion of carbenoids into O-H with SpiroBOX ligand

Considering the difficulty and cost associated with gaining access to enantiopure SPINOL ligands and the promising activity of the SPIROL ligands developed in previous

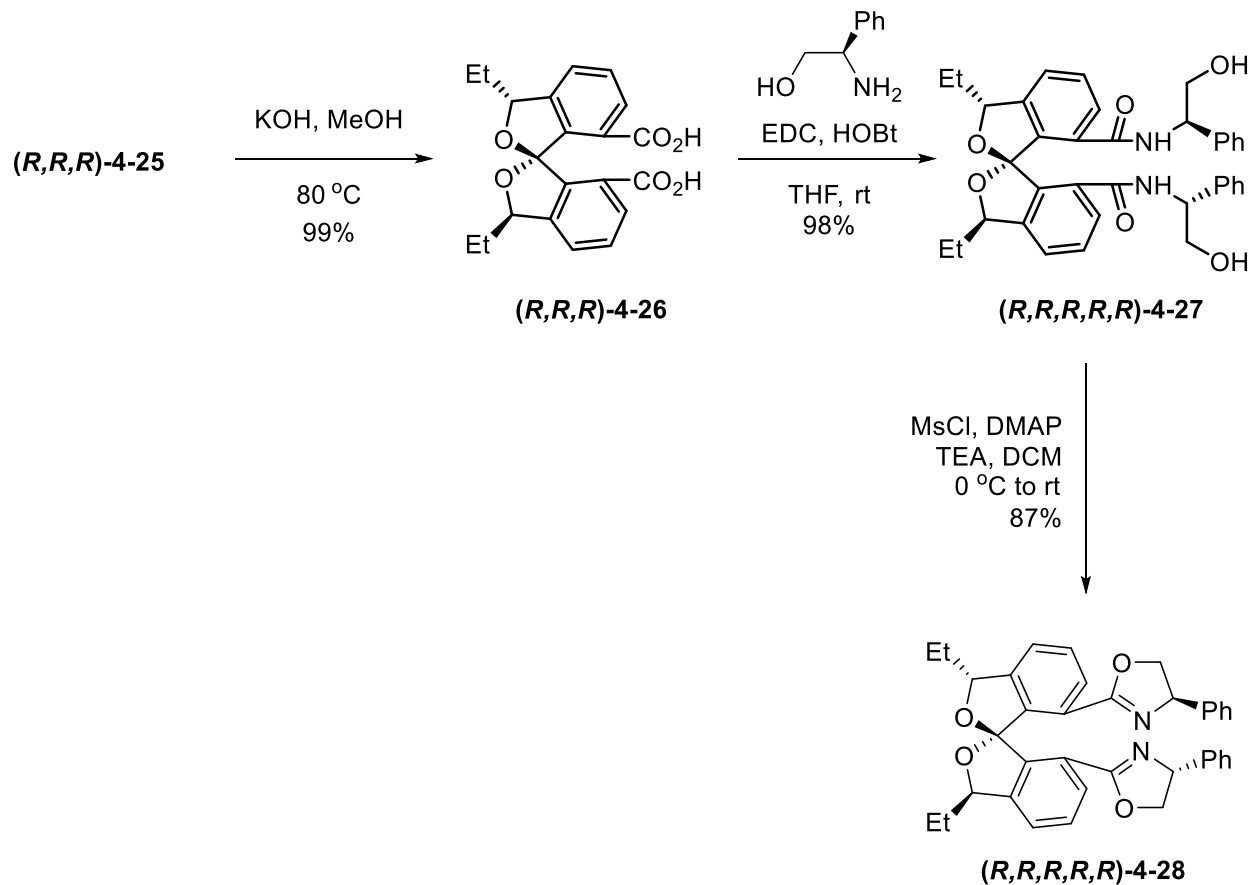
chapters, we have pursued the synthesis and evaluation of the C₂-symmetric SPIROL ligands functionalized with oxazolines. This chapter summarizes the development of SPIROL-based oxazoline ligands (SPIROXs) and their exploration in asymmetric Cu(I)-catalyzed reaction α -diazoesters and phenols.

4.3. Synthesis of C₂-symmetric SPIROL-based bisoxazoline ligands (SPIROX)



Scheme 4.6 Synthesis of compound 4-25

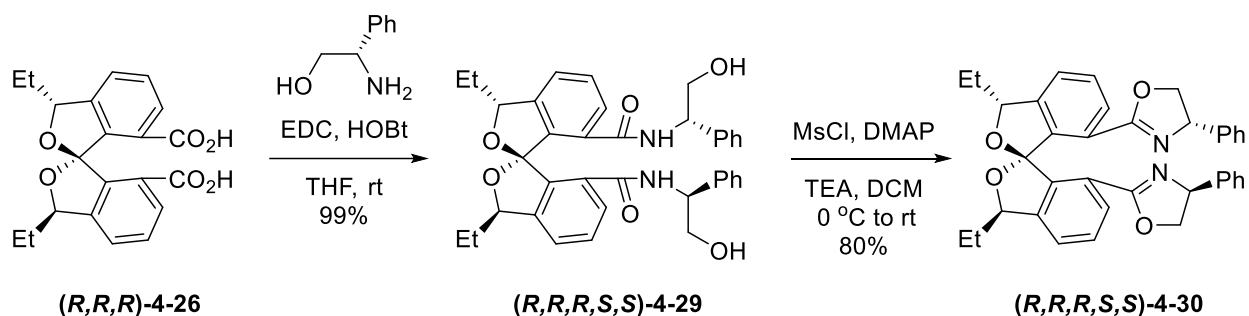
Our studies commenced with the triflation of *endo*-SPIROL (***R,R,R***-4-1), which was obtained in enantiopure form after recrystallization according to our previous report.³³ The *bis*-triflate derivative (***R,R,R***-4-2) was conveniently synthesized in 97% yield by a reaction of (***R,R,R***-4-1) with triflic anhydride and pyridine. The carbonylation of compound (***R,R,R***-4-2) using carbon monoxide (1 atm), methanol and catalytic Pd(OAc)₂ (10 mol%) at reflux provided diester (***R,R,R***-4-3) in 78% yield after the purification with no observable epimerization of the spiroketal stereocenter. We realized that 1,3-bis(diphenylphosphino)propane (dppp) is the crucial ligand for this step, as the yield was dramatically decreased with either 1,1'-bis(diphenylphosphino)ferrocene (dppf) or 1,4-bis(diphenylphosphino)butane (dppb).



Scheme 4.7 Synthesis of SPIROX (R,R,R,R,R)-4-28

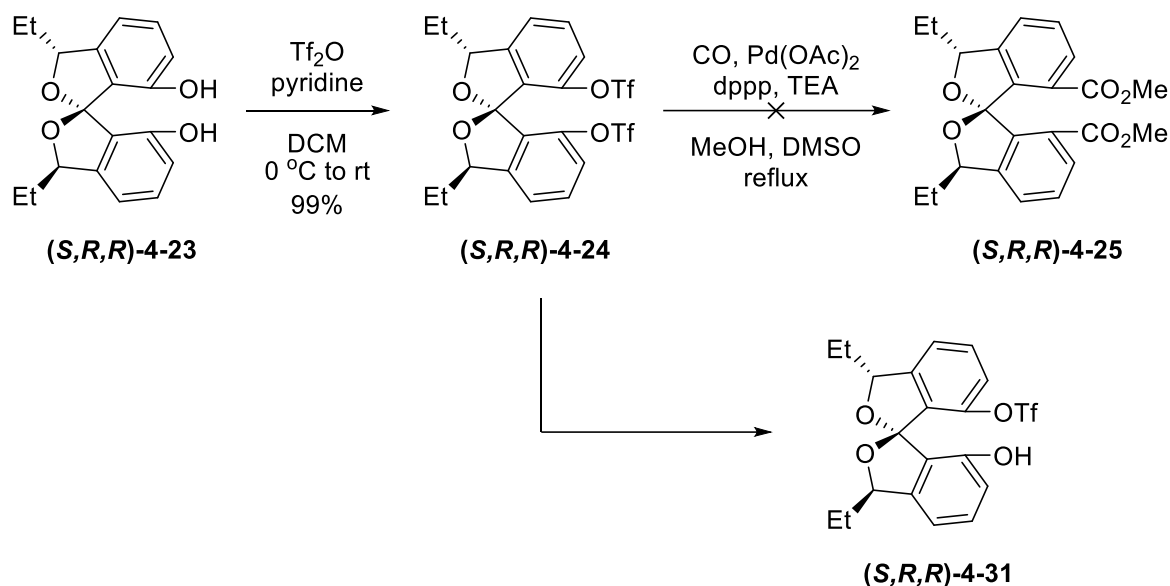
Biscarboxylic acid (R,R,R)-4-26 was subsequently accessed via hydrolysis with KOH refluxing in methanol followed by an acidic work up. Since the resulting carboxylic acid (R,R,R)-4-26 is already axially chiral, condensation with an optically active amino alcohol may produce two distinct diastereomers. Although *N,N'*-dicyclohexylcarbodiimide (DCC) was cheaper than EDC, the dicyclohexylurea byproduct generated from DCC could not be completely removed from the product after the work-up nor even the column chromatography. Therefore, EDC was used as the dehydrating agent, and the urea byproduct was separated from the main product during the purification process. (*R*)- or (*S*)-2-phenylglycinol was used with the presence of hydroxybenzotriazole (HOBT) and 1-ethyl-3-(3-dimethylaminopropyl)carbodiimide (EDC), and either pseudoenantiomeric bisamides (R,R,R,R,R)-4-27 or (R,R,R,S,S)-4-29 was

synthesized, respectively. **(R,R,R,R,R)-4-26** was accessed from (*R*)-2-phenylglycinol, and 98% yield was obtained. The oxazoline ring formation was achieved by treatment with methanesulfonyl chloride (MsCl), 4-dimethylaminopyridine (DMAP) and triethylamine, and the final bisoxazoline ligand SPIROX **(R,R,R,R,R)-4-28** was synthesized with 87% yield.



Scheme 4.8 Synthesis of SPIROX **(R,R,R,S,S)-4-30**

The same strategy was applied for the synthesis of **(R,R,R,S,S)-4-31** that **(R,R,R,S,S)-4-29** was prepared with 99% yield from **(R,R,R)-4-26**, and good conversion provided **(R,R,R,S,S)-4-30** with 80% yield.

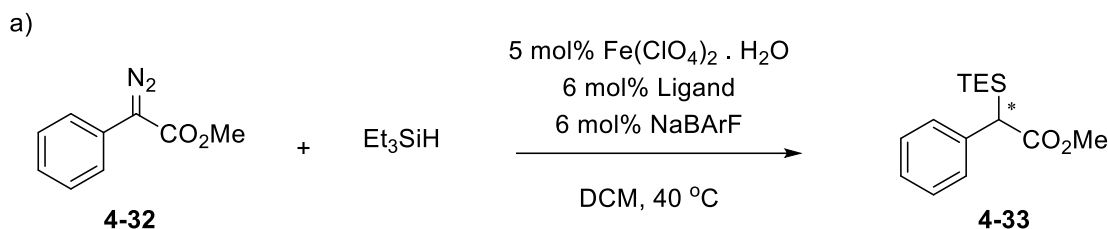


Scheme 4.9 Failed attempts towards (S,R,R) -4-31

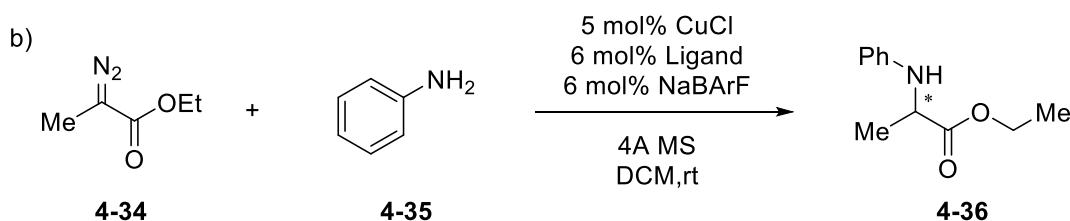
In addition, we also attempted our synthesis with diastereomeric (S,R,R) -4-23. Reaction with triflic anhydride and pyridine successfully provided (S,R,R) -4-24 with 99% yield. However, the following carbonylation with compound (S,R,R) -4-24 was problematic. With 1 atm of carbon monoxide and methanol at reflux, the reaction did not have any conversion, so we decided to perform the reaction on the same scale in an autoclave. To our surprise, even under the pressure of 25 psi of carbon monoxide, and temperature elevated to 70 °C, no reaction was observed and the unreacted (S,R,R) -4-24 was recovered. Later even when we heated the reaction to 90°C, only trace of (S,R,R) -4-25 but with the majority of (S,R,R) -4-31 was isolated. There are still ongoing efforts to optimize carbonylation for (S,R,R) -4-24, and we are very interested in performance with this non-SPINOL-like ligand.

4.4. Application of SPIROX ligands in asymmetric insertion of carbenoids into Si-H, N-H and O-H bonds

Table 4.1 Evaluation of SPIROX ligands for asymmetric insertion into a) Si-H and b) N-H



Entry	Ligand	Conversion ^b	ee ^c
1	(<i>R,R,R,R,R</i>)-4-28	< 1% conv.	-
2	(<i>R,R,R,S,S</i>)-4-30	< 1% conv.	-

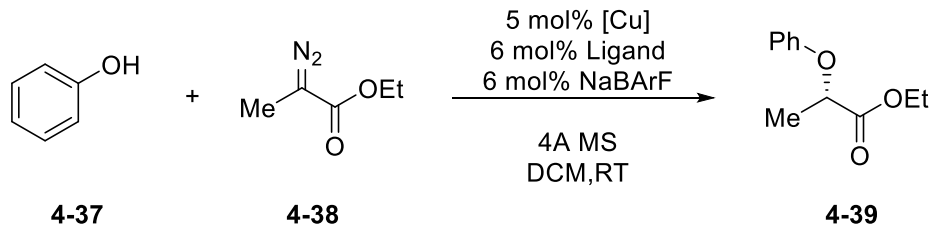


Entry	Ligand	Conversion ^b	ee ^c
1	(<i>R,R,R,R,R</i>)-4-28	99%	50% ee
2	(<i>R,R,R,S,S</i>)-4-30	99%	-20% ee

^aReactions were carried out at r.t with [Cu] (0.01 mmol) or [Fe] (0.01 mmol), ligand (0.012 mmol), NaBARF (0.012 mmol), 4A molecular sieves (300 mg) and DCM (2.0 mL) while stirring under nitrogen for 2 h; then phenol (1.0 mmol) and ethyl α -diazopropionate (0.2 mmol) were added, and the reaction mixture was stirred for another 3 h. ^bDetermined by NMR. ^cDetermined by chiral HPLC using a Chiralcel OD-H column.

To test reactivity and enantioselectivity, we first examined the performances of two SPIROX ligands (*R,R,R,R,R*)-4-28 and (*R,R,R,S,S*)-4-30 for the insertion of ethyl diazoacetate into the N-H bond of aniline³⁵ and Si-H bond of triethylsilane⁴¹ based on previous reports. Unfortunately, there was almost no conversion for the iron-catalyzed insertion into Si-H bonds, and only up to 50% ee was achieved in the reactions of diazoester and aniline (cf. Table 4.1).

Table 4.2 Evaluation of SPIROX ligands for Cu-catalyzed asymmetric O-H insertion^a



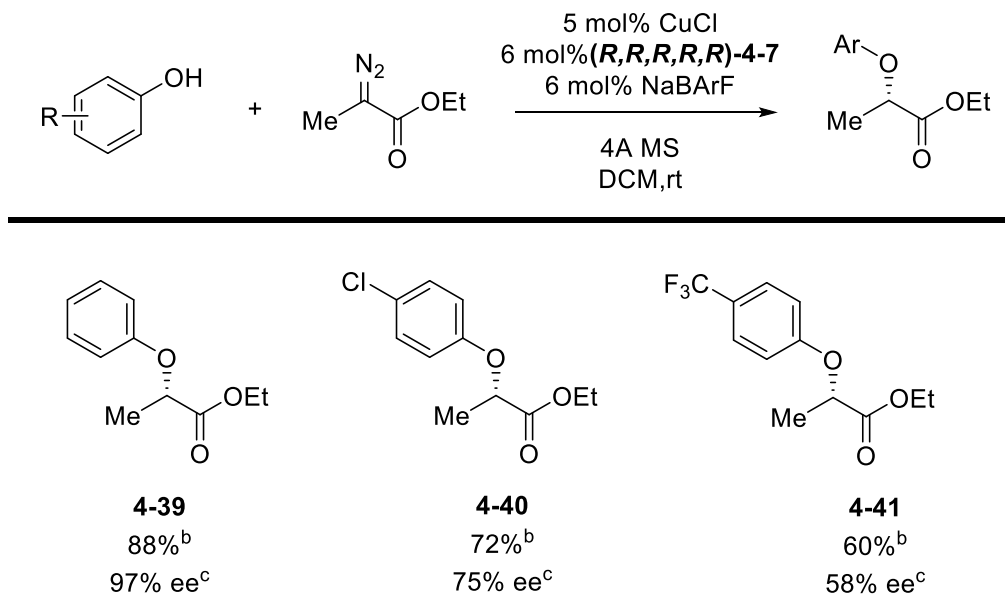
Entry	Ligand	[Cu]	Conversion ^b	ee ^c
1	(<i>R,R,R,R,R</i>)-4-28	CuCl	99%	97% ee
2	(<i>R,R,R,S,S</i>)-4-30	CuCl	99%	-22% ee
3	(<i>R,R,R,R,R</i>)-4-28	Cu(OTf) ₂	99%	95% ee
4	(<i>R,R,R,S,S</i>)-4-30	Cu(OTf) ₂	99%	-62% ee

^aReactions were carried out at rt with [Cu] (0.01 mmol), ligand (0.012 mmol), NaBARF (0.012 mmol), 4A molecular sieves (300 mg) and DCM (2 mL) while stirring under nitrogen for 2 h; then phenol (1.0 mmol) and ethyl α -diazopropionate (0.2 mmol) were added, and the reaction mixture was stirred for another 3 h. ^bDetermined by NMR.

^cDetermined by chiral HPLC using a Chiralcel OD-H column.

Despite the unsatisfied performances of SPIROX ligands in the aforementioned examples, the subsequent study exploring the reaction of diazoester **4-38** with phenol **4-37** using the established by the Zhou group conditions was more successful.³⁶ This reaction was carried out in DCM as the solvent with 5 mol% of copper salt, sodium tetrakis[3,5-bis(trifluoromethyl)phenyl]borate (NaBARF) and 4Å molecular sieves (*cf.* Table 4.2). When copper(I) chloride was used as the copper source, full conversion was observed with both (*R,R,R,R,R*)-4-28 and (*R,R,R,S,S*)-4-30 ligands. While (*R,R,R,R,R*)-4-28 had a comparable enantioselectivity (97% ee) with what was previously observed by Zhou group with the SPINOL-based ligands, the diastereomeric (*R,R,R,S,S*)-4-30 behaved as its pseudoenantiomer and produced the opposite enantiomer of the product in lower selectivity (-22% ee). Copper triflate was also tested with the same reaction condition and (*R,R,R,R,R*)-4-28 had a slightly decreased enantioselectivity (95%). However, to our surprise, (*R,R,R,S,S*)-4-30 has a significant increase with such reaction condition when copper triflate was employed. We then used our

optimized condition to test ligand with other phenols. The results showed that the product **4-39** could be obtained with 88% isolated yield and 97% ee, while lower yields and enantioselectivities were observed for products **4-40** and **4-41**.



^aReactions were carried out at r.t with CuCl (0.01 mmol), ligand (0.012 mmol), NaBARF (0.012 mmol), 4A molecular sieves (300 mg) and DCM (2 mL) while stirring under nitrogen for 2 h; then phenol (1.0 mmol) and ethyl α -diazopropionate (0.2 mmol) were added, and the reaction mixture was stirred for another 3 h. ^bIsolated yield. ^cDetermined by chiral HPLC using a Chiralcel OD-H column.

Figure 4.6 Substrate scope of CuCl-catalyzed asymmetric O-H insertion

4.5. Conclusions

In conclusion, we have successfully developed the new SPIROL-based oxazoline ligands (*R,R,R,R*)-**4-28** and (*R,R,R,S,S*)-**4-30** in 5 steps (59-64% overall yield) from *endo*-SPIROL (*R,R,R*)-**4-23**. These ligands have been evaluated in catalytic enantioselective reactions of diazoesters with aniline, silanes and phenols. While poor reactivities and selectivities were observed for the insertion into Si-H and N-H bonds, the O-H insertion reactions proceeded in good yields and selectivities. Future studies by the Nagorny group will be focused on further

exploration of the potential of (***R,R,R,S,S***)-**4-30** as the ligand for the metal-catalyzed reactions of α -diazoesters and various X-H group containing molecules. In addition, other diastereomeric scaffolds such as (***S,R,R***)-**4-25**, epimeric at the spiroketal stereocenter will also be explored.

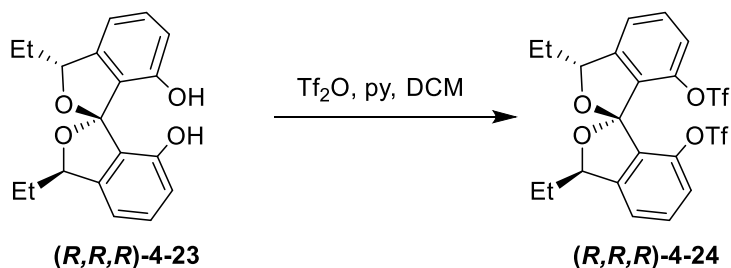
4.6. Experimental information

General Information

Unless otherwise stated, all reagents were purchased from commercial suppliers and used without further purification. All reactions were carried out under an atmosphere of nitrogen in flame-dried glassware with magnetic stirring, unless otherwise noted. Air-sensitive reagents and solutions were transferred via syringe or cannula and were introduced to the apparatus through rubber septa. Reactions were cooled via external cooling baths: ice water (0 °C), dry ice-acetone (-78 °C), or Neslab CB 80 immersion cooler (0 to -60 °C). Heating was achieved using a silicone oil bath with regulated by an electronic contact thermometer. Deionized water was used in the preparation of all aqueous solutions and for all aqueous extractions. Solvents used for extraction and column chromatography were ACS or HPLC grade. Dry tetrahydrofuran (THF), dichloromethane (DCM), toluene (PhMe), and diethyl ether (Et₂O) were prepared by filtration through a column (Innovative Technologies) of activated alumina under nitrogen atmosphere. Reactions were monitored by nuclear magnetic resonance (NMR, see below) or thin layer chromatography (TLC) on silica gel precoated glass plates (0.25 mm, SiliCycle, SiliaPlate). TLC plate visualization was accomplished by irradiation with UV light at 254 nm or by staining with a potassium permanganate (KMnO₄) or cerium ammonium molybdate (CAM) solution. Flash chromatography was performed using SiliCycle SiliaFlash P60 (230-400 mesh) silica gel. Powdered 4 Å molecular sieves were pre-activated by flame-drying under vacuum before use.

Proton (^1H), carbon (^{13}C), and fluorine (^{19}F) NMR spectra were recorded on Varian VNMRS 700 (700 MHz), Varian VNMRS 600 (600 MHz), Bruker Avance Neo 500 (500 MHz), Varian VNMRS 500 (500 MHz), Varian INOVA 500 (500 MHz), or Varian MR400 (400 MHz). ^1H , ^{13}C , and ^{19}F NMR spectra are referenced on a unified scale, where the single reference is the frequency of the residual solvent peak in the ^1H NMR spectrum. Chemical shifts (δ) are reported in parts per million (ppm) relative to tetramethylsilane for ^1H and ^{13}C NMR and trichlorofluoromethane for ^{19}F . Data is reported as (br = broad, s = singlet, d = doublet, t = triplet, q = quartet, m = multiplet; coupling constant(s) in Hz; integration). Slight shape deformation of the peaks in some cases due to weak coupling (e.g., aromatic protons) is not explicitly mentioned. High resolution mass spectra (HRMS) were recorded on the Agilent 6230 TOF HPLC-MS. The enantiomeric excesses were determined by HPLC analysis employing a chiral stationary phase column and conditions specified in the individual experiment. HPLC experiments were performed using a Waters Alliance e2695 Separations Module instrument. Optical rotations were measured at room temperature in a solvent of choice on a JASCO P-2000 digital polarimeter at 589 nm (D-line). Fourier-transform infrared spectroscopy (FT-IR) were performed at room temperature on a Thermo-Nicolet IS-50 equipped with an ATR accessory with a diamond crystal and converted into inverse domain (wavenumbers in cm^{-1}).

Synthesis of SPIROX ligands



**(1*R*,3*R*,3'*R*)-3,3'-diethyl-3*H*,3'*H*-1,1'-spirobi[isobenzofuran]-7,7'-diyl
bis(trifluoromethanesulfonate) ((*R,R,R*)-4-24)**

Enantiopure (*R,R,R*)-4-23 diol⁴⁰ (500.0 mg, 1.60 mmol, 1.0 equiv.) and pyridine (2.85 mL, 37.8 mmol, 23.6 equiv.) were dissolved with DCM (25.0 mL) in a dry round-bottom flask under nitrogen and cooled to 0 °C. Trifluoromethanesulfonic anhydride (2.68 mL, 16.0 mmol, 10.0 equiv.) was added to the solution with a syringe over 30 minutes at 0 °C. Reaction mixture was then warmed to room temperature with stirring. After 2 hours a saturated aqueous solution of NaHCO₃ (25.0 mL) was added. After separating layers, the aqueous phase was extracted with DCM (2 x 15.0 mL). Combined organic was dried over Na₂SO₄ and concentrated in vacuo. The crude product was purified by the column chromatography (SiO₂, 10% EtOAc in hexanes) to afford the product as a slight yellow oil (895 mg, 97%).

¹H NMR (500 MHz, Chloroform-*d*) δ 7.51 (t, *J* = 7.9 Hz, 2H), 7.29 (d, *J* = 7.6 Hz, 2H), 7.23 (d, *J* = 8.2 Hz, 2H), 5.38 (dd, *J* = 7.3, 4.6 Hz, 2H), 2.05 – 1.84 (m, 4H), 1.05 (t, *J* = 7.4 Hz, 6H).

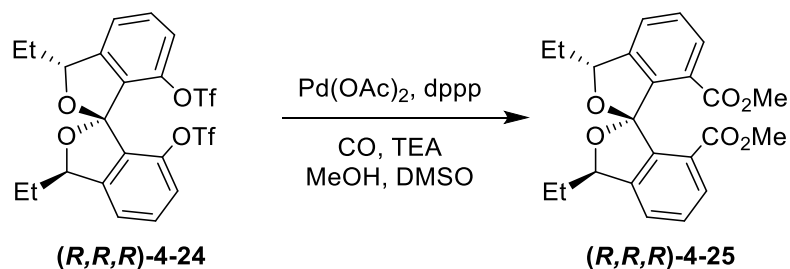
¹³C NMR (126 MHz, Chloroform-*d*) δ 147.3, 144.7, 132.0, 130.3, 121.2, 119.6, 118.8 (q, *J* = 320.1 Hz, CF₃), 114.5, 84.7, 30.0, 9.4.

¹⁹F NMR (471 MHz, Chloroform-*d*) δ -74.59.

ESI-HRMS Calcd. for C₂₁H₁₉F₆O₈S₂⁺ 577.0426 [M+H]⁺, found 577.0418.

IR (film): ν_{max} = 2973, 2880, 1470, 1422, 1207, 1137, 935, 852, 749 cm⁻¹

[α]_D: +3.21 (c = 1.0 in CHCl₃)



Dimethyl (1*R*,3*R*,3'*R*)-3,3'-diethyl-3*H*,3'*H*-1,1'-spirobi[isobenzofuran]-7,7'-dicarboxylate ((*R,R,R*)-4-25)

(*R,R,R*)-4-24 (894.8 mg, 1.55 mmol, 1.0 equiv.), Pd(OAc)₂ (35.9 mg, 0.16 mmol, 0.1 equiv.) and 1,3-bis(diphenylphosphino)propane (66.0 mg, 0.16 mmol, 0.1 equiv.) were added to a dry round-bottom flask in the glovebox and then carried outside. Distilled triethylamine (3.80 mL), methanol (9.40 mL) and DMSO (15.00 mL) were added to the flask at room temperature, and the reaction atmosphere was then carefully purged with CO balloon. Reaction mixture was heated to and maintained at reflux for overnight. After TLC indicated a full consumption of the starting material the reaction mixture was cooled to room temperature and concentrated to approximately half of its volume. The crude product was purified by the column chromatography (SiO₂, 20% EtOAc in hexanes) to afford the product as white solids (479 mg, 78%).

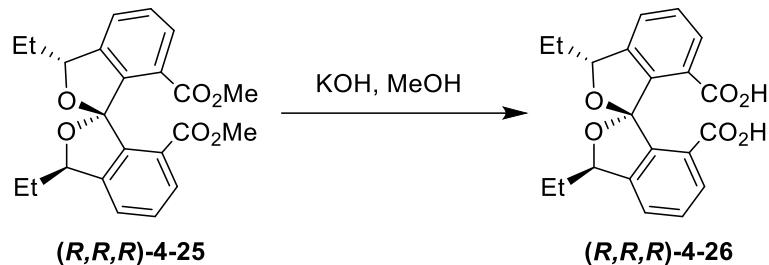
¹H NMR (500 MHz, Chloroform-*d*) δ 7.94 (dd, *J* = 7.1, 1.8 Hz, 2H), 7.51 – 7.43 (m, 4H), 5.22 (dd, *J* = 7.7, 4.1 Hz, 2H), 3.29 (s, 6H), 2.06 – 1.85 (m, 4H), 1.09 (t, *J* = 7.4 Hz, 6H).

¹³C NMR (126 MHz, Chloroform-*d*) δ 165.8, 145.2, 140.2, 130.4, 128.7, 125.6, 125.0, 118.2, 84.2, 51.3, 30.4, 9.9.

ESI-HRMS Calcd. for C₂₃H₂₅O₆⁺ 397.1645 [M+H]⁺, found 397.1640.

IR (powder): ν_{max} = 2965, 2936, 2876, 1717, 1456, 1433, 1297, 1263, 1196, 1144, 1007, 923, 747 cm⁻¹

[α]_D: -88.84 (c = 2.0 in CHCl₃)



(1*R*,3*R*,3'*R*)-3,3'-diethyl-3*H*,3'*H*-1,1'-spirobi[isobenzofuran]-7,7'-dicarboxylic acid ((*R,R,R*)-4-26)

(*R,R,R*)-4-25 (479.1 mg, 1.21 mmol, 1.0 equiv.), 30% KOH aqueous solution (3.00 mL) and MeOH (3.00 mL) were added to a round-bottom flask, and reaction mixture was heated to 80 °C. After TLC indicated a full conversion, the reaction mixture was cooled to room temperature and concentrated to half of its volume. 1M HCl was slowly added to the reaction mixture until the solution pH is around 5-6, and then DCM (15.0 mL) was added to the mixture. After separating layers, the aqueous phase was extracted with DCM (4 x 15.0 mL). Combined organic was dried over Na₂SO₄ and concentrated in vacuo. The crude product was purified by the column chromatography (SiO₂, 5% MeOH in DCM) to afford the product as white solids (445 mg, 99%).

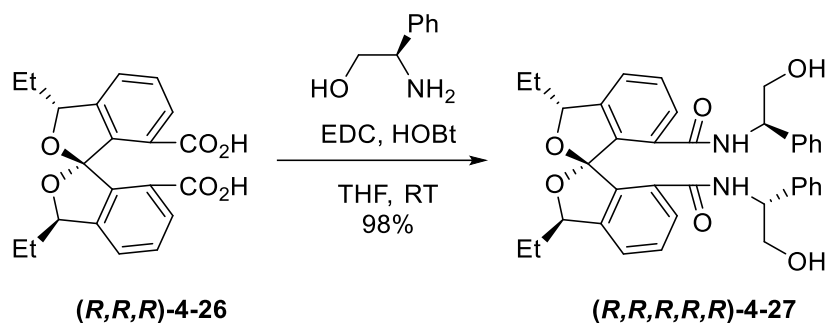
¹H NMR (400 MHz, Methanol-*d*₄) δ 7.85 (dd, *J* = 6.2, 2.6 Hz, 2H), 7.57 – 7.36 (m, 4H), 5.18 (dd, *J* = 7.6, 3.9 Hz, 2H), 1.96 (ddq, *J* = 11.0, 7.6, 3.8 Hz, 2H), 1.83 (dt, *J* = 14.3, 7.3 Hz, 2H), 1.02 (t, *J* = 7.4 Hz, 6H).

¹³C NMR (100 MHz, cd₃od) δ 167.2, 145.4, 140.1, 129.8, 128.4, 126.2, 124.6, 118.5, 84.2, 29.6, 8.8.

ESI-HRMS Calcd. for C₂₁H₂₀O₆Na⁺ 391.1152 [M+Na]⁺, found 391.1158.

IR (powder): ν_{max} = 3021(br), 2964, 2926, 2876, 2654, 1703, 1601, 1459, 1264, 1194, 1011, 928, 758 cm⁻¹

[α]_D: -42.40(c = 0.20 in CHCl₃)



(1*R*,3*R*,3'*R*)-3,3'-diethyl-*N*⁷,*N*^{7'}-bis((*R*)-2-hydroxy-1-phenylethyl)-3*H*,3'*H*-1,1'-spirobi[isobenzofuran]-7,7'-dicarboxamide ((*R,R,R*)-4-27)

(*R,R,R*)-4-26 (130.0 mg, 0.35 mmol, 1.0 equiv.), (*R*)-(-)-2-phenylglycinol (288.1 mg, 2.10 mmol, 6.0 equiv.), 1-hydroxybenzotriazole hydrate (222.2 mg, 1.65 mmol, 4.7 equiv.) and EDCI (332.4 mg, 2.14 mmol, 6.1 equiv.) were added to a round-bottom flask under nitrogen. Dry THF (15.0 mL) was added to the flask and cooled to 0 °C. After 1 hour, the reaction mixture was spontaneously warmed to room temperature and stirred for overnight. After TLC indicated a full conversion, the reaction mixture was concentrated in vacuo. The crude product was purified by the column chromatography (SiO₂, 5% MeOH in DCM) to afford the product as white solids (208 mg, 98%).

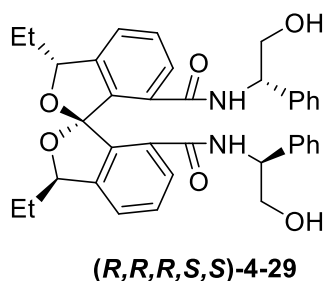
¹H NMR (700 MHz, Chloroform-*d*) δ 7.45 (d, *J* = 7.5 Hz, 2H), 7.40 (t, *J* = 7.5 Hz, 2H), 7.33 (d, *J* = 7.5 Hz, 2H), 7.29 (dd, *J* = 8.1, 6.3 Hz, 4H), 7.06 (dd, *J* = 7.0, 1.9 Hz, 4H), 7.00 (d, *J* = 6.5 Hz, 2H), 4.97 (dd, *J* = 8.1, 4.9 Hz, 2H), 4.65 (td, *J* = 6.8, 3.7 Hz, 2H), 3.49 (dd, *J* = 11.4, 3.8 Hz, 2H), 3.35 (dd, *J* = 11.4, 6.9 Hz, 2H), 1.98 – 1.86 (m, 4H), 1.06 (t, *J* = 7.4 Hz, 6H).

¹³C NMR (176 MHz, Chloroform-*d*) δ 168.2, 145.3, 137.8, 135.2, 131.5, 129.7, 128.7, 128.0, 127.9, 126.9, 123.4, 84.2, 66.3, 56.6, 30.6, 10.4.

ESI-HRMS Calcd. for C₃₇H₃₉N₂O₆⁺ 607.2803 [M+H]⁺, found 607.2790.

IR (powder): ν_{\max} = 3327(br), 3062, 2966, 2934, 2875, 2244, 1643, 1521, 1453, 1340, 1268, 1007, 906, 726 cm^{-1}

[\alpha]_D: +39.98 (c = 0.30 in CHCl_3)



(1*R*,3*R*,3'*R*)-3,3'-diethyl-*N*⁷,*N*^{7'}-bis(*S*)-2-hydroxy-1-phenylethyl)-3*H*,3'*H*-1,1'-spirobi[isobenzofuran]-7,7'-dicarboxamide ((*R,R,R,S,S*)-4-29)

(*R,R,R,S,S*)-4-29 was obtained with (*S*)-(-)-2-phenylglycinol (288.5 mg, 2.10 mmol, 6.0 equiv) as white solids (213 mg, 99%).

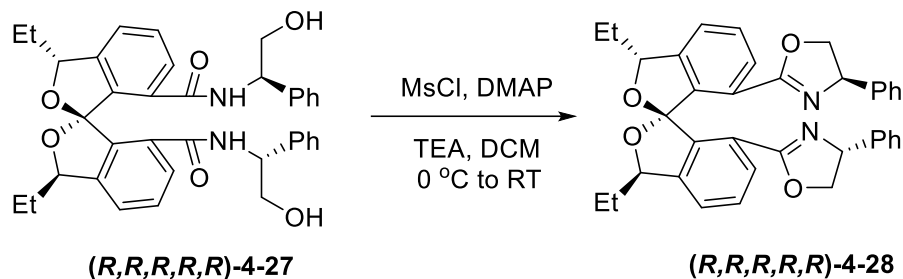
¹H NMR (500 MHz, Chloroform-*d*) δ 7.56 – 7.49 (m, 4H), 7.38 (d, J = 7.6 Hz, 4H), 7.27 – 7.19 (m, 6H), 6.88 (d, J = 6.9 Hz, 2H), 4.53 (td, J = 5.8, 3.4 Hz, 2H), 4.42 (dd, J = 8.4, 4.6 Hz, 2H), 3.93 – 3.86 (m, 2H), 3.71 (dt, J = 11.5, 5.7 Hz, 2H), 3.44 – 3.36 (m, 2H), 1.96 – 1.77 (m, 4H), 1.01 (t, J = 7.4 Hz, 6H).

¹³C NMR (176 MHz, Chloroform-*d*) δ 168.3, 146.0, 138.7, 135.3, 131.2, 129.6, 128.8, 128.0, 127.4, 127.1, 124.0, 84.0, 65.9, 56.7, 30.3, 10.4.

ESI-HRMS Calcd. for $\text{C}_{37}\text{H}_{39}\text{N}_2\text{O}_6^+$ 607.2803 $[\text{M}+\text{H}]^+$, found 607.2797.

IR (powder): ν_{\max} = 3259(br), 3062, 2964, 2925, 2875, 1644, 1598, 1534, 1454, 1359, 1270, 1214, 1053, 1008, 933, 747 cm^{-1}

[\alpha]_D: +86.80 (c = 0.10 in CHCl_3)



(4*R*,4'*R*)-2,2'-((1*R*,3*R*,3'*R*)-3,3'-diethyl-3*H*,3'*H*-1,1'-spirobif[isobenzofuran]-7,7'-diyl)bis(4-phenyl-4,5-dihydrooxazole) ((*R,R,R,R*)-4-28)

A solution of (*R,R,R,R*)-4-27 (208.3 mg, 0.34 mmol, 1.0 equiv.) and DMAP (4.4 mg, 0.034 mmol, 10 mol%) in dry DCM (20.0 mL) was cooled to 0 °C under nitrogen. Distilled triethylamine (0.20 mL) and MsCl (120.0 μ L) were added and the solution was stirred at 0 °C for 30 minutes. Additional triethylamine (1.00 mL) was added, and the reaction mixture was spontaneously warmed to room temperature and stirred for overnight. After TLC indicated a full conversion, the reaction mixture was concentrated in vacuo. The crude product was purified by the column chromatography (SiO₂, 6% EtOAc in DCM) to afford the product as white solids (168 mg, 87%)

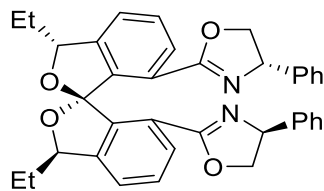
¹H NMR (500 MHz, Chloroform-*d*) δ 7.93 (d, *J* = 7.6 Hz, 2H), 7.33 (t, *J* = 7.6 Hz, 2H), 7.27 – 7.17 (m, 8H), 6.97 – 6.92 (m, 4H), 5.17 (dd, *J* = 7.7, 4.2 Hz, 2H), 5.00 (dd, *J* = 10.2, 7.8 Hz, 2H), 3.92 (dd, *J* = 10.2, 8.3 Hz, 2H), 3.81 (t, *J* = 8.3 Hz, 2H), 1.94 (ddq, *J* = 28.8, 14.1, 7.7, 7.2 Hz, 4H), 1.10 (t, *J* = 7.3 Hz, 6H).

¹³C NMR (126 MHz, Chloroform-*d*) δ 163.3, 145.8, 142.0, 138.7, 129.6, 128.6, 128.5, 127.2, 126.5, 123.4, 123.0, 118.1, 84.2, 74.1, 69.7, 30.2, 10.0.

ESI-HRMS Calcd. for C₃₇H₃₅N₂O₄⁺ 571.2592 [M+H]⁺, found 571.2588

IR (powder): ν_{\max} = 3061, 3028, 2964, 2933, 2875, 2242, 1953, 1647, 1590, 1493, 1477, 1453, 1364, 1315, 1266, 1172, 1130, 1008, 942, 754 cm⁻¹

$[\alpha]_D$: +78.13 ($c = 0.10$ in CHCl_3)



(4*S*,4'*S*)-2,2'-((1*R*,3*R*,3'*R*)-3,3'-diethyl-3*H*,3'*H*-1,1'-spirobi[isobenzofuran]-7,7'-diyl)bis(4-phenyl-4,5-dihydrooxazole) ((*R,R,R,S,S*)-4-30)

(*R,R,R,S,S*)-4-30 was obtained as white solids (155 mg, 80%).

$^1\text{H NMR}$ (500 MHz, Chloroform-*d*) δ 7.90 (d, $J = 7.7$ Hz, 2H), 7.36 – 7.28 (m, 4H), 7.23 – 7.17 (m, 6H), 7.01 – 6.96 (m, 4H), 5.14 (dd, $J = 7.8, 4.3$ Hz, 2H), 4.90 – 4.82 (m, 2H), 4.38 – 4.30 (m, 2H), 3.29 – 3.21 (m, 2H), 2.01 – 1.92 (m, 4H), 1.12 (dd, $J = 8.6, 6.5$ Hz, 6H).

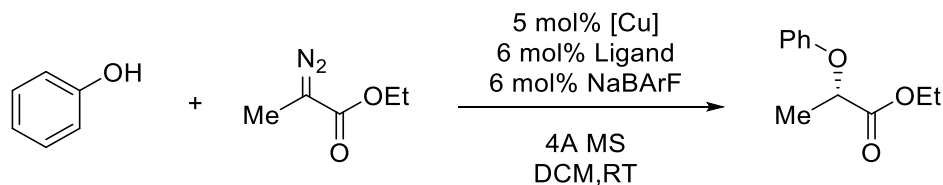
$^{13}\text{C NMR}$ (176 MHz, Chloroform-*d*) δ 163.4, 145.9, 141.7, 138.6, 129.6, 128.6, 128.4, 127.3, 126.8, 123.4, 123.1, 117.7, 84.2, 74.6, 69.9, 30.4, 10.2.

ESI-HRMS Calcd. for $\text{C}_{37}\text{H}_{35}\text{N}_2\text{O}_4^+$ 571.2592 $[\text{M}+\text{H}]^+$, found 571.2604

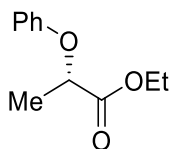
IR (powder): $\nu_{\text{max}} = 3062, 3028, 2962, 2919, 2850, 1980, 1643, 1592, 1493, 1453, 1364, 1266, 1175, 1131, 1010, 946, 757 \text{ cm}^{-1}$

$[\alpha]_D$: -27.05 ($c = 1.00$ in CHCl_3)

Typical procedure for the asymmetric insertion



The CuCl (1.0 mg, 0.01 mmol), (*R,R,R,R*)-4-28 (6.8 mg, 0.012 mmol), NaBARF (11.3 mg, 0.012 mmol) and 300 mg 4Å molecular sieves were introduced into an oven-dried 1-dram vial. DCM (2.0 mL) was added, and the solution was stirred at room temperature under nitrogen for 2 hours. Phenol (94.1 mg, 1.0 mmol) and ethyl α -diazopropionate (26.0 mg, 0.2 mmol) were added to the reaction mixture, and the resulting mixture was stirred at room temperature for 3 hours. After filtrating and removing solvent in vacuum the product was purified by the column chromatography (SiO₂, 6% Et₂OAc in hexanes) to afford the product as a clear oil (34 mg, 88%, 97% ee)



ethyl (*S*)-2-phenoxypropanoate (4-39)

¹H NMR (600 MHz, Chloroform-*d*) δ 7.30 – 7.26 (m, 2H), 6.97 (td, $J = 7.4, 1.1$ Hz, 1H), 6.90 – 6.86 (m, 2H), 4.75 (q, $J = 6.8$ Hz, 1H), 4.22 (q, $J = 7.1$ Hz, 2H), 1.62 (d, $J = 6.8$ Hz, 3H), 1.25 (t, $J = 7.1$ Hz, 3H).

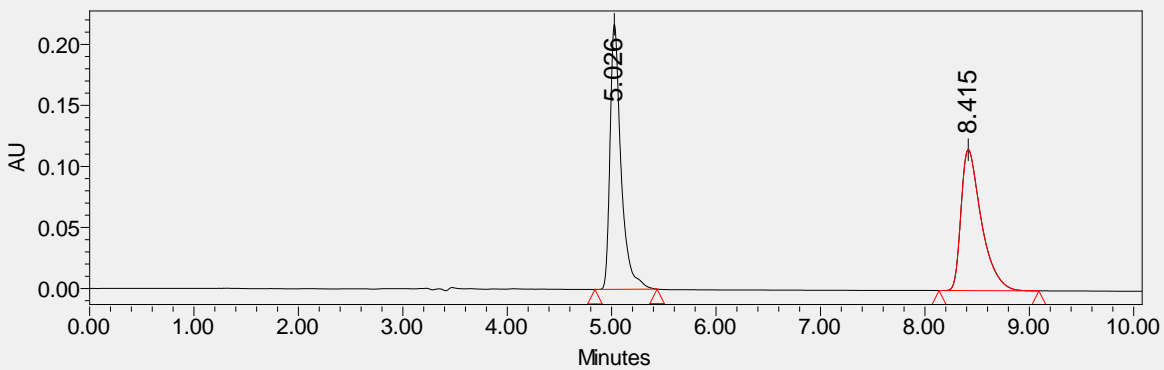
¹³C NMR (176 MHz, Chloroform-*d*) δ 172.2, 157.5, 129.5, 121.5, 115.0, 72.6, 61.2, 18.5, 14.1.

ESI-HRMS Calcd. for C₁₁H₁₅O₃⁺ 195.1016 [M+H]⁺, found 195.1011

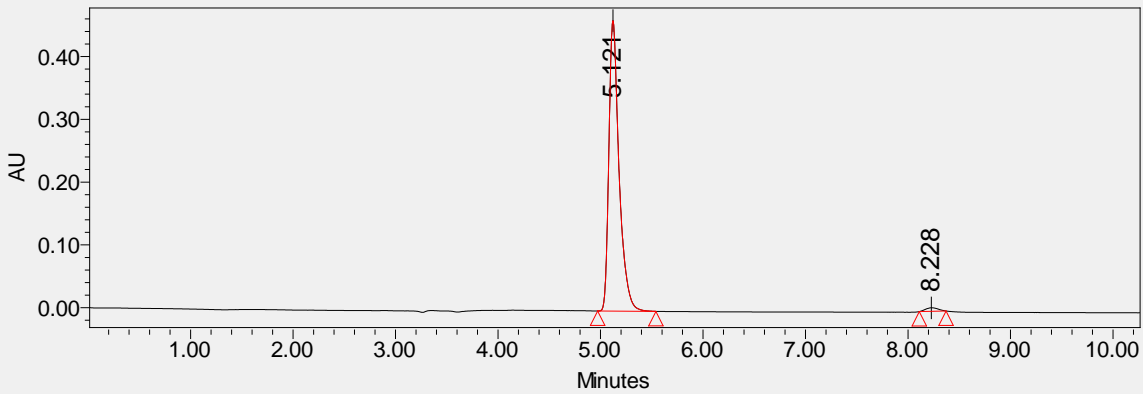
IR (film): $\nu_{\text{max}} = 2986, 2938, 2125, 1751, 1732, 1600, 1588, 1494, 1445, 1375, 1273, 1238, 1191, 1174, 1132, 1096, 1078, 1049, 1017, 945, 884, 750, 624$ cm⁻¹

[α]_D: -23.20 (c = 2.00 in CHCl₃) [Literature⁴²: **[α]_D**: -41.3 (c = 0.8 in CHCl₃) for 90% ee]

ee: 97% ee [HPLC condition: Chiralcel OD-H column, n-Hexane/*i*-PrOH = 90:10, flow rate = 1.0 mL/min, , $t_{\text{R}} = 5.02$ min for (*S*)-enantiomer, $t_{\text{R}} = 8.41$ min for (*R*)-enantiomer]



	Retention Time	Area	% Area	Height	Amount	Peak Type
1	5.026	1435038	50.48	195282		Unknown
2	8.415	1407630	49.52	104333		Unknown



	Retention Time	Area	% Area	Height	Amount	Peak Type
1	5.121	3199041	98.52	462566		Unknown
2	8.228	47974	1.48	5682		Unknown

4.7. References

- (1) Buchner, E.; Feldmann, L. Diazoessigester Und Toluol. *Berichte Dtsch. Chem. Ges.* **1903**, 36 (3), 3509–3517. <https://doi.org/10.1002/cber.190303603139>.
- (2) Carbenes. In *IUPAC Compendium of Chemical Terminology*; Nič, M., Jiráč, J., Košata, B., Jenkins, A., McNaught, A., Eds.; IUPAC: Research Triangle Park, NC, 2009. <https://doi.org/10.1351/goldbook.C00806>.
- (3) Nozaki, H.; Moriuti, S.; Yamabe, M.; Noyori, R. Reactions of Diphenyldiazomethane in the Presence of Bis(Acetylacetonato) Copper (II). Modified Diphenylmethylen Reactions. *Tetrahedron Lett.* **1966**, 7 (1), 59–63. [https://doi.org/10.1016/S0040-4039\(01\)99630-3](https://doi.org/10.1016/S0040-4039(01)99630-3).
- (4) Taber, D. F.; Amedio, J. C.; Sherrill, R. G. Palladium-Mediated Diazo Insertions: Preparation of 3-Alkyl-2-Carbomethoxycyclopetenones. *J. Org. Chem.* **1986**, 51 (17), 3382–3384. <https://doi.org/10.1021/jo00367a030>.
- (5) Simmons, H. E.; Smith, R. D. A NEW SYNTHESIS OF CYCLOPROPANES FROM OLEFINS. *J. Am. Chem. Soc.* **1958**, 80 (19), 5323–5324. <https://doi.org/10.1021/ja01552a080>.
- (6) Simmons, H. E.; Smith, R. D. A New Synthesis of Cyclopropanes1. *J. Am. Chem. Soc.* **1959**, 81 (16), 4256–4264. <https://doi.org/10.1021/ja01525a036>.
- (7) Paulissen, R.; Reimlinger, H.; Hayez, E.; Hubert, A. J.; Teyssié, Ph. Transition Metal Catalysed Reactions of Diazocompounds - II Insertion in the Hydroxylic Bond. *Tetrahedron Lett.* **1973**, 14 (24), 2233–2236. [https://doi.org/10.1016/S0040-4039\(01\)87603-6](https://doi.org/10.1016/S0040-4039(01)87603-6).
- (8) Yates, P. The Copper-Catalyzed Decomposition of Diazoketones1. *J. Am. Chem. Soc.* **1952**, 74 (21), 5376–5381. <https://doi.org/10.1021/ja01141a047>.
- (9) Anciaux, A. J.; Demonceau, A.; Noels, A. F.; Warin, R.; Hubert, A. J.; Teyssié, P. Transition Metal Catalyzed Reactions of Diazoesters: Cyclopropanation of Dienes and Trienes. *Tetrahedron* **1983**, 39 (13), 2169–2173. [https://doi.org/10.1016/S0040-4020\(01\)91934-9](https://doi.org/10.1016/S0040-4020(01)91934-9).

- (10) Doyle, M. P.; McKervey, M. A.; 1938-; Ye, T.; 1963-. *Modern Catalytic Methods for Organic Synthesis with Diazo Compounds*; Wiley, 1998.
- (11) Ford, A.; Miel, H.; Ring, A.; Slattery, C. N.; Maguire, A. R.; McKervey, M. A. Modern Organic Synthesis with α -Diazocarbonyl Compounds. *Chem. Rev.* **2015**, *115* (18), 9981–10080. <https://doi.org/10.1021/acs.chemrev.5b00121>.
- (12) Bettoni, G.; Loiodice, F.; Tortorella, V.; Conte-Camerino, D.; Mambrini, M.; Ferrannini, E.; Bryant, S. H. Stereospecificity of the Chloride Ion Channel: The Action of Chiral Clofibrin Acid Analogs. *J. Med. Chem.* **1987**, *30* (8), 1267–1270. <https://doi.org/10.1021/jm00391a002>.
- (13) Chimichi, S.; Boccalini, M.; Cravotto, G.; Rosati, O. A New Convenient Route to Enantiopure 2-Coumarinyloxypropanals: Application to the Synthesis of Optically Active Geiparvarin Analogues. *Tetrahedron Lett.* **2006**, *47* (14), 2405–2408. <https://doi.org/10.1016/j.tetlet.2006.01.151>.
- (14) Maier, T. C.; Fu, G. C. Catalytic Enantioselective O–H Insertion Reactions. *J. Am. Chem. Soc.* **2006**, *128* (14), 4594–4595. <https://doi.org/10.1021/ja0607739>.
- (15) Lowenthal, R. E.; Abiko, A.; Masamune, S. Asymmetric Catalytic Cyclopropanation of Olefins: Bis-Oxazoline Copper Complexes. *Tetrahedron Lett.* **1990**, *31* (42), 6005–6008. [https://doi.org/10.1016/S0040-4039\(00\)98014-6](https://doi.org/10.1016/S0040-4039(00)98014-6).
- (16) Müller, D.; Umbricht, G.; Weber, B.; Pfaltz, A. C₂-Symmetric 4,4',5,5'-Tetrahydrobi(Oxazoles) and 4,4',5,5'-Tetrahydro-2,2'-Methylenebis[Oxazoles] as Chiral Ligands for Enantioselective Catalysis Preliminary Communication. *Helv. Chim. Acta* **1991**, *74* (1), 232–240. <https://doi.org/10.1002/hlca.19910740123>.
- (17) Evans, D. A.; Woerpel, K. A.; Hinman, M. M.; Faul, M. M. Bis(Oxazolines) as Chiral Ligands in Metal-Catalyzed Asymmetric Reactions. Catalytic, Asymmetric Cyclopropanation of Olefins. *J. Am. Chem. Soc.* **1991**, *113* (2), 726–728. <https://doi.org/10.1021/ja00002a080>.
- (18) Corey, E. J.; Imai, N.; Zhang, H. Y. Designed Catalyst for Enantioselective Diels-Alder Addition from a C₂-Symmetric Chiral Bis(Oxazoline)-Iron(III) Complex. *J. Am. Chem. Soc.* **1991**, *113* (2), 728–729. <https://doi.org/10.1021/ja00002a081>.
- (19) Evans, D. A.; Peterson, G. S.; Johnson, J. S.; Barnes, D. M.; Campos, K. R.; Woerpel, K. A. An Improved Procedure for the Preparation of 2,2-Bis[2-[4(S)- Tert-Butyl-1,3-

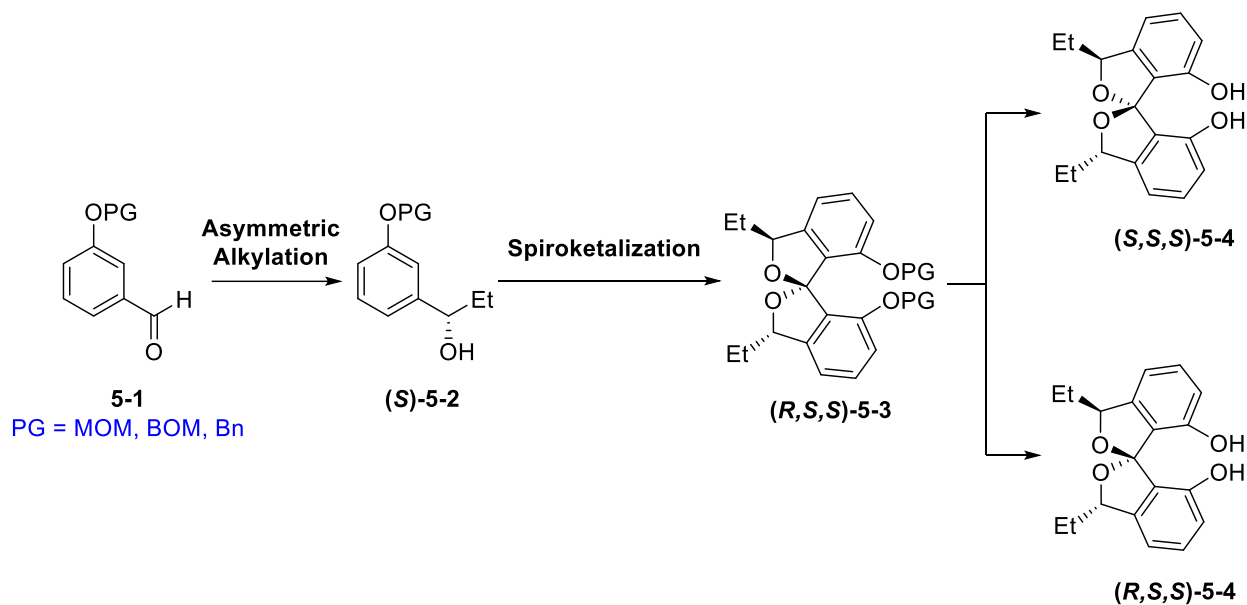
- Oxazolinyll]Propane [(S,S)-Tert-Butylbis(Oxazoline)] and Derived Copper(II) Complexes. *J. Org. Chem.* **1998**, *63* (13), 4541–4544. <https://doi.org/10.1021/jo980296f>.
- (20) Evans, D. A.; Burgey, C. S.; Kozlowski, M. C.; Tregay, S. W. C₂-Symmetric Copper(II) Complexes as Chiral Lewis Acids. Scope and Mechanism of the Catalytic Enantioselective Aldol Additions of Enolsilanes to Pyruvate Esters. *J. Am. Chem. Soc.* **1999**, *121* (4), 686–699. <https://doi.org/10.1021/ja982983u>.
- (21) Evans, D. A.; Burgey, C. S.; Paras, N. A.; Vojkovsky, T.; Tregay, S. W. C₂-Symmetric Copper(II) Complexes as Chiral Lewis Acids. Enantioselective Catalysis of the Glyoxylate–Ene Reaction. *J. Am. Chem. Soc.* **1998**, *120* (23), 5824–5825. <https://doi.org/10.1021/ja980549m>.
- (22) Marigo, M.; Kjærsgaard, A.; Juhl, K.; Gathergood, N.; Jørgensen, K. A. Direct Catalytic Asymmetric Mannich Reactions of Malonates and β -Keto Esters. *Chem. – Eur. J.* **2003**, *9* (10), 2359–2367. <https://doi.org/10.1002/chem.200204679>.
- (23) Evans, D. A.; Willis, M. C.; Johnston, J. N. Catalytic Enantioselective Michael Additions to Unsaturated Ester Derivatives Using Chiral Copper(II) Lewis Acid Complexes. *Org. Lett.* **1999**, *1* (6), 865–868. <https://doi.org/10.1021/ol9901570>.
- (24) Cichowicz, N. R.; Kaplan, W.; Khomutnyk, Y.; Bhattarai, B.; Sun, Z.; Nagorny, P. Concise Enantioselective Synthesis of Oxygenated Steroids via Sequential Copper(II)-Catalyzed Michael Addition/Intramolecular Aldol Cyclization Reactions. *J. Am. Chem. Soc.* **2015**, *137* (45), 14341–14348. <https://doi.org/10.1021/jacs.5b08528>.
- (25) Bhattarai, B.; Nagorny, P. Enantioselective Total Synthesis of Cannogenol-3-O- α -l-Rhamnoside via Sequential Cu(II)-Catalyzed Michael Addition/Intramolecular Aldol Cyclization Reactions. *Org. Lett.* **2018**, *20* (1), 154–157. <https://doi.org/10.1021/acs.orglett.7b03513>.
- (26) Lee, J.; Wang, S.; Callahan, M.; Nagorny, P. Copper(II)-Catalyzed Tandem Decarboxylative Michael/Aldol Reactions Leading to the Formation of Functionalized Cyclohexenones. *Org. Lett.* **2018**, *20* (7), 2067–2070. <https://doi.org/10.1021/acs.orglett.8b00607>.
- (27) Nelson, T. D.; Meyers, A. I. The Asymmetric Ullmann Reaction. 2. The Synthesis of Enantiomerically Pure C₂-Symmetric Binaphthyls. *J. Org. Chem.* **1994**, *59* (9), 2655–2658. <https://doi.org/10.1021/jo00088a066>.

- (28) Homochiral 2,2'-Bis(Oxazolyl)-1,1'-Binaphthyls as Ligands for Copper(I)-Catalyzed Asymmetric Cyclopropanation. *Tetrahedron Asymmetry* **1996**, *7* (6), 1603–1606. [https://doi.org/10.1016/0957-4166\(96\)00193-0](https://doi.org/10.1016/0957-4166(96)00193-0).
- (29) Uozumi, Y.; Kato, K.; Hayashi, T. Catalytic Asymmetric Wacker-Type Cyclization. *J. Am. Chem. Soc.* **1997**, *119* (21), 5063–5064. <https://doi.org/10.1021/ja9701366>.
- (30) Uozumi, Y.; Kyota, H.; Kato, K.; Ogasawara, M.; Hayashi, T. Design and Preparation of 3,3'-Disubstituted 2,2'-Bis(Oxazolyl)-1,1'-Binaphthyls (Boxax): New Chiral Bis(Oxazoline) Ligands for Catalytic Asymmetric Wacker-Type Cyclization. *J. Org. Chem.* **1999**, *64* (5), 1620–1625. <https://doi.org/10.1021/jo982104m>.
- (31) Tietze, L. F.; Ma, L.; Reiner, J. R.; Jackenkroll, S.; Heidemann, S. Enantioselective Total Synthesis of (–)-Blennolide A. *Chem. – Eur. J.* **2013**, *19* (26), 8610–8614. <https://doi.org/10.1002/chem.201300479>.
- (32) Ganapathy, D.; Reiner, J. R.; Löffler, L. E.; Ma, L.; Gnanaprakasam, B.; Niepötter, B.; Koehne, I.; Tietze, L. F. Enantioselective Total Synthesis of Secalonic Acid E. *Chem. – Eur. J.* **2015**, *21* (47), 16807–16810. <https://doi.org/10.1002/chem.201503593>.
- (33) Ganapathy, D.; Reiner, J. R.; Valdomir, G.; Senthilkumar, S.; Tietze, L. F. Enantioselective Total Synthesis and Structure Confirmation of the Natural Dimeric Tetrahydroxanthone Dicerandrol C. *Chem. – Eur. J.* **2017**, *23* (10), 2299–2302. <https://doi.org/10.1002/chem.201700020>.
- (34) Liu, B.; Zhu, S.-F.; Wang, L.-X.; Zhou, Q.-L. Preparation and Application of Bisoxazoline Ligands with a Chiral Spirobiindane Skeleton for Asymmetric Cyclopropanation and Allylic Oxidation. *Tetrahedron Asymmetry* **2006**, *17* (4), 634–641. <https://doi.org/10.1016/j.tetasy.2006.02.010>.
- (35) Liu, B.; Zhu, S.-F.; Zhang, W.; Chen, C.; Zhou, Q.-L. Highly Enantioselective Insertion of Carbenoids into N–H Bonds Catalyzed by Copper Complexes of Chiral Spiro Bisoxazolines. *J. Am. Chem. Soc.* **2007**, *129* (18), 5834–5835. <https://doi.org/10.1021/ja0711765>.
- (36) Chen, C.; Zhu, S.-F.; Liu, B.; Wang, L.-X.; Zhou, Q.-L. Highly Enantioselective Insertion of Carbenoids into O–H Bonds of Phenols: An Efficient Approach to Chiral α -Aryloxycarboxylic Esters. *J. Am. Chem. Soc.* **2007**, *129* (42), 12616–12617. <https://doi.org/10.1021/ja074729k>.

- (37) Zhu, S.-F.; Song, X.-G.; Li, Y.; Cai, Y.; Zhou, Q.-L. Enantioselective Copper-Catalyzed Intramolecular O–H Insertion: An Efficient Approach to Chiral 2-Carboxy Cyclic Ethers. *J. Am. Chem. Soc.* **2010**, *132* (46), 16374–16376. <https://doi.org/10.1021/ja1078464>.
- (38) Zhu, S.-F.; Chen, C.; Cai, Y.; Zhou, Q.-L. Catalytic Asymmetric Reaction with Water: Enantioselective Synthesis of α -Hydroxyesters by a Copper–Carbenoid O H Insertion Reaction. *Angew. Chem. Int. Ed.* **2008**, *47* (5), 932–934. <https://doi.org/10.1002/anie.200704651>.
- (39) Zhu, S.-F.; Cai, Y.; Mao, H.-X.; Xie, J.-H.; Zhou, Q.-L. Enantioselective Iron-Catalysed O–H Bond Insertions. *Nat. Chem.* **2010**, *2* (7), 546–551. <https://doi.org/10.1038/nchem.651>.
- (40) Sun, S.; Nagorny, P. Exploration of Chiral Diastereomeric Spiroketal (SPIROL)-Based Phosphinite Ligands in Asymmetric Hydrogenation of Heterocycles. *Chem. Commun.* **2020**, *56* (60), 8432–8435. <https://doi.org/10.1039/D0CC03088K>.
- (41) Gu, H.; Han, Z.; Xie, H.; Lin, X. Iron-Catalyzed Enantioselective Si–H Bond Insertions. *Org. Lett.* **2018**, *20* (20), 6544–6549. <https://doi.org/10.1021/acs.orglett.8b02868>.
- (42) Le Maux, P.; Carrié, D.; Jéhan, P.; Simonneaux, G. Asymmetric O–H Insertion Reaction of Carbenoids Catalyzed by Chiral Bicyclo Bisoxazoline Copper(I) and (II) Complexes. *Tetrahedron* **2016**, *72* (31), 4671–4675. <https://doi.org/10.1016/j.tet.2016.06.044>.

Chapter 5

Closing Remarks



Scheme 5.1 SPIROL synthesis

In summary, this dissertation describes the development and exploration of two new types of spirocyclic ligands, the axial chirality of which was dependent on the configuration of the spiroketal stereocenter. These scaffolds could be easily accessed from commercially available starting material **5-1** in just 2 steps. Spiroketalization with **5-2** constructed the ligand core **5-3** with excellent yield and perfect diastereoselectivity, where various protecting groups were also tolerated and utilized for late-stage functionalizations. Two distinct diastereotopic SPIROLs **5-4** could be derived from **5-3** separately without chiral resolution, and readily available for the synthesis of different ligands.

The efforts summarized in this dissertation resulted in the development of various mono- and bidentate ligands. The subsequent exploration of these ligands highlighted the structural differences between the diastereomeric (*S,S,S*)- and (*R,S,S*)-SPIROL scaffolds. While the (*S,S,S*)-series of ligands was found to be structurally similar to SPINOL-based ligands, structurally different (*R,S,S*)-SPIROLs exhibited different reactivity and selectivity profiles. Importantly, both SPIROL pseudoenantiomers could be prepared from the same readily accessible intermediate **5-3**, which enabled the described studies and commercialization of (*S,S,S*)- and (*R,R,R*)-SPIRAP ligands through Sigma Aldrich.

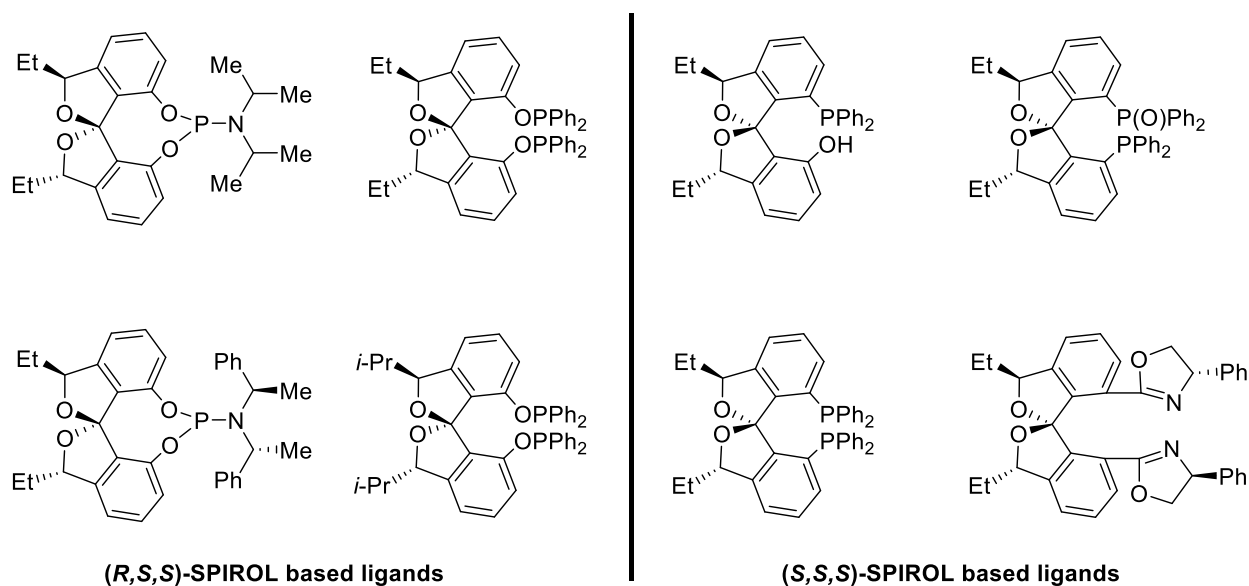


Figure 5.1 Selected examples of available ligands

With the utility demonstrated in this dissertation of both diastereomeric series of ligands, some of the future efforts will be focused on utilizing these scaffolds for the development of new asymmetric reactions. Considering the challenges associated with the access to SPINOL-based phosphoramidite ligands, we are interested in generating their (*R,S,S*)-SPIROL and (*S,S,S*)-SPIROL equivalents for the subsequent exploration in the synthesis of natural products. The promising profiles observed for the *i*-Pr-substituted SPIRAPO ligands warranty the future

exploration of the modified SPIROL scaffolds containing substituents other than *i*-Pr or Et groups. This would help to evaluate the steric and electronic effects of these substituents on the overall performance of the ligand/metal complexes and may result in new strategies to fine-tune the reactivity of SPIROLs. (*R,S,S*)-SPIROL is significantly different from (*S,S,S*)-SPIROL and SPINOL structurally. Hence, further exploration of this new subtype of spirocyclic ligands may lead to identifying unique catalytic profiles. Finally, the additional introduction of other chiral groups into (*R,S,S*)-SPIROL backbone represents an exciting new direction to pursue.

Appendix A

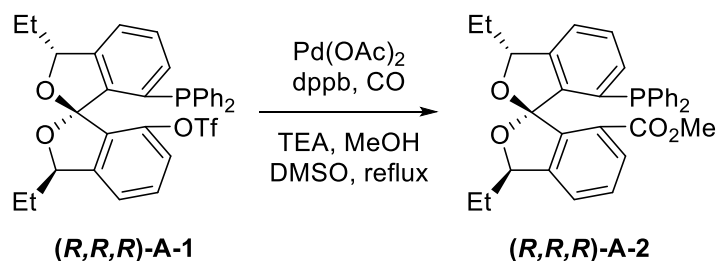
Experimental information for other important SPIROL-based ligands

General Information

Unless otherwise stated, all reagents were purchased from commercial suppliers and used without further purification. All reactions were carried out under an atmosphere of nitrogen in flame-dried glassware with magnetic stirring, unless otherwise noted. Air-sensitive reagents and solutions were transferred via syringe or cannula and were introduced to the apparatus through rubber septa. Reactions were cooled via external cooling baths: ice water (0 °C), dry ice-acetone (-78 °C), or Neslab CB 80 immersion cooler (0 to -60 °C). Heating was achieved using a silicone oil bath with regulated by an electronic contact thermometer. Deionized water was used in the preparation of all aqueous solutions and for all aqueous extractions. Solvents used for extraction and column chromatography were ACS or HPLC grade. Dry tetrahydrofuran (THF), dichloromethane (DCM), toluene (PhMe), and diethyl ether (Et₂O) were prepared by filtration through a column (Innovative Technologies) of activated alumina under nitrogen atmosphere. Reactions were monitored by nuclear magnetic resonance (NMR, see below) or thin layer chromatography (TLC) on silica gel precoated glass plates (0.25 mm, SiliCycle, SiliaPlate). TLC plate visualization was accomplished by irradiation with UV light at 254 nm or by staining with a potassium permanganate (KMnO₄) or cerium ammonium molybdate (CAM) solution. Flash chromatography was performed using SiliCycle SiliaFlash P60 (230-400 mesh) silica gel. Powdered 4 Å molecular sieves were pre-activated by flame-drying under vacuum before use.

Proton (^1H), carbon (^{13}C), and fluorine (^{19}F) NMR spectra were recorded on Varian VNMRS 700 (700 MHz), Varian VNMRS 600 (600 MHz), Bruker Avance Neo 500 (500 MHz), Varian VNMRS 500 (500 MHz), Varian INOVA 500 (500 MHz), or Varian MR400 (400 MHz). ^1H , ^{13}C , and ^{19}F NMR spectra are referenced on a unified scale, where the single reference is the frequency of the residual solvent peak in the ^1H NMR spectrum. Chemical shifts (δ) are reported in parts per million (ppm) relative to tetramethylsilane for ^1H and ^{13}C NMR and trichlorofluoromethane for ^{19}F . Data is reported as (br = broad, s = singlet, d = doublet, t = triplet, q = quartet, m = multiplet; coupling constant(s) in Hz; integration). Slight shape deformation of the peaks in some cases due to weak coupling (e.g., aromatic protons) is not explicitly mentioned. High resolution mass spectra (HRMS) were recorded on the Agilent 6230 TOF HPLC-MS. The enantiomeric excesses were determined by HPLC analysis employing a chiral stationary phase column and conditions specified in the individual experiment. HPLC experiments were performed using a Waters Alliance e2695 Separations Module instrument. Optical rotations were measured at room temperature in a solvent of choice on a JASCO P-2000 digital polarimeter at 589 nm (D-line). Fourier-transform infrared spectroscopy (FT-IR) were performed at room temperature on a Thermo-Nicolet IS-50 equipped with an ATR accessory with a diamond crystal and converted into inverse domain (wavenumbers in cm^{-1}).

Synthesis of phosphine/oxazoline ligand



(R,R,R)-A-1 (1.55 mmol, 1.0 equiv.), Pd(OAc)_2 (35.9 mg, 0.16 mmol, 0.1 equiv.) and 1,3-bis(diphenylphosphino)propane (66.0 mg, 0.16 mmol, 0.1 equiv.) were added to a dry round-

bottom flask in the glovebox and then carried outside. Distilled triethylamine (3.80 mL), methanol (9.40 mL) and DMSO (15.00 mL) were added to the flask at room temperature, and the reaction atmosphere was then carefully purged with CO balloon. Reaction mixture was heated to and maintained at reflux for overnight. After TLC indicated a full consumption of the starting material the reaction mixture was cooled to room temperature and concentrated to approximately half of its volume. The crude product was purified by the column chromatography (SiO₂, 20% EtOAc in hexanes) to afford the product as white solids.

¹H NMR (700 MHz, Chloroform-*d*) δ 7.49 (dt, $J = 7.6, 0.9$ Hz, 1H), 7.37 (dt, $J = 7.5, 1.1$ Hz, 1H), 7.31 (t, $J = 7.6$ Hz, 1H), 7.29 – 7.26 (m, 2H), 7.25 – 7.22 (m, 3H), 7.22 – 7.18 (m, 1H), 7.07 (tdd, $J = 7.3, 3.5, 1.9$ Hz, 4H), 6.88 (ddd, $J = 6.9, 4.7, 2.7$ Hz, 1H), 6.74 (td, $J = 7.9, 1.4$ Hz, 2H), 5.44 – 5.39 (m, 1H), 5.22 (dd, $J = 7.7, 4.1$ Hz, 1H), 3.29 (s, 3H), 2.04 – 1.96 (m, 2H), 1.89 (ddp, $J = 28.4, 14.2, 7.3$ Hz, 2H), 1.11 (t, $J = 7.4$ Hz, 3H), 1.00 (t, $J = 7.4$ Hz, 3H).

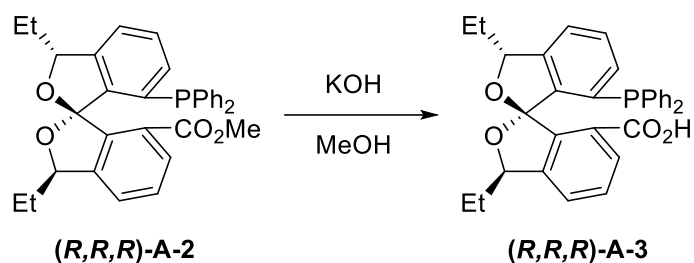
¹³C NMR (176 MHz, Chloroform-*d*) δ 164.9, 145.6, 145.6, 145.5, 145.5, 143.3, 143.2, 139.7, 137.3, 137.2, 135.4, 135.4, 133.6, 133.5, 133.4, 133.4, 133.3, 131.6, 131.5, 130.5, 129.1, 128.5, 128.4, 128.1, 128.0, 128.0, 127.8, 127.8, 126.2, 125.2, 121.3, 118.5, 118.5, 85.0, 83.6, 83.5, 51.1, 30.4, 29.7, 10.0, 9.2.

³¹P NMR (243 MHz, cdcl₃) δ -18.58.

ESI-HRMS Calcd. for C₃₃H₃₂O₄P⁺ 523.2033 [M+H]⁺, found 523.2040.

IR (powder): $\nu_{\max} = 3053, 2966, 2936, 2877, 1733, 1584, 1455, 1432, 1338, 1264, 1193, 1149, 1004, 914, 754$ cm⁻¹

[α]_D: -22.56 (c = 1.00 in CHCl₃)



(R,R,R)-A-2 (430 mg, 0.82 mmol, 1.0 equiv.), 30% KOH aqueous solution (1.80 mL) and MeOH (9.30 mL) were added to a round-bottom flask, and reaction mixture was heated to 80 °C. After TLC indicated a full conversion, the reaction mixture was cooled to room temperature and concentrated to half of its volume. 1M HCl was slowly added to the reaction mixture until the solution pH is around 4-5, and then DCM (15.0 mL) was added to the mixture. After separating layers, the aqueous phase was extracted with DCM (4 x 15.0 mL). Combined organic was dried over Na₂SO₄ and concentrated in vacuo. The crude product was purified by the column chromatography (SiO₂, 5% MeOH in DCM) to afford the product as white solids (99%).

¹H NMR (500 MHz, Chloroform-*d*) δ 10.45 (br s, 1H), 7.37 (dt, *J* = 7.6, 0.9 Hz, 1H), 7.33 (dt, *J* = 7.7, 1.0 Hz, 1H), 7.27 – 7.20 (m, 3H), 7.18 – 7.13 (m, 3H), 7.10 (tq, *J* = 7.5, 1.3 Hz, 1H), 6.98 (td, *J* = 7.5, 1.8 Hz, 2H), 6.90 (ddd, *J* = 8.5, 5.4, 1.6 Hz, 2H), 6.81 – 6.74 (m, 1H), 6.62 (td, *J* = 8.0, 1.4 Hz, 2H), 5.43 – 5.34 (m, 1H), 5.15 (dd, *J* = 7.9, 4.1 Hz, 1H), 2.02 – 1.72 (m, 4H), 1.07 (t, *J* = 7.3 Hz, 3H), 0.93 (t, *J* = 7.4 Hz, 3H).

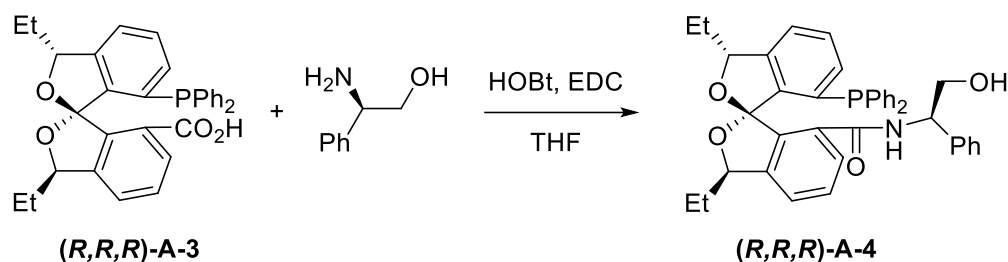
¹³C NMR (176 MHz, Chloroform-*d*) δ 168.6, 145.7, 144.6, 144.5, 143.7, 143.6, 140.1, 137.1, 137.1, 135.2, 135.1, 133.5, 133.5, 133.4, 133.3, 133.2, 131.7, 131.6, 131.1, 129.3, 128.8, 128.4, 128.1, 128.1, 126.0, 125.4, 121.1, 118.4, 85.2, 83.9, 83.9, 30.3, 29.6, 10.1, 9.1.

³¹P NMR (203 MHz, Chloroform-*d*) δ -18.32.

ESI-HRMS Calcd. for C₃₂H₃₀O₄P⁺ 509.1875 [M+H]⁺, found 509.1858.

IR (film): ν_{\max} = 3054, 3007, 2965, 2925, 2875, 1694, 1599, 1457, 1433, 1264, 1215, 1084, 1005, 920, 758 cm^{-1}

[α]_D: -22.51 ($c = 0.35$ in CHCl_3)



(*R,R,R*)-A-3 (0.82 mmol, 1.0 equiv.), (*R*)-(-)-2-phenylglycinol (359 mg, 2.62 mmol), 1-hydroxybenzotriazole hydrate (251 mg, 1.86 mmol) and EDCI (374 mg, 2.41 mmol) were added to a round-bottom flask under nitrogen. Dry THF (25.0 mL) was added to the flask and cooled to 0 °C. After 1 hour, the reaction mixture was spontaneously warmed to room temperature and stirred for overnight. After TLC indicated a full conversion, the reaction mixture was concentrated in vacuo. The crude product was purified by the column chromatography (SiO_2 , 5% MeOH in DCM) to afford the product as white solids (518 mg, 99%).

^1H NMR (700 MHz, Chloroform-*d*) δ 7.60 (d, $J = 7.6$ Hz, 1H), 7.44 (t, $J = 7.6$ Hz, 1H), 7.33 – 7.26 (m, 5H), 7.21 (tt, $J = 7.6, 4.1$ Hz, 4H), 7.14 (td, $J = 7.6, 1.5$ Hz, 2H), 7.12 – 7.07 (m, 2H), 6.99 (td, $J = 8.2, 7.7, 1.5$ Hz, 2H), 6.92 (tdd, $J = 7.5, 4.7, 2.4$ Hz, 3H), 6.92 – 6.87 (m, 1H), 4.85 (td, $J = 6.6, 3.8$ Hz, 1H), 4.68 (dd, $J = 7.5, 4.3$ Hz, 1H), 4.63 (dd, $J = 8.6, 4.5$ Hz, 1H), 3.56 – 3.52 (m, 1H), 3.39 (dd, $J = 11.3, 7.0$ Hz, 1H), 2.68 (s, 1H), 1.94 – 1.72 (m, 4H), 1.27 – 1.22 (m, 1H), 1.02 (t, $J = 7.4$ Hz, 3H), 0.95 (t, $J = 7.3$ Hz, 3H).

^{13}C NMR (176 MHz, Chloroform-*d*) δ 167.4, 145.8, 143.7, 143.6, 143.4, 143.4, 138.3, 136.7, 135.7, 135.5, 135.4, 134.0, 133.8, 133.7, 133.5, 133.4, 133.3, 133.2, 132.0, 129.7, 129.3, 129.0,

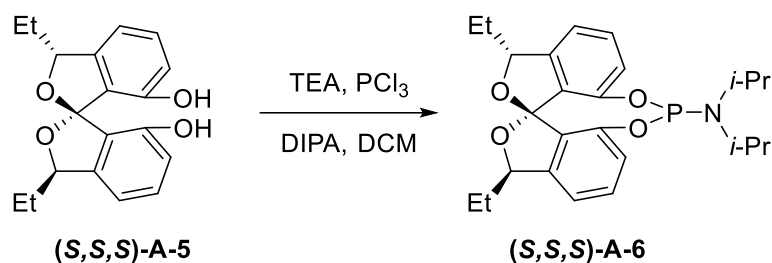
128.7, 128.6, 128.3, 128.3, 128.1, 127.9, 127.9, 127.9, 127.1, 123.6, 121.9, 83.9, 83.9, 65.9, 56.5, 30.8, 30.1, 10.5, 9.7.

^{31}P NMR (283 MHz, Chloroform-*d*) δ -19.10.

ESI-HRMS Calcd. for $\text{C}_{40}\text{H}_{39}\text{NO}_4\text{P}^+$ 628.2610 $[\text{M}+\text{H}]^+$, found 628.2596.

IR (powder): ν_{max} = 3331(br), 3055, 3003, 2964, 2931, 2874, 1649, 1515, 1460, 1433, 1265, 1006, 945, 915, 744 cm^{-1}

$[\alpha]_{\text{D}}$: +101.41 ($c = 0.425$ in CHCl_3)



PCl_3 (44 μL) was added to 2.5mL of DCM in a round-bottom flask under nitrogen, and the solution was cooled to 0 $^\circ\text{C}$. TEA (0.35 mL) was added dropwise into an ice-cold solution and stirred at 0 $^\circ\text{C}$ for 5 minutes. The mixture was then allowed to warm to room temperature and the diisopropylamine (70 μL) was added dropwise to the flask. The mixture was stirred at room temperature for 5 hours and then the DCM solution of **(S,S,S)-A-5** was added and stirred for 18 hours. After full consumption of **(S,S,S)-A-5** indicated by TLC, the reaction was dried by blowing nitrogen. The product was purified by base-treated column chromatography (hexanes/TEA, 20/1 v/v), and obtained the compound as white foam, which is stored in the glove box.

^1H NMR (500 MHz, C_6D_6) δ 7.07 – 6.99 (m, 3H), 6.91 (d, $J = 7.9$ Hz, 1H), 6.79 (d, $J = 7.4$ Hz, 1H), 6.68 (d, $J = 6.8$ Hz, 1H), 4.76 (dd, $J = 9.5, 4.8$ Hz, 1H), 4.61 (dd, $J = 9.6, 5.0$ Hz, 1H), 2.98

(dp, $J = 12.6, 6.4$ Hz, 2H), 2.27 (ddt, $J = 29.4, 15.4, 7.3$ Hz, 2H), 1.91 (ddp, $J = 20.9, 13.9, 7.1$ Hz, 2H), 1.12 – 1.01 (m, 18H)

^{13}C NMR (126 MHz, C_6D_6) δ 149.0, 148.5, 147.6, 146.2, 146.2, 133.2, 131.5, 130.7, 130.2, 122.3, 121.8, 121.7, 117.8, 116.7, 84.9, 84.6, 44.9, 44.8, 30.6, 30.6, 24.3, 24.2, 11.3, 11.1.

^{31}P NMR (283 MHz, C_6D_6) δ 141.79.